PALACKÝ UNIVERSITY
FACULTY OF MEDICINE AND DENTISTRY

Programme DSP: Medical genetics and fetal medicine

PROTEOTOXIC STRESS, DNA DAMAGE RESPONSE AND CANCER

Katarína Chromá, M.Sc.

Supervising department:

Institute of Molecular and Translational Medicine, Faculty of Medicine and Dentistry, Palacký University and University Hospital in Olomouc

Supervisor:

Juraj Kramara, Msc, PhD

Olomouc 2017

Statement:

I hereby declare that I wrote this dissertation entitled: " Proteotoxic stress, DNA damage response and cancer." by myself. The research was carried out at the Institute of Molecular and Translational Medicine, Laboratory of Genome Integrity, Olomouc.

Acknowledgment:

First, I want to thank my supervisor, Juraj Kramara Ph.D. for his invaluable ideas, help and support by his endless optimism throughout my PhD study. Secondly, to Prof. MUDR. Jiří Bártek and Martin Mistrík Ph.D for giving me the chance to work on this exciting project and mediating my internship in highly motivating research area of Genome Integrite Unit Group in Copenhagen, Denmark. I would like to thank also to doc. MUDR Jaroslav Bačovský and the department of hematooncology- Faculty hospital Olomouc, for his willigness to collaborate on the clinical part of this project providing patient's samples diagnosed for multiple myeloma.

I am also grateful to all my labmates from Laboratory of Genome Integrity in Olomouc for the motivating atmosphere they created.

My special thanks go to my mother, whole the family, my boyfriend and friends without whose support none of this would have been possible.

Research on these projects was supported by grants: IGA MZČR NT13569, GAČR 303/09/H048, IGA LF_2012_017, IGA UP LF_2013_015 a BIOMEDREG CZ.1.05/2.1.00/01.0030., NPU1 LO1304

Olomouc …….

March 2017 Katarína Chromá, M.Sc.

Bibliografická identifikácia

Meno a priezvisko autora:	Katarína Chromá
Názov práce:	Proteotoxický stres, odpoveď na poškodenie DNA a rakovina
Typ práce:	Dizertačná
Pracovisko:	Ústav molekulární a translační medicíny, Lékařské fakulty, Univerzity Palackého v Olomouci
Vedúci práce:	Juraj Kramara, Msc, Ph.D
Rok obhajoby práce:	2017
Kľúčové slová:	Odpoveď na poškodenie DNA, dvojvláknový zlom DNA, Nehomologické spájanie koncov, Homologická rekombinácia, RNF168, 53BP1
Jazyk:	Anglický

Bibliographical identification:

Author's name and surname:	Katarína Chromá
Title:	Proteotoxic stress, DNA damage response and cancer
Type of thesis:	Dissertation
Department:	Institute of Molecular and Translational Medicine, Faculty of Medicine and Dentistry, Palacký University Olomouc
Supervisor:	Juraj Kramara, Msc, Ph.D
The year of defence:	2017
Keywords:	DNA damage response, DNA double-strand break, Non-homologous end-joining, Homologous recombination, RNF168, 53BP1
Language:	English

ABSTRACT

DNA double-strand break (DSB) signaling and repair is crucial to preserve genomic integrity and maintain cellular homeostasis. During DNA damage response (DDR), histone ubiquitylation by RNF168 is a critical event, which orchestrates the recruitment of downstream effectors, e.g. BRCA1 and 53BP1. While 53BP1 licenses the non-homologous end joining (NHEJ), BRCA1 initiates DNA resection thus enabling homologous recombination (HR). When recruited to a DSB, 53BP1 "reads" the RNF168 created ubiquitylated histone mark along with histone methylation.

Under conditions of ubiquitin starvation, mostly resulting from proteotoxic stress, the ubiquitin dependent accrual of DDR proteins at the sites of damage is impaired and the ubiquitin mediated DDR is attenuated. A common manifestation of the attenuation is disappearance of the 53BP1 and BRCA1 proteins from irradiation induced foci (IRIF). However, we have identified several cancer cell lines that display 53BP1 recruitment to IRIFs under the conditions of proteasome inhibitor (Bortezomib or MG132) induced proteotoxic stress *i.e.* under substantial depletion of nuclear free ubiquitin levels. We show that central to this phenotype is elevated level of the E3 ubiquitin ligase RNF168 that enables more efficient exploitation of the residual free ubiquitin. Elevated RNF168 levels harbouring cells are more resistant to combined treatment by gamma irradiation and proteasome inhibitor which implies that the RNF168 upregulation may have arisen as an adaptation to constant proteotoxic stress experienced by tumor cells. Moreover, the overabundance of the E3 ligase shifts the balance between NHEJ and HR towards NHEJ, a scenario accompanied by enhanced chromosomal instability shown as micronuclei formation. Importantly, this imbalance might account for increased sensitivity of particular HR proficient breast cancer lines towards PARP1 and topoisomerase inhibitors.

Key words: DNA damage response, DNA double-strand break, Non-homologous end-joining, Homologous recombination, RNF168, 53BP1

ABSTRAKT

Signalizácia a oprava poškodenia DNA dvojvláknových zlomov (DSB) sú považované za nevyhnutné mechanizmy z hľadiska udržiavania integrity genómu ako aj bunkovej homeostázy. V priebehu odpovede na DNA poškodenie (DDR) dochádza ku kľúčovému momentu a to ubiquitylácii histónov prostredníctvom proteínu RNF168, ktorej výsledkom je väzba efektorových proteínov, BRCA1 a 53BP1. Zatiaľ čo proteín 53BP1 spúšťa opravu dvojvláknových zlomov DNA prostredníctvom nehomologického spájania koncov DNA (NHEJ), proteín BRCA1 iniciuje resekciu DNA a homologickú rekombináciu (HR). V priebehu väzby 53BP1 proteínu na dvojvláknovy zlom DNA dochádza k rozpoznaniu histónových modifikácii; metylácie a ubiquitylácie indukovanej prostredníctvom proteínu RNF168.

V podmienkach proteotoxického stresu, ktorý je sprevádzaný nedostatkom voľného ubiquitínu dochádza k poklesu väzobnej schopnosti DDR proteínov k miestam poškodenia a teda k utlmeniu DDR závislej na ubiquitíne. Všeobecným prejavom spomínanej inhibície DDR je strata opravných proteínov 53BP1 a BRCA1 z fokusov indukových gamma žiarením (IRIF). Napriek tomuto všeobecne akceptovanému javu sa nám podarilo identifikovať niekoľko nádorových bunkových línií s prítomnosťou 53BP1 v IRIF (žiarením indukované fokusy) za podmienok deficitu ubuquitínu, teda indukovaného proteotoxického stresu prostredníctvom inhibítora proteazómu (Bortezomib alebo MG132). Objasnili sme rozhodujúcim menovateľ pre daný fenotyp, ktorým je zvýšená hladina E3 ubiquitín ligázy RNF168 umožňujúca efektívne využitie reziduálneho ubiquitínu prítomného v bunke. Bunky so zvýšenou hladinou RNF168 sú rezistentnejšie na kombinovanú terapiu gamma žiarenia a inhibítor proteazómu, čo naznačuje možnú spojitosť deregulácie RNF168 s adaptáciou danej rakovinovej bunky na endogénny proteotoxický stres, ktorému je takáto bunka prirodzene vystavená. Navyše, nadbytok tejto E3 ligázy posúva rovnováhu medzi opravnými dráhami dvojvláknových zlomov DNA, NHEJ a HR, bližsie k NHEJ, čo je sprevádzané zvýšenou nestabilitou chromozómov identifikovanou vo forme zvýšeného počtu mikrojadierok. Takto vzniknutá nerovnováha môže mať za následok zvýšenú citlivosť špecifických HR-pozitívnch nádorových línií prsníka k inhibítorom PARP1 a topoizomeráz.

Kľúčové slová: Odpoveď na poškodenie DNA, DNA dvojvláknový zlom, Nehomologické spájanie koncov, Homologická rekombinácia, RNF168, 53BP1

TABLE OF CONTENTS

1 INTRODUCTION 10
2 DNA DAMAGE RESPONSE 11
3 DNA DOUBLE-STRAND BREAKS (DSBs) 14
3.1 SENSING A DNA DOUBLE-STRAND BREAK 16
3.2 SIGNALING EVENTS FOLLOWING A DNA DOUBLE-STRAND BREAK 18
Chromatin mediated regulation of DSB repair outcome……...22
3.3 DOUBLE-STRAND BREAK REPAIR PATHWAYS 24
3.3.1 Homologous recombination (HR) 25
3.3.2 Non-homologous end-joining (NHEJ) 27
NHEJ as a source of genomic instability……29
3.3.3 Regulation of DSB repair pathway choice 31
4 POST-TRANSLATIONAL MODIFICATION WITH UBIQUITIN 33
4.1 UBIQUITIN AND UBIQUITIN CONJUGATION TO SUBSTRATES 34
Ubiquitin ligases……36
4.2 FUNCTION OF UBIQUITYLATION AND THE ‘UBIQUITIN CODE‘ 37
5 ROLE OF UBIQUITYLATION IN DNA DOUBLE-STRAND BREAK REPAIR 40
5.1 DOUBLE-STRAND BREAK SIGNALING BY RNF8 AND RNF168 40
5.2 UBIQUITYLATION IMPACTS ON 53BP1 AND BRCA1 FUNCTIONS 43
53BP1 localization at sites of DNA double-strand breaks……44
BRCA1 localization at sites of DNA double-strand breaks……...48
6 LINK BETWEEN THE UBIQUITIN-PROTEASOME SYSTEM AND THE DNA DAMAGE RESPONSE 50
6.1 PROTEASOME AS FUNCTIONAL COMPONENT OF DNA REPAIR PROCESS .. 52
6.2 THE USE OF PROTEASOME INHIBITORS IN CANCER TREATMENT 55
6.2.1 Bortezomib- the first proteasome inhibitor used in therapy of cancer 57
7 AIMS OF THE THESIS 60
8 MATERIALS AND METHODS 61
8.1 CELL CULTURE AND GENERATION OF DSBs 66
8.2 MICROIRRADIATION 66

8.3 PLASMID AND SiRNA TRANSFECTION 67
8.5 IMMUNOBLOTTING 68
8.6 BIOCHEMICAL CELL FRACTIONATION-ISOLATION OF CHROMATIN-BOUND PROTEINS 68
8.7 IMMUNOFLUORESCENCE AND MICRONUCLEI STAINING 69
8.8 GENERATION OF LENTIVIRUSES AND LENTIVIRAL TRANSDUCTION 70
8.9 FLOW-CYTOMETRIC ANALYSIS OF DNA REPAIR PATHWAY CHOICE 70
8.10 CELL CYCLE ANALYSIS 70
8.11 LONG-TERM CELL SURVIVAL ASSAY 70
8.12 PATIENT's SAMPLES 71
8.13 BM COLLECTION AND ISOLATION OF SINGLE CELL SUSPENSION 71
8.14 IMMUNOMAGNETIC ENRICHMENT OF CD138 POSITIVE CELLS AND IMMUNOPHENOTYPING ANALYSES 71
9 RESULTS AND DISCUSSION 73
9.1 53BP1 IS RECRUITED TO DNA DAMAGE SITES DESPITE PROTEASOME INHIBITOR INDUCED PROTEOTOXIC STRESS IN THE MDA-MB-231 CELL LINE 73
9.2 MDA-MB-231EXHIBIT STANDARD RESPONSE TO PROTEASOME INHIBITION AND STANDARD DDR 74
9.3 MDA-MB-231 AND U2OS DISPLAY SIMILAR LEVELS OF 53BP1 NEGATIVE REGULATORS, PLAYING NONE OR MINOR ROLE IN OBSERVED PROTEOTOXIC STRESS RESISTANT DSB RESPONSE 77
9.4 THE RIF1 AND REV7 EFFECTOR PROTEINS ARE RECRUITED TO MICROIRRADIATION INDUCED DNA DAMAGE UNDER PROTEOTOXIC STRESS IN MDA-MB-231 CELL LINE 79
9.5 ABSENCE OF 53BP1 MUTATED IN ITS UDR-MOTIF AT DSB SITES UNDER PROTEOTOXIC STRESS 81
9.6 THE PROTEOTOXIC STRESS RESISTANT DDR PHENOTYPE DEPENDS ON DDR ASSOCIATED UBIQUITIN SIGNALING WITH RNF168 PLAYING A CENTRAL ROLE 82
9.7 WIDER OCCURENCE OF THE PROTEOTOXIC-STRESS RESISTANT PHENOTYPE AMONG CANCER CELL LINES WITH DIFFERENT ORIGIN 90
9.8 PROTEOTOXIC STRESS-RESISTANT DSB RESPONSE PHENOTYPE EXPERIENCED BY MULTIPLE MYELOMA CANCER CELLS 93

9.9 OVERABUNDANT RNF168 SHIFTS DSB REPAIR TOWARDS NHEJ, ENHANCES GENOMIC INSTABILITY AND VULNERABILITY TO PARPi AND CAMPTOTHECIN 95

9.10 OVEREXPRESSION OF RNF168 CORRELATES WITH INCREASED ENDOGENOUS PROTEOTOXIC STRESS IN BONE MARROW SAMPLES OF PATIENTS DIAGNOSED FOR MULTIPLE MYELOMA 100

10 SUMMARY 106

11 SÚHRN 107

12 REFERENCES 109

13 ABBREVIATIONS 133

14 BIBLIOGRAPHY 137

14.1 ORIGINAL ARTICLES AND REVIEWS 137

14.2 CONFERENCE LECTURES AND POSTER PRESENTATIONS 137

15 APPENDIX-FULL TEXT PUBLICATIONS RELATED TO THE THESIS

15.1 APPENDIX A

15.2 APPENDIX B

15.3 APPENDIX C

15.4 APPENDIX D

1 INTRODUCTION

Maintaining genome integrity and transmission of intact genetic information is critical for the viability and fitness of any living cell and organism. DNA is continuously exposed to genotoxic insults inflicted by endogenous as well as exogenous sources (Barnes and Lindahl, 2004; Jackson and Bartek, 2009). Therefore to avoid the adverse outcomes of DNA distortions, cells have evolved the ability to sense DNA damage, activate the cell cycle checkpoint and initiate DNA repair. Failure to properly repair damaged DNA leads to somatic mutations and chromosomal rearrangements, thus increasing genomic instability, the main feature of tumorigenesis (Jeggo and Löbrich, 2007). Defects in DNA damage sensing and repair are therefore particularly associated with numerous cancer predisposing clinical syndromes as well as other pathologies characterized by accelerated aging, infertility and impaired development of the nervous and immune systems (Callén et al., 2007; McKinnon and Caldecott, 2007).

Efficient detection and repair of damaged DNA requires recruitment and activity of number of specific proteins that are subject to extensive post-translational modification (PTM) (Lukas et al., 2011; Polo and Jackson, 2011). This complex signaling network is termed the DNA damage response (DDR) (Ciccia and Elledge, 2010; Jackson and Bartek, 2009).

A PTM called ubiquitylation has emerged as an important regulatory mechanism that impacts almost every aspect of the DNA damage response. Signaling processes mediated by ubiquitin are especially crucial for the cellular response to DNA double-strand breaks (DSBs) (Stewart et al., 2009), one of the most deleterious types of DNA lesions. In particular, the DSB response critically relies on the active ubiquitin-signaling cascade comprised of UBC13-RNF8-RNF168 proteins (Doil et al., 2009; Huen et al., 2007; Kolas et al., 2007; Stewart et al., 2009; Wang and Elledge, 2007). Sequential action of these proteins producing specific K63-linked ubiquitin chains on chromatin is known to be essential for proper DSB signaling by creating a binding platform for the downstream DSB repair effector proteins (Fradet-Turcotte et al., 2013; Panier et al., 2012).

This work provides an overview of the DNA damage response focusing on the detection and repair of DNA double-strand breaks. Furthermore, current understanding of the role of ubiquitylation within the DDR is discussed. We report that this pathway is hampered by

limited supply of ubiquitin caused by chronic proteotoxic stress in cancer cells. Importantly, this limitation might be circumvented by dysregulation of the ubiquitin driven DDR, particularly by overexpression of the E3 ubiquitin ligase RNF168. In the Results and Discussion sections we further address the following questions: i) what is the mechanism behind the aberrant 53BP1-DSB recruitment in MDA-MB-231 breast cancer cell line after inhibition of protesome followed by gamma irradiation ii) what is the triggering mechanism for the RNF168 upregulation in cancer cells, iii) what are the possible benefits of the proteotoxic stress resistant DSB signaling for the cancer cells and iv) what are the functional consequences of the phenotype for genomic integrity.

2 DNA DAMAGE RESPONSE

Genome of living organisms is constantly challenged by physical and chemical DNA damaging agents, of both physiological and environmental origins. Although DNA is considered to be a highly stable molecule, as one would expect for genetic information storage molecule, it is still susceptible to certain spontaneous changes, due to its complex polymeric and organic nature. In order to prevent accumulation and propagation of mutations, it is essential to detect and repair damaged DNA before the DNA is replicated and passed to daughter cells.

Organisms have developed elaborate cellular pathways that encompass the sensing, signaling and repair of damaged DNA, collectively termed the DNA damage response (DDR) (Ciccia and Elledge, 2010; Jackson and Bartek, 2009). The cascade of events that takes place following an insult to DNA involves the recruitment and local accumulation of DNA damage sensor and mediator proteins at the site of DNA damage, which can be visualized through microscopic imaging as visible subnuclear foci (Bekker-Jensen et al., 2010; Polo and Jackson, 2011). Signaling pathways link these, often chromatin-associated complexes, with transducer/effector proteins that amplify the DNA damage signal and coordinate global as well as more localized cellular changes. These include interruption of ongoing replication and transcription and initiation of damaged DNA repair, eventually resulting in signaling of the repair process completion. Severe or irreparable DNA damage is also recognized by DDR and

leads to permanent cell cycle arrest (cellular senescence) or programmed cell death by apoptosis (Bartek et al., 2007; Mallette et al., 2007; Rich et al., 2000; Zhivotovsky and Kroemer, 2004)

DNA damage may result from endogenous sources, such as reactive oxygen species or other by-products of cellular metabolism, DNA mismatches during replication or from abortive topoisomerase activity. Alternatively, exogenous sources of DNA damage include ionizing radiation (IR), ultraviolet light (UV) and environmental carcinogens (Jackson and Bartek, 2009).

From a structural point of view, there are various types of DNA lesions including damaged DNA bases, DNA mismatches, intra and interstrand cross-links, DNA-protein crosslinks, single- strand breaks (SSBs) and double-strand breaks (DSBs) - considered to be the most cytotoxic (Figure 2.1) (Hoeijmakers, 2001).

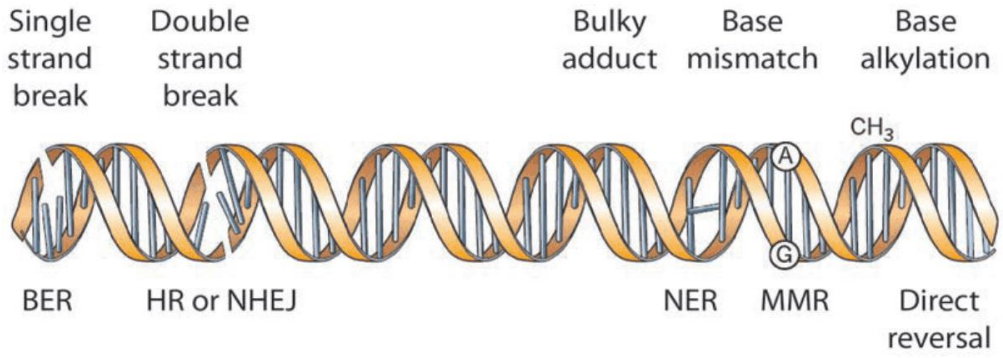

Figure 2.1: Different DNA repair pathways are employed to repair of different types of DNA damage. BER – base excision repair, HR – homologous recombination, NHEJ non-homologous end joining, NER – nucleotide excision repair, MMR – mismatch repair. (Adopted from Lord, 2012)

Besides DNA DSBs repair pathways which will be discussed in more detail below, each individual type of DNA damage is engaged by specialized cellular pathway (Figure 2.1, Table 2.1)

Table 2.1 Brief description of DNA repair pathways in human cells (adopted from Brown and Jackson, 2016)

DNA REPAIR PATHWAYS	
mismatch repair (MMR)	DNA mismatches can arise during DNA replication and are repaired through MMR pathways involving the collective actions of a nudease, polymerase, and ligase (Jiricny, 2006).
SSB Repair	SSBs are recognized predominantly by PARP enzymes which synthesize PAR chains and thereby stimulate the recruitment of DNA repair factors such as XRCC1 and LIG3 to sites of break (Caldecott, 2008). SSBs can arise as a result of IR, treatment with various chemical agents and also as intermediate during BER and NER (see below).
base excision repair (BER)	Involves recognition, excision and replacement of damaged bases in cells, employing the overlapping enzymes with those required for SSB repair (Dianov and Hübscher, 2013).
nudeotide excision repair (NER)	NER machinery removes a wide spectrum of DNA helix distorting lesions, in particular the UV-induced photo lesions: CPD (cyclobutane pyrimidine dimers) and 6-4PP (pyrimidone photoproducts). Two subpathways of NER, global genome NER (GG-NER) and transcription coupled NER (TC-NER) are capable of recognition of DNA damage, single strand incisions and excision of the lesion-containing DNA fragment followed by DNA repair synthesis/ligation. GG-NER operates throughout whole the genome while TC-NER is initiated when DNA lesion encounters the transcribed strand of active genes (Fousteri and Mullenders, 2008).
trans-lesion synthesis (TLS)	TLS is mechanism of DNA damage bypass that protects against DSB break generation following replication fork stalling. It involves specialized DNA polymerases from Y-family to replicate past the DNA damage and therefore is intrinsically error-prone (Sale, 2012).
DNA Interstrand cross-link (ICL) repair	ICL can arise following exposure to various environmental mutagens, particularly alkylating and platinum based chemical compounds (Deans and West, 2011). Proteins from Fanconi aneamia family (FANCA, B. C, E, F, G, L, M) are required for detection and repair of ICLs. Presence of ICLs can stall replication fork progression, causing replication fork collapse and generation of DSBs triggering sequential action of translesion synthesis and homologous recombination repair mechanisms (Sale, 2012).

Clinical syndromes arising due to hereditary defects in genes encoding DDR proteins are characterized by immunodeficiency, infertility, neurodegeneration, cancer predisposition and accelerated aging. This highlights the importance of the physiological processes that rely on functional DNA repair pathways (Ciccia and Elledge, 2010; Jackson and Bartek, 2009).

Deficiency in DNA repair pathways is a typical hallmark of cancer cells characterized by number of chromosomal aberrations leading to genomic instability. This together with the intrinsic replication stress (RS) present in most tumors provides a therapeutic window for novel cancer therapies (O'Connor, 2015).

Current cancer therapeutics research therefore aims at developing of small molecule inhibitors of key DDR enzymes as well as cytotoxic chemotherapeutics acting through generation of DNA damage in tumor cells (Basu et al., 2012; Curtin, 2012; Furgason and Bahassi, 2013).

Among broad spectrum of DNA lesions encountered daily by any mammalian cell (Lindahl and Barnes, 2000), DNA double-strand breaks represent the most deleterious one (Wyman and Kanaar, 2006).

Given the key biological role of the double strand break repair pathways in safeguarding the genome stability, this work predominantly focuses on the most recent progress in the fields of signaling and repair of DNA double-strand breaks, highlighting the relevance of ubiquitylation in the process.

3 DNA DOUBLE-STRAND BREAKS (DSBs)

DSBs result from **exogeno**us agents such as ionizing irradiation (IR) and action of chemotherapeutic drugs. The latter group of chemical compounds, (being the mainstay of cancer therapy for decades), involves drugs that induce covalent crosslinks between DNA bases (cisplatin, carboplatin, oxaliplatin and mitomycin C), drugs that attach alkyl groups to bases (methyl methanesulphonate and temozolomide) and agents that may cause DSBs by trapping topoisomerase enzyme I or II on DNA (camptothecin and etoposide) (Ciccia and Elledge, 2010). Other drugs, impairing the progression of DNA replication, by either inhibiting the activity of DNA replicative polymerase or depleting deoxyribonucleotide pool, include aphidicolin and hydroxyurea. For more detailed insight into mechanism of action, induced phenotypes and cellular readouts of some previously mentioned agents please refer to our recent review article " Common chemical inductors of replication stress: focus on cell-based studies" attached in the chapter 15.4.

Endogenous processes also represent a challenge for the genome integrity. Major causes of such inherent DSBs are oxidized DNA bases generated by reactive oxygen species (ROS) via normal cellular metabolism. Similarly, during unperturbed cell cycle, errors in DNA replication as well as numerous natural obstacles lead to pause/stall or block of DNA replication fork and may eventually result in formation of DNA double-strand breaks. DSBs may also arise due to defective metabolism of chromosome ends (telomeres) (d'Adda di Fagagna et al., 2001)

In parallel with these stochastic DSBs, programmed DSBs play an essential role in various biological processes in a cell. These intentional DSBs are instrumental during development of the immune system and during meiosis. In the first case they occur as an intermediate during developmentally regulated rearrangements, such as V(D)J recombination and immunoglobulin class-switch recombination (CSR) during lymphocytes maturation (Alt et al., 2013). DSBs are also generated in meiosis, during gamete maturation in sexually reproducing organisms to initiate recombination between homologous chromosomes (de Massy, 2013).

DNA DSBs are considered to be of particular biological importance because their repair is intrinsically more difficult than that of other types of DNA lesions. DNA DSBs are generated when the both complementary strands of DNA double helix are simultaneously broken at the same time. As a consequence, the two DNA ends produced by a DSB are susceptible to become physically dissociated from one another, making subsequent repair difficult to perform and also providing the opportunity for inappropriate recombination with other sites in the genome. Another obstacle to rapid and error-free DSB repair is the fact that the DNA termini often involve also persisted base damage, therefore the DSB ligation step cannot occur until processing by DNA polymerase and/or nuclease has taken place (Jackson, 2002).

Defective rejoining of DNA DSBs may occur, leading to the loss and/or amplification of chromosomal material that is characteristic trait of many cancer cells. Under certain conditions such inappropriate DSB repair leads to chromosomal translocations, which might be associated with the inactivation of tumor suppressor loci and activation of proto-oncogenes, respectively (Mitelman et al., 2007).

There is a large amount of experimental evidence supporting the causal link between DSBs, induction of genomic mutations, chromosomal aberrations and cell transformation. As will be discussed later, mutations in many components of DSB signaling and repair lead to increased predisposition to cancer in humans and animal models. Therefore accurate repair is not only essential to safeguard genome stability, but also to counteract the malignant transformation of cells (Jackson and Bartek, 2009)

Cells initiate a robust signaling based response to DSBs that activates cell cycle checkpoints, coordinates DNA repair and changes in chromatin structure, regulates gene

expression and, in some cases, induces p53-driven apoptosis if damage proves too severe (Figure 3.1) (Bekker-Jensen and Mailand, 2010; Luijsterburg and van Attikum, 2011; Rouse and Jackson, 2002; Zhou and Elledge, 2000).

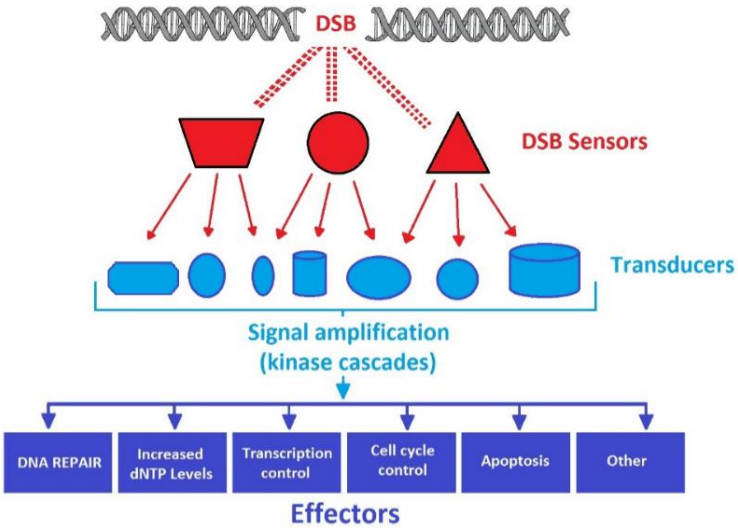

Figure 3.1: Schematic representation of cellular response to DNA double-strand breaks. Multiple sensor proteins physically recognize DNA damage, while number of transducer proteins then amplifies and diversify the DNA-damage signal, and a range of downstream effectors regulates various aspects of cellular functions (adopted from Jackson, 2002).

3.1 SENSING A DNA DOUBLE-STRAND BREAK

A DSB is detected rapidly by various DSB `sensor` proteins that subsequently direct signaling and repair via one of the two predominant DSB repair pathways in human cells: homologous recombination (HR) and non-homologous end joining (NHEJ).

One of these DSB sensors is the heterodimeric Ku protein, formed by two structurally related polypeptides of 70 and 83 kDa (Ku70 and Ku80, respectively) (Griffith et al., 1992; Mimori et al., 1986). Ku is a highly abundant DNA-binding protein, binding rapidly to free DNA ends independently of their DNA sequence, being necessary for NHEJ repair of DSBs (Britton et al., 2013; Mari et al., 2006; Smider et al., 1994; Taccioli et al., 1994; Uematsu et al., 2007). Ku protein is able to self-associate, and binding of two heterodimers at each side of the DSB enables bridging and stabilization of the two DNA ends, while allowing access to the DNA ends by ligation enzymes (Cary et al., 1997; Ramsden and Gellert, 1998; de Vries et al., 1989). In addition, Ku serves as a docking site for all the other core components of the NHEJ

complex, including DNA-PKcs (catalytic subunit of DNA-dependent Protein Kinase) (Gottlieb and Jackson, 1993; Smith and Jackson, 1999; Uematsu et al., 2007), XRCC4/LIG4 (X-ray Cross-Complementation group 4) (Costantini et al., 2007; Hsu et al., 2002), XLF (Yano et al., 2008) and the recently identified PAXX protein (PAralog of XRCC4 and XLF) (Ochi et al., 2015; Xing et al., 2015).

Another DSB sensor is the MRN protein complex comprised of MRE11 (Meiotic Recombination 11), RAD50 (DNA repair protein RAD50) and NBS1 (Nijmegen breakage syndrome 1) (Dolganov et al., 1996; Ogawa et al., 1995; Trujillo et al., 1998; Usui et al., 1998). MRE11 has intrinsic DNA-binding activity (de Jager et al., 2001), as well as endo- and exonuclease activity that is required for nucleolytic processing of DNA ends before NHEJ can proceed (Paull and Gellert, 1998, 1999). It is also important for short-range stabilization of DNA ends and, together with its binding partner CtIP (also known as RBBP8; RetinoBlastoma Binding Protein 8), initiates the process of DNA end resection, driving step of HR (Jazayeri et al., 2006; Sartori et al., 2007).

The poly(ADP-ribose) polymerase proteins **PARP1** and **PARP2 are** also employed in detection of both DNA single– and double-stranded breaks being responsible for the most of cellular poly (ADP-ribosylation) (PAR) activity following the DNA breakage (El-Khamisy et al., 2003; Mortusewicz et al., 2006; Wang et al., 2006).

Upon detecting DNA damage, the PARP enzymes are first automodified which leads to signal amplification and selective recruitment of poly ADP-ribose binding effector proteins to the vicinity of DNA breaks (Bramson et al., 1993; D'Silva et al., 1999; Lindahl et al., 1995). The primary effects of the PARP-automodification comprise changes in chromatin architecture (by poly ADP-ribose attached to histones) (Kim et al., 2004), recruitment of the BER machinery (by specific binding of XRCC1 and LIG3) (El-Khamisy et al., 2003; Mortusewicz et al., 2006), or removal of damaged nuclear proteins (by direct activation of the nuclear 20S proteasome) (Mayer-Kuckuk et al., 1999; Ullrich et al., 1999).The current view on PARP1 in repair of DSBs distinguishes a role of PARP1 in slower alternative NHEJ (aNHEJ) repair mechanism from its function in a fast classical NHEJ (cNHEJ) pathway. PARP1 has been described as component of an error-prone backup alternative pathway of NHEJ together with DNA Ligase III and XRCC1, being essential for cell survival predominantly in the absence of cNHEJ (Audebert et al., 2004; Wang et al., 2006). However,

recent findings emphasized the role of PARP1 in modulating the efficiency of classical NHEJ (cNHEJ) in chromatin environment. Findings of Luijsterburg and colleagues suggested a model in which PARP1- associated PAR chains attract the chromatin-remodeling activity of CHD2 to deposit histone variant H3.3 and generate an accessible chromatin environment that promotes the efficient assembly of NHEJ complexes at DSBs (Luijsterburg and van Attikum, 2011).

It is still not clear how a particular DSB might promote the recruitment of one over another DNA damage sensing molecule. However, recent studies have shown that both Ku and MRN might co-localize at some DSBs, at least in the first stages of DSB recognition (Britton et al., 2013).

3.2 SIGNALING EVENTS FOLLOWING A DNA DOUBLE-STRAND BREAK

Even a single DSB can evoke a complex cellular response that occurs not only in the vicinity but also globally, coordinating the most appropriate outcome. This includes stimulation of DNA repair, cell cycle checkpoint activation, transcriptional reprogramming, or apoptosis if damage proves too severe (Bao, 2011). To prevent oncogenic genome rearrangements resulting from inaccurate DDR, repair pathways that sense and signal DNA damage must be highly sensitive, but at the same time, selective and reversible. DNA DSB signaling events are largely coordinated by three major phosphatidylinositol 3-kinase-related kinases (PIKKs): ATM, ATR (Ataxia telangiectasia and Rad3-related protein) and DNA-PKcs. These kinases preferentially phosphorylate serine or threonine residues followed by glutamine residue (S/TQ) (Kim et al., 2004).

ATM and DNA-PK are critical for the signaling of DSBs while ATR is mainly playing role in the response to DNA single strand breaks and stalled replication forks (Bartek and Lukas, 2007; Shiloh and Kastan, 2001). DSBs trigger rapid activation of the ATM kinase in a process that involves its acetylation by Tip60 (KAT5) and interaction with NBS1 (Falck et al., 2005; Paull and Lee, 2005; Uziel et al., 2003). The ATR protein is activated by RPA (replication protein A)- bound to single-stranded DNA (ssDNA). This can arise either as a result of replication stress leading to accumulation of long ssDNA stretches or following DNA

end resection prior to HR-mediated DNA repair (Costanzo and Gautier, 2003). ATR is recruited to RPA coated ssDNA by its obligate binding partner ATRIP (ATR-interacting protein), while its kinase activity being enhanced by TOPBP1 (topoisomerase binding partner 1) (Cimprich and Cortez, 2008; Nam and Cortez, 2011; Zou and Elledge, 2003).

Germline mutations in ATM or ATR result in ataxia-telangiectasia (A-T) and Seckel syndrome, respectively a human hereditary disorders characterized by primary immunodeficiency, radiosensitivity and progressive neurodegeneration (Shiloh and Kastan, 2001; Ziv et al., 1997).

The catalytic activity of DNA-PK triggered via Ku-mediated DNA binding is essential for NHEJ (Gottlieb and Jackson, 1993) as well as V(D)J recombination and the maturation T and B cell lymphocytes (Blunt et al., 1995; Finnie et al., 1995; Kurimasa et al., 1999). Therefore germline mutations in DNA-PKcs result in severe combined immunodeficiency phenotype (SCID) (van der Burg et al., 2009) .

Additionally, the elevated DNA-PKcs activity or expression level, mutations and polymorphisms in *DNA-PKcs* gene (also referred to as *Prkdc* or *XRCC7*) have been identified in clinical tumor samples of different origin characterized by poor patient survival. Therefore, various anti-DNA-PKcs strategies have been developed and tested in preclinical studies to exploit the benefit of DNA-PKcs inhibition in sensitization of radiotherapy and in combined modality therapy with other antitumor agents (Hsu et al., 2012).

As well as mediating the local recruitment of mediator proteins to DNA DSBs, the PIKKs also phosphorylate effector molecules that regulate more global cellular responses, including transcription, apoptosis, senescence and delayed cell cycle progression. Following induction of DSBs, the DDR leads to activation of cell cycle checkpoints allowing the cell time to repair and to avoid damage propagation to daughter cells. Therefore, it is very important to emphasize direct linkage among the sensing response (Figure 3.1), checkpoint response (Figure 3.2) and the repair response to DNA damage (Figure 3.4). Loss of cell cycle checkpoints is a key event in tumorigenesis, and generally occurs through mutation of checkpoint proteins (i.e. p53, RB etc) (Berger et al., 2011; Hanahan and Weinberg, 2000).

Checkpoints are largely controlled by ATM and ATR kinases which are activated by the mechanisms described above depending on the cell cycle stage in which the damage is recognized (Abraham, 2001).

G1-phase Checkpoint:

The major proximal checkpoint kinase activated in response to IR- or radiomimetic agent-induced DNA damage during G1 is the ATM kinase, which acts on many targets, including CHK2, MDM2 and p53(Lavin and Kozlov, 2007; Matsuoka et al., 2007). ATM is known to enhance p53 accumulation by triggering its release from MDM2, a protein that targets p53 for ubiquitylation, nuclear export, and proteosomal degradation (Freedman et al., 1999; Juven-Gershon and Oren, 1999). When ATM is activated, MDM2 is phosphorylated and prevented from regulating p53-turnover. The checkpoint kinase CHK2, also activated by ATM driven phosphorylation, further phosphorylates p53 (Caspari, 2000). All these events contribute to p53 stabilization and its action as a transcription factor to variety of genes, including p21WAF inhibitor of cyclin-dependent kinases (Beckerman and Prives, 2010). Inhibition of CDC25A phosphatase by p21WAF blocks the dephosphorylation of CDK2 which is required for hyperphosphorylation of RB to drive initiation of S-phase (Saha et al., 1997). Simultaneously, CHK2 phosphorylates CDC25A and prevents its activity in a more rapid fashion (Falck et al., 2005). Together, these two pathways lead to accumulation of cells near the G1/S boundary (Tannock et al., 2004; Weinberg, 2006).

S-phase Checkpoint:

The intra-S-phase checkpoint network activated by genotoxic insults causes largely transient, reversible inhibition of the firing from those origins of DNA replication that have not yet been initiated. In S-phase cells experiencing DNA resulting from genotoxic stress induced by UV, IR or agents that interfere with DNA replication (aphidicolin, hydroxyurea), the proximal kinase activated is ATR. Recently it has become clear that this stress also contributes to ATM activation and ATM, ATR kinases share some substrates (Jazayeri et al., 2006; Matsuoka et al., 2007; Stiff et al., 2006). Both kinases activate structural maintenance of chromosomes protein 1 (SMC1) and Nijmegen breakage syndrome protein 1 (NBS1), leading to slowing down of replication progression (Bartek et al., 2004). A parallel pathway involves activation of the CHK1 and CHK2 proteins that phosphorylate CDC25A and CDC25C. This leads to CDC25C binding to the 14-33σ (a p53 target) and this complex along with CDC25A block CDK2 function to prevent further replication origin firing (Cimprich and Cortez, 2008). This

mechanism is explained through disability of DNA polymerase alpha loading to chromatin, which is initiated by cell division protein 45- CDC45, when CDK2 becomes activated (Bartek and Lukas, 2003; Bartek et al., 2004).

G2 Checkpoints:

The G2 checkpoint (also known as the G2/M checkpoint) prevents cells from entering mitosis when they experience DNA damage during G2, or when they progress into G2 with some unrepaired damage inflicted during previous S or G1 phases (Nyberg et al., 2002; Xu et al., 2002). The accumulation of cells in G2 may also reflect a contribution of the so-called DNA replication checkpoint (often referred to as the S/M checkpoint) that may sense some of the persistent DNA lesions from the previous S phase as being inappropriately or not fully replicated DNA. There are actually two distinct "checkpoints" enacted during G2 phase. The first more rapid one is termed the G2/M checkpoint and is dependent on ATM but independent of IR-dose (Xu et al., 2002). Like the intra-S phase checkpoint ATM-mediated activation of CHK2 induces phosphorylation of CDC25C and its association with 14-3-3σ prevents dephosphorylation of CDC2 (CDK1) and mitotic entry (Lopez-Girona et al., 1999; Matsuoka et al., 1998).. The second G2 "checkpoint" is more accurately termed the G2-accumulation. The G2-accumulation occurs through currently poorly understood ATR-CHK1 mediated pathway and is dominant in mutants that lack G1/S or intra-S-phase checkpoints. It is proposed that this pathway may act as a final salvage mechanism to prevent mitotic entry of cells that were unable to arrest and remove DNA damage at earlier cell cycle stages.

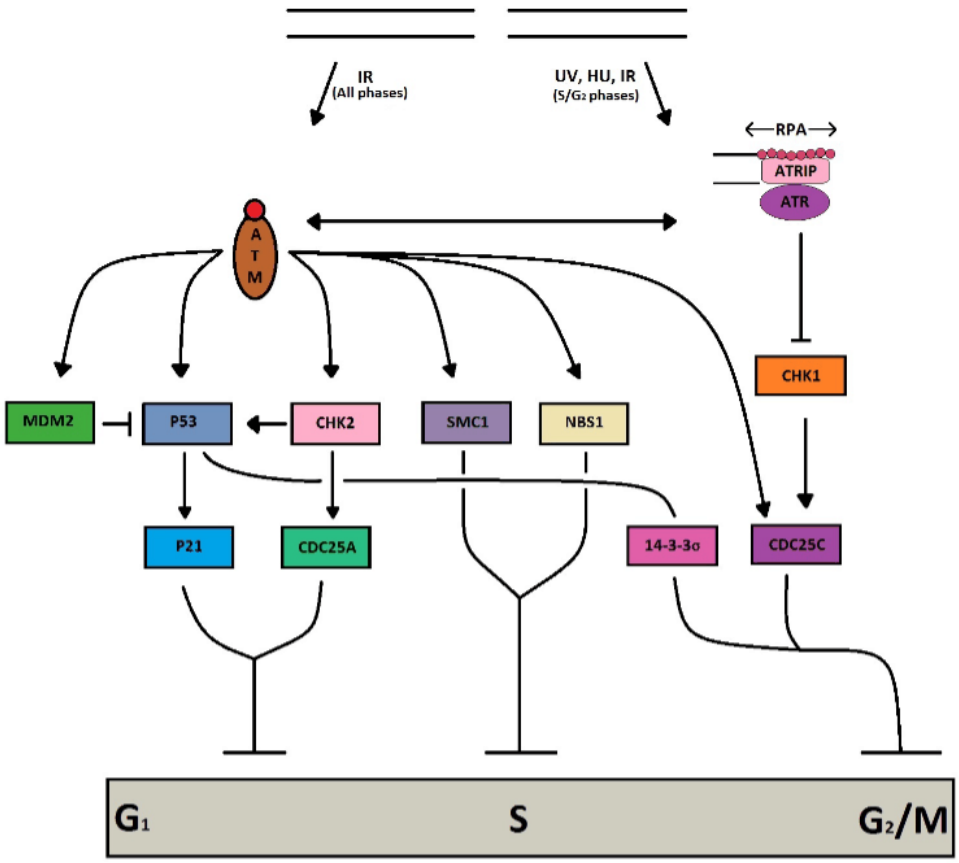

Figure 3.2: DSB-induced Cell Cycle Checkpoints. DSB induction by IR activates ATM leading to accumulation of p53 and transactivation of its target genes, such as p21. Simultaneous phosphorylations of CHK2, SMC1 and NBS1 lead to G1/S checkpoints and intra-S phase cell cycle delay by mediating CDKs as described in the text. DNA damage incurred during S-phase (i.e. by IR or UV) may create ssDNA, leading to activation of ATR. This activates CHK1 and likely ATM-mediated targets to enact the G2/M checkpoint and G2- accumulation as described in the text.

Chromatin-Mediated Regulation of DSB Repair Outcome

When studying the DDR in its cellular context, it is necessary to consider that the physiological substrate for the DDR machinery in the cell nucleus is DNA wrapped around histone proteins in the form of chromatin, the basic unit of which is the nucleosome (Kornberg, 1977; Luger et al., 1997). Although chromatin acts as a physical barrier to the detection and repair of DNA lesions, it is also a dynamic structure that can be modulated by DNA methylation (Kulis and Esteller, 2010), incorporation of histone variants (Bernstein and Hake, 2006), nucleosome repositioning by ATP-dependent remodeling complexes (Clapier and Cairns, 2009) and histone post-translational modifications (Kouzarides, 2007) to be more accessible for DSB repair complexes.

As critical early step in the cellular response to DNA DSBs in context of chromatin, is phosphorylation of the key histone variant H2AX on serine 139 (termed yH2AX) (Rogakou et al., 1998. Following induction of DNA DSB, ATM kinase rapidly phosphorylates H2AX, containing a unique phosphorylation site in its C-terminal tail (Rogakou et al., 1998). In the next step MDC1 (mediator of DNA damage checkpoint protein 1) directly recognizes yH2AX through its carboxy terminal BRCT domain and amplify the yH2AX signal by both promoting its phosphorylation and inhibiting its dephosphorylation (Stucki et al., 2005). Spreading of yH2AX to over a megabase from the site of the initial lesion (Rogakou et al., 1998) is required to sustain the DNA damage signal sufficiently to recruit and retain mediator proteins such as the tumorsuppressors: 53BP1/TP53BP1 (TP53; tumor protein p53 binding protein 1) and BRCA1 (breast cancer susceptibility protein 1) at DSB sites. MDC1 also serves as a binding site for recruitment of other DDR proteins on the damaged chromatin and is considered to be a cornerstone molecule for linkage between phosphorylation and ubiquitylation signaling cascades in DDR (Coster and Goldberg, 2010).

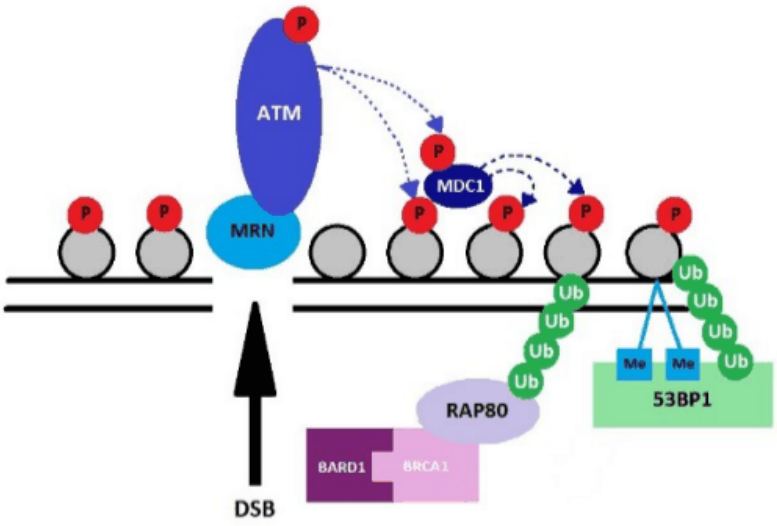

Figure 3.3: Simplified illustration of the major protein players and their PTMs involved in signalling of DSB induction. See above text for details. Horizontal lines represent DNA. P, phosphorylation; Ub ubiquitylation; Me, methylation (adopted from Brown and Jackson, 2016).

3.3 DOUBLE-STRAND BREAK REPAIR PATHWAYS

DSBs are repaired by multiple mechanisms, however human cells prefer two major DSB repair pathways- the Non-Homologous End Joining (NHEJ) and the Homologous Recombination (HR), that differ in speed, accuracy and availability during the cell cycle.These pathways are largely distinct from one another and function in a complementary fashion to accomplish effective DSB repair (Cromie et al., 2001; Essers et al., 2000; Haber, 2000; Takata et al., 1998). Homologous recombination mainly functions during S and G2 phases, when a newly synthesized sister chromatid is available as a template to promote high fidelity DSB repair (Heyer et al., 2010). This pathway is employed for repair of more complex DSBs which, together with the crucial DNA-resection step, slows down its repair kinetics compared to NHEJ.

In contrast, the NHEJ is a relatively simple DNA repair pathway which brings about the ligation of two unprocessed (or minimally processed) DNA ends. The NHEJ pathway does not require undamaged partner DNA molecule to guide the repair and is therefore considered to be error prone (Shrivastav et al., 2008). Consequently, small-scale mutations, such as additions and deletions can be introduced at the break junctions during NHEJ.

Both pathways are highly conserved throughout the eukaryotic evolution but their relative importance differs from one organism to another. Simple eukaryotes such as the yeast species *Saccharomyces cerevisiae* and *Schizosaccharomyces pombe* rely mainly on HR to repair DNA DSBs. In contrast, in mammals the NHEJ pathway dominates almost throughout the entire cell cycle-particularly in G_0 and G_1.The amount of DNA in a mammalian cell compared to a yeast cell is dramatically higher, and to accommodate this, DNA is in higher range compacted into HC (heterochromatin).

Therefore, the choice of pathway for repair of individual breaks is influenced by more parameters, except of already mentioned cell cycle status. Important for such decision is complexity of DNA break and also chromatin structure of present DSB (whether it residues in aneuchromatic or heterochromatic region of the genome) (Ceccaldi et al., 2016).

3.3.1 Homologous recombination (HR)

HR, known as an error-free DSB repair pathway, uses a sequence similar or identical to the broken DNA as a template for accurate repair (Figure 3.3.1). The repair requires significant DNA end

processing and is initiated following 3'-5' DNA end resection coordinated by CtIP(C terminal interacting protein) and the MRN complex, generating 3'-single stranded DNA (ssDNA) (Ciccia et Elledge, 2010). The resulting ssDNA is stabilized through RPA coating, to remove secondary structure (Sugiyama et al., 1997). Subsequently, BRCA2 (breast cancer type 2 susceptibility protein), with the help of BRCA1 (breast cancer type 1 susceptibility protein), and PALB2 (partner and localizer of BRCA2), mediates the replacement of RPA by RAD51 (RAD51 recombinase), to form a nucleoprotein filament that searches for the homologous sequence on the sister chromatid. RAD51 then catalyzes strand invasion of a homologous DNA sequence in a sister chromatid and DNA end extension using the intact sequence as a template. After restoration of any lost sequence information, the second end of the broken DNA is captured and the junctions are resolved to give a precisely repaired DSB (Pardo et al., 2009). Finally, after migration, the DNA crossovers are resolved by cleavage and ligation to yield two intact DNA molecules (Pardo et al., 2009).

Loss of HR in vertebrate cells precludes successful termination of the S-phase, probably due to an inability to restart replication at collapsed DNA replication forks which encountered endogenously generated DNA lesions such as DNA single-strand breaks. It is likely that the inability to restart replication also underlies the unviability of vertebrate tissue culture cells and the early embryonic lethality in mouse models with inactivated essential HR genes such as RAD51, BRCA1 (Lim and Hasty, 1996; Sharan et al., 1997; Sonoda et al., 1998; Tsuzuki et al., 1996). Moreover, the observed unviability of vertebrate cells disrupted for MRE11, RAD50 or NBS1 may be also related to defects in HR (Luo et al., 1999; Xiao and Weaver, 1997; Yamaguchi-Iwai et al., 1999; Zhu et al., 2001). In particular, HR fails to occur efficiently if genes encoding components of the MRN complex, CtIP, ATM, MDC1, gH2AX, PALB2, BRCA1, BRCA2 or RAD51 are silenced or mutated at critical residues. Mutations that limit function of these proteins, as well as other participants in the HR process, are often found in cancers (Roy et al., 2011). High-grade serious ovarian and breast cancer is

characterized by BRCA1 and BRCA2 mutations resulting in genomic instability, being a hallmark of rapid progression of ovarian cancer (Cancer Genome Atlas Research Network).

Early studies found that BRCA1- or BRCA2-deficient cells are hypersensitive to PARP inhibitors. In particular, cells lacking BRCA1 or BRCA2 were more susceptible to PARP inhibitor-induced apoptosis and showed more profound growth inhibition when treated as xenografts in nude mice (Bryant et al., 2005; Farmer et al., 2005). Subsequent investigation demonstrated that cells deficient in other HR components, including NBS1, ATM, ATR, CHK1, CHK2, RAD51, RAD54, FANCD2, FANCA, PALB2, or FANCC, are also hypersensitive to PARP inhibitors (McCabe et al., 2006; Weston et al., 2010; Williamson et al., 2010). Inhibitors of PARP activity comprising molecules such as olaparib/LynparzaTM (AstraZeneca) inhibit function of PARP1 protein playing critical role in BER (Dantzer et al., 1999; De Vos et al., 2012). Initial explanation for the ability of PARP inhibitor to selectively kill HR-deficient cells is based on the interplay between BER and HR. DNA damage induced by endogenous ROS or replication errors results in DNA SSBs, which are ordinarily known to be repaired by BER. Persisted unrepaired SSBs are converted into DSBs following interactions with transcription complexes and replication machinery. In HR proficient cells, such DSBs would be repaired by HR. In cells lacking BRCA1, BRCA2 or other HR proteins, impaired repair would result in persistence of these breaks leading to apoptosis. Another alternative model which could account for synthetic lethality of PARP inhibitors to HR-deficient cells describes trapping of PARP1 on DNA in the presence of inhibitory, thereby diminishing the access of other repair proteins to damaged DNA (Satoh and Lindahl, 1992).

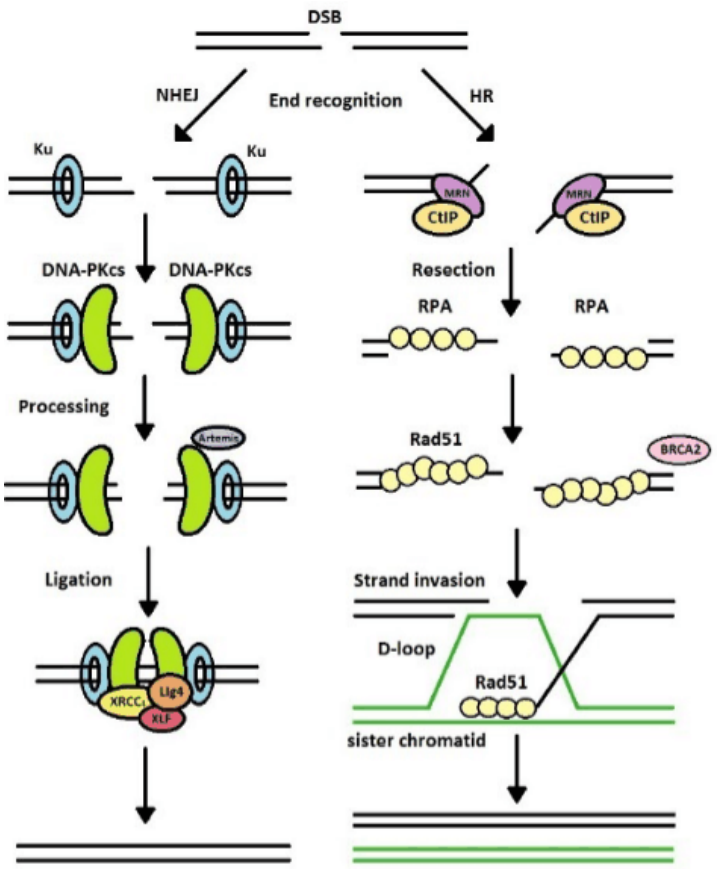

Figure 3.3.1: **A simplified model for HR and NHEJ repair pathways**
Left - NHEJ starts with recognition of the DNA ends by the Ku70/80 heterodimer, which recruits DNA-PKcs. If the ends are incompatible, nucleases such as Artemis can trim the ends. The XRCC4-DNA Ligase IV-XLF ligation complex seals the break.
Right – HR**.** The MRN-CtIP complex starts resection on the breaks to generate single stranded DNA (ssDNA). After resection the break can no longer be repaired by NHEJ. The ssDNA is first coated by RPA, which is subsequently replaced by Rad51 with the help of BRCA2. These Rad51 nucleoprotein filaments mediate strand invasion on the homologous template (adopted from Lorenzo et al., 2013).

3.3.2 Non-homologous end-joining (NHEJ)

NHEJ is a relatively simple and rapid DSB repair pathway that occurs in all cell cycle stages (Figure 3.3.1). Like most DNA repair processes, NHEJ requires a nuclease to resect damaged DNA, polymerases to synthetize new DNA, and a ligase to restore integrity to the DNA strands.

When a DNA double-strand break arises in vertebrates, Ku70/Ku80 heterodimer is the first DNA end binding protein complex, recruiting then the catalytic subunit of the DNA dependent protein kinase (DNA-PKcs) (Ciccia and Elledge, 2010). If necessary, the ends can

be trimmed by nucleases, such as Artemis or filled in by DNA polymerases such as Polμ or Polλ, to create compatible ends (Lieber, 2010). In the final step, the ligation complex, consisting of DNA ligase IV, X-ray cross-complementation group 4 (XRCC4) and Xrcc4 Like factor (XLF)/Cernunnos ligates the processed ends (Ahnesorg et al., 2006)

One might think of Ku as a toolbelt which, when bound to a DNA end, serves as a docking site for the NHEJ nuclease, polymerase and ligase enzymes (Lieber, 2010). It has been suggested that there is a Ku: DNA complex at both DNA ends being joined, thereby permitting each DNA end to be modified in preparation for joining. Each Ku—DNA end complex can recruit the nuclease, polymerase and ligase activities in any order (Figure 3.3.2) (Lieber, 2010; Ma et al., 2004). This flexibility is the basis for the diverse array of outcomes that can arise from identical starting ends. The conformation of DNA bound Ku is most likely different from that of Ku present in solution without DNA. This is due to its inability to form stable complexes with DNA-PKcs in the absence of DNA ends (Yaneva et al., 1997) and the same appears to be the case for its interactions with polymerases mu and lambda (Pol μ and λ) and with XRCC4:DNA ligase IV (Chen et al., 2000; Nick McElhinny et al., 2000).

Except for 5' exonuclease activity, the Artemis—DNA-PKcs complex possesses different array of endonuclease activities including 5' endonuclease activity, 3' endonuclease activity and hairpin opening activity (Ma et al., 2002). Once bound to the DNA terminus, DNA-PKcs phosphorylates itself, the Artemis nuclease and a number of other proteins that can process DNA ends such as polynucleotide kinase phosphorylase, and various DNA polymerases. This broad spectrum of nucleolytic activities allows the Artemis:DNA-PKcs complex to endonucleolytically process a variety of damaged DNA overhangs (Ma et al., 2005; Yannone et al., 2008).

Polymerases mu and lambda are both able to bind to the Ku: DNA complexes by their BRCT domain located at the N-terminal part of respective polymerase (Ma et al., 2004) Additional polymerases appear to substitute for mu and lambda when neither of these two polymerases is present (Bertocci et al., 2006; Wilson and Lieber, 1999). Pol mu is particularly well-suited for functioning in NHEJ because it is capable of template-independent synthesis, in addition to template dependent synthesis. Pol lambda also has more flexibility than replicative polymerases (Ma et al., 2004).

A complex of XLF:XRCC4—DNA ligase IV is the most flexible ligase known, with the ability to ligate incompatible DNA ends and ligate substrate across gaps (Gu et al., 2007a, 2007b). It can also ligate one strand when the other has a complex configuration (e.g., bearing flaps), and it can ligate single-stranded DNA, though with limited efficiency and substantial sequence preferences (Gu et al., 2007a, 2007b)

Altogether, the NHEJ nucleases, polymerases and ligases have much greater mechanistic flexibility than their counterparts in other repair pathways. This flexibility permits these structure-specific proteins to act on a wider range of starting DNA end structures. One consequence of such flexibility in vertebrates may be the substantial diversity of junctional outcomes observed, even from identical starting ends (Ma et al., 2004, 2005).

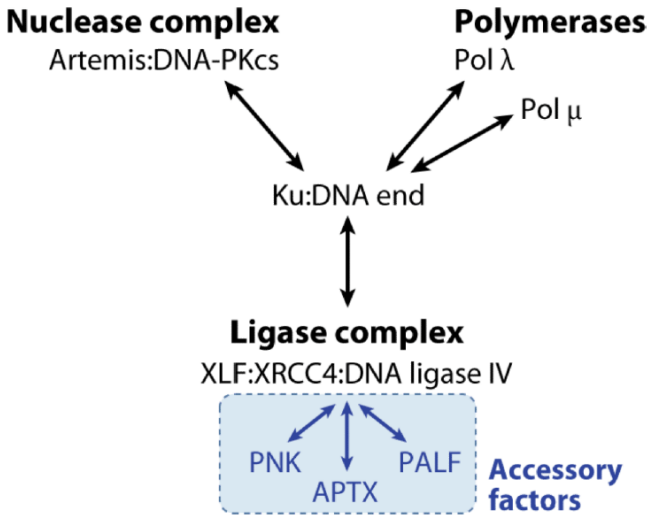

Figure 3.3.2: Summary of the physical interactions among NHEJ components (adopted from Lieber, 2010

NHEJ as a source of genomic instability

Several repair pathways have been proposed to be involved in the formation of translocations which are currently estimated to drive about 20% of cancer cases (Hastings et al., 2009; Mitelman et al., 2007). Probably the most prominent among them is NHEJ that generates translocations often leading to gene fusions. The fusions result from joining of DNA DSBs that arise at different sites of non-homologous chromosomes (Stephens et al., 2011).

Several studies have concluded that disruption of key NHEJ factors such as Ku70, Ku80 or LIG4 reduces genomic instability and the appearance of chromosome-rearrangements

in cells lacking BRCA1 or FANC complementation group proteins (Adamo et al., 2010; Bunting et al., 2010, 2012; Pace et al., 2010). Chemical inhibition of DNA-PKcs has been also reported to reduce genomic instability in BRCA1 and BRCA2 deficient backgrounds (Patel et al., 2011).

One possible explanation to the NHEJ linked increased genomic instability is the differential activity of NHEJ and HR pathways throughout the cell cycle. While, HR is activated only in S and G2 phases when a template for faithful repair is available, NHEJ acts upon DSBs in G1 when there is no newly replicated template present. In the absence of functional BRCA1, DNA lesions occurring in S-phase that are normally repaired through error-free HR are instead channeled into mutagenic NHEJ, resulting in the formation of highly aberrant end joining products such as chromosomal radials (Bunting et al., 2010). Hence, BRCA1-deficiency confers exquisite sensitivity toward chemotherapeutic agents that damage DNA in S-phase cells, such as previously described poly(ADP-ribose) polymerase inhibitors (PARPi) (Bunting et al., 2010; Farmer et al., 2005; Shen et al., 1998) or camptothecin.

Importantly, this PARP inhibitor-induced increase in chromosomal rearrangements and mutations can be diminished by simultaneous treatment of HR deficient cells with a selective DNA-PK inhibitor. Similiarly, the cytotoxicity of PARP inhibitors in BRCA1 deficient background is abrogated by manipulations, diminishing NHEJ activation,including depletion of Ku80 (Patel et al., 2011), DNA-PKcs inhibition (Patel et al., 2011), DNA-PKcs deficiency (Murai et al., 2011; Patel et al., 2011; Williamson et al., 2012), or deletion of 53BP1, which is required for NHEJ pathway activation (Bunting et al., 2010).

In generally accepted model, endogenously induced DSBs are predominantly repaired by the high fidelity HR pathway, in HR proficient cells. In cells, lacking functional HR, however, the end resection dependent mutagenic NHEJ is activated (Patel et al., 2011) and contributes to error prone DSB repair increasing chromosomal rearrangements leading to genomic instability. Consistent with this model, loss of 53BP1 was shown to rescue the lethality of deleterious BRCA1 mutation in mouse models (Bouwman et al., 2010; Cao et al., 2009) , suggesting that BRCA1 deficiency kills mouse cells by activating NHEJ. Moreover, previously described 53BP1 deficiency positively correlates with triple-negative status and poor survival in patients with breast cancer (Bouwman et al., 2010) .

Collectively, these results suggest that, when mammalian DNA repair pathways (such as HR) are defective, the NHEJ pathway can increase the level of genomic instability and therefore, accelerate the accumulation of mutations that contribute to cancer.

3.3.3 Regulation of DSB repair pathway choice

The two major DSB repair mechanisms– HR and NHEJ differ in kinetics, accuracy and availability during the cell cycle (Ceccaldi et al., 2016; Chapman et al., 2012a; Mehta and Haber, 2014). The choice between the two pathways is regulated in a cell cycle dependent manner- DSBs formed in S phase are preferentially repaired by HR, whereas in G1 DSBs, including those formed at immunoglobulin loci, are repaired by NHEJ (Figure 3.3.3). As mentioned above, when this regulation fails, translocations and other genome rearrangements may arise, diminishing cell viability and increasing the chance of tumorigenic changes. Therefore the DSB repair pathway choice is critical for the maintenance of genomic stability and is tightly controlled during different cell cycle phases (Chapman et al., 2012b). The crucial determinant of the cellular choice between the two mechanisms is the requirement of DNA-end processing/ end-resection (Symington and Gautier, 2011).

Homologous recombination depends entirely on the extensive 5` to 3` nucleolytic resection of DNA surrounding the DSB, forming 3` single-strand overhang coated by RPA (Dynan and Yoo, 1998; Heyer et al., 2010). On the other hand, DNA end resection is not needed for NHEJ and most likely prevents the engagement of Ku70/Ku80.

Among various molecules accumulating at DSBs, the tumorsuppressors 53BP1 and BRCA1 are generally the best known and studied proteins with defined role in regulation of DSB repair pathway choice.

53BP1 is considered to be an NHEJ-promoting protein protecting DSB ends from processing by the DNA end-resection machinery during the G1 phase of the cell cycle. Although 53BP1 does not have any intrinsic enzymatic activity, it plays a key role in DSB repair decision by recognition of particular ubiquitylated histone mark in DSB surrounding area and further locally assemble additional factors shielding DSBs against resection (Boersma et al., 2015; Bunting et al., 2010; Callen et al., 2013; Chapman et al., 2013; Escribano-Díaz et al., 2013; Feng et al., 2013; Wang et al., 2014; Xu et al., 2015;

Zimmermann et al., 2013). Several groups have revealed crucial role of these 53BP1 interacting proteins involved in this process, namely REV7- the recently discovered 53BP1 associated protein, RIF1 (Rap1 interacting factor 1) and PTIP (PAX transcription activation domain interacting protein). All three factors cooperate to suppress DNA double-strand break end resection in G1 phase cells. Both RIF1 and PTIP directly interacting with ATM-phosphorylated form of 53BP1, (Chapman et al., 2013; Di Virgilio et al., 2013; Escribano-Díaz et al., 2013; Xu et al., 2015; Zimmermann et al., 2013). Moreover, 53BP1, RIF1, and PTIP all seem to prevent unscheduled hyper-resection of DSBs resulting into switch from error-free HR gene conversion driven by RAD51 to mutagenic HR subpathway-single strand annealing by RAD52 (Ochs et al., 2016).

In contrast to 53BP1 and its effectors, BRCA1 is a key positive regulator of DNA end resection, promoting HR. This crucial function of BRCA1 in HR is based on observation of impaired resection at DSBs as well as failure of RAD51 chromatin loading in BRCA1 deficient cells (Bhattacharyya et al., 2000; Huber et al., 2001; Schlegel et al., 2006). However, the exact mechanism of BRCA1 action in HR was uncovered just recently. During S/G2 phase, cyclin-dependent kinase 1 (CDK1)-mediated phosphorylation of CtIP stimulates its activity at break sites, promotes CtIP binding to BRCA1 which both together prevent 53BP1-RIF1 chromatin association and subsequently drive the resection of duplex DNA to form 5' single-strand overhang (Prakash et al., 2015; Yun and Hiom, 2009). DSB resection starts with DNA incision by the MRE11-CtIP nuclease complex, continues with more processive resection by Exo1 exonuclease and the BLM-DNA2 helicase-endonuclease complex (Mehta and Haber, 2014; Symington, 2014), followed by stabilization of 3'-ss DNA filament by RPA protein. BRCA1 further recruits PALB2 and BRCA2 proteins, and their coordinated action then facilitates RPA-RAD51 replacement required for error-free HR (Zhang et al., 2009). Moreover, the most recent model proposed by Morris and collaborators revealed the precise mechanism by which BRCA1 abrogates 53BP1 recruitment to DNA ends. The process involves the ubiquitylation activity of BRCA1-BARD1 complex which was shown to have a new essential role in regulation of DSB repair pathway choice. Their observations point to a role of the BRCA1-BARD1 ubiquitin ligase activity in driving of chromatin modification that is necessary for the activity of chromatin remodeler SMARCAD1, which in turn repositions 53BP1 thereby allowing the completion of resection (Densham et al., 2016).

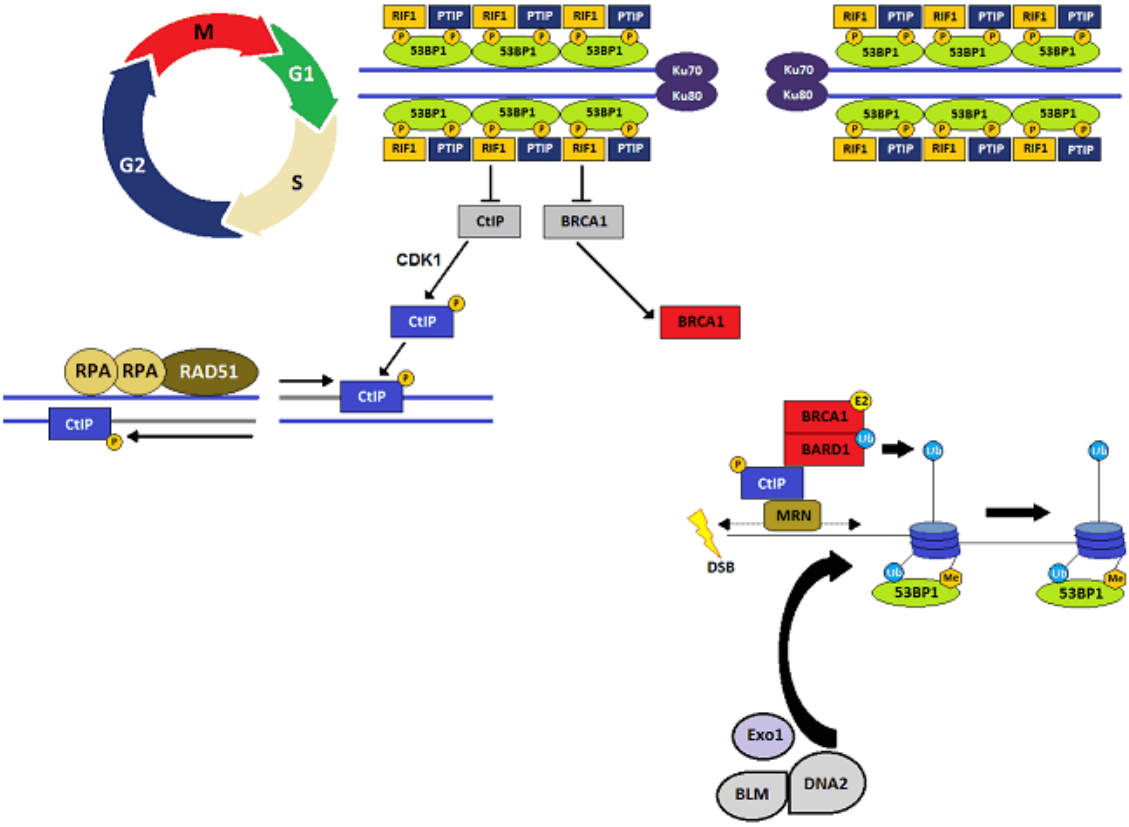

Figure 3.3.3: Regulation of DSB repair pathway choice
Non-homologous end-joining mediated by Ku70 and Ku80 is favored in G1 phase, when the activities of BRCA1 and CtIP are repressed by a complex of 53BP1, PTIP and RIF1, which coats the chromatin in the vicinity of double-strand breaks. During the transition to S/G2 phase, BRCA1 acquires the ability to bind at break sites, where it drives chromatin remodeling being necessary for mobilizing of 53BP1 and allowing recruitment of HR repair factors. Also during S/G2 phase, CDK1-mediated activating phosphorylation of CtIP leads to resection of duplex DNA and formation of a 5´ single-strand overhang. Commitment to homologous recombination is mediated by loading of replication protein A (RPA) and RAD51 at the single-stranded DNA region formed by resection at the DNA break site. (Adopted from Bunting et Nussenzweig, 2013; Densham et Garvin, 2016)

4 POST-TRANSLATIONAL MODIFICATION WITH UBIQUITIN

Post-translational modifications (PTM) play a crucial role in coordinating cellular response to DNA damage. Utilization of specific post-translational modifiers allows temporal

and spatial control over protein localization and interactions, and may represent a means for trans-regulatory activation of protein activities.

The posttranslational modification with ubiquitin (Ub), a process referred to as ubiquitylation, controls, like most other PTMs, many vital metabolic functions. Protein ubiquitylation was discovered in the early 1980s as a process, in which lysine residues in target proteins are modified with a small, 76 amino acid long polypeptide of ~8500 Da (Ciehanover et al., 1978). The initial research on Ub revealed the predominant function of this PTM- regulation of protein turnover by their labelling for degradation in the proteasome complex (Ciehanover et al., 1978). For this and additional discoveries regarding the ubiquitin-proteasome system Aaron Ciechanover, Avram Hershko and Irwin Rose were awarded the Nobel Prize in Chemistry in 2004 (Giles, 2004).

Surprisingly, further research reported additional unexpected functions of protein ubiquitylation. For example, binding of ubiquitin to target protein was shown to induce conformational changes, change subcellular localization, modulate enzymatic activity, alter protein-protein interactions, or modify stability/lifespan of the modified protein (Komander, 2009).

Given the emerging complexity of protein ubiquitylation, there has been an intense interest concerning the role of this modification in pathways of DNA damage response and signaling. In recent years, different groups reported the essential role of ubiquitylation in DDR and in several DNA repair mechanisms (Pinder et al., 2013). A paradigmatic example of DDR coordination via ubiquitylation is represented by the signaling pathway triggered by DNA double-strand breaks that will be discussed in more detail below.

4.1 UBIQUITIN AND UBIQUITIN CONJUGATION TO SUBSTRATES

Ubiquitin is a highly conserved, small (76 amino acid residues) protein, originally discovered owing to its ability to mediate ATP-dependent and lysosome independent pathway of intracellular protein degradation (Ciehanover et al., 1978).

There are four genes encoding ubiquitin in the human genome- UBC, UBB, UBA52 and UBA80, which are first translated either fused to ribosomal proteins (UBA52, UBA80), or as linear poly-ubiquitin chains that require processing to yield ubiquitin monomers

(UBC,UBB) (Baker and Board, 1987; Ozkaynak et al., 1987; Wiborg et al., 1985). Full-length ubiquitin is a precursor peptide requiring cleavage to expose a carboxy-terminal di-glycine motif Ubiquitin is then covalently attached via its C-terminal glycine residue to target proteins, generally to the ε-amino group of a substrate lysine residue. This conjugation involves a sophisticated three-step enzymatic cascade (Dye and Schulman, 2007; Pickart, 2001). In an ATP-dependent first step, an E1 ubiquitin-activating enzyme 'charges' an E2 ubiquitin conjugating enzyme with ubiquitin, i.e. the ubiquitin C terminus is attached to the E2 catalytic cysteine residue via a thioester linkage. The E3 ubiquitin ligase further serves as an adaptor that binds both the substrate and charged E2 and so facilitates isopeptide bond formation between ubiquitin and the substrate (Figure 4.1) (Ciechanover et al., 1982; Hershko et al., 1983).

A pyramid of enzymatic complexity exists to enable conjugation of ubiquitin to a plethora of substrates. In humans, there are eight known E1s two of which are specific for ubiquitin (UBA1 and UBA6) (Schulman and Harper, 2009), 35 E2s (van Wijk and Timmers, 2010) and more than 1000 E3s (Berndsen and Wolberger, 2014).

Ubiquitylation is a reversible process, as ubiquitin conjugated to a substrate can be released by deubiquitinating enzymes (DUBs),-or recycled in the process of proteasome mediated protein degradation for further use by different combination of E1, E2 and E3 enzymes.

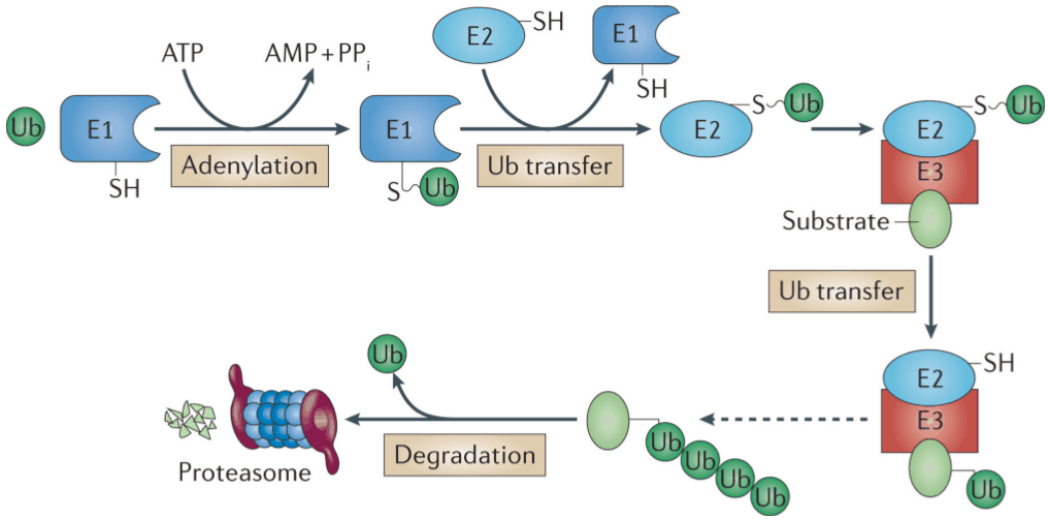

Figure 4.1: Schematic overwiev of the ubiquitylation cascade.

First, ubiquitin is activated by an E1 via an ATP-dependent reaction forming E1-Ub thioester bond. Activated ubiquitin is then transferred to an E2 protein. Finally, an E3 catalyzes the transfer of a ubiquitin to a target protein through formation of an isopeptide bond between the carboxyl-terminus of ubiquitin and a lysine (K) residue on the target protein. Lys48-linked ubiquitin chains are common signals for 26S proteasomes where deubiquitylating enzymes release and recycle ubiquitin during substrate protein degradation (adopted from Maupin-Furlow, 2011).

In general, it is the E3 enzyme that confers the majority of the substrate specificity to the ubiquitylation cascade through recognition of a distinct set of target proteins.

Ubiquitin ligases

E3s, as the widest group of Ub-associated proteins, can be divided into three major families: HECT (Homology to E6AP Carboxyl-Terminus), RING (Really Interesting New Gene) and RBR (Ring Between Ring) (Figure 4.2) (Berndsen and Wolberger, 2014; Mattiroli and Sixma, 2014).

In the case of HECT, ubiquitin is transferred from an E2 to an active site cysteine in the E3 and then to the substrate (Kim and Huibregtse, 2009; Rotin and Kumar, 2009).

The RING E3s bind to the ubiquitin-charged E2 and substrate at the same time (either directly, or through E3-binding partners), transferring ubiquitin to the substrate without direct interaction of the E3 and ubiquitin. The RING domain contains seven highly conserved histidine residues being crucial for E2 binding through recognition of its two central Zn^{2+} ions (Deshaies and Joazeiro, 2009). The generally used term RING E3 ligase is rather an inaccurate term for RING E3s, as they possess no intrinsic catalytic activity, although they do catalyse the transfer from the E2 to substrate by positioning the ubiquitin moiety into a favorable position for conjugation (Plechanovová et al., 2012).

The third class of E3-ligases, RBR, was shown to use both RING and HECT-like mechanisms of action (Wenzel et al., 2011). The transfer of ubiquitin is initiated by the interaction of an E2~ubiquitin with the RBR (Smit et al., 2012; Stieglitz et al., 2012; Wenzel et al., 2011), similar to the interaction between E2s and classical RING E3-ligases (Marín et al., 2004; Smit et al., 2012; Stieglitz et al., 2012). However, in RBRs this interaction further facilitates the formation of a HECT-like thioester intermediate between ubiquitin and an active site cysteine on RBR RING2 domain before it is coupled to its substrate.

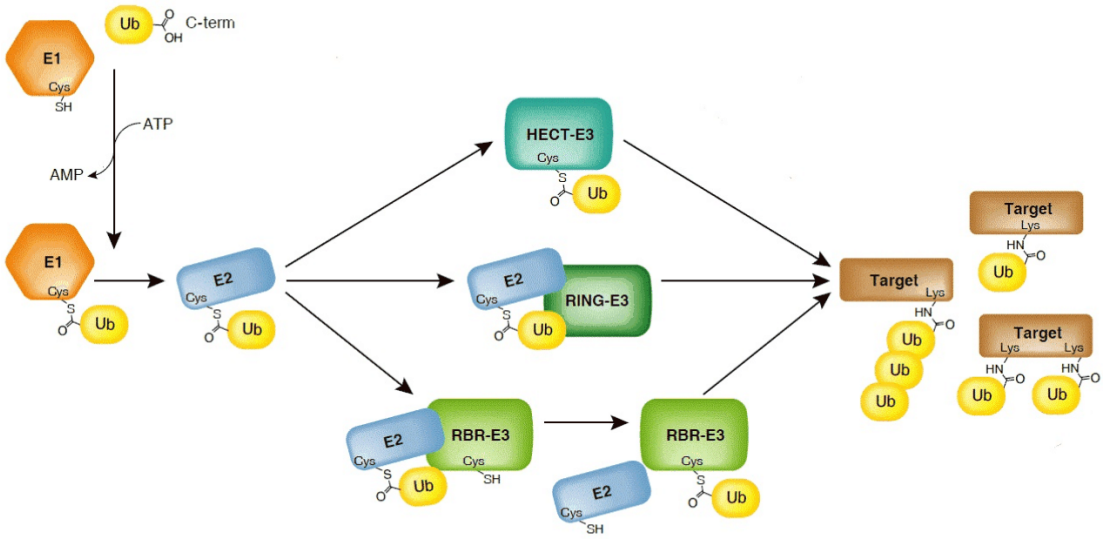

Figure 4.2: Three major types of ubiquitin-ligases (E3).
The ubiquitin (Ub) C-terminus is activated in an ATP-dependent manner by an E1 activating enzyme, and is subsequently transferred to form a thioester intermediate on an E2 conjugase. The final transfer of ubiquitin onto its target is mediated by E3-ligases that either form a thioester intermediate with the ubiquitin (HECT E3-ligases), mediate a direct transfer of the ubiquitin from the E2 onto its target (RING E3-ligases), or function as RING/HECT-type hybrids (RBR E3-ligases). Through this cascade of E1, E2 and E3 enzymes, the ubiquitination machinery mediates the formation of mono ubiquitination, multi-mono-ubiquitination, or ubiquitin chain formation on its targets (Adopted from Smit and Sixma, 2014).

4.2 FUNCTION OF UBIQUITYLATION AND THE ‘UBIQUITIN CODE‘

Ubiquitylation is a versatile regulatory process that can result either in the attachment of a single ubiquitin moiety (mono-ubiquitylation) or in the formation of poly-ubiquitin chains (Figure 4.4). Mono-ubiquitylation has been shown to regulate lysosomal degradation of proteins (Mukhopadhyay and Riezman, 2007) and also mediates protein-protein interactions. One example is the recruitment of translesion synthesis polymerases following mono-ubiquitylation of PCNA after DNA damage (Bienko et al., 2005).

Ubiquitin, contains seven lysine residues (K6, K11, K27, K29, K33, K48, K63), enabling the formation of ubiquitin chains and thus the poly-ubiquiylation of substrates. In addition to these, linear ubiquitin chains can be also formed using the amino-terminal methionine of ubiquitin (Panier and Durocher, 2009) (Figure 4.3).

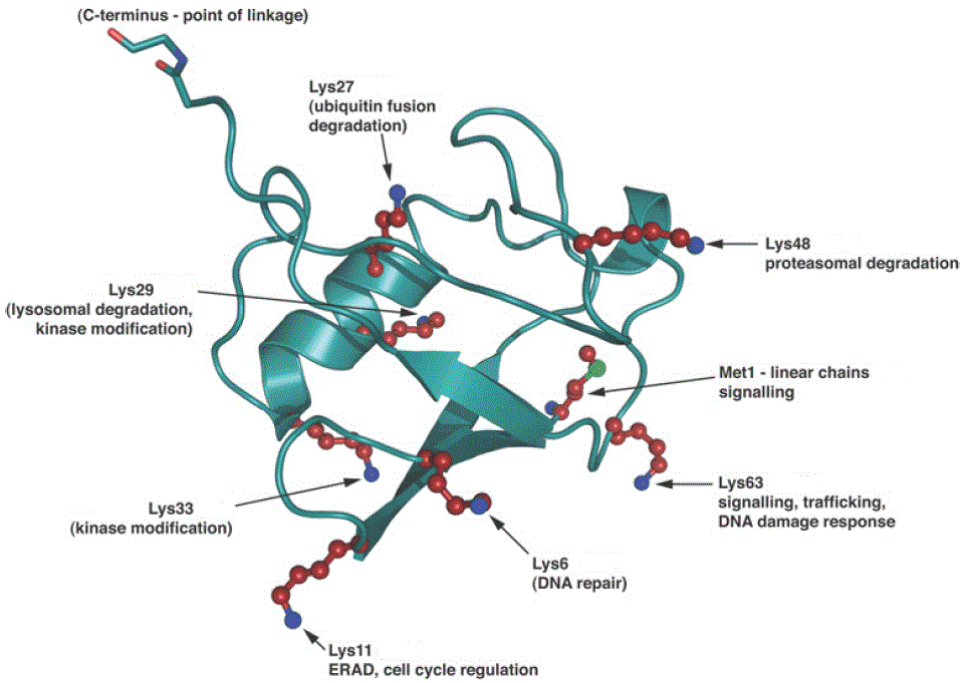

Figure 4.3: Ubiquitin and its lysine residues.
The structure of ubiquitin reveals that all seven lysine residues (red, with blue nitrogen atoms) reside on different surfaces of the molecule. Met1 (with a green sulfur atom) is the linkage point in linear chains, and is spatially close to Lys63. The C-terminal Gly75-Gly76 motif involved in isopeptide bond formation is indicated (red oxygen atoms, blue nitrogen atoms). Lysine residues are labelled and description bellow represents their potential role in cells (adoptef from Komander, 2009).

The linkage specificity is mainly determined by the pairing of specific E2s and E3s (Rieser et al., 2013) . Initially, it was recognized, that protein degradation via the proteasome is not initiated by monoubiquitylation, but rather by K48 polyubiquitin chains that mark the potentially most harmful, misfolded or damaged proteins that need to be destroyed rapidly (Hershko and Ciechanover, 1998).

With the exception of K63 chains, all the other chains were observed to accumulate after proteasome inhibition in yeast. This suggested at least partial role of all the non-K63 chains in directing proteasomal degradation (Xu et al., 2009).

The “degradation role only” paradigm was challenged in 1999/2000 by the teams of C, Pickart and Z. Chen who described a novel ubiquitin linkage that did not have the canonical protein degradation function (Deng et al., 2000; Hoffmann et al., 2016). They found a protein complex consisting of an E2 enzyme UBE2N/Ubc13 and one of two ‘pseudo-E2s’ (E2 fold proteins lacking catalytic residues) MMS2 or Uev1a, which together specifically assembled Lys63-linked ubiquitin chains. It turned out that these K63 polyubiquitin chains served non-

degradative roles, and are important in regulation of DNA-damage response, as well as in signaling processes leading to the activation of the transcription factor NF-κB (nuclear factor κB) (Chen and Sun, 2009).

Given the heterogeneity of the ubiquitin code, it is not surprising that ubiquitylation regulates a wide range of biological processes, including cell cycle progression, transcription, apoptosis and inflammation, as well as DNA damage signaling and repair. Its dysfunction is therefore associated with various diseases, especially neurodegenerative disorders, viral diseases and cancer. Consequently, targeting the components of ubiquitin-system is currently an active area for drug (Deshaies, 2014).

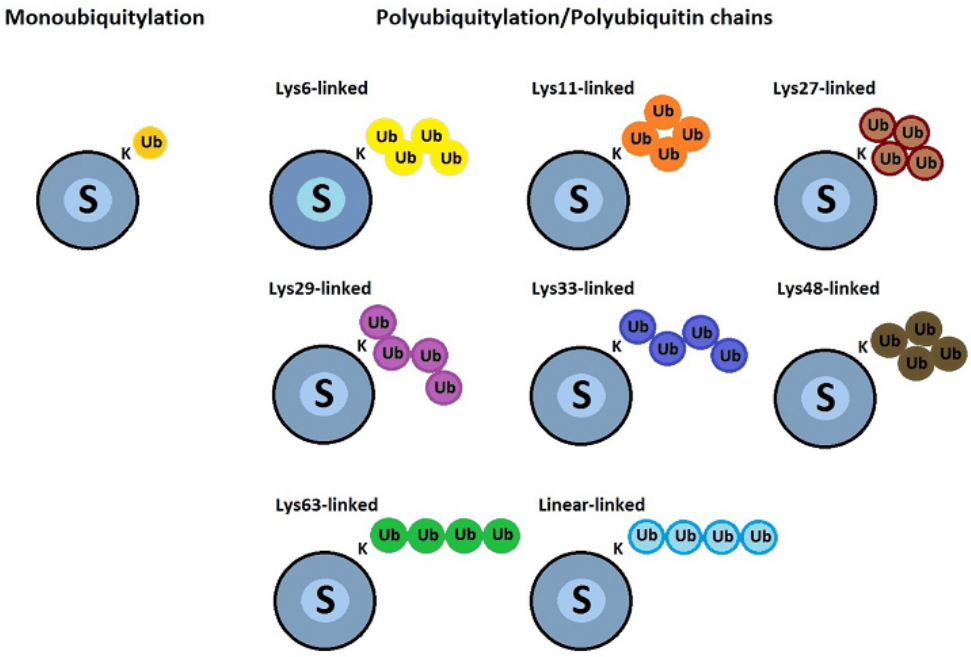

Figure 4.4: Monoubiquitylation and forms of polyubiquitylation
Forms of homotypic polyubiquitination, where each ubiquitin chain contains a single linkage type. Individual linkages may lead to distinct ubiquitin chain structure, and Lys48- and Lys63-linked/linear chains have different conformations. Structures of the remaining chain types are unknown (adopted from Komander, 2009).

The non-degradative K63 chains are particularly important in coordination of the DNA damage response, regulating signaling pathways triggered by DSBs and are therefore described in following chapter. Moreover, recent findings revealed an indirect role of proteasome in the DDR signaling. Hence the role of proteasome in the DDR as well as the possibilities of pharmacologic modulation of this ub signaling pathway, the DDR related

functions of ubiquitin-proteasome system will be discussed in the following sections in more detail.

5 ROLE OF UBIQUITYLATION IN DNA DOUBLE-STRAND BREAK REPAIR

In response to DSBs, cells mount a response that can be cytologically followed via the accumulation of numerous signaling and repair factors on the chromatin surrounding the DNA break. This protein accumulation at DSB sites of chromatin is manifested by the formation of the above mentioned-distinct subnuclear structures called `foci` (Lukas and Bartek, 2004).

The last few years of research in the field have shown, that the assembly of the foci is largely dependent on ubiquitylation which regulates particularly the early signaling events following DNA DSBs formation (Panier and Durocher, 2009).

5.1 DOUBLE-STRAND BREAK SIGNALING BY RNF8 AND RNF168

Chromatin in the vicinity of DSB sites is enriched in K63 ubiquitin chains (Doil et al., 2009; Stewart et al., 2009).

The first E3 ubiquitin ligase acting in the DSB signaling cascade is the RNF8 (RiNg Finger protein 8). RNF8 provides a critical link between phosphorylation and ubiquitylation events in the DDR through binding to ATM-phosphorylated MDC1 via its FHA (Figure 5.1) (forkhead-associated domain) (Huen et al., 2007; Kolas et al., 2007; Mailand et al., 2007). Utilizing its RING domain RNF8 recognizes the E2 enzyme UBE2N (also known as UBC13) and mediates K63-linked ubiquitylation of several different targets required for downstream signaling and recruitment of both major DSB effector proteins- 53BP1 and BRCA1 (and the associated complexes such as the RAP80 complex) (Figure 5.2).

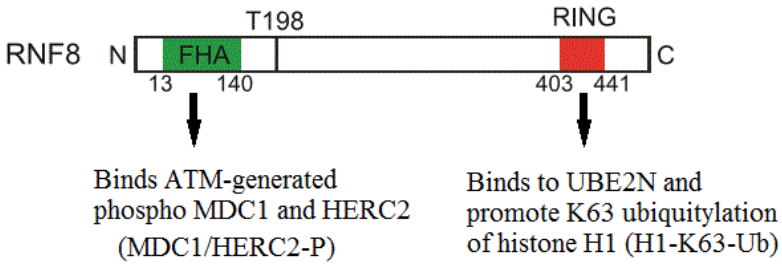

Figure 5.1: RNF8 domains organization and functions
FHA, forkhead-associated domain; N, N terminus; C, C terminus (Adopted from Orthwein et al., 2014)

Recent work of Thorslund and colleagues revealed a long undefined target of UBE2N-RNF8-driven K63 ubiquitylation. They established the H1- type linker histone as the major chromatin associated target of this RNF8 driven Ub modification which in turn enables the recruitment of the second major DDR E3 ligase- RNF168 and corresponding downstream factors to the DSB sites (Figure 5.2) (Thorslund et al., 2015).

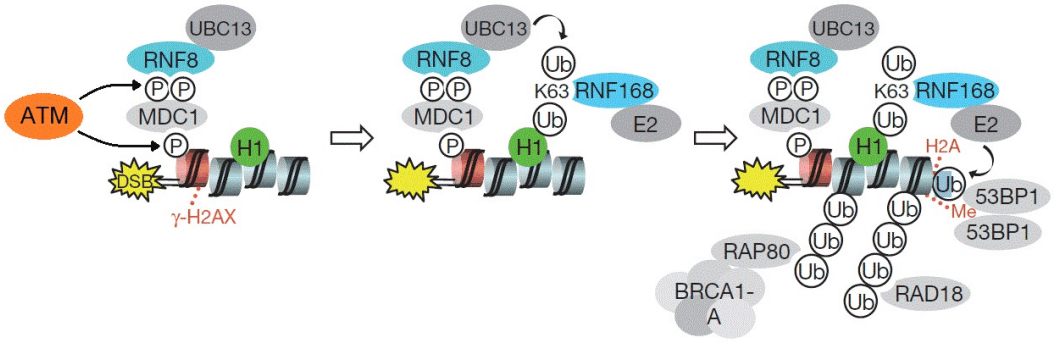

Figure 5.2: Model of RNF8–UBC13 and RN168 driven DSB signaling.
Chromatin ubiquitylation by the RNF8–RNF168 pathway has a central role in recruiting repair factors to DSB sites. Following recognition and initial DSB signal transmission, phosphorylated H2A variant γH2AX generates a direct binding site for the scaffold protein MDC1. ATM-dependent phosphorylation of MDC1 then recruits RNF8–UBC13, which promotes K63-linked polyubiquitylation of H1-type linker histones, a modification that is directly recognized by RNF168. RNF168 potently ubiquitylates H2A-type histones at K13 and K15, generating recruitment platforms for a range of ubiquitin-binding domain (UBD)-containing repair factors, including 53BP1 and RAP80-BRCA1, RAD18 and their associated proteins. RNF168 itself recognizes ubiquitylated forms of H2A,thus amplifying DSB-induced ubiquitylatin signal promoting accumulation of DSB repair factors, along the chromatin fibre (adopted from Thorslund et al., 2015).

In addition to binding phosphorylated MDC1, the FHA domain of RNF8 was also shown to interact with ATM-phosphorylated HERC2 (also a RING E3 ligase), forming an MDC1-RNF8-HERC2 complex following DNA damage (Bekker-Jensen et al., 2010). HERC2

has been reported to stabilize the RNF8-UBE2N interaction and maintain sufficient levels of RNF8 to promote downstream ubiquitylation events at DNA damage sites (Bekker-Jensen et al., 2010).

As mentioned above, the ubiquitylation signal required for signaling of DSBs is not maintained by RNF8 alone, but is largely dependent on the activity of the second RING E3 ubiquitin ligase, RNF168. RNF168 contains two DSB-targeting modules (Figure 5.3), both of which contain ubiquitin-binding domains (Figure 5.3) (Doil et al., 2009; Pinato et al., 2011; Stewart et al., 2009).

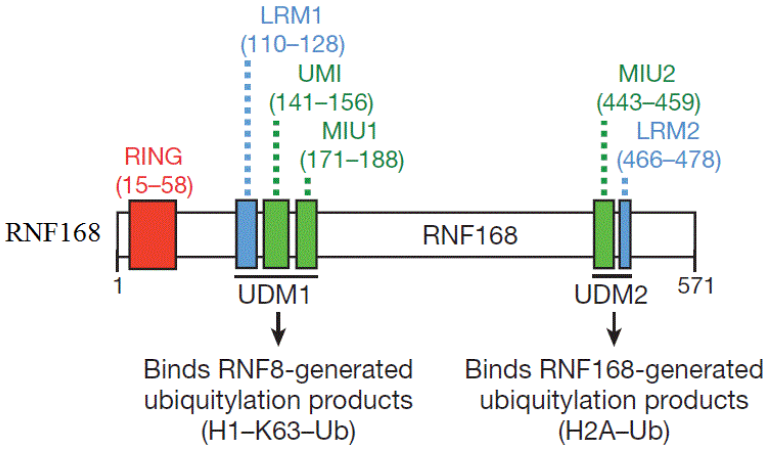

Figure 5.3: Composition and reported functions of ubiquitin dependent DSB recruitment modules (UDMs) in human RNF168 (Adopted from Thorslund et al., 2015)

The N-terminal LRM1-UMI-MIU region termed ubiquitin dependent DSB recruitment module 1 (UDM1) binds to the RNF8-ubiqitylated histone H1, promoting an initial localization of RNF168 at DSB sites. RNF168 then triggers mono-ubiquitylation of histone H2A K13/K15, creating a binding platform for assembly of 53BP1 and the BRCA1/RAP80 complex at the sites of DNA damage (Figure 5.3) (Mattiroli et al., 2012). RNF168 itself also interacts with ubiquitylated histone H2A through its UDM2, consisting of MIU2 and LRM2, and amplifies the H2AK13/K15 monoubiquitin histone mark (Panier et al., 2012; Thorslund et al., 2015).

First indicatation of the existence of a putative DNA double-strand break repair protein that functions upstream of 53BP1 and contributes to the normal development of the human immune system came from the Durocher lab (Stewart et al., 2009). Initially, they showed that cells from a patient with previously unknown syndrome that was later termed RIDDLE syndrome (Radiosensitivity, Immunodeficiency, Dysmorphic features, Learning difficulties)

exhibited hypersensitivity to ionizing irradiation, cell cycle checkpoint abnormalities and impaired end joining in the recombined switch regions. Intriguingly, all the observed effects stemmed from defects in the 53BP1-mediated DNA damage signaling. Their further investigation revealed that the gene mutated in the RIDDLE syndrome codes for the RNF168 ubiquitin ligase (Stewart et al., 2009). Importantly, their study defined physiological neccessity of protein ubiquitylation cascade controlled by RNF8 and RNF168 for 53BP1 function in response to DSBs in human cells. In addition to, a parallel study from the laboratory of J. Lukas and J. Bartek has emphasized crucial role of RNF168 in amplification of ub conjugates on damaged chromosomes thus allowing accumulation of the DSB effectors 53BP1 and BRCA1 on chromatin (Doil et al., 2009).

In line with mentioned immunodeficiency associated with dysfunctional RNF168, other studies have also described the role of RNF8/168 in immunoglobulin class-switch recombination (Kracker and Durandy, 2011). Furthermore, these enzymes were reported to function also in processes of telomere end protection (Peuscher and Jacobs, 2011; Rai et al., 2011) and transcriptional repression at DNA damage sites (Shanbhag et al., 2010).

Of note, the Ub-driven DSB signaling pathway comprising E3-RNF8, RNF168 was shown to be inhibited during mitosis. Preventing the localization of 53BP1, a crucial NHEJ factor, to DNA damage in mitosis, seems to be a crucial step in prevention of cellular genomic instability resulting from deleterious mitotic telomere fusions (Orthwein et al., 2014). The phosphorylation of RNF8 and 53BP1 by mitotic kinases inhibits their recruitment to DSB flanking chromatin, thus blocking the progression of DSB repair in M phase. The rationale behind the necessity to block mitotic DSB repair in response to genotoxic stressors is the harmful DSB repair processing on uncapped sister telomeres leading to chromosome missegregation and aneuploidy. Based on this study, cells generally invoke DSB repair in all the cell cycle stages except of mitosis, when they trigger transient inactivation of the major genome-maintenance pathway to avoid problems caused by underprotected mitotic telomeres.

5.2 UBIQUITYLATION IMPACTS ON 53BP1 AND BRCA1 FUNCTIONS

Probably the most extensively studied ubiquitin driven DDR signaling and repair process is the recruitment of 53BP1 and BRCA1 to DSB sites (Figure 12). These two key

DSB response effectors with antagonistic functions are recruited to a DNA lesion surrounding chromatin in a series of histone ubiqutinylation steps driven by the RNF8/168 E3 ligases (Smeenk and Mailand, 2016)

53BP1 localization at sites of DNA double-strand breaks

53BP1 is a bivalent histone modification reader, recognizing two histone modification marks- nucleosomes modified with H4K20me2 and the DNA damage-inducible H2AK15ub mark (Botuyan et al., 2006; Fradet-Turcotte et al., 2013). First model of 53BP1 recruitment to DSB flanking chromatin describes recognition of dimethylated histone 4 on lysine 20 (H4K20me2) by its TUDOR domain (Figure 5.4) (Botuyan et al., 2006). Later identification of 53BP1 ubiquitylation damage response domain UDR) motif recognizing H2A ubiquitinated on Lys 15 (H2AK15ub), further corroborated the crucial role of the E3 RNF168 ubiquitin driven signaling for 53BP1 accumulation at DSB sites (Fradet-Turcotte et al., 2013) (Figure 5.4).

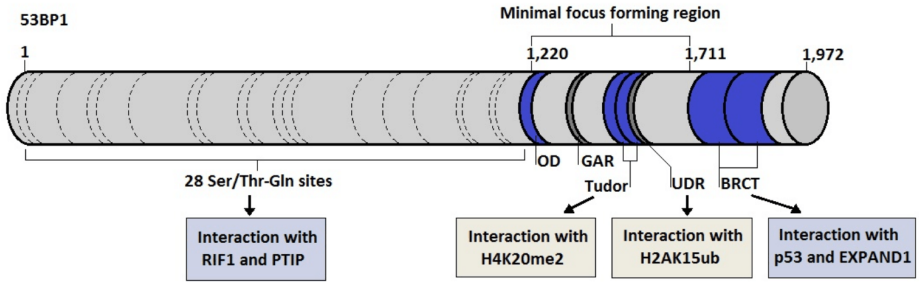

Fig 5.4: Domain structure and interaction partners of 53BP1 (S/T-Q) sites in 53BP1 N terminus are phosphorylated by ATM and promote the binding of its effectors RIF1 and PTIP. The C terminus contains tandem BRCT (BRCA1carboxy-terminal) domains that bind to p53 and EXPAND1. The minimal focus-forming region in 53BP1 contains an oligomerization domain (OD), a Gly- and Arg-rich (GAR) motif, a tandem Tudor motif that binds to dimethylated Lys20 of histone 4 (H4K20me2) and a ubiquitin damage response domain (UDR) motif that interacts with ubiquitylated H2AK15 (H2AK15ub) (Adopted from Panier et Boulton, 2014).

Based on the two affore mentioned histone marks recognized by 53BP1, there are also two proposed models of its attachment to sites of DSBs, both requiring the activity of RNF168 (Figure 5.5.).

Following formation of a DSB, the sequential action of ub conjugating enzyme-UBC13 and E3 ubiquitin ligase RNF8 activates the apical E3 RNF168 which catalyses K63

ubiquitylation of H2AK15, the crucial recognition histone binding motif of 53BP1 (Fradet-Turcotte et al., 2013) (Figure 5.5b).

However, the K48 ub chains have been also shown to play essential role in the second mode of 53BP1 recruitment to DSB flanking chromatin. In non-stressed cells, the H4K20me2 histone mark recognized by the 53BP1-TUDOR domains is occupied by several other proteins including the JMJD2A (JuMonJi Domain 2 protein A) and L3MBTL1 (Lethal (3)malignant brain tumor-like protein 1) demethylases (Figure 5.5.a). Presence of DNA damage triggers RNF8-RNF168 mediated K48-ubiquitylation and directs the two demethylases proteins to proteasome degradation, thus exposing H4K20me2 to be recognized by 53BP1 (Mallette and Richard, 2012).

The most recent proposed model describes the cooperation of both 53BP1 histone modification recognition motifs playing role in its proper positioning at DSB sites. The engagement of H4K20me2 by the Tudor domain was shown to be important for the correct orientation of the UDR in contacting the epitope formed by H2AK15ub. Therefore the current understanding of 53BP1 DSB-nucleosome binding status is described to be minimally a dimeric structure (Fradet-Turcotte et al., 2013) (Figur 5.5.c). In addition, the most recent structural studies of a dimerized 53BP1 revealed that recognition of H4K20me2 and H2AK15ub further involves intimate contacts with multiple nucleosomal elements including the acidic patch, producing highly specific chromatin binding of 53BP1(Wilson et al., 2016).

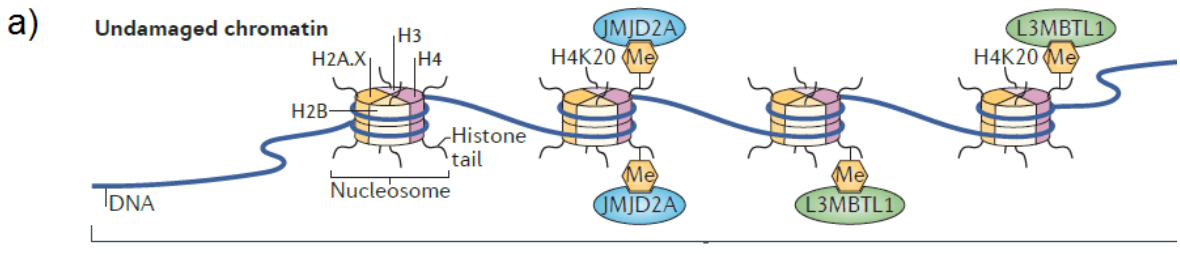

Figure 5.5continues on the next page

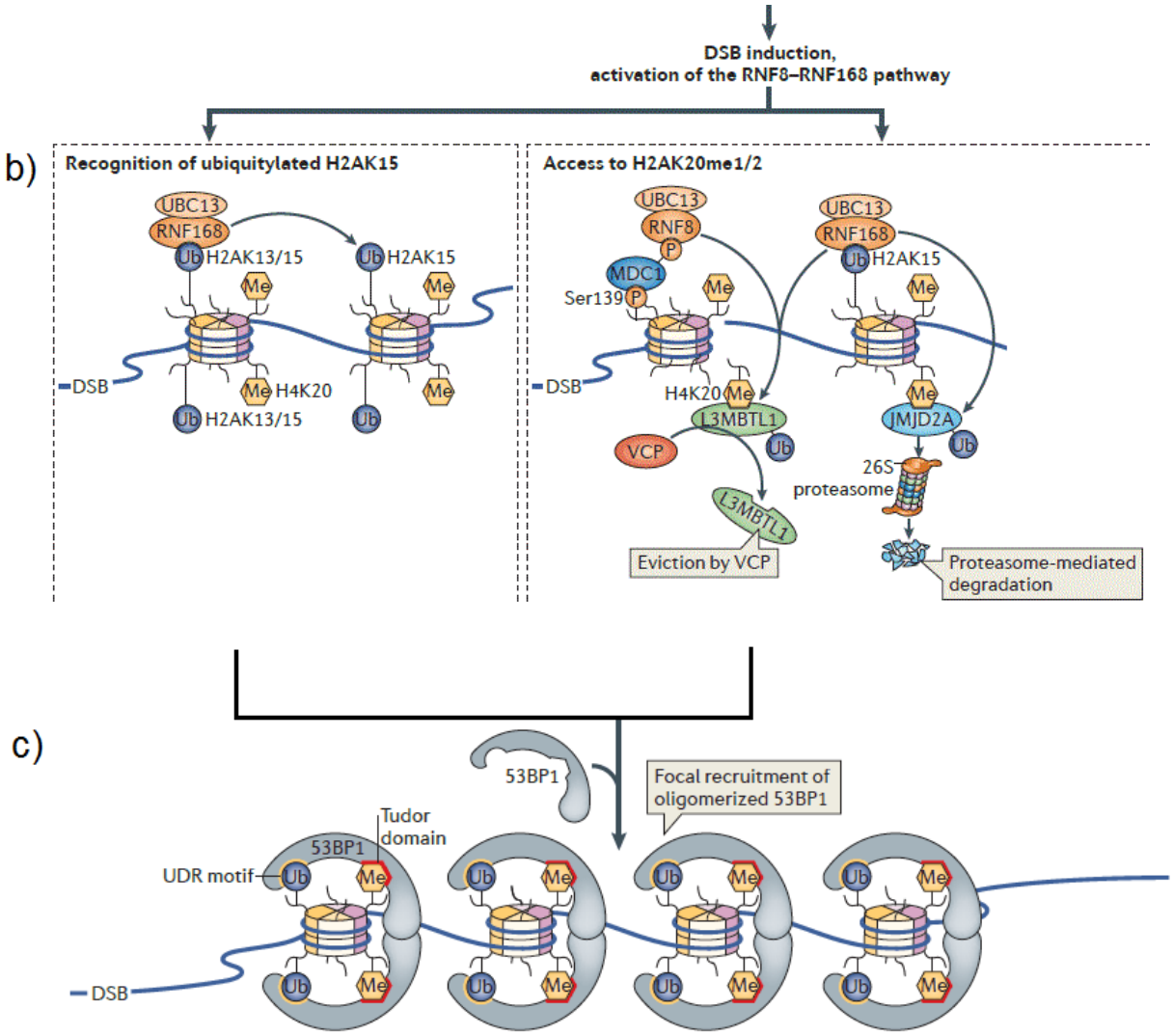

Figure 5.5: Model of 53BP1 recruitment to DSBs on damaged chromatin

a) Histone demethylases- L3MBTL1 and JMJD2A are bound to H4K20me2 in the absence of DNA damage.

b) After DSB formation the focal recruitment of 53BP1 relies on RNF168 mediated ubiquitylation of H2AK15 and increased access of 53BP1 to H4K20me2. E3s RNF8 and RNF168 promote the ub-dependent eviction of L3MBTL1 and JMJD2A from chromatin, by VCP segregase and proteasome.

c) 53BP1 binds minimally as a dimer, selectively to nucleosomes that are both ubiquitylated at H2AK15 and methylated at H4K20.

(Panier and Boulton, 2014).

Given the critical role of ubiquitylation in coordinating the accuracy of DSB response, there also needs to be a tight regulation of the process. Recent studies provided evidence on the crucial importance of homeostasis in the ubiquitin-controlled events after DNA breakage, which can be subverted during tumorigenesis (Gudjonsson et al., 2012). An uncontrolled

amplification of chromatin ubiquitylation driven by RNF168 may have deleterious consequences on genome stability resulting from massive spreading of ubiquitin conjugates. Excessive histone ubiquitylation may result in the hyperaccumulation of ubiquitin-regulated genome caretakers such as 53BP1 and BRCA1, affecting the balance and fidelity of DSB response pathways (Gudjonsson et al., 2012).

Two E3 ligases- TRIP12 and UBR5 were reported to monitor and negatively regulate RNF168 abundance, thus guard against improper RNF168 ub signaling on chromatin (Gudjonsson et al., 2012). Furthermore, a number of specific deubiqutylating enzymes (DUBs) have been linked to reversing RNF8/RNF168-mediated chromatin ubiquitylation to regulate the stringency of DNA damage signaling (Mosbech et al., 2013; Nakada et al., 2010).

Similar observations were made by Zong and colleagues who showed that the supraphysiological level of the E3 ubiquitin ligase RNF168 results in the expanded 53BP1spreading and accelerated DSB repair by error-prone NHEJ proceeding even during the S phas (Zong et al., 2015). As mentioned above, BRCA1-deficiency confers exquisite chemosensitivity towards chemotherapeutic agents that damage DNA in S-phase cells, such as poly(ADP-ribose) polymerase inhibitor (PARPi). Based on this fact, Zong and colleagues suggested a model in which the heterogeneity in the RNF168/53BP1 expression level found in human tumors promotes the genome instability and alters chemosensitivity of BRCA1 deficient cells to PARPi (Zong et al., 2015).

Another unique property of RNF168 to selective regulate 53BP1 activity on DSB surrounding areas was described by team of R. Hakem (Bohgaki et al., 2013). They have shown that RNF168 directly interacts with 53BP1 and promotes its K63 polyubiquitylation, reported to be critical for initial recruitment of 53BP1 to DSB sites and its function in DDR and genomic stability.

Altogether, current model describes E3 RNF168 as a key upstream multistep regulator of 53BP1, controlling its initial recruitment and retention on the DSB flanking chromatin thereby ensuring the proper NHEJ progression during the cell cycle (Fradet-Turcotte et al., 2013).

BRCA1 localization at sites of DNA double-strand breaks

BRCA1 is a large phosphoprotein that contains tandem BRCT domains in its C-terminal region that recognizes phosphorylated proteins that are primarily involved in the DNA damage response, such as Abraxas or CtIP (Figure 5.6) (Callebaut and Mornon, 1997). It also harbors an N-terminal RING domain which mediates specific interaction with the structurally related protein BARD1, forming a stable heterodimer with ubiquitin ligase activity (Brzovic et al., 2003). Their interaction is inhibited by BRCA1-associated protein 1 (BAP1) (Miki et al., 1994; Wu et al., 1996). The BRCA1 Coiled-coil domain was found to be recognized by the PALB2 and BRCA2 factors, both essential components of homologous recombination mediated DNA repair (Figure 5.6) (Xia et al., 2007).

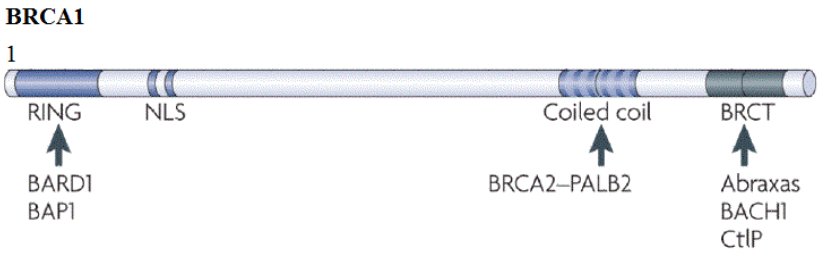

Figure 5.6: BRCA1 domain organization and interaction partners (Adopted from Huen et al. 2010)

BRCA1 is a part of two distinct multi-protein complexes with opposing roles in two different DSB repair pathways. These BRCA1-containing complexes can differentially affect HR in a manner dependent on DNA damage-induced ubiquitylation by RNF8/RNF168 K63 ubiquitin chains on chromatin (Kolas et al., 2007; Mailand et al., 2007).

Strikingly, while the BRCC complex consisting of BRCA1-PALB2-BRCA2-RAD51 promotes HR, the BRCA1-A complex containing BRCA1-Abraxas-RAP80-MERIT40 functionally antagonizes this repair process either by inhibiting DNA end resection or by sequestering BRCA1 away from HR sites by binding to RNF8/RNF168 ubiquitylated chromatin (Coleman and Greenberg, 2011; Hu et al., 2011; Kakarougkas et al., 2013; Kim et al., 2007; Sobhian et al., 2007; Wang and Elledge, 2007; Wang et al., 2007). It is supposed, that in the course of IR inflicted DDR, RAP80 complexes suppress the premature and prolonged localization of BRCA1 at IRIFs, without affecting the cell cycle progression (Hu et al., 2011)

Association of BRCA1 with ubiquitin conjugates through RAP80 is also known to inhibit the HR by BRCA1 removal from DSB flanking chromatin, thus performing BRCA1-HR tuning function (Hu et al., 2011). Typas and colleagues recently proposed a model for RNF168-dependent regulation of HR (Figure 5.7): RNF168-induced ubiquitin conjugates recognized by RAP80 involved in BRCA1-A complex spread away into more distal chromatin regions, sequestering BRCA1 from the ssDNA and inhibiting the HR (Typas et al., 2016). They identified two deubiquitylating enzymes USP26 and USP37 removing RNF168-induced ubiquitin conjugates distal from DSBs, thus preventing the ubiquitin-dependent sequestration of BRCA1 through the BRCA1-A complex, while promoting the association and cooperation of BRCA1 with the BRCC complex during HR (Typas et al., 2016).

In line with this model, supraphysiological level of RNF168 triggers extensive ubiquitylation of H2A accompanied by reduction of HR efficiency (Typas et al., 2016).

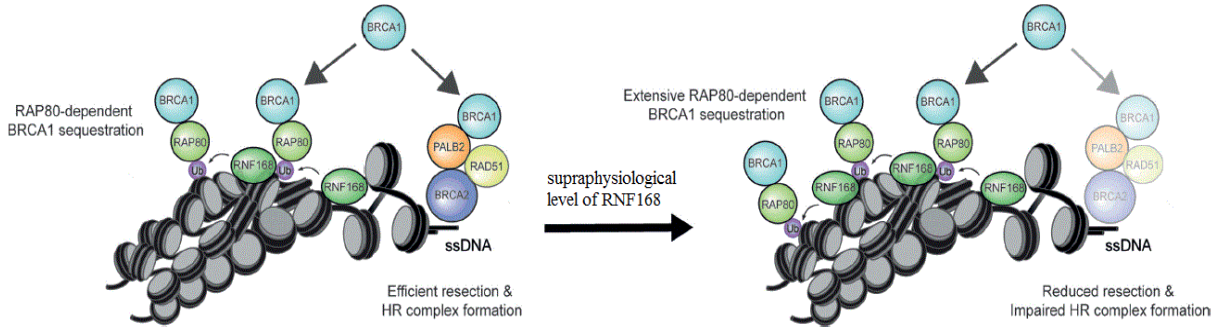

Figure 5.7: Possible molecular role of RNF168 in regulation of BRCA1 recruitment to DSB and HR.
RNF168 sequesters BRCA1 away from chromatin, thereby preventing its function with PALB2-BRCA2-RAD51 in HR. Additionally, the more extensive spreading of RAP80 reduces DNA-end resection, which also has a negative impact on HR (Modified from Typas et al., 2016).

Hereditary BRCA1 mutations confer a high risk of breast and ovarian cancer, that is characterized by excessive genome instability. Studies support the idea that BRCA1 exerts its tumor suppression function primarily through its involvement in cell cycle checkpoint control and DNA damage repair, including regulation of replication fork stability, DNA cross-link repair and DNA double-strand break repair (Jiang and Greenberg, 2015; Long and Walter, 2012; Schlacher et al., 2012). Therefore, in the absence of functional BRCA1, DNA lesions occurring in S-phase that are normally repaired by error-free HR are instead directed into mutagenic NHEJ triggered by 53BP1. The result of this abnormal repair pathway choice under

such conditions results in accumulation of chromosomal aberrations and lastly to heightened sensitivity to PARPi (Zong et al., 2015). However, the combined BRCA1/53BP1 deficiency rescues HR, resulting in resistance to PARPi (Bunting et al., 2010; Farmer et al., 2005; Shen et al., 1998). Recently, Ochs and colleagues explained that such cells can repair DSBs at the cost of increasing reliance on RAD52-mediated HR, which may trigger genome instability (Ochs et al., 2016). Based on these findings, they proposed a model in which 53BP1 play an unexpected role in fostering the HR fidelity, rather than suppressing DNA end resection when challenging DSBs (Ochs et al., 2016).

Therefore, further studies getting deeper insight into the complex relationship between 53BP1 and BRCA1as well as complete knowledge about mechanisms behind the DSB repair pathway choice could be later exploited for clinical purposes to enhance PARPi-based therapy.

6 LINK BETWEEN THE UBIQUITIN-PROTEASOME SYSTEM AND THE DNA DAMAGE RESPONSE

The ubiquitin proteasome system (UPS) is the major cellular housekeeping mechanism eliminating mutant, misfolded, and damaged proteins which are then degraded in the cytoplasm and nucleus of eukaryotic cells. Proteins destined to be degraded by the UPS are modified by ubiquitin chain which are recognized by ubiquitin receptors in the 26S proteasome complex (Hershko and Ciechanover, 1998).

Proteasome is a large (2.5 megadalton) multisubunit proteolytic complex that consists (Finley, 2009) of two major components: the core particle (also known as the 20S subunit) and the regulatory particle (also known as the 19S subunit) (Figure 6.1). All Ub chain types irrespective of conformation can be bound by the regulatory 19S particle where they are recognized simultaneously by the high affinity Ub receptors PSMD4 and ADRM1, and the PSMC3 subunit that binds ubiquitin with lower affinity than the two aforementioned proteins (Peth et al., 2009). Following the ubiquitin binding, the proteasome associated deubiquitinating enzymes (DUBs), mainly the ubiquitin specific protease (USP)14 mediates opening of the narrow pore formed by the 19S alfa-rings to allow entry of the substrate into

the 20S proteolytic core where the three proteolytic activities - chymotryptic-, tryptic- and caspase-like reside (Peth et al., 2009, 2010). K63-linked Ub-substrates are rescued from degradation by removal of ub moieties by proteasomal DUBs prior to their recognition in 19S (Cooper et al., 2009; Johnson et al., 1995; Matilla et al., 2001) while the most abundant chains, linked by K48, plus those linked by K11 and K29 and possible other chains, act as signal for degradation (Xu et al., 2009).

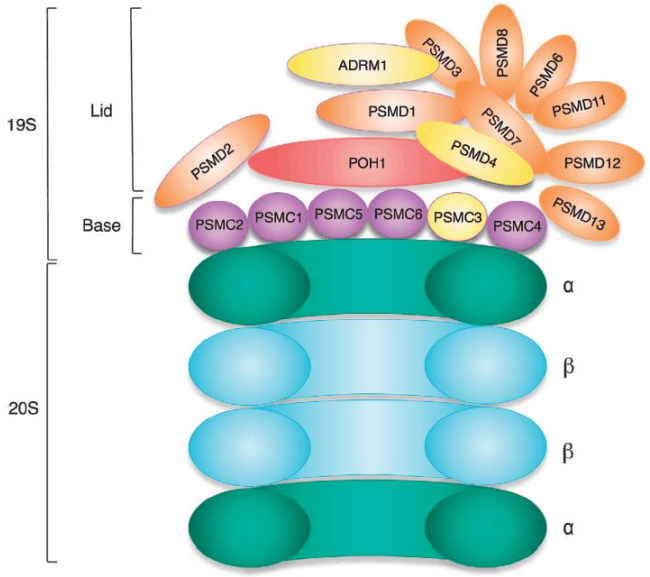

Figure 6.1: Schematic 2D representation of the proteasome.
The 20S core consists of two b-rings (blue) flanked by two a-rings (turquoise). The 19S lid is split into two subcomplexes; the base contains six AAA+ ATPases; PSMC1,2,4,5,6 (purple) and proteasome (prosome, macropain) 26S subunit, ATPase 3 (PSMC3; yellow). The lid comprises PSMD1, PSMD2, PSMD3, PSMD4, PSMD6, PSMD7, PSMD8, PSMD11, PSMD12, PSMD13, PSMD14/POH1 and ADRM1subunits. POH1 (red) is a JAMM-type DUB, which removes chains 'en block' from substrates committed for degradation (adopted from Stone et Morris, 2013).

Recent reports show that the sites of DSBs in mammalian cells are selectively enriched in the proteasome complex. This part of my work will address 3 possible mechanisms of proteasome involvement in DSB repair:

1. as a functional component of DNA repair mechanism itself

2. as a deubiquitinase that antagonizes the chromatin ubiquitylation resulting from DSB signaling

3. as a major regulator component indirectly coordinating ub-dependent recruitment of DSB effector proteins

Altogether, findings of various research groups show, that proteasome is functionally more versatile as previously thought which might be exploited in the design of novel therapeutic targets for cancer treatment as will be described later.

6.1 PROTEASOME AS FUNCTIONAL COMPONENT OF DNA REPAIR PROCESS

Direct role of the proteasome at sites of DNA damage

1. The first indications that proteasome has a functional role in DSB repair was came from yeast. Krogan and colleagues discovered that a small acidic 19S proteasome subunit protein DSS1/sem1 9deleted in split-hand/split foot 1) is recruited to sites of damage and required for DSB repair (Krogan et al., 2004). DSS1 was also found to promote HR in mammals where it interacts with BRCA2 and induces BRCA2-mediated RAD51 displacement of RPA-ssDNA (Kojic et al., 2005; Kristensen et al., 2010; Liu et al., 2010; Zhou et al., 2007) (Figure 6.2). Moreover, formation of DSS1 foci after IR-induced DSBs is dependent on 19S proteasomal activator POH1 suggesting a functional role of proteasome in DDR (Butler et al., 2012).

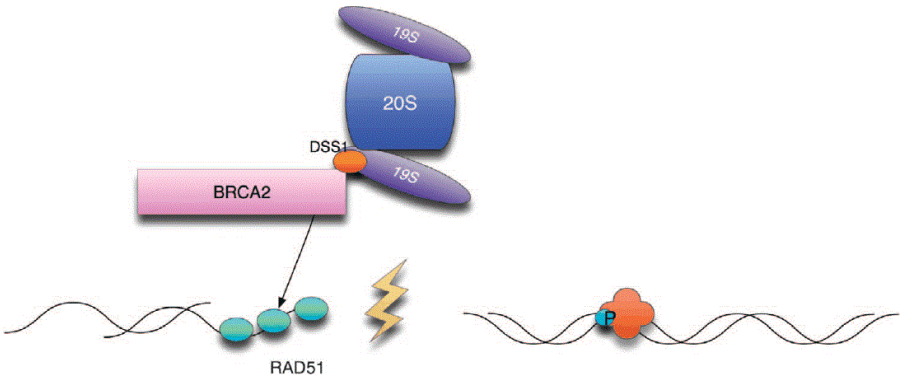

Figure 6.2: The proteasome as a component of the DDR
The proteasome promotes the enrichment of DSS1, a co-factor of BRCA2 and promotes RAD51 loading and homologous recombination (Adopted from Stone and Morris, 2013)

2. A second direct role of proteasome emerged when a role for the 19S JAMM-type deubiquitylating enzyme POH1 in the restriction of DNA damage-associated Ub conjugates (Butler et al., 2012) was described. POH1 is important in the two main pathways employed to repair of DSBs. In NHEJ, it acts to restrain 53BP1 accumulation through counteracting both

RNF8/168 K63-driven ubiquitylation and JMJD2A chromatin eviction (Figure 6.3). In HR repair, POH1 acts independently of its influence on 53BP1 and promotes RAD51 loading through regulation of DSS1 enrichment at sites of damage (Butler et al., 2012). The exogenous DSS1 expression in POH1-depleted cells was reported to restore both the RAD51 foci and HR repair, confirming the major role of donwnstream associated protein DSS1 in initial steps of HR (Butler et al., 2012).

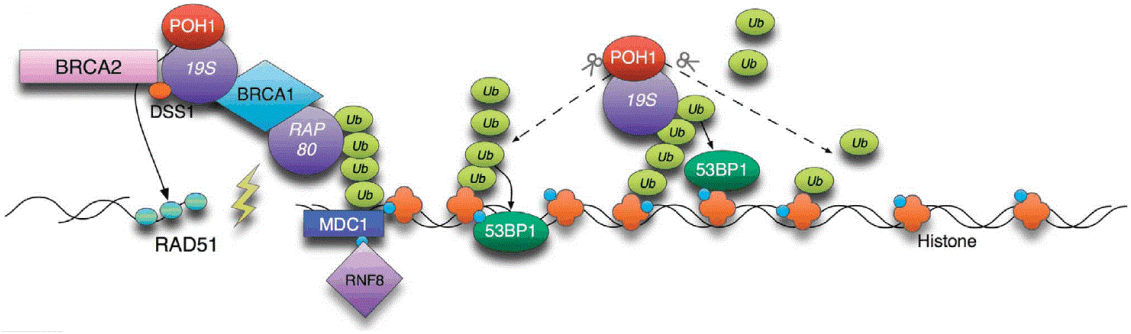

Figure 6.3: Model of POH1 function in DSB response.
POH1-mediated promotion of RAD51 loading: The 19S interacts with BRCA1 and BRCA2 at sites of DNA damage and POH1 promotes DSS1 enrichment and the loading of RAD51. POH1 also counters the K63-poly-Ub on chromatin to further restrict 53BP1 accumulation on chromatin (Adopted from Butler et al., 2012).

In addition to direct roles of proteasome components in DDR, the majority of cellular proteins acting in the response to DSBs are turned over by proteasome degradation triggered by K48 protein ubiquitylation.

However, there is one more significant mechanism involving the removal of K48 Ub-modified proteins by the AAA+ type ATPase Valosin containing protein (VCP/p97/Cdc480) in connection to DNA repair (Figure 6.4). VCP is recruited to poly-Ub modified proteins by recognition of K48-linked chains and promotes the extraction of ubiquitylated proteins from complexes and eviction of proteins from chromatin (Franz et al., 2011; Raman et al., 2011). Some studies show that VCP hands substrates over to a shuttling factor before being delivered to the proteasome (Richly et al., 2005) while others suggest that VCP is required for substrate unfolding at the proteasome (Verma et al., 2011). Surprisingly, VCP was shown to be directly involved in process of DNA repair. After its localization to sites of DNA damage in an RNF8

dependent manner, VCP removes K48-Ub protein conjugates from sites of DNA damage to orchestrate proper association of 53BP1, BRCA1 and RAD51 components with damaged chromatin (Meerang et al., 2011). The best described role of VCP is illustrated in the dynamic assembly of 53BP1 linked to efficient repair of DSBs. VCP was reported to act in parallel to the canonical RNF168-53BP1 pathway, promoting extraction of L3MBTL1-competitor of 53BP1 for binding to H4K20me2, therefore being crucial component of NHEJ repair pathway (Acs et al., 2011)

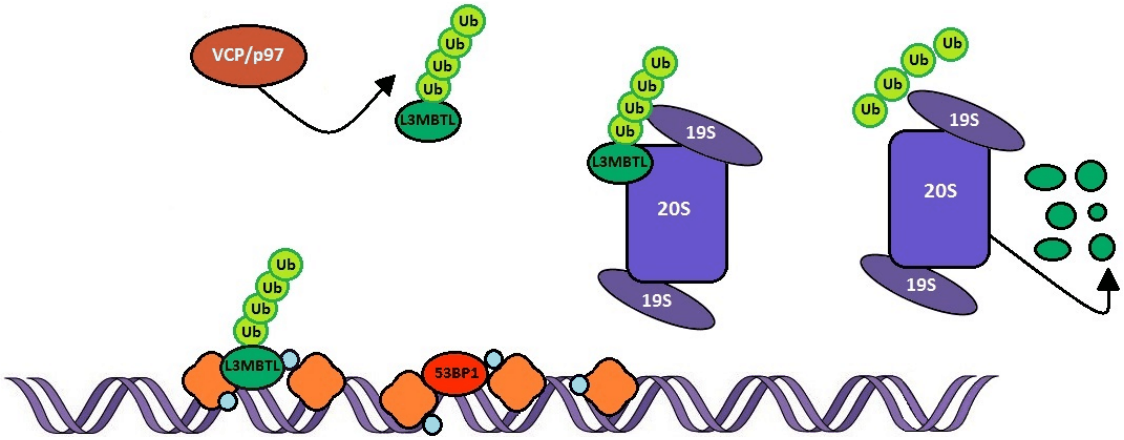

Figure 6.4: Degradation of proteins evicted from chromatin. Proteins such as L3MBTL1, JMJD2A are evicted from chromatin following Ub modification, this may require VCP/p97, and lead to subsequent proteasome mediated degradation (Adopted from Stone and Morris, 2013)

3. Indirect role of proteasome in response to DSBs

The proteasome is required, indirectly, for Ub signaling in the DDR. Treatment with proteasome core inhibitors, such as MG132 or Bortezomib, before or shortly after induction of DNA damage, results in failure of the damage response to progress. This is most likely due to the inability of DNA repair ligases to attach Ub moiety to their targets under condition of Ub starvation brought about by acute proteasome inhibition (Figure 6.5) (Acs et al., 2011; Dantuma et al., 2006; Mailand et al., 2007; Meerang et al., 2011). Under these conditions the Ub-independent recruitment of DDR proteins (e.g MDC1) is sustained, while BRCA1 and 53BP1 do not recruit and both non-homologous end joining and homologous recombination repair mechanisms are attenuated (Dantuma et al., 2006; Gudmundsdottir et al., 2007; Jacquemont and Taniguchi, 2007; Meerang et al., 2011; Murakawa et al., 2007; Shi et al.,

2008). Moreover, depletion of both 20S and 19S subunits was found to increase genomic instability and reduce RAD51 loading in mammalian cells,underlining the importance of functional proteasome components in recruitment of DDR proteins to DNA damage sites (Ben-Aroya et al., 2010; Jacquemont and Taniguchi, 2007).

This suggests a critical role of proteasome, particularly its intrinsic recycling capacity for Ub, to be necessary for further ubiquitin-dependent processes and proper DSB repair progression.

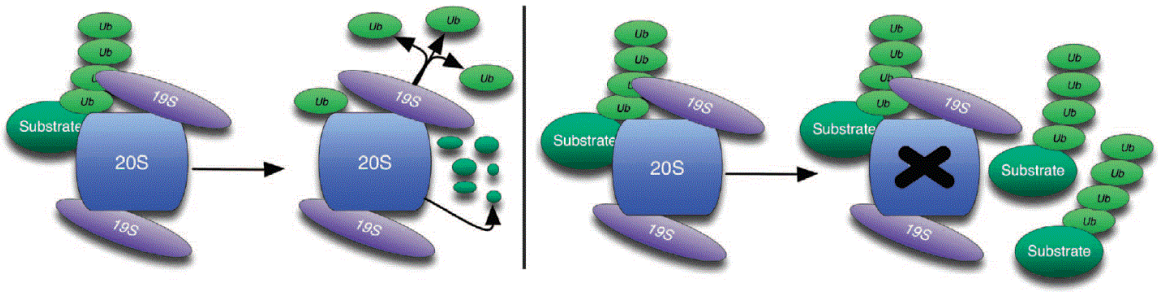

Figure 6.5: Indirect role of proteasome in response to DSBs
The proteasome has an indirect role on the DDR. Protein degradation is coupled to release of Ub monomers, replenishing the free Ub pool (left-hand panel). Upon acute proteasome inhibition Ub is captured in high molecular weight conjugates (right-hand panel), without compensation by increased Ub transcription. As a consequence the free pool is diminished and induced Ub conjugation events prevented (adopted from Stone et Morris, 2013).

6.2 THE USE OF PROTEASOME INHIBITORS IN CANCER TREATMENT

Several lines of evidence suggest that cancer cells have a heightened dependency on mechanisms of protein homeostasis (proteostasis) (Balch et al., 2008), including the ubiquitin proteasome system. Cancer cells are typically carriers of dozens to hundreds of point mutations in protein coding sequences (Vogelstein et al., 2013) giving rise to mutant proteins with increased degradation rate via the UPS (Figure 6.7). In addition, cancer cells genomes often contain large deletions, duplications, inversions, and translocations as well as altered copy of entire chromosomes (aneuploidy). The excess chromosomes continues to be expressed, and therefore protein synthesis in aneuploid cancer cells is often imbalanced, with increased protein production by extra chromosomes compared to carriers having physiologically normal two copies of each chromosome (Torres et al., 2010; Williams et al., 2008). This creates a problem mainly in the case of proteins that assemble to form

stoichiometric complexes such as the ribosome. In such cases, the excess proteins cannot achieve a stable conformation and therefore are degraded by proteasome (Dephoure et al., 2014; Warner et al., 1985). Such a dysregulated hyperaccumulation of modified cancer-related unfolded, misfolded or dysfunctional proteins may then result in proteasome overload reported as cell status called proteotoxic stress (Figure 6.6).

In theory, this make cancer cells to be more dependent on protein quality control of UPS (Guo et al., 2013; Luo et al., 2009; Whitesell and Lindquist, 2005; Williams and Amon, 2009), suggesting them to be more sensitive to proteasome inhibitors in comparison to normal cells. The best known example of the intrinsic proteotoxic stress, being linked to higher cancer cell sensitivity to proteasome inhibition, is described by blood cell malignancy called Multiple myeloma. Tumor myeloma cells originate from malignant transformation of B cells and due to their physiological role in production of large quantity of antibodies these cells are supposed to have increased level of endogenous proteotoxic stress (Leung-Hagesteijn et al., 2013; Meister et al., 2007) and lower threshold for induction of lethal unfolded protein response (Obeng et al., 2006).

Importantly, the inhibition of proteasome results in the abnormal accumulation of ubiquitylated or misfolded intracellular proteins leading to cell condition called exogenous or induced “proteotoxic stress”, being even more pronounced under cancer related conditions.
The presence of persistent proteotoxic stress, as in the case of proteasome inhibition, then leads to signaling of cell cycle arrest and activation of pro-apoptotic signaling, what are the major causes of cell death (Balch et al., 2008).

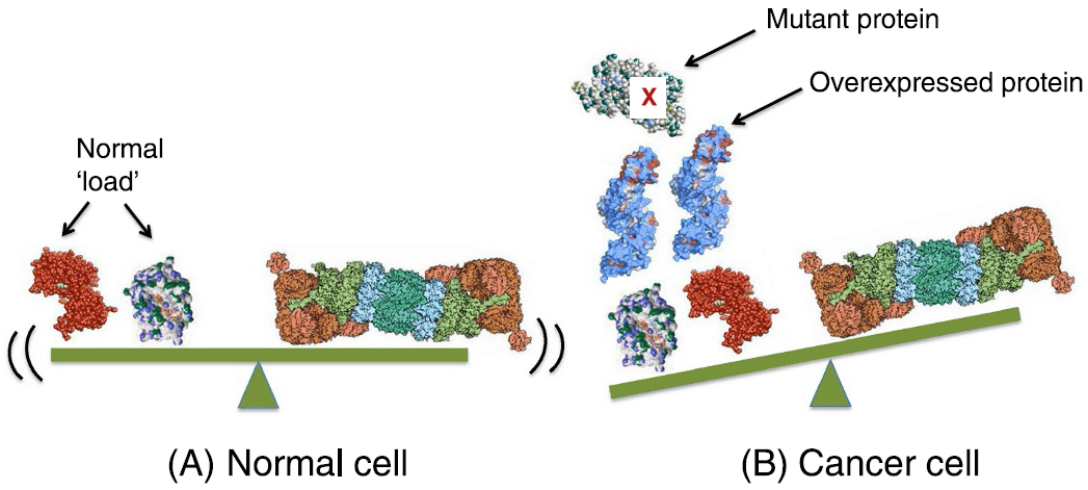

Figure 6.6: Protetoxic stress in cancer cells. (adopted from Deshaies, 2014)
(A) In normal cells, the natural load of degradation substrates on the left is in balance with the capacity of the cellular ubiquitin-proteasome system (UPS), signified by the proteasome on the right.
(B) In cancer cells, the load is increased due to expression of mutant proteins and/or expression of excess proteins due to aneuploidy. This results in an imbalance where the degradation load exceeds the capacity of the UPS.

6.2.1 Bortezomib- the first proteasome inhibitor used in therapy of cancer

Bortezomib (Velcade, formerly known as PS-341) was the first selective, reversible inhibitor of the 26S proteasome approved by FDA (Food and Drug Administration) for treatment of blood malignancies- multiple myeloma (Kane et al., 2006) , later expanded for treatment of mantle cell lymphoma (Kane et al., 2007). Bortezomib is modified dipeptidyl boronic acid, specifically inhibiting chymotrypsin-like active site of β5 subunit, which is sufficient to inhibit the proteolytic actvity of the proteasome complex (Chen et al., 2011).

Multiple myeloma described as a malignant B-cell tumour is second most common haematological cancer (after non-Hodkin`s lymphoma). Based on in vitro studies, myeloma cells are up to 1000 fold more sensitive to bortezomib-induced apoptosis than normal plasma cells (Hideshima et al., 2001). Initially, it seemed that a key factor in this differential response is the ability of proteasome inhibitor to block the activation of the prosurvival transcription factor NF-κB. Multiple myeloma cells are known to constitutively express this factor to transcriptionally regulate antiapoptotic factors, inflammatory molecules, cell adhesion molecules and cytokines, which altogether promote the growth of myeloma cells (Barnes and Karin, 1997). Proteasome inhibitors block the degradation of the NF-κB inhibitor-IκB by proteasome, thereby inhibiting inducible NF-κB activity (Palombella et al., 1994). However, recent findings favours an alternative cause of the increased multiple myeloma cells sensitivity to bortezomib. This second explanation for the enhanced bortezomib sensitivity is most probably linked to lower threshold of multiple myeloma plasmatic cells for induction of a lethal dose of unfolded proteins triggering apoptosis (Obeng et al., 2006).

Although, the proteasome has a number of cellular roles, recent findings describing its direct and indirect involvement in DDR, makes it a good target, for combined anticancer therapy with DNA damaging agents. Bortezomib has been combined with doxorubicin, thalidomide, melphalan, dexamethasone, and lenalidomide, and has generally been

successfully combined with other agents without increased toxicity. There are currently over 200 active clinical trials involving bortezomib, the majority of which are investigating novel combination therapy for haematological malignancies, particularly multiple myeloma and lymphoma (www.clinicaltrials.gov).

As mentioned above, recent research highlighted a role for the UPS in regulating repair of the most deleterious DNA lesion-DNA double-strand breaks (reviewed in Montegi et al., 2009). Proteasome inhibitors impact two major DSB repair pathways through the depletion of available nuclear ubiquitin resulting in an accumulation of nondegraded polyubiquitylated proteins. This depletion of free ubiquitin results in a loss of monoubiquitylated histones in the nucleus and consequently impairs the activity of mentioned DSB repair pathways effectors-tumorsupressors-53BP1 and BRCA1.

Therefore, further research will be instrumental for understanding of how cancer cells tolerate the impact of proteotoxic stress and associated ubiquitin shortage in terms of DNA damage repair and signaling. Importantly, further research efforts may reveal mechanisms of cancer cells resistance to bortezomib treatment suggest new possible alternative therapies for non-responsive malignancies.

In the presented experimental study, we have identified MDA-MB-231 breast cancer cell line displaying exceptional phenotype-recruitment of 53BP1 protein to IRIFs under the conditions of proteasome inhibitor (Bortezomib or MG132) induced proteotoxic stress. We show that central to this phenotype is elevated level of the E3 ubiquitin ligase RNF168 that enables more efficient exploitation of the residual free ubiquitin. In addition, we have shown that proteotoxic stress resistant DSB response phenotype is more widespread among cancer cell lines of different origin with upregulated E3 RNF168. Elevated RNF168 levels harbouring cells are more resistant to combined treatment by gamma irradiation and proteasome inhibitor. Moreover, the overabundance of the E3 ligase shifts the balance between NHEJ and HR towards the mutagenic Non-homologous end joining (mutNHEJ), a scenario accompanied by enhanced chromosomal instability/micronuclei formation and sensitivity under replication stress-inducing treatments with camptothecin or poly(ADP-ribose) polymerase (PARP) inhibitor.

As tumors often display heterogeneity in RNF168 expression, upregulation of the RNF168/53BP1 pathway could provide a useful biomarker for assessment of tumor sensitivity to S phase genotoxins- PARP inhibitors and camptothecin.

Following experimental part of my thesis provides a deeper insight into the observed proteotoxic stress resistant DDR phenotype. Data described in chapter of Results explain the mechanism responsible for this phenomenon, its main characteristics shared by different cancer cell lines and eventually direct to potential implications of this cancer feature for clinical practice and targeted cancer therapies.

7 AIMS OF THE THESIS

1. Elucidation of the mechanism responsible for the proteotoxic stress-resistant DSB response phenotype observed in the proteasome inhibitor-treated MDA-MB-231 cell line.
2. Experimental induction and/or detection of the proteotoxic stress resistant DDR in other cancer cell line models; describing the common features.
3. Probe the functional consequences of the phenotype for genomic integrity and overall repair capacity of cancer cells (repair pathway preference, damage accumulation, DDR inhibitor sensitivity)
4. Assess possible benefits/functional significance of the proteotoxic stress resistant DSB in cancer cells of various origin
5. Suggest an alternative model for treatment of proteasome inhibitor resistant tumor malignancies.

8 MATERIALS AND METHODS

List of used antibodies

Antibody	Origin	Clonality	Dilution	Method
γH2AX (Merck Millipore, Billerica, MA, USA)	mouse	monoclonal	1 : 1000	Immunofluorescence
PS139-γH2AX (Cell Signaling)	rabbit	polyclonal	1:300	Laser striping
RNF8 (B-2) (Santa Cruz)	mouse	monoclonal	1:500	Immunobloting
HERC2 (BD Transduction Laboratories)	mouse	monoclonal	1:500	Immunobloting
GAPDH (GT239) (GeneTex)	mouse	monoclonal	1:1000	Immunobloting
REV7 (BD Bioscience)	mouse	monoclonal	1:200	Laser striping
RIF1 (Bethyl Laboratories)	rabbit	polyclonal	1:500	Laser striping
53BP1(-H300) (Santa Cruz Biotechnology)	rabbit	polyclonal	1:500 1:400	Immunofluorescence Laser striping
BRCA1 (Santa Cruz Biotechnology)	rabbit	polyclonal	1:500	Immunofluorescence
TRIP12 (Abcam)	rabbit	polyclonal	1:500	Immunobloting
UBR5 (Sigma Aldrich)	rabbit	polyclonal	1:500	Immunobloting
FK2 (Enzo Life Sciences)	rabbit	polyclonal	1:500	Immunobloting
RNF168 (gift from N. Mailand)	rabbit	polyclonal	1:5000 1:500	Immunobloting Immunofluorescence
RNF169 (gift from N. Mailand)	rabbit	polyclonal	1:1000	Immunobloting
MEK1 (Santa Cruz Biotechnology)	rabbit	polyclonal	1:500	Immunobloting
LAMIN B (Santa Cruz Biotechnology)	goat	polyclonal	1:1000	Immunobloting
MUM1 (Cell signaling)	rabbit	polyclonal	1:1000	Immunobloting

BiP (Abcam)	rabbit	polyclonal	1:500	Immunobloting
CD138-PE (MACS Milenyi Biotec)	mouse	monoclonal	1:11 for up to 10^7 cells in buffer	Flow cytometry analysis

List of used cell lines with applied cell culture media

Cell line	Origin	Growth mode	Cell culture media
MDA-MB-231 ATCC	Human breast adenocarcinoma	adherent	DMEM (high glucose)
MDA-MB-436	Human breast adenocarcinoma	adherent	DMEM (high glucose)
HeLa ATCC	Human cervix carcinoma	adherent	DMEM (high glucose)
BJ	Human fibroblasts-foreskin	adherent	DMEM (high glucose)
U2OS	Human bone osteosarcoma	adherent	DMEM (high glucose)
U2OS RNF168-GFP	Human bone osteosarcoma (RNF168-GFP construct)	adherent	DMEM (high glucose)
MCF7	Human breas adenocarcinoma	adherent	RPMI-1640
MMS1 Gift fromProf. Dr. Christoph Driessen laboratory (Kantonsspital St. Gallen)	Human B lymphoblast-immunoglobulin A lambda myeloma	suspension	RPMI-1640
AMO1 Gift fromProf. Dr. Christoph Driessen laboratory (Kantonsspital St. Gallen)	Human plasma cell myeloma	suspension	RPMI-1640

*if not stated otherwise, cell lines were obtained from the collection of Danish Cancer Society

List of used reagents and chemical compounds

Name	Application
FuGene (Roche)	plasmid transfection
Lipofectamin RNAiMAX (Invitrogene)	siRNA transfection
Polybrene (Sigma Aldrich)	lentiviral cell transduction
ECL detection reagent (Thermo Fisher Scientific)	chemiluminiscence
DAPI containing Vectashield (Vector laboratories)	fluorescent nuclear staining
Whole Blood Column Kit (MACS Miltenyi Biotec)	magnetic separation of blood cells
Whole Blood and bone marrow CD138 microbeads (MACS Milteney Biotec)	magnetic separation of CD138 positive plasma cells
Separation (Running) buffer (MACS Milteneyi Biotec)	magnetic separation
Bortezomib (PS-341) (Sigma Aldrich)	proteasome inhibitor
MG132 (Sigma Aldrich)	proteasome inhibitor
Camptothecin (CPT) (Sigma-Aldrich)	topoisomerase I inhibitor
KU 58948 (AstraZeneca)	PARP1 inhibitor

List of used plasmids

Name	Application
pGFP-53BP1-Fl-wt (gift from D. Durocher's lab)	plasmid transfection
pGFP-53BP1-Fl-L1619A (gift from D. Durocher's lab)	plasmid transfection
pGFP-53BP1-Fl-D1521	lentiviral cell transduction

(Sigma Aldrich)	
pAcGFP-C1-RNF168 C16RING (gift from J.Lukas's lab)	plasmid transfection
pAcGFP-C1-RNF168 C16MIU (gift from J.Lukas's lab)	plasmid transfection
pMD2.G (31476, 31482) (Addgene #12259)	generation of lentiviruses
psPAX2 (12260) (Addgene #12260)	generation of lentiviruses
pCVL SFFV d14GFP EF1s HA.NLS.Sce(opt) (Addgene #31476)	traffic light system
pCVL traffic light reporter 1.1 (Sce target) Ef1a Puro (Addgene #31482)	traffic light system
Tet- pLKO- puro (Addgene #21915)	Inducible expression of shRNA

List of used oligonucleotides

Name	Sequence
shRNA RNF168 sense (Generi Biotech)	CCGGGGCGAAGAGCGATGGAGGACTCGAGTCCTCCATCGCTCTTCGCCTTTTT (5'–3')
shRNA RNF168 antisense (Generi Biotech)	AATTAAAAAGGCGAAGAGCGATGGAGGACTCGAGTCCTCCATCGCTCTTCGCC (5'–3')
53BP1 DD2013 (MWG Operon)	GAGAGCAGAUGAUCCUUUAtt (5'–3')
RNF168qPCR_F1 (Generi Biotech)	CAGGGCAAGACACAGAAATAGA (5'–3')
RNF168qPCR_R1 (Generi Biotech)	GGCAC CACAGGCACATAA (5'–3')
RNF168qPCR_F2 (Generi Biotech)	CTCCCTACAGCCTAGCATTTC (5'–3')
RNF168 qPCR_R2	AGATCACAAAGCACTCCCTTTA (5'–3')

(Generi Biotech)	
GAPDH-F (Generi Biotech)	GAAGATGGTGATGGGATTTC (5'–3')
GAPDH-R (Generi Biotech)	GAAGGTGAAGGTCGGAGT (5'–3')

List of used siRNAs

Name	Company
siRNA #1 Negative control (ID#4390843)	Thermo Fisher Scientific
siRNF168 (#126171)	Thermo Fisher Scientific
siRNF8 (#17200)	Thermo Fisher Scientific
siUBC13	Santa Cruz Biotechnology
siJMJD2A	Thermo Fisher Scientific
siTRIP12	Thermo Fisher Scientific
siUBR5	Thermo Fisher Scientific

List of used machines and lab equipment

Name	Method
Xylon Smart160E/1.5 device	gamma irradiation of cells
Zeis Axio Observer.Z1 inverted microscope combined with LSM 780 confocal module	confocal microscopy
Nano Light Cycler (Roche)	qPCR
Chemi-Doc-Systém (Bio-Rad)	Chemiluminiscence detection
Vi-Cell XR Cell viability analyzer	cell number analyses
Influx (BD Biosciences) instrument	FACS/flow cytometry analysis

FACS verse instrument	flow cytometry analysis
MACS separator	magnetic cell sorting

8.1 CELL CULTURE AND GENERATION OF DSBs

Most cell lines used in this work were cultured in Dulbecco's modified Eagle's medium and RPMI-1640 supplemented with 10% fetal bovine serum (PAA, Pasching, Austria) and penicillin/streptomycin (Sigma-Aldrich) in a humidified atmosphere of 5% CO2 at 37 °C. X-ray irradiation was done using the YXLON.SMART 160E/1.5 device (YXLON, Horsens, Denmark) at the following settings: 150 kV, 6 mA, 11 mGy/s.

8.2 MICROIRRADIATION

Cells were grown on plastic discs (17mm diameter) that were cut using CNC cutter from the bottom of standard 10-cm cultivation dish (TPP) sterilized by UV and placed inside the wells of a 12-well plate. Next day, BrDU (0.5 mM final concentration) was added into each well to pre-sensitize the cells towards UV-A wavelength. Twenty-four hours after BrdU addition, cells were either treated for 2 hours with 5 μM MG132 or mock treated (0,5% DMSO). Subsequently, the plastic discs with cells were removed, covered by a coverslip and immediately placed inside Zeiss AxioObserver Z.1inverted microscope combined with LSM 780 confocal module. Cells were irradiated at 20 °C via 340 water immersion objective (ZeissC-Apo 403/1.2WDICIII), using 355nm 65mW laser set on 100% power. The total laser dose that could be further manipulated by the amount of irradiation cycles was empirically set to six cycles. Laser track was pre-defined to cover all the cells within the acquisition area with at least one stripe across the nucleus. After the irradiation process the coverslip was gently removed and plastic disk was quickly placed back into the same well of the 12-well plate and incubated for another 45 min at standard cultivation conditions. The plastic disks with laser-irradiated cells were first processed for immunofluorescent staining at 4 °C. Cells were washed by PBS (4 °C), equilibrated for 2 min in sucrose buffer 1 (10mM PIPES, pH 6.8, 100mM NaCl, 1.5mM MgCl2 and 300mM sucrose) on ice and then pre-extracted for 15 min

on ice, on slow moving shaker using sucrose buffer 2 (10mMPIPES, pH6.8, 100mMNaCl, 1.5mM MgCl2, 300mM sucrose, 0.5% Triton X-100, 1mM dithiothreitol (DTT) supplemented with protease inhibitor. After the pre-extraction cells were washed by PBS (4 °C) and fixed by 4% paraformaldehyde (PFA) for 15 min at room temperature. PFA was washed out three times by PBS. The disks were further processed as standard coverslips (that is, blocking in blocking solution (DMEM plus 20% FBS) for 1 h followed by incubation with primary antibodies involving REV7, RIF1, pS139- H2AX and 53BP1 for 1 h at room temperature, and with appropriate secondary antibodies coupled to Alexa Fluor 488 and Alexa Flour 568 fluorophores. Both primary and secondary antibodies were dissolved in the blocking solution. After washes in PBS, the disks were incubated in 1 μgml-1 DAPI in dH2O at room temperature for 5 min and air dried. Dried disks were placed on a standard microscopy glass (cell layer face up) and anchored by two rubber bands laced over the glass. Stained cells were mounted using Vecta Shield (Vector Labs) mounting medium and covered by a coverslip. The samples were examined using Zeiss Axio-Observer Z.1 inverted microscope combined with LSM 780 confocal module using 340 oil objective (Zeiss EC PlnN 403/1.3 Oil DICII).

8.3 PLASMID AND SiRNA TRANSFECTION

Most plasmids were transfected using the FuGENE 6 reagent following the manufacturer's instructions. When required, plasmid DNA was transfected by nucleofection using the Neon (Life Technologies) device at settings recommended by the manufacturer for the respective cell line. The pGFP-53BP1-Fl-wt, pGFP-53BP1-Fl-L1619A and pGFP-53BP1-Fl-D1521 plasmids carrying the 53BP1 UDR and Tudor domains mutations were a gift from D Durocher (Samuel Lunenfeld Research Institute, Ontario, Canada). The pAcGFP-C1-RNF168 plasmids harboring the C16S RING and MIU mutations were described previously (Doil et al., 2009). The Traffic light repair template, the I-SceI lentiviral constructs (Certo et al., 2011 38) as well as the lentivirus production plasmids pMD2.G and psPAX2 (D Trono, unpublished) were purchased from Addgene (plasmids no·s 31476, 31482, 12259 and 12260). The inducible shRNA RNF168 knockdown lentiviral plasmids were constructed as described in Wiederschain et al. (Wiederschain et al., 2009).

The backbone pLKO-Tet-On Puro (Wee et al., 2008; Wiederschain et al., 2009) plasmid was obtained from Addgene (plasmid no. 21915). SiRNA's were transfected with the Lipofectamine RNAiMAX (Invitrogen) reagent following the manufacturer's instructions.

8.4 OLIGONUCLEOTIDES AND qPCR

The abundance of RNF168 mRNA level was probed by quantitative PCR using a Nano LightCycler (Roche) instrument. GAPDH primers were used as an internal control. PCR product abundance was quantified using the Light Cycler Nano software (Roche).

8.5 IMMUNOBLOTTING

Protein lysates were collected using 2x Laemmli sample buffer (2x LSB): using 300µl of LSB to lyse cells from confluent 60mm Petri dish, incubated at 95°C for 5,5 min with shaking (1250 rpm). Whole-cell lysates were subsequently separated using self-cast 10% sodium dodecyl sulfate–polyacrylamide gel or pre-cast SDS-PAGE (4−15% gradient) (Biorad) ectrophoresis gel and transferred to a nitrocellulose membrane (GE Healthcare). The membrane was blocked in 5 % (w/v) skim milk in Tris-buffered saline supplemented with in 0.1% (v/v) Tween-20 and probed with a primary antibody overnight at 4 °C. Subsequently, the membrane was incubated with horseradish peroxidase-labeled secondary anti-mouse or anti-rabbit antibodies (Santa Cruz Biotechnology) for 1h at room temperature and the signals were visualized using ECL detection reagents (Thermo Fisher Scientific) and the ChemiDoc system (Bio-Rad). Band intensity quantification was performed in the ImageJ software (http://imagej.nih.gov/ij/).

8.6 BIOCHEMICAL CELL FRACTIONATION-ISOLATION OF CHROMATIN-BOUND PROTEINS

To isolate chromatin, cells growing on 60mm Petri dish were incubated for 10 min in 400µl of ice-cold buffer A (10mM HEPES-KOH, 10mM KCl, 1.5mM Mg_2Cl, 0.34M sucrose, 10% glycerol, 0.1% TritonX-100) enriched for 5µl 1M DTT, 10 µl 0.5M NaF, 10 µl β glycerophosphate, 250 µl Protease inhibitor cocktail) directly before use. Supernatant of cells was collected into ice-cold eppendorf tubes and spin down at maximum speed (15 000 rpm)

15-30min at 4°C. 360 µl of supernatant was further resuspend in 120 µl of 4x concentrated Laemmli buffer and incubated at 95°C for 5,5 min with shaking (1250 rpm) to get the soluble protein fraction (S) of cells. The same 60mm Petri dishes with cells from the first step were washed with Buffer A for 5min and after removal of buffer A cells were lysed in 400 µl of Laemmli buffer. To get the chromatin enriched fraction of cells (CHR) prepared cell lysates were incubated at 97°C for 7 min with shaking (1400 rpm).

8.7 IMMUNOFLUORESCENCE AND MICRONUCLEI STAINING

Cells grown on 12-mm coverslips were fixed with 4% paraformaldehyde in phosphate-buffered saline (PBS) for 15 min and then permeabilized with PBS containing 0.2% (v/v) Triton X-100 for 5 min. Suspension cells were cytospinned onto microscopic slides before fixation using the Cyto-Tek Sakura instrument (Sakura Finetek). Fixed cells were blocked with 5% (v/v) fetal bovine serum in PBS for 30 min and incubated overnight at 4 °C with primary antibodies (diluted in 5% (w/v) bovine serum albumin in PBS). Coverslips were washed three times in PBS supplemented with 0.1% (v/v) Tween-20, once with PBS and then incubated with an appropriate secondary goat anti-rabbit or goat anti-mouse Alexa Fluor 488 or Alexa Fluor 568 conjugated (Invitrogen) secondary antibody (diluted in in 5% (w/v) bovine serum albumin in PBS) for 60 min at room temperature. Slips were then washed as above and mounted onto slides using the 4,6-diamidino-2-phenylindole (DAPI) containing Vectashield mounting reagent (Vector Laboratories) or and incubated with Hoechst 33342 at room temperature for 5 min before mounting.. Coverslips for micronuclei analysis were fixed and washed as above, stained with DAPI diluted in PBS and subsequently mounted with the Vectashield reagent (without DAPI). Slides were visualized by the Axio Observer.Z1/Cell Observer Spinning Disc microscopic system (Yokogawa, Tokyo, Japan and Zeiss) equipped with an Evolve 512 (Photometrix, Tucson, AZ, USA) EMCCD camera. Zeiss Plan Apochromat 63x and 100x/1.40 NA objectives were used. For quantitative image analysis, a series of random fields were recorded automatically, using the ScanR imaging workstation (Olympus, Tokyo, Japan; with an EM charge-coupled device camera (C9100; Hamamatsu Photonics, Hamamatsu City, Japan), a U Plan S Apochromat 40 × /0.9 NA objective, and an image resolution of 200 × 200 nm/pixel). The number and intensity of micronuclei and IR-induced nuclear foci were quantified using the ScanR image analysis software (Olympus).

8.8 GENERATION OF LENTIVIRUSES AND LENTIVIRAL TRANSDUCTION

Lentiviruses were generated by co-transfecting 293T cells with 4 μg of pMD2.G, 7 μg of psPAX2 and 9 μg of a lentiviral plasmid of interest using the CaPO4 precipitation method (Tiscornia et al., 2006). Six to eight hours post-transfection, the cells were washed briefly with pre-warmed PBS and medium was changed. Lentivirus containing supernatant was collected 48 h later. Target cellswere transduced at multiplicity of infection of 1–10 with the supernatant supplemented with 4 μg/ml polybrene (Sigma-Aldrich). Twenty-four hours post-transduction, the medium was changed and when required, the cells were selected in 1 μg/ml puromycin.

8.9 FLOW-CYTOMETRIC ANALYSIS OF DNA REPAIR PATHWAY CHOICE

Cells harboring the Traffic light reporter were seeded in a 12-well plate and 24-h later transduced with the I-SceI and GFP repair template containing construct using the procedure above. Seven days later, the cells were trypsinized, fixed with formaldehyde and analyzed by an Influx instrument. GFP was measured using a 488 nm laser for excitation and a 530/40 filter, whereas mCherry was excited using a 561 nm laser and acquired with a 610/20 filter. Data were analyzed using the FACS Sortware software.

8.10 CELL CYCLE ANALYSIS

Cells were fixed in 70% ethanol and stained with propidium iodide for flow cytometric analysis. Fixed cells were analyzed on a FACS Verse instrument and cell cycle distribution was assigned using the FAC Suite software.

8.11 LONG-TERM CELL SURVIVAL ASSAY

In all, 1 × 105 cells were seeded in triplicate to ø 6 cm plates and left to attach overnight. Next day, the medium was replaced by inhibitor or dimethylsulfoxide (mock) containing medium. Seven days later, the cells were trypsinized and cell number was scored using a Vi-Cell XR Cell Viability Analyzer equipped with the ViCELL XR software. The IR resistance of proteotoxic stress DDR-resistant lines was assessed as above with following modifications:

attached cells were pretreated with 5 μM MG132 or dimethylsulfoxide (mock) for 2 h and subsequently irradiated with 2 Gy. Then medium was changed and cell survival was assayed as above 7 days later.

8.12 PATIENT's SAMPLES

Between September 2016 and December 2016, 6 bone marrow (BM) samples were obtained by routine prognostic procedure at the Department of Hematooncology of the Faculty Hospital Olomouc after an appropriate informed consent was signed. Described BM samples were derived from 4 patients diagnosed for multiple myeloma (MM) and 2 patients diagnosed for driving stage of MM -monoclonal gammopathy of uknown significance (MGUS). All the BM samples studied were from females in age between 50-65 years.

8.13 BM COLLECTION AND ISOLATION OF SINGLE CELL SUSPENSION

Bone marrow samples (3-7ml) were mixed with 5ml of RPMI-1640 containing 100U/ml heparin to prevent coagulation of blood cells. Collected bone marrow samples were first deprived of red blood cells by applying pre-chilled red blood cell lysis buffer (RBC) (0.15M NH4Cl; 10mM KHCO3; 0.1mM EDTA; pH 7.3) for 30min. Remaining cells were passed through wet 100μm MACS SmartStrainers to remove bone fragments and cell clumps and centrifuged at 445xg for 10min at 20 °C in a swinging bucket rotor without braking. Cell pellets were resuspended in separation buffer (autoMACS Running Buffer) to the original volume of obtained bone marrow sample. To obtain single-cell suspension before magnetic labeling cells were passed through 30 μm nylon mesh.

8.14 IMMUNOMAGNETIC ENRICHMENT OF CD138 POSITIVE CELLS AND IMMUNOPHENOTYPING ANALYSES

Cells were magnetically labeled for 15 min with 50 μl of CD138 Microbeads per 1 ml of single cell suspension at 4°C. Subsequently, cells were washed by 2-5ml of Separation buffer per 1ml of obtained bone marrow sample and centrifuged at 445xg for 10 min in a swinging bucket rotor without braking. Cell pellets were resuspended with Separation buffer to a total volume equal to volume of single-cell suspension. Magnetically labeled cell suspensions were

applied to whole blood columns placed in the magnetic field of MACS Separator prewashed 3x with Separation buffer. The collected flow-through represented the CD138 negative unlabeled cells. Whole blood columns were 3x washed with 3ml of Separation buffer and collected pass through was combined with the previous effluent of CD138 negative cells. Subsequently, whole blood columns were removed from the separator and placed into new collection tube. To obtain the CD138 positive plasma cells, 5ml of Whole Blood Column Elution Buffer was apllied onto the Whole Blood Column and the magnetically labeled cells were immediately flushed out by firmly pushing the plunger into the column.

Fraction of cells deprived of red blood cells, CD138- fraction and CD138+ fraction (0.05-0.1x10^6) were further analysed by flow cytometry as reported previosly (Kovarova et al., 2009). For plasma cells determination, monoclonal fluorescently labeled antibody CD138-PE (phycoerythrine) was used.

9 RESULTS AND DISCUSSION

9.1 53BP1 IS RECRUITED TO DNA DAMAGE SITES DESPITE PROTEASOME INHIBITOR INDUCED PROTEOTOXIC STRESS IN THE MDA-MB-231 CELL LINE

As mentioned in the previous chapter theoretical part of my thesis, inhibition of the proteasome in mammalian cells is accompanied by depletion of free ubiquitin pool and abrogates the recruitment of multiple key players of DDR pathway, including the 53BP1 and BRCA1 proteins. However, our observation of persisting IR-induced 53BP1 focal accumulation in the breast cancer MDA-MB-231 cell line pretreated with proteasome inhibitor MG132, contradicts this generally believed phenomenon. Intriguingly, in the MDA-MB-231 cell line, even a 2 hour pre-treatment with the proteasome inhibitor, MG132, followed by gamma irradiation did not lead to diminished 53BP1 irradiation induced foci (IRIF) formation and over 40 % of cells contained >5 53BP1 IRIFs (Figures 9.1 A, B). On the other hand, in the U2OS cell line that served as a control, the same treatment diminished 53BP1 IRIF formation completely (Figures 9.1A, B). We also employed a primary line control (BJ) that behaved in the same fashion as U2OS (Figures 9.1 A, B).

There are several possible scenarios in which MDA-MB-231 cells may promote 53BP1 DSB association even under conditions of ubiquitin starvation. First, it is possible that MDA-MB-231 cells might exhibit non-standard response to proteasome inhibition, being less sensitive and thus sustaining sufficient pool of free ubiquitin for ongoing ubiquitin driven processes including 53BP1 recruitment to its chromatin binding sites. Second alternative for persisted 53BP1 foci under protesome inhibition might be downregulation of its direct competitors for recognition of H4K20me2 histone binding motif- JMJD2A and L3MBTL1 in the MDA-MB-231 cell line (Mallette and Richard, 2012). A the same time, the recruitment of 53BP1 might be independent of ubiquitylation in MDA-MB-231 cell line, utilizing ubiquitin like molecule NEDD8, shown to be involved in certain pathways of DNA damage signaling (Huang et al., 2004) and suggested to compensate ubiquitin especially under condition of acute ubiquitin starvation (Hjerpe et al., 2012). Another thinkable explanation for described unexpected phenotype in MDA-MB-231 cells could be supraphysiologial level of key DSB

response related ubiquitin conjugating enzyme – UBC13 (UBE2N) and E3 ubiquitin ligases RNF8 and RNF168. Given its capacity for amplification of the ubiquitin driven DDR signaling, hyperactive RNF168 might efficiently compete for residual pool of free ubiquitin (after proteasome inhibition) and still perform the H2AK15 monoubiquitylation, known to be crucial for 53BP1 recruitment (Fradet-Turcotte et al., 2013).

9.2 MDA-MB-231EXHIBIT STANDARD RESPONSE TO PROTEASOME INHIBITION AND STANDARD DDR

Firstly, we reasoned that the MDA-MB-231 cells might exhibit a non-standard response to core proteasome inhibition resulting in less pronounced drop in free ubiquitin levels thus enabling sustained 53BP1 IRIF formation. Nevertheless, immunoblotting analysis of total ubiquitin showed accumulation of high molecular weight ubiquitin conjugates and depletion of free ubiquitin in both MDA-MB-231 and U2OS control upon MG132 treatment (Figure 9.1 C). As in the case of free ubiquitin depletion, accumulation of high molecular ubiquitin conjugates is a sign of proteasome inhibition, hence we concluded that altered sensitivity to proteasome inhibitors is unlikely causing the observed MDA-MB-231 phenotype. In both MDA-MB-231 and U2OS we also observed disappearance of ubiquitin conjugates (detected by the FK2 antibody) at sites of gamma irradiation inflicted DNA damage (Figure 9.2 A). It has been shown that upon proteasome inhibition, ubiquitin is cleaved off the histones and other nuclear proteins and shuttled to cytoplasmic proteins awaiting degradation in the proteasome complex (Dantuma et al., 2006).

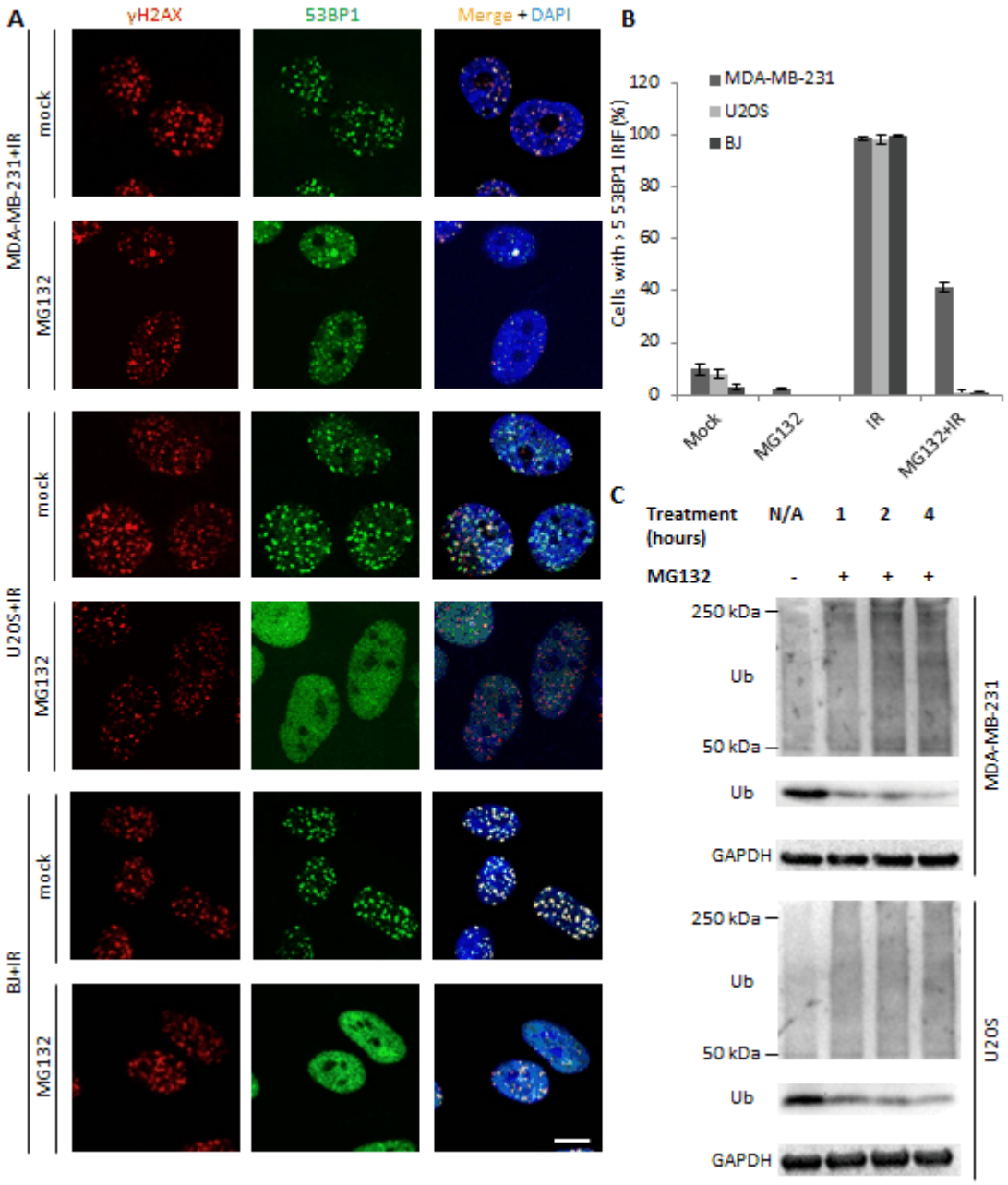

Figure 9.1: 53BP1 is recruited to DNA damage sites despite proteotoxic stress in MDA-MB-231 cells. (a) MDA-MB-231, U2OS and BJ cells were mock- or MG132 (5 μM) treated for 2 h and subsequently irradiated with 2 Gy. One hour post-irradiation, the cells were fixed and immunostained for γH2AX and 53BP1. Scale 10 μM. (b) Cells with >5 53BP1 IRIFs were scored for all three lines after mock, MG132 or either of the treatments combined with irradiation (2 Gy). (c) MDA-MB-231 and U2OS cells were mock and MG132 treated, lysed at various time points and subsequently probed for free ubiquitin and ubiquitin conjugate levels using immunoblotting. In (b), results are mean ±s.d. of three independent experiments.

This result again shows that MDA MB 231 respond to proteasome inhibition in a standard mode and the depletion of free ubiquitin pool takes place also in the nucleus with no nucleus-specific compensatory mechanism taking place that would allow for the sustained 53BP1 accrual at the sites of damage.

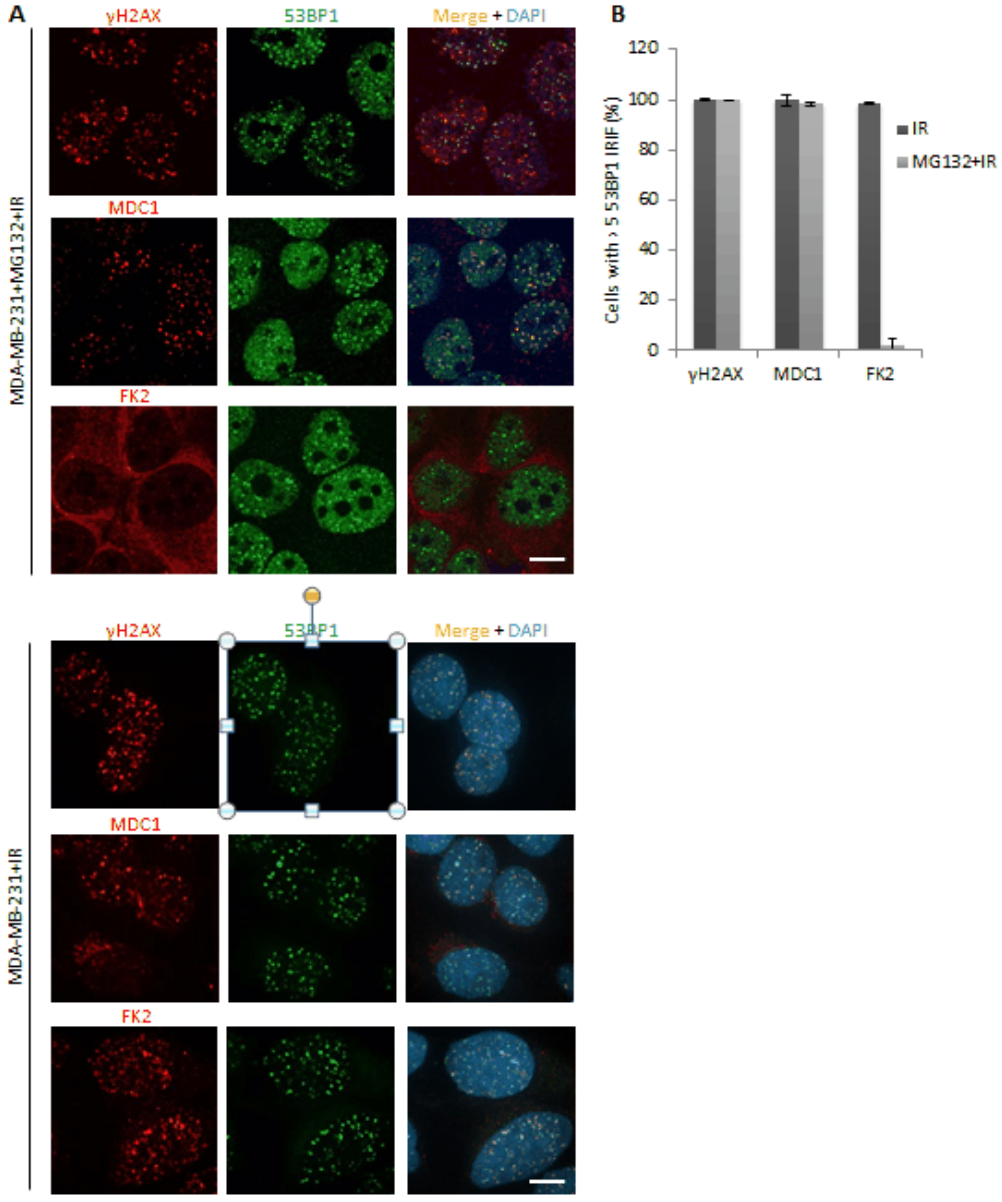

Figure 9.2: Probing DSB response upstream of 53BP1 in MG132-treated MDA-MB-231 and U2OS cells. (a) MDA-MB-231 cells were pretreated with MG132 for 2 h, irradiated with 2 Gy and 1h post-irradiation immunostained for the indicated proteins or protein modifications known to be present in IRIFs. Scale 10 μM. (b) Graphical summary of nuclei with >5 γH2AX, FK2 or MDC1 IRIFs, scored in cells bearing 45 53BP1 IRIFs. Results are mean ±s.d. of three independent experiments.

Additionally, we detected recruitment of key DDR proteins acting upstream of 53BP1 to IRIF in mock-treated and proteasome inhibitor-treated MDA-MB-231 cells. With the exception of the above mentioned ubiquitin conjugates, the IRIF contained the key DDR proteins such as the phosphorylated histone H2AX and MDC1 (Figure 9.2 A, B). This suggested that the upstream steps of the DSB response pathway react to proteasome inhibition largely in a standard mode in MDA-MB-231 cell line.

9.3 MDA-MB-231 AND U2OS DISPLAY SIMILAR LEVELS OF 53BP1 NEGATIVE REGULATORS, PLAYING NONE OR MINOR ROLE IN OBSERVED PROTEOTOXIC STRESS RESISTANT DSB RESPONSE

To gain insight into the mechanism responsible for observed persisted DSB response in MDA-MB-231 cell line we turned our attention to 53BP1 upstream and downstream regulators, whose up- or downregulation in the examined cell line might affect 53BP1 recruitment to the DNA damage sites. We probed the levels of various 53BP1 positive (described in the text later Figure 9.6.2 C) and negative regulators (Figure 9.3 A) which could alter the IR induced 53BP1 recruitment in the presence of proteasome inhibitor.

We suggested that our experiments can shed some light on the competition based mode of 53BP1 recruitment that reportedly requires two proteins, hitone demethylase- JMJD2A and polycomb group protein- L3MBTL1 to be removed from chromatin flanking the DSBs and degraded in order to expose the H4K20me2 that can be subsequently bound by the 53BP1's tandem TUDOR domains (Mallette and Richard, 2012).

However, none or subtle changes in abundance of JMJD2A and L3MBTL1 were observed by immunoblotting using MDA-MB-231 and U2OS cell lysates (Figure 9.3 A). In addition to this, both proteins displayed similar abundance in MDA-MB-231 compared to U2OS when checked even more specifically for its level in separated soluble and chromatin fraction of cells (Figure 9.3 A). However, efficient siRNA mediated knockdown of JMJD2A in both tested cell lines resulted in increased number of 53BP1 positive nuclei after MG132 treatment and more pronounced signal of 53BP1 monitored in IRIF (Figure 9.3 B, C). In addition to this, we detected none change in the level of RNF169 protein, described to

compete with 53BP1 for its association with ub-modified chromatin (data not schown) (Panier and Boulton, 2014; Poulsen et al., 2012).

As we have observed sustained 53BP1 recruitment under conditions of proteasome inhibition, it seems unlikely that JMJD2A and L3MBTL1 proteins have to be degraded to allow for 53BP1 recruitment to chromatin. We favor a model in which the clearance of the competing proteins from the DSB-flanking chromatin is sufficient and does not have to be accompanied by their degradation in order to permit 53BP1 recruitment. According to such modified model, the RNF168- mediated ubiquitination of JMJD2A would serve primarily as a chromatin eviction signal and the subsequent degradation of these demethylases is not essential for 53BP1 recruitment.

A

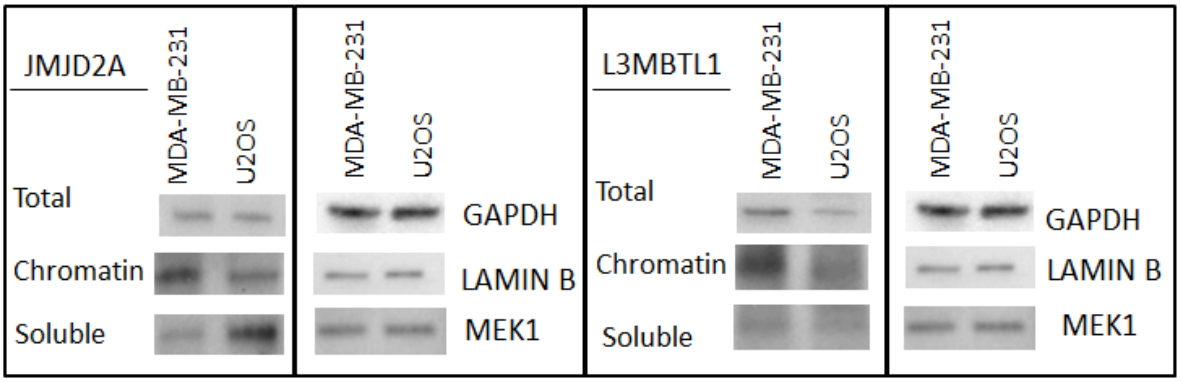

Figure 9.3 continues on the next page

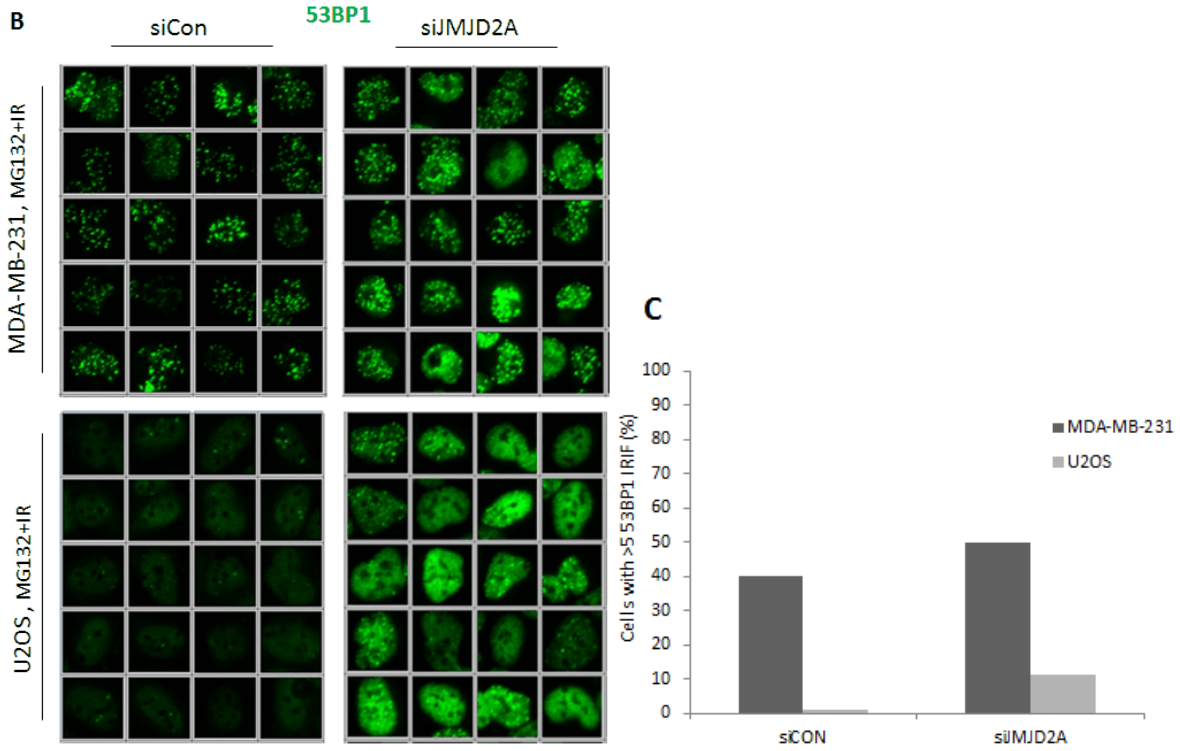

Figure 9.3: Similiar levels of 53BP1- direct competitors, JMJD2A and L3MBTL1 in MDA-MB-231 and U2OS cell line. (a) MDA-MB-231 and U2OS total cell lysates as well as chromatin and soluble fractions were analyzed by immunoblotting for abundance of JMJD2A and L3MBTL1 histone demethylase. (b) MDA-MB-231 and U2OS cells transfected with indicated siRNAs were treated with MG132 (2h, 5μM), irradiated (2Gy) and 1h post-irradiation immunostained for 53BP1. (c) Cells with >5 53BP1 IRIF from (b) were scored.

9.4 THE RIF1 AND REV7 EFFECTOR PROTEINS ARE RECRUITED TO MICROIRRADIATION INDUCED DNA DAMAGE UNDER PROTEOTOXIC STRESS IN MDA-MB-231 CELL LINE

The results of the immunofluorescence experiments presented above imply that the DDR exhibited by the proteotoxic stress resistant DDR cells under proteasome inhibition is a standard one. To further verify the chromatin DSB response pathway at the level of 53BP1in cell treated by proteasome inhibitor, we probed MDA-MB-231 and U2OS cells for recruitment of two known 53BP1 effectors-RIF1 (Chapman et al., 2013; Zimmermann et al., 2013) and REV7 (Xu et al., 2015) to laser microirradaiation induced DNA damage sites.

In contrast to U2OS, in the MDA-MB-231 both RIF1 and REV7 were recruited to laser induced ‘stripes’, even after MG132 treatment (Figure 9.4). These results imply that the

upstream steps of the DSB response pathway operate normally, and the unorthodox DSB response in the MDA-MB-231 cells under proteotoxic stress is shared by 53BP1 and its downstream effectors.

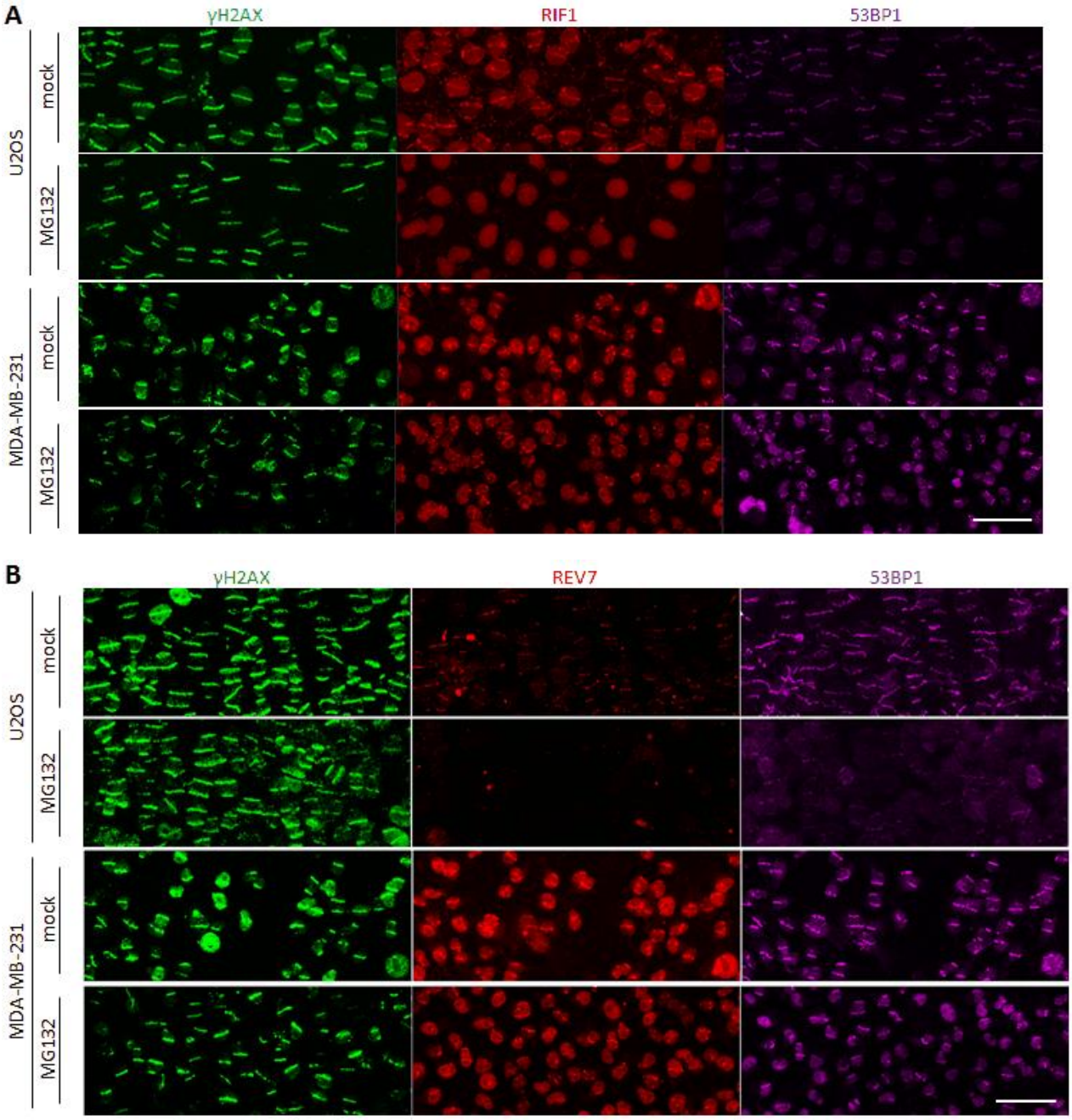

Figure 9.4: Probing DSB response downstream of 53BP1 in MG132-treated MDA-MB-231 and U2OS. (a) Mock or MG132-treated (5μM, 2h) MDA-MB-231 and U2OS cells were laser-microirradiated and immunostained for γH2AX, 53BP1 and RIF1. (b) As in (a), but staining for γH2AX, 53BP1 and REV7. Scale bar 50 μM

9.5 ABSENCE OF 53BP1 MUTATED IN ITS UDR-MOTIF AT DSB SITES UNDER PROTEOTOXIC STRESS

As reported recently, 53BP1 binds to two chromatin modifications at the DSBs – dimethylated histone H4 (H4K20) and ubiquitinated histone H2A (H2AK15Ub). The H2AK15Ub mark is recognized by the Ubiquitin Damage Response domain (UDR) at the C-terminal part of 53BP1 (Fradet-Turcotte et al., 2013). To test wether ubiquitin is indeed required for 53BP1 accumulation at DSBs in MDA-MB-231 under condition of proteotoxic stress, we utilized a 53BP1 UDR mutant incapable of binding to its cognate site.

While a 53BP1 wild type green fluorescent protein (GFP) fusion protein was recruited to IRIFs, cells expressing a GFP labelled UDR mutant (L1619A) (Fradet-Turcotte et al., 2013) did not form 53BP1 IRIFs (Figure 9.5). Furthermore, a GFP tagged Tudor domain 53BP1 mutant (D1521R) (Fradet-Turcotte et al., 2013) behaved similarly and was not recruited to IRIFs.

Although 53BP1 recruitment is regulated also by other modifications including NEDDylation and acetylation (Ma et al., 2013; Tang et al., 2013) and NEDDylation was suggested to compensate for ubiquitylation when proteasome is inhibited (Hjerpe et al., 2012) our own experiments using inhibitors of NEDD conjugation and deacetylation did not support this possibility (our unpublished data).

Taken together, this suggested that in the MDA-MB-231 cells, 53BP1 recruitment operates in standard mode still requiring ubiquitin driven signaling and each of its binding domains to recognize H4K20me2 and H2AK15Ub respectively, even when cellular level of free ubiquitin becomes limiting.

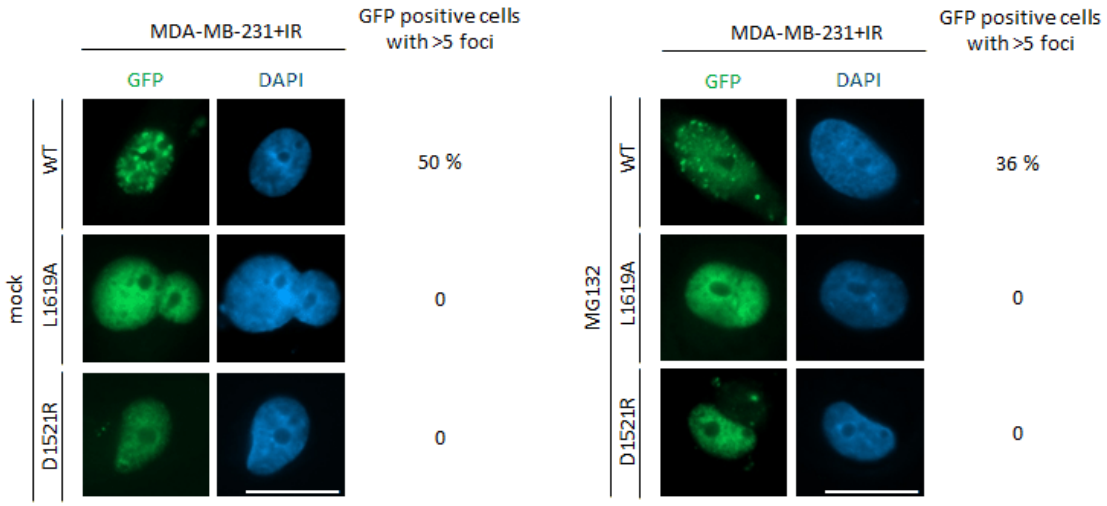

Figure 9.5: 53BP1 recruitment to sites of damage in MDA-MB-231 is methylation and ubiquitination dependent. MDA-MB-231 cells transfected with siRNA against 53BP1 and expression vectors for the indicated siRNA-resistant GFP-tagged versions of 53BP1 were mock or MG132 treated (2h, 5μM), irradiated with 2Gy and after 1h processed for GFP imaging. Scale 20μM. Results are mean of two independent experiments.

9.6 THE PROTEOTOXIC STRESS RESISTANT DDR PHENOTYPE DEPENDS ON DDR ASSOCIATED UBIQUITIN SIGNALING WITH RNF168 PLAYING A CENTRAL ROLE

As the response to DSBs in the MDA-MB-231 line is still fueled by ubiquitin under proteotoxic stress, a mechanism should exist that provides sufficient amount of free ubiquitin to sustain the process. One thinkable way of bypassing an acute decrease in free ubiquitin level is overexpression of the E2 and/or E3 ubiquitin conjugating enzymes/ligases. Elevated pool of an E2 ligase that was charged with ubiquitin prior to the drop in free ubiquitin level might serve as a temporary reservoir for downstream processes. On the other hand, an overexpressed E3 ligase might outcompete remaining E3 ligases in the uptake of residual ubiquitin after introduction of proteotoxic stress.

Hence, we examined the levels of key DSB response relating ubiquitin conjugating enzyme – UBC13 (UBE2N) and E3 ligases RNF8 and RNF168 in the MDA-MB-231 line. Strikingly, all three enzymes displayed substantially elevated levels in this cell line (Figure 9.6.1 A). When normalized to glyceraldehyde 3-phosphate dehydrogenase (GAPDH), both RNF8 and RNF168 showed more than twofold higher levels than those in the U2OS cells, while UBC13 level was even higher – more than fivefold fold higher compared to the U2OS

line (Figure 9.6.1 B). The overabundance of these three enzymes was even more profound when the normal diploid BJ cells were compared with MDA-MB-231 cells: more than fourfold for UBC13, sixfold for RNF8 and more than eightfold in the case of RNF168 (Figure 9.6.1 B).Importantly, the level of the 53BP1 protein was comparable in all three cell types (Figure 9.6.1 B).

Our results showing the profound change in the level of RNF168 among indicated cell lines together with the recent finding of other laboratories (Fradet-Turcotte et al., 2013; Gudjonsson et al., 2012) corroborated the functional significance of the RNF168-centered ubiquitin-mediated signaling pathway in the studied exceptional DSB response in MDA-MB-231 cells. To further support our hypothesis, we monitored increased endogenous level of RNF168 in MDA-MB-231 compared to U2OS by two additional experimental approaches: i) measuring signal intensity of RNF168 present in IRIF (Figure 9.6.1 E) ii) detecting the abundance of RNF168 present in chromatin fraction of cells (Figure 9.6.1 F). Taken together, these results supported the functional significance of the RNF168-centered ubiquitin-mediated signaling pathway in the altered DSB response in MDA-MB-231 cells.

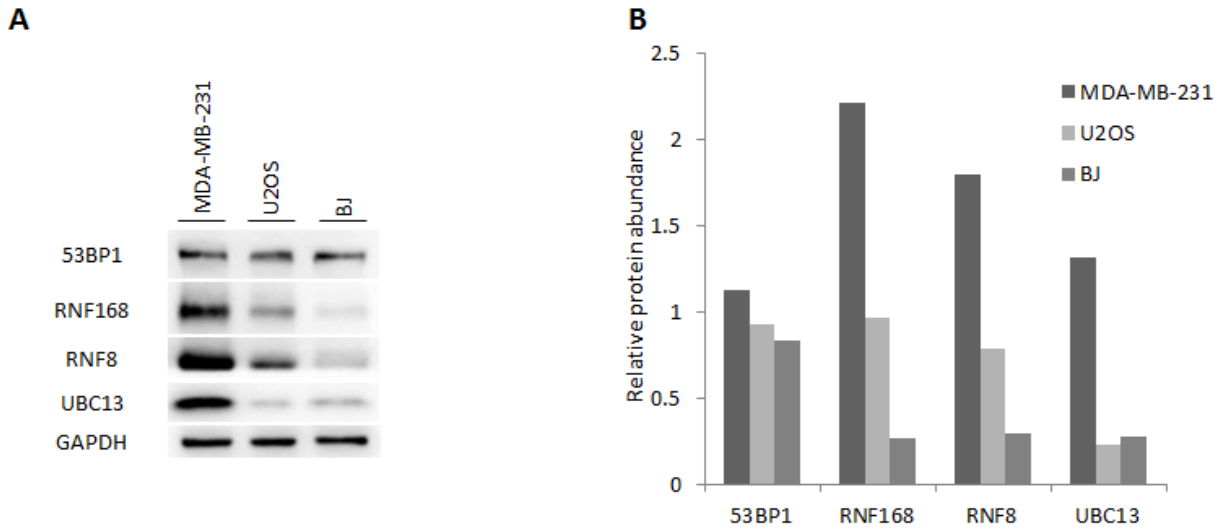

Figure 9.6.1 continues on the next page

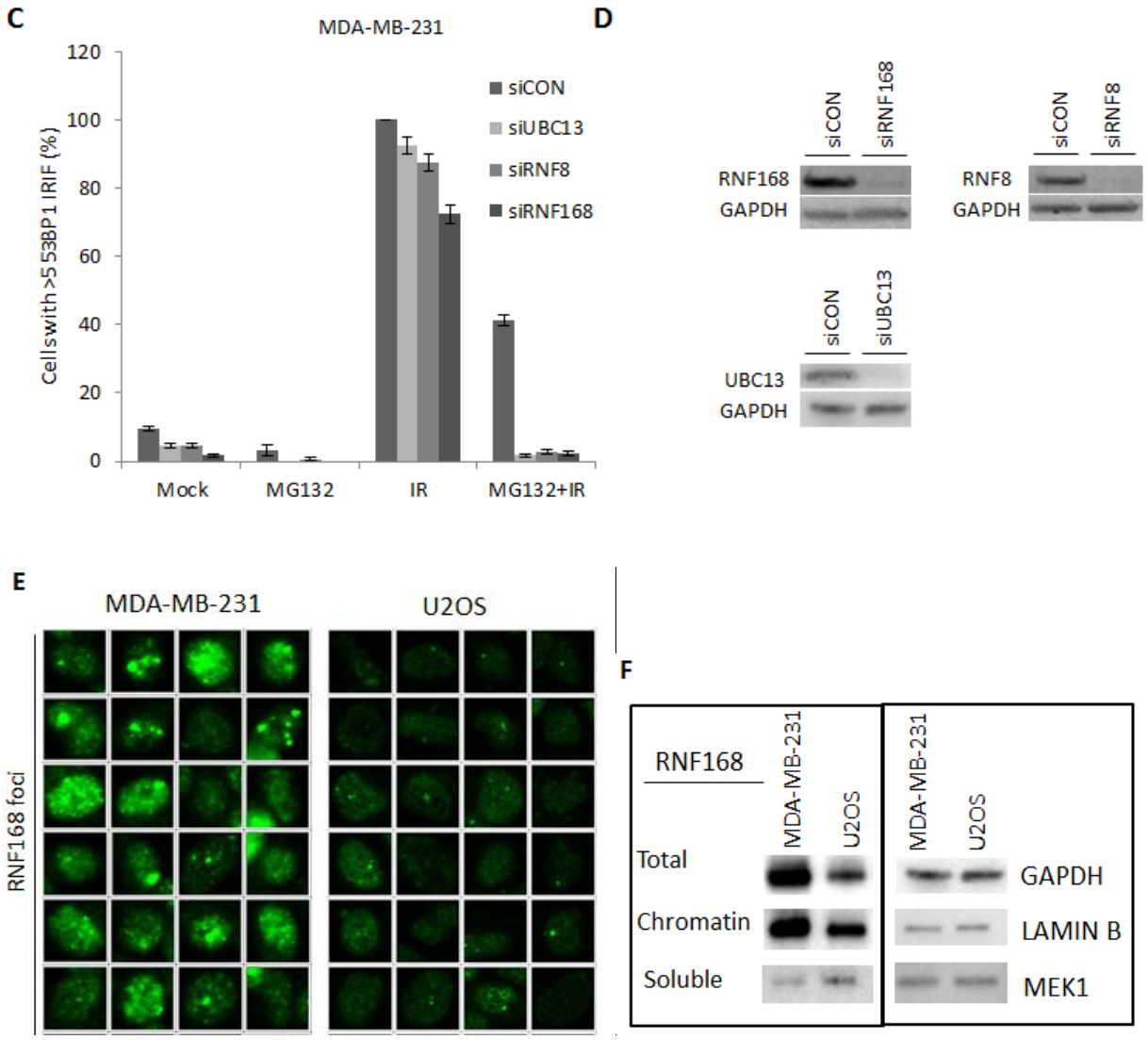

Figure 9.6.1: Elevated levels and impact of ubiquitin-mediated DSB signaling-related enzymes in MDA-MB-231 cells. (a) MDA-MB-231, U2OS and BJ cell lysates were analyzed by immunoblotting for abundance of 53BP1 and the major DSB ubiquitin signaling enzymes RNF8, RNF168 and UBC13. (b) Protein abundance was calculated using densitometric analysis of the immunoblot shown in a. Band intensities were normalized to corresponding GAPDH bands. (c) MDA-MB-231 cells were transfected with indicated siRNAs, mock and MG132 treated (2h, 5μM) with and without irradiation (2Gy) and 1h post-irradiation stained for 53BP1. Cells with >5 53BP1 IRIF were scored. Results are mean± s.d. of three independent experiments (d) Knockdown efficiency in (c) was verified by probing corresponding cell lysates by immunobloting using indicated antibodies (e) MDA-MB-231 and U2OS immunostained for endogenous RNF168. (f) MDA-MB-231 and U2OS total cell lysates, chromatin and soluble fractions were analyzed by immunoblotting for the level of RNF168.

Quantitative PCR and cycloheximide chase experiments demonstrated that the heightened levels of RNF168 E3 ligase in the MDA-MB-231 cells stem from transcriptional upregulation and stability of the proteins is unaltered (Figure 9.6.2 A, B). It remains to be elucidated how MDA-MB-231 cancer cells acquire the elevated expression of RNF168 and/or other ubiquitin ligases and conjugating enzymes. Analogous to other tumor-associated changes in gene expression, the most likely candidates are mutations in gene regulatory sequences, genome rearrangements or transcription suppressor/activator mutations. One of the likely candidates that might drive the cancer-related RNF168 overexpression is the family of FOXO transcription factors shown to regulate various stress response genes including components of the DDR machinery (Greer and Brunet, 2005; Tran et al., 2002). Moreover, dysregulation of the FOXO3a transcription factor was detectedin in breast cancer (Greer and Brunet, 2005) which implies that this protein (and possibly other FOXO family members) might fuel the elevated RNF168 also in MDA-MB-231 cell line.

Interestingly, we have monitored almost fourfold shorter RNF168 protein half-life in MDA-MB-231 compared with U2OS cell line. Indeed, the accelerated turnover of RNF168 protein was consistent with detected overabundant TRIP12 and UBR5 in MDA-MB-231 (Figure 9.6.2 C), the two E3 ligases critical for ubiquitin/proteasome-mediated degradation of RNF168 (Gudjonsson et al., 2012). The elevated TRIP12 and UBR5 might reflect a fine-tuning mechanism in MDA-MB-231 cells, possibly providing a negative feedback loop to limit the overabundant RNF168 to levels that are not overly harmful to cells, a scenario that occurs upon experimental gross overexpression of RNF168 (Gudjonsson et al., 2012). Consistently, depletion of either TRIP12 or UBR5 in MDA-MB-231 led to an even more pronounced DSB response phenotype resistant to proteasome inhibition (Figure 9.7D), possibly due to further increase in the abundance of RNF168. Our results are in line with observation of Gudjonsson and colleagues showing massive spreading of ubiquitin conjugates and hyperaccumulation of ubiquitin-regulated genome caretakers such as 53BP1 and BRCA1 after depletion of these two HECT domain ubiquitin E3 ligases (Gudjonsson et al., 2012) . However, in their hands, depletion of free ubiquitin by MG132 treatment (10μM) abrogated 53BP1 foci formation 1 hour after IR in U2OS cell line irrespective of TRIP12/UBR5 depletion. This contradiction in our results may be due to lower dose of MG132 used in our case, allowing persistence of some residual ubiquitin which can be still utilized by the

abundant RNF168 molecules in absence of TRIP12 and UBR5 for establishment of the ubH2AK15 53BP1 docking site.

In addition, we observed moderately elevated levels of the HERC2 ubiquitin ligase (Figure 9.6.2 C), previously described possible regulator of 53BP1 recruitment (Bekker-Jensen et al., 2010) and the chromatin remodeler KAP1 (data not shown). As HERC2 is responsible for stabilization of RNF8 interaction with UBC13 (Danielsen et al., 2012), this observation seems to go in line with the key role of RNF168 ubiquitin ligases in the phenotype.

Overall, these results supported the functional significance of the RNF168-centered ubiquitin-mediated signaling pathway in the altered DSB response in MDA-MB-231 cells.

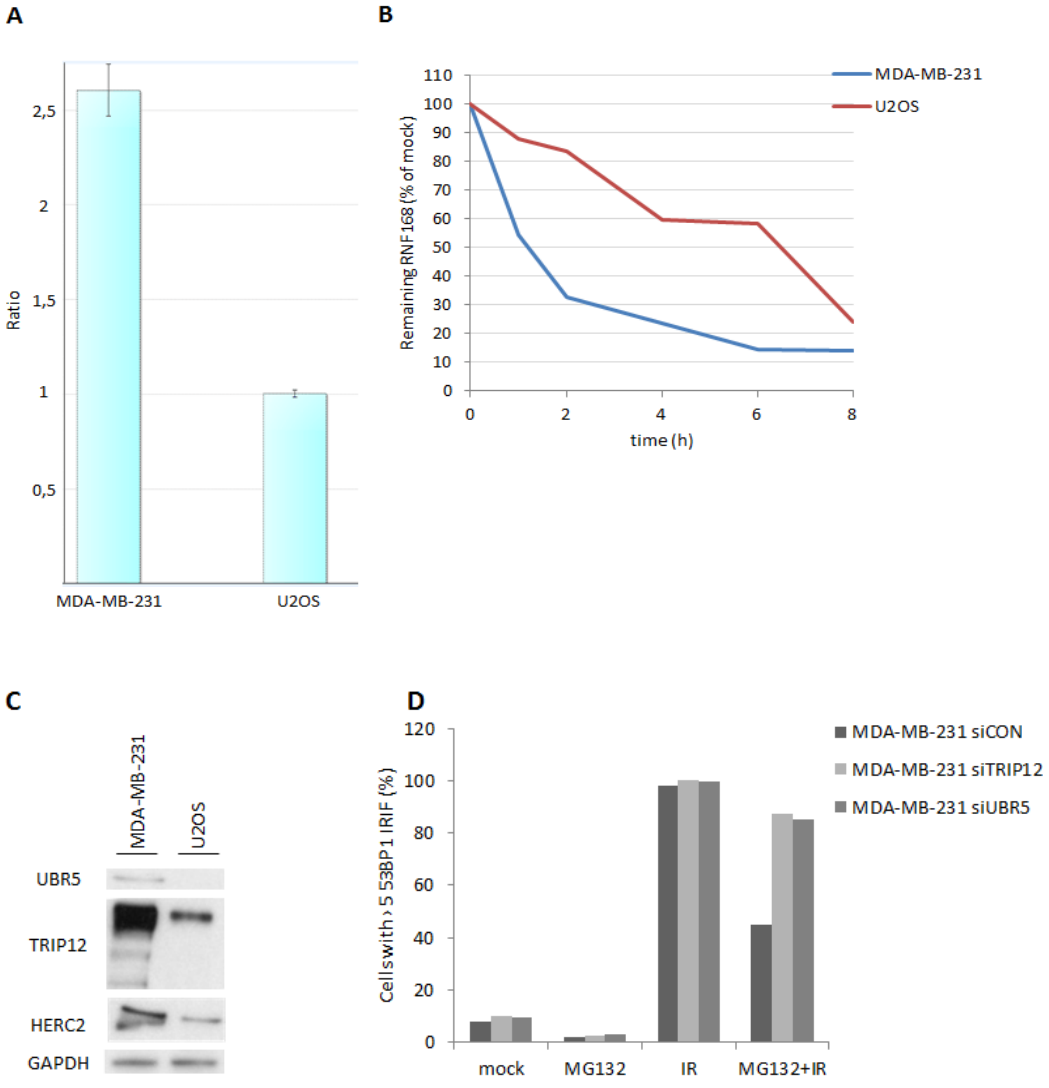

Figure 9.6.2: RNF168 stability and mRNA levels in MDA-MB-231 and U2OS cells. (a) RNF168 mRNA levels were quantified by real time qRT-PCR. GAPDH was used as a reference gene. (b) Cells were treated with cycloheximide (300 µM) and RNF168 levels were probed by immunoblotting at indicated time points. Protein levels were estimated by densitometric analysis compared to GAPDH internal standard. (c) Change in the levels of selected RNF168 stability and 53BP1 recruitment regulators in MDA-MB-231 and U2OS cell lines. The level of selected proteins was probed by immunoblotting. (d) MDA-MB-231 cells were transfected with indicated siRNAs, mock- or MG132 treated (2 h, 5 µM), irradiated (2 Gy) and 1 h post-irradiation stained for 53BP1 and scored for nuclei with >5 53BP1 IRIFs. The chart shown represents one of three consistent experiments.

Importantly, this our notion was further confirmed by functional experiments, in which small interfering RNA (siRNA)-mediated knockdown of UBC13, RNF8 or RNF168 completely abolished the proteotoxic stress-resistant DSB response phenotype in the proteasome inhibitor-treated MDA-MB-231 cells (Figures 9.6.1 C, D). Based on available mechanistic insights (Gudjonsson et al., 2012) we hypothesized that central to this unorthodox DSB response phenotype in MDA-MB-231 could be the RNF168 ligase.

To validate and extend this hypothesis, we performed partial knockdown of RNF168 with increasing amounts of siRNA resulted in gradual decrease of cells containing >5 53BP1 IRIF (Figure 9.6.2 A). In addition, we demonstrated that the phenotype could not be rescued by expression of siRNA resistant mutant version of RNF168 bearing a mutation (C16S) in the catalytic RING domain (Figure 9.6.2 B). Based on our results, we propose a model whereby ubiquitin is still used under proteotoxic stress to relay the DSB chromatin signaling, provided that the RNF168 E3 ligase is overabundant and hence can preferentially channel the remaining available ubiquitin to the RNF168- mediated pathway.

To verify our hypothesis of RNF168 having a central role in studied phenotype, we overexpressed the enzyme in a cell line incapable of sustaining DSB signaling under proteotoxic stress might mimic the situation seen in MDA-MB- 231. Indeed, an U2OS derived cell line overexpressing a RNF-168-GFP fusion protein exhibited 53BP1 IRIF in nearly all nuclei after proteasome inhibition (Figure 9.6.3 C, D). As in the case of MDA MB 231, the number of 53BP1 IRIF positive cells correlated with the level of RNF168 (Figure 9.6.3 E) and the phenotype was dependent on RNF8 (Figure 9.6.3 F). Of note, changes in RNF8 level had less profound effect on the phenotype as in the case of RNF168 underlining the major role of RNF168 in the proteotoxic stress resistant DSB response (Figure 9.6.3 F). Furthermore, the number of persisted 53BP1 foci in U2OS GFP-RNF168 nuclei cells correlated with their RNF168-GFP signal intensity after proteasome inhibition (Figure 9.6.3 G). Overall, these data

were consistent with the emerging key role of RNF168 abundance in the proteotoxic stress-resistant DSB response.

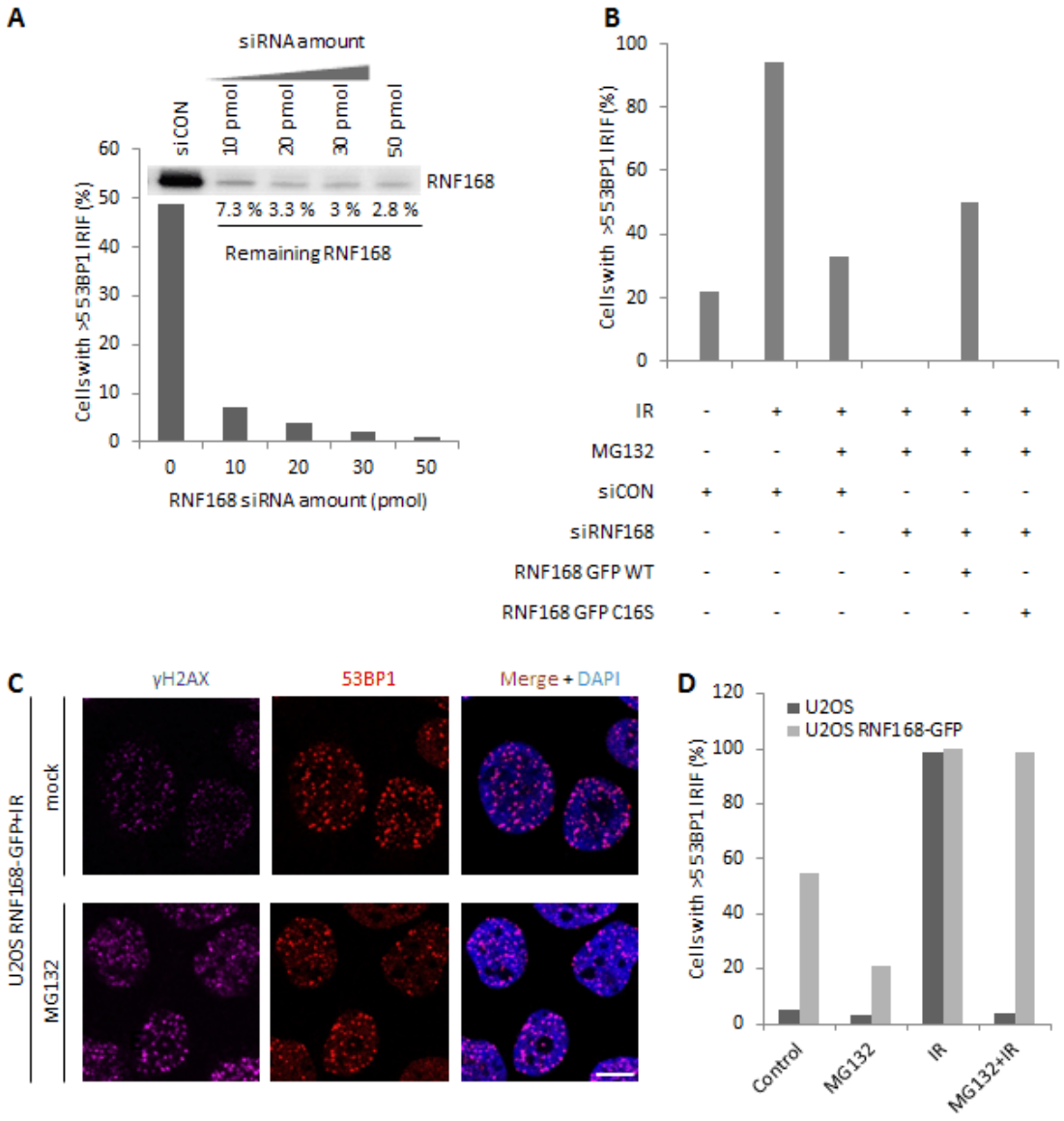

Figure 9.6.3 continues on the next page

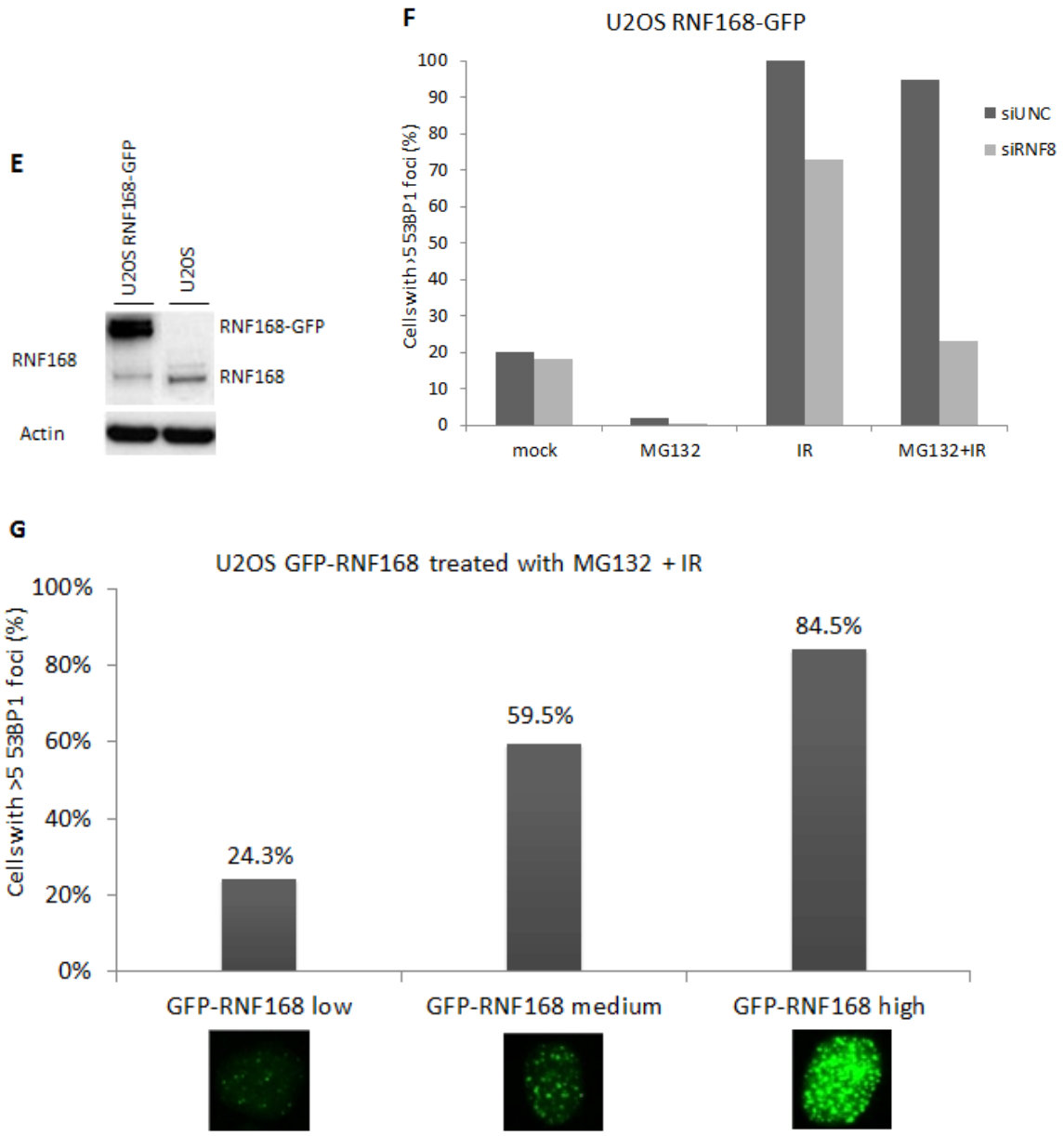

Figure 9.6.3: The proteotoxic stress-resistant DSB response phenotype depends on RNF168.

a) MDA-MB-231 cells were transfected with increasing amounts of RNF168 siRNA, treated with 5 μM MG132 (2h), irradiated (2Gy) and 1h post-irradiation stained for 53BP1. Nuclei with >5 53BP1 IRIFs were scored. Inset—siRNA transfected MDA-MB-231 cells were lysed and analyzed by immunoblotting for remaining RNF168 level. (b) MDA-MB-231 cells were co-transfected with control or RNF168 siRNA and siRNA-resistant plasmids carrying GFP-tagged WT or the C16S RING mutant version of RNF168. Transfected cells were mock or MG132 treated (2h, 5μM), irradiated (2Gy) and 1 h post-irradiation stained for 53BP1 and scored for nuclei with >5 53BP1 IRIFs. (c) U2OS RNF168-GFP cells were pre-treated with MG132 for 2h, irradiated with 2Gy and 1h post-irradiation immunostained for γH2AX and 53BP1. Scale bar 10 μM. (d) U2OS RNF168-GFP cells were mock or MG132 treated (2h, 5μM), irradiated (2Gy) and 1h post-irradiation stained for 53BP1 and scored for nuclei with45 53BP1 IRIFs. The chart shows one of three consistent repeats. (e) U2OS and U2OS RNF168-GFP cells were lysed and probed for RNF168 levels by immunoblotting. The total level of RNF168 in U2OS RNF168-GFP is approximately fivefold higher than in U2OS. In (A, B and D), the

charts show one out of three consistent experiments (f) The U2OS RNF168-GFP line was transfected with indicated siRNAs, treated with MG132 (5μM, 2 h), irradiated (2 Gy) and 1 h post-irradiation stained for 53BP1. Cells with >53BP1 IRIF were counted.
(g) U2OS RNF168-GFP line was treated with MG132 (5μM, 2 h), irradiated (2G)y and 1h post-irradiation analysed for number of 53BP1 foci and RNF-GFP signal intensity.

9.7 WIDER OCCURENCE OF THE PROTEOTOXIC-STRESS RESISTANT PHENOTYPE AMONG CANCER CELL LINES WITH DIFFERENT ORIGIN

Next, we asked whether the observed phenotype in MDA-MB-231 cell line is unique or can be more widespread.

The wider occurrence of proteotoxic stress resistant DDR among different tumor cell lines would raise a question whether it might represent a means of adaptation or provide some selective advantage(s) during tumorigenesis. Cancer cells suffer from increased endogenous proteotoxic stress that stems from such features as aneuploidy, mutation overload, variation of gene copy number and levels of transcription which eventually leads to accumulation of altered/aberrant proteins (Deshaies, 2014; Luo et al., 2009). We propose that apart from placing a significant burden on the protein quality control mechanisms (Luo et al., 2009) , proteotoxic stress also impacts on DSB response via attenuating the ubiquitin driven signaling at damaged chromatin. Of note, the load of endogenous DSBs increases during cell transformation and tumor progression because of enhanced replication stress evoked by diverse oncogenes and loss of some tumor suppressors (Bartkova et al., 2005, 2006; Burrell et al., 2013; Di Micco et al., 2006; Gorgoulis et al., 2005). Given its pathophysiological significance, aberrations in the DSB ubiquitination signaling pathway might profoundly affect genome integrity of tumor cells.

Firstly, we tested a panel of human cancer cell lines treated by proteasome inhibitor for occurrence of 53BP1 IRIF. Surprisingly, we observed the proteotoxic stress-resistant DSB response phenotype in several other cancer cell lines apart from MDA MB 231 (Figure 9.7 A). Breast cancer cell line MCF7 and cervical cancer-derived HeLa cells were proficient for proteotoxic stress-resistant phenotype analogous to MDA-MB-231 while another breast cancer cell line MDA-MB-436 was phenotypically similar to the control U2OS cells (Figure 9.7 A). Importantly, all cell lines displaying proteotoxic stress-resistant DSB response showed elevated RNF168 (Figure 9.7 B and C). The protein levels of RNF8 and UBC13 in MCF7 and

HeLa cell lines showed only slightly if any increase, in contrast to more pronounced elevation of RNF168 (Figure 9.7 B).The situation in these lines seems to be reminiscent of that in the RNF168-GFP overexpressing U2OS line underlining the central role of the RNF168 ligase in the phenotype.

Given the wide occurrence of the phenotype, we asked whether it might represent some kind of phenotypical adaptation beneficial for tumor cells. Cancer cells are known to experience higher load of genotoxic stress including DSBs (Bartek et al., 2007; Halazonetis et al., 2008) and enhanced proteotoxic stress (Deshaies, 2014), which might possibly attenuate the ubiquitin-mediated DSB response pathway through chronic limitation of free ubiquitin. We hypothesized that a proteotoxic stress-resistant DSB response may help cells to counteract the adverse effects of proteotoxic stress on DSB signaling and thereby support cancer cell viability. When four cell lines from our panel were treated with MG132 and subsequently irradiated, their survival positively correlated with their respective abilities to sustain the DSB response under such proteotoxic stress conditions. The cell lines MDA-MB-231 and MCF7 that display the proteotoxic stress-resistant DSB response showed significantly higher survival compared with the control U2OS and BJ cells (Figure 9.7 E). One of the most prominent signs of chronic proteotoxic stress is accumulation of ubiquitin-conjugated proteins because of cellular protein quality control and UPS overload. The accumulation is detectable by immunoblotting and immunostaining techniques using antibodies recognizing protein-conjugated ubiquitin. To test whether the increased resistance to combined irradiation and proteasome inhibition (Figure 9.7 E) correlated with higher loads of endogenous proteotoxic stress, we compared the levels of conjugated ubiquitin in our panel of cell lines (Figure 9.7 D) by immunoblotting using an antibody against K48 linked ubiquitin. Pronounced conjugate accumulation in both MDA-MB-231 and MCF7 cells was apparent compared with BJ and U2OS cells (Figure 9.7 D). This finding was consistent with our hypothesis that the increased tolerance to simultaneous irradiation and proteasome inhibition in the MDA-MB-231 and MCF7 lines might reflect adaptation to chronic inherent proteotoxic stress experienced by tumor cells.

Altogether, our findings show that attenuation of DSB signaling because of proteotoxic stress might be circumvented by upregulation of one or more key ubiquitin ligases involved in the DDR, particularly RNF168.

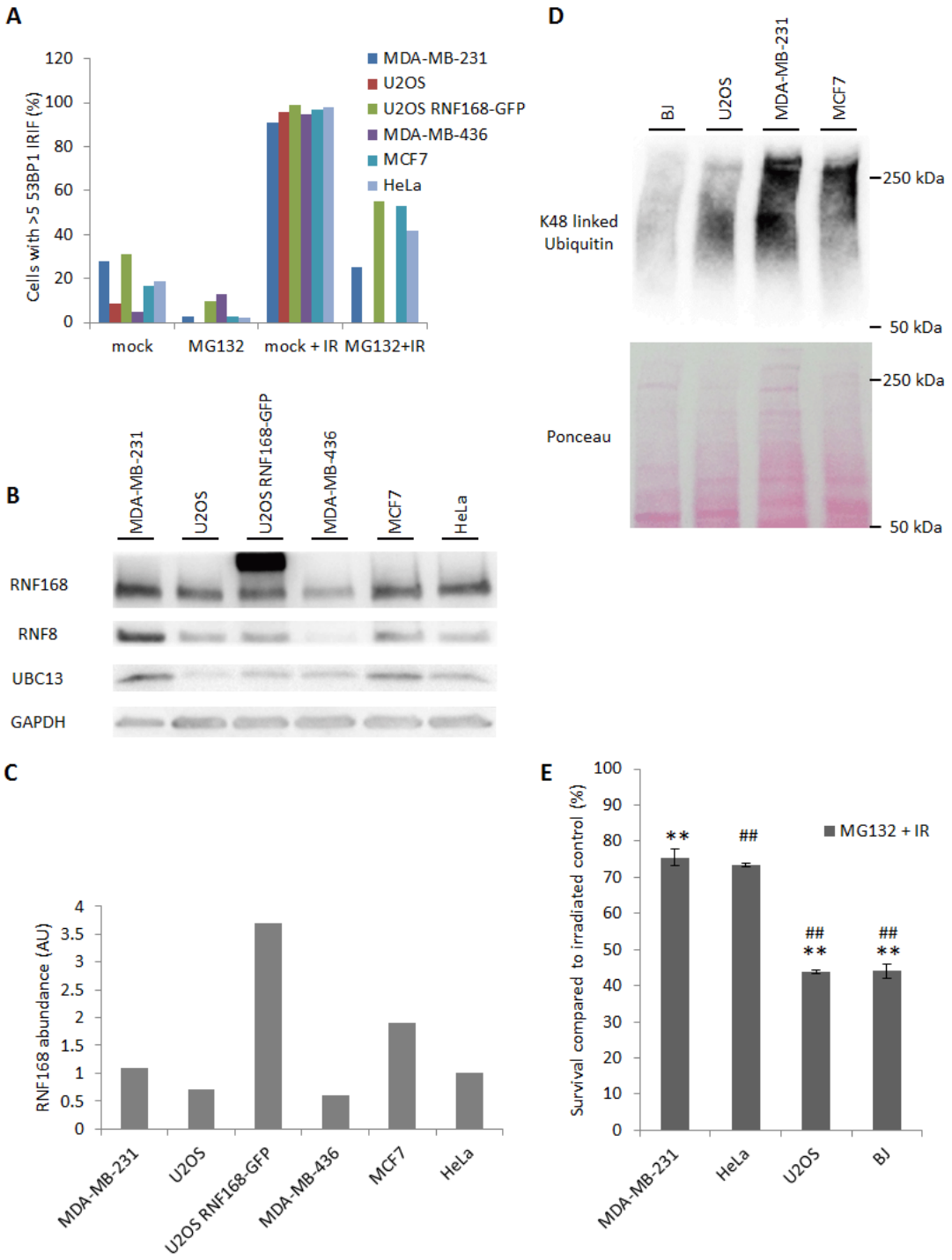

Figure 9.7: The proteotoxic stress-resistant DSB response phenotype is shared by other cancer cell lines. (a) Indicated cells lines were mock- and MG132 treated (2h, 5µM), either with or without irradiation (2Gy) and 1h post-irradiation stained for 53BP1. Nuclei with >5 53BP1 IRIFs were scored. (b) Lysates prepared from the lines in (a) were probed for RNF8, RNF168 and UBC13 levels by immunoblotting. (c) RNF168 band intensity was quantified and normalized according to the total protein levels in the indicated lines. (d) Indicated cell lines were probed for the level of conjugated K48 linked ubiquitin by immunoblotting. Equal protein amounts were loaded for all the cell lines. (e) Indicated cell lines displaying various levels of RNF168 expression were pretreated with 5µM MG132

(2 h), irradiated with 2Gy and 1h post-treatment seeded to Petri dishes. Six days post-irradiation, the cells were trypsinized and counted using an automated cell counter. In (a and e), results are mean±s.d. of three independent experiments. Statistical significance was determined with two-tailed unpaired Student's t-test; **,##P‹0.005.

9.8 PROTEOTOXIC STRESS-RESISTANT DSB RESPONSE PHENOTYPE EXPERIENCED BY MULTIPLE MYELOMA CANCER CELLS

Proteasome inhibitors have been successfully used in the treatment of multiple myeloma and other hematological malignancies (Chauhan et al., 2005) . Besides pro-apoptotic effects, one of the proposed modes of action of these inhibitors is further exacerbation of the high intrinsic proteotoxic stress in the immunoglobulin producing myeloma cells thus causing a lethal unfolded protein response (Deshaies, 2014). Given the high endogenous levels of proteotoxic stress in myeloma cells, we asked whether myelomas show a similarly 'adapted' DSB response, reminiscent of some carcinoma cell lines such as MDA-MB-231.

We therefore probed two human myeloma cell lines, AMO1 and MMS1, for their ability to form 53BP1 IRIFs after MG132 treatment. Strikingly, the proteotoxic stress-resistant DSB response phenotype in these myeloma cell lines was even more pronounced than in the MDA-MB-231 cells, as 60% and 90% of AMO1 and MMS1 myeloma cells, respectively, formed more than five 53BP1 IRIFs under proteasome inhibition conditions (Figures 9.8 A and B). Similarly to MDA-MB-231 and other cancer cell lines that share the proteotoxic stress-resistant DSB response, the ability to sustain 53BP1 IRIF formation after MG132 treatment correlated with elevated RNF168. Protein levels of RNF168 in AMO1 and MMS1 cells exceeded not only those seen in BJ and U2OS cells, but even that in MDA-MB-231 cells (Figure 9.8 C). As expected, both AMO1 and MMS1 cell lines showed grossly elevated levels of intrinsic proteoxic stress manifested by accumulation of poly-ubiqutinated proteins and the BiP protein an established marker of proteotoxic stress and ubiquitin-proteasome response (UPR) activation (Figure 9.8 C) (Gething, 1999).

Taken together, these results further support the possibility that the proteotoxic stress-resistant DSB response indeed represents an adaptation to chronic proteotoxic stress experienced by tumors.

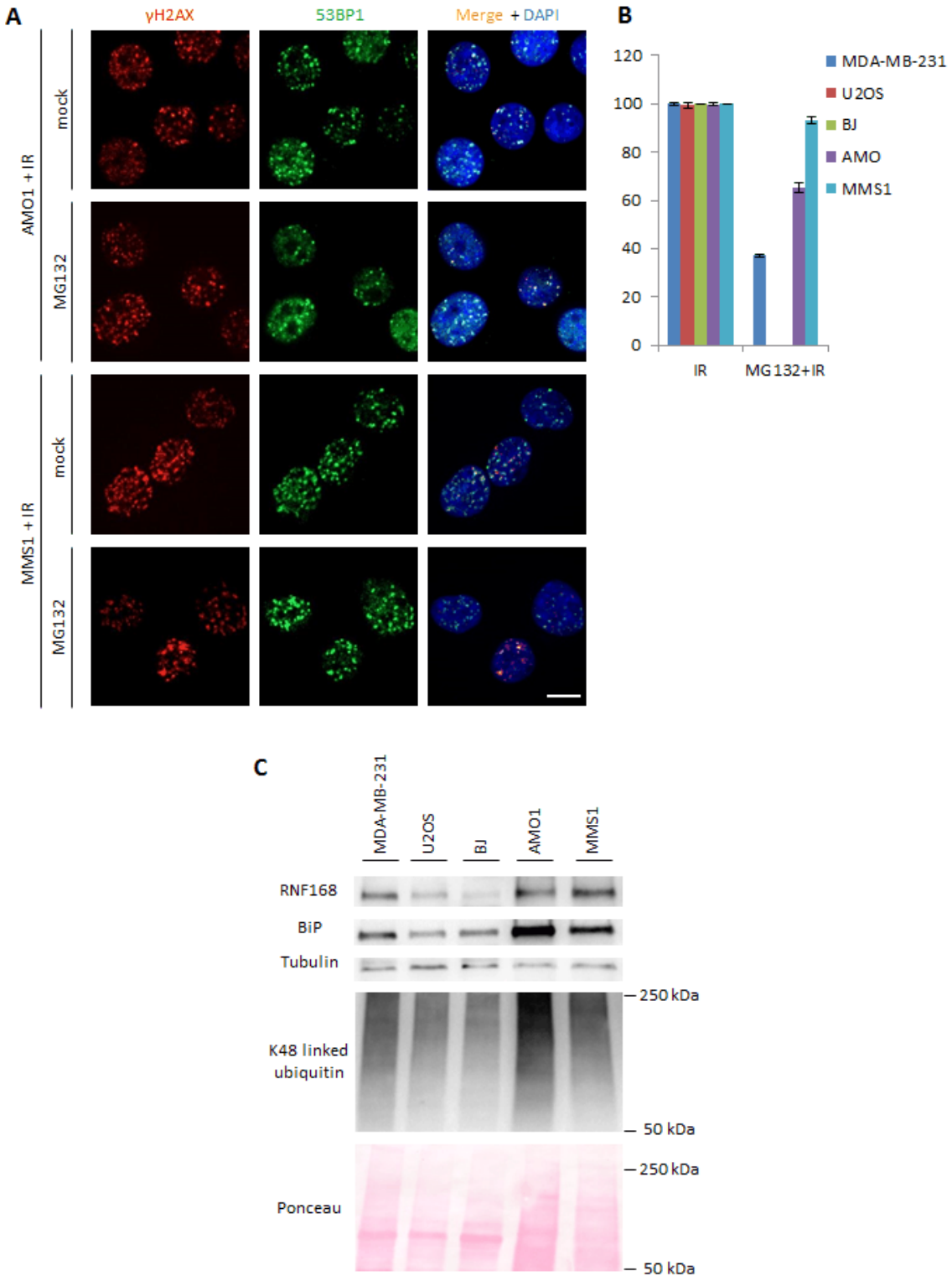

Figure 9.8: Multiple myeloma cell lines exhibit the RNF168-fueled proteotoxic stress-resistant DSB response. (A and B) AMO1 and MMS1 cell lines were mock- and MG132-treated (2h, 5μM), either with or without irradiation (2Gy) and 1h post-irradiation stained for >53BP1. Nuclei with 5 53BP1 IRIFs were scored. Scale 10μM. (C) Indicated cell lines were probed for the level of conjugated

K48 linked ubiquitin, RNF168 and BiP by immunoblotting. Equal protein amounts were loaded for all the cell lines. In (b), results are mean ±s.d. of three independent experiments.

9.9 OVERABUNDANT RNF168 SHIFTS DSB REPAIR TOWARDS NHEJ, ENHANCES GENOMIC INSTABILITY AND VULNERABILITY TO PARPi AND CAMPTOTHECIN

Based on previous results, we hypothesized that MDA-MB-231 and some other cancer cell line capable of DSB signaling despite proteotoxic stress may deviate from normal cells and from other cell lines in various aspects of their genome integrity control.

53BP1 is known to promote mutagenic NHEJ by blocking end resection which results in hypersensitivity towards chemotherapeutic agents that damage DNA in S-phase cells, such as PARP inhibitors (PARPi) and topoisomerase inhibitors (Bunting et al., 2010). Given the overt, RNF168 driven recruitment of 53BP1 we expected the MDA-MB-231 and other cancer cell line to exhibit a shift in DNA repair pathway preference towards the NHEJ that would lead to substantial sensitivity to the above mentioned inhibitors, acting mainly in S-phase. This might mimic previously described situation of cells depleted for BRCA1, known to limit 53BP1 chromatin loading during S phase. Under such conditions, the RNF168-driven 53BP1 recruitment was shown to preclude DSB end resection and thereby HR, whereas boosting DNA repair by the mutagenic NHEJ pathway (Muñoz et al., 2012, 2014; Zong et al., 2015).

Immunofluorescence analysis indicated that while 60% of S-phase MDA-MB-231 cells treated by a PARPi displayed over 10 53BP1-positive foci per nucleus, in U2OS the fraction of such cells was significantly lower (Figure 9.9.1 A, B). Given the similar cell cycle phase profiles of both cell lines (data not shown) and the fact that the DSBs caused by PARPi commonly occur during S phase and are particularly repaired by HR the efficiency of which is affected by 53BP1 recruitment (Bouwman et al., 2010; Bunting et al., 2010) these results suggested that such unscheduled recruitment of 53BP1 might alter the balance between the major DSB repair pathways.

The latter possibility would also correlate with the ability of 53BP1 to promote mutagenic NHEJ (mutNHEJ) by blocking DSB end resection, resulting in hypersensitivity toward chemotherapeutic agents that damage DNA in S-phase cells, including PARPi and camptothecin (Bouwman et al., 2010; Bunting et al., 2010). To test this assumption in a

syngeneic system, we employed generated clones of MDA-MB-231 cells expressing a doxycycline (DOX)-inducible shRNA against RNF168 to validate the partial knockdown of RNF168 in these models by immunoblot (Figure 9.9.1 C). Next, we measured the ratio of mutNHEJ/HR repair modes by introducing into the RNF168-regulatable cell lines the so-called Traffic light system (Certo et al., 2011), a reporter that enables flow-cytometric analysis of repair pathway choice at individual I-SceI induced DNA breaks. Quantification of red (mutNHEJ) and green (HR) repair events then provides information on the overall proportion of the two pathways in the analyzed cell population. A representative example of such experiment shown in Figure 9.9.1 D indeed supports the RNF168-dependent repair shift, as the cells with DOX-induced partial RNF168 knockdown showed a lower mutNHEJ/HR ratio. Furthermore, consistent with the high and low levels of RNF168,respectively, the mutNHEJ/HR ratio was more than sixfold higher in the parental MDA-MB-231 cells compared with the parental U2OS cells (Figure 9.9.1 E).

Excessive mutNHEJ leads to frequent chromosome aberrations and genome rearrangements that might contribute to tumor heterogeneity (Rodgers and McVey, 2016; Zong et al., 2015). To examine whether the RNF168-driven upregulation of mutNHEJ makes the MDA-MB-231 line more prone to genome rearrangements, we used the DOX-inducible RNF168 knockdown model in MDA-MB-231 cells and compared numbers of micronuclei in DOX-induced and non-induced cells pretreated by a topoisomerase I inhibitory drug camptothecin (CPT). The number of micronuclei was indeed significantly lower in the Dox-induced cells with lowered RNF168 level and hence a more proficient HR repair because of less robust recruitment of 53BP1 (Figure 9.9.1 F).

These results support a plausible scenario that the aberrantly upregulated RNF168 protects cancer cells from adverse effects of proteotoxic stress on the DDR, however, only at the expanses of increased genomic instability.

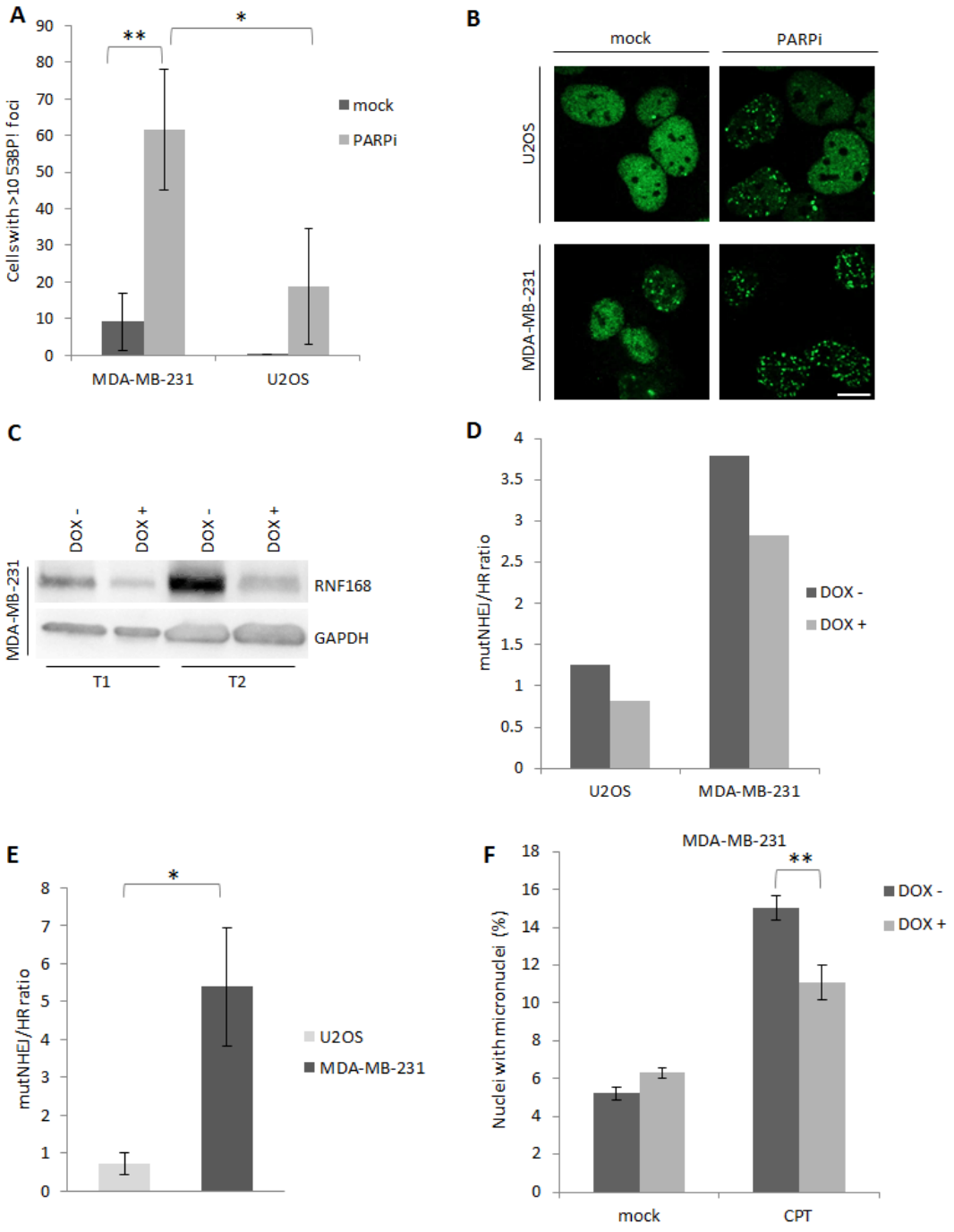

Figure 9.9.1: Overabundant RNF168 causes unscheduled 53BP1 recruitment, increased mutNHEJ pathway activity and micronuclei formation.
(a) MDA-MB-231 and U2OS cells were mock or PARPi (10μM, 24h) treated, immunostained for 53BP1 and cyclin A. Cyclin A-positive cells with >10 53BP1 foci were scored. (b) Representative images of 53BP1 immunostained cells from (a). Scale 10 μM. (c) The MDA-MB-231 DOX-inducible knockdown cells were pretreated with DOX (DOX, 100ng/ml; 72 h: T1 or 96 h: T2), lysed and probed for RNF168. After the 72h pre-treatment, the RNF168 levels were >2.5 times lower in the DOX-treated cells compared with controls (T1). The endpoint (96-h knockdown) RNF168 levels are shown in the T2 panel. (d) The effect of RNF168 level on the mutNHEJ/HR ratio was assessed in the MDA-

MB-231 and U2OS cell lines bearing the DOX-inducible RNF168 knockdown and the Traffic light reporter. Stable reporter cell lines were pretreated with DOX as in (a) and subsequently transduced with a lentivirus carrying an HR repair template and an I-SceI gene. Five days posttransduction, cells were examined by flow cytometry for mCherry and GFP signal. The NHEJ/HR ratio was calculated by correlating the numbers of red (NHEJ) and green (HR). (e) Analogous to (d), assessed in the parental U2OS and MDA-MB-231 cell lines only. (f) MDA-MB-231 cells were pretreated with DOX as above, then mock or CPT treated (10 nM. 24 h) and nuclei/micronuclei were counterstained with DAPI. Fraction of micronuclei in the DAPI-stained objects was determined. In (a, e and f), results are mean±s.d. of three independent experiments. Statistical significance was determined with two-tailed unpaired Student's t-test; *Po0.05; **P‹0.005.

Based on previously reported results showing the altered balance of DSB repair pathway choice toward higher mutNHEJ in cells with dysregulated RNF168-53BP1 pathway, we wanted to test , whether this can impact cell viability under exposure to S-phase genotoxic insults, that require HR for efficient DNA repair (Zong et al., 2015). We employed a MDA-MB-231 cell line that enabled doxycycline (DOX) inducible partial shRNA knockdown of RNF168. As illustrated in the figure 9.9.2 A, the DOX-induced cells with decreased RNF168 levels were significantly less sensitive to CPT, than the noninduced counterpart cells. We interpret the observed decrease in CPT sensitivity upon RNF168 knockdown as further evidence for upregulation of NHEJ and the following genomic instability in the MDA-MB-231 cells driven by increased level of RNF168. Surprisingly, the MDA-MB-231 knockdown cell line did not show a significant change in sensitivity toward PARP1 inhibition, which is also known to be particularly toxic to cells with deregulated NHEJ (Bunting et al., 2010). We reasoned that this might be caused by only slight degree of RNF168 knockdown achieved in the MDA-MB-231 cells. To verify this possibility, we established and tested a MCF7- derived RNF168 knockdown cell line for sensitivity to CPT and the KU58948 PARP1 inhibitor. Indeed, MCF7 cells that share with MDA-MB-231 cells also the RNF168-fueled proteotoxic stress-sresistant DSB response proved to be more amenable to the DOX inducible RNF168 knockdown as the RNF168 level dropped >3.5- fold upon DOX treatment (Figure 9.9.2 B). Another important reason for including MCF7 was the fact that, along with MDA-MB-231, MCF7 cells exhibited significant PARPi sensitivity, despite both these breast cancer cell lines are BRCA1/BRCA2 proficient (Bunting et al., 2010). We suggested that the observed sensitivity to PARPi might be at least partly attributable to the RNF168 overabundance and the ensuing shift of the mutNHEJ/HR ratio, thereby creating a partial, relative ‘HR deficiency’ despite the proficient BRCA1/2 genes. Consistent with such possibility, the MCF7 cells

showed significantly lower cell sensitivity toward both CPT and the PARPi upon RNF168 partial knockdown (Figure 9.9.2 C).

Thus, apart from providing another piece of evidence for aberrant upregulation of NHEJ in these cell lines, this result might also represent an important clue for better understanding of PARPi sensitivity in BRCA1/2-proficient tumors.

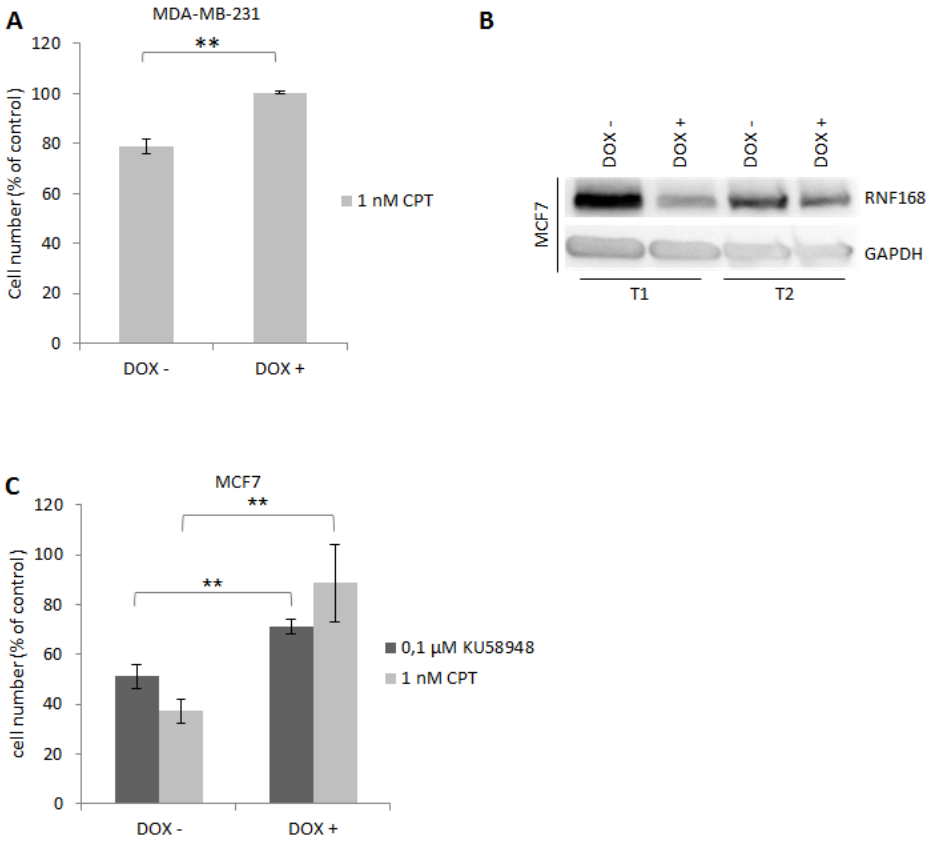

Figure 9.9.2: RNF168 overabundance sensitizes MDA-MB-231 and MCF7 cells to CPT and PARPi. (a) Sensitivity of the MDA-MB-231 RNF168 knockdown cells toward CPT was assessed by a cell survival assay. The cells were pretreated with DOX as above and then treated with 1 nM CPT. After 6 days, the cells were trypsinized and counted using an automated cell counter. (b) The MCF7 DOX-inducible knockdown cell line was pretreated with DOX (DOX, 100 ng/ml; 72h: T1 or 96 h: T2), lysed and probed by immunoblotting for RNF168. After the 72h pre-treatment, the RNF168 levels were >3.5-fold lower in the DOX-induced cells than in the non-treated control cells (T1). (c) Sensitivity of the MCF7 RNF168 knockdown cells toward CPT and KU58948 was assessed as in (a). In (a and c), results are mean ±s.d. of three independent experiments. Statistical significance was determined with two-tailed unpaired Student's t-test; **P‹0.005.

Taken together, our findings show that BRCA1-proficient cells bearing overabundant RNF168 mimic, at least to some extent, the BRCA1-deficient phenotype by displaying lower levels of HR at the expense of upregulated mutNHEJ. We show that this is most likely caused by aberrantly enhanced 53BP1 recruitment in S-phase cells that is fueled by the excess of RNF168. Similar scenario was proposed in studies involving mouse B cells and embryonic fibroblasts, where it has been shown that the overabundant RNF168 inhibits efficient DSB end resection and fuels DSB repair by the mutagenic NHEJ pathway (Zong et al., 2015). The RNF168 overexpression seems to derail the physiological balance of the DSB repair pathways toward 53BP1 recruitment and mutNHEJ. We speculate that this imbalance leads to 'conditional HR deficiency' especially under chronic proteotoxic stress conditions, and might account for (or contribute to) the observed increased sensitivity of certain BRCA1-proficient (and principally also HR-proficient) tumorssuch as subsets of triple-negative breast carcinomas, toward PARPis (Inbar-Rozensal et al., 2009; Livraghi and Garber, 2015).

9.10 OVEREXPRESSION OF RNF168 CORRELATES WITH INCREASED ENDOGENOUS PROTEOTOXIC STRESS IN BONE MARROW SAMPLES OF PATIENTS DIAGNOSED FOR MULTIPLE MYELOMA

To validate our experimental data from multiple myeloma cell lines also in clinical regimen, we decided to further analyse malignant plasma cells (PCs) derived from bone marrow patients diagnosed for multiple myeloma (MM). Multiple myeloma, a malignancy of terminally differentiated B-Lymphocytes- plasma cells is characterized by proliferation of plasma cell clones producing abnormal antibody called paraprotein mainly in the bone marrow (Kyle et al., 2003). The disease is known to be preceded by a pre-malignant condition of monoclonal gammopahy of uknown significance (MGUS), shifted to MM and becoming more aggressive in association with obtained genetic mutations, chromosomal abnormalities and gene expression signatures (Bergsagel and Kuehl, 2005; Chapman et al., 2011; Fonseca et al., 2009; Magrangeas et al., 2011).

MM cells, similar to their normal counterparts, produce significant excess amount of proteins (namely paraprotein, immunoglobulins), making them more dependent on homeostatic mechanism of unfolded protein response (UPR) (Meister et al., 2007). This

together with other specific MM properties (elevated level of NF-kB, lower threshold of lethal UPR etc) is the key feature for MM cells sensitivity to perturbation of protein degradation by proteasome inhibitors (PIs) (Meister et al., 2007).

Therefore the inhibition of proteasome by bortezomib (BTZ) is highly cytotoxic to plasma cells of multiple myeloma and bortezomib has been effective therapy for treating patients with this disease (Hideshima et al., 2005). However, while initially effective, patients eventually relapse to proteasome inhibitor class of drugs and become (Anderson, 2016; Greenlee et al., 2000). This is opening a window for further research of molecular pathways and proteins involved in mechanisms of cellular homeostasis enabling a compensatory response to proteasome inhibition, such contributing to MM drug resistance. Furthemore, specific association of intrinsic proteotoxic stress in MM patient's cells with function or expression level of some ub-related enzymes might reveal a new important diagnostic and prognostic biomarker in MM.

As described in a Figures 9.7 D and 9.8 C, the hightened intrinsic proteotoxic stress in cancer cells correlates with elevated level of RNF168 ligase, which likely reflects adaptation to the chronic free ubiquitin shortage. In order to validate our finding on clinical material, we processed and analysed bone marrow samples from 6 patients diagnosed either for MGUS or MM having different clinical history. The samples were acquired in cooperation with hematoncology department (University Hospital in Olomouc). We isolated MM plasma cells using immunomagnetic separation method applying magnetic beads conjugated with CD138 antibidy (syndecan 1; SCD1), which is generally preferred because of its plasma cell specificity (Lin et al., 2004; San Miguel et al., 2006). We confirmed efficient immunomagnetic separation of CD138+ plasma cells by FACS analysis, detecting signal of CD138-PE antibody and percentage of isolated CD138+ plasma cells from starting sample of the bone marrow, CD138- and CD138+ fraction (Figure 9.12 A).

In order to identify RNF168 level in tested samples we performed immunoblot of CD138+ plasma cells and their negative counterpart for presence of RNF168 as well as BiP, previously established marker of endogenous proteotoxic stress (Gething, 1999). To further asses the magnitude of RNF168 upregulation we analysed MM patient's samples in parallel with BJ- low RNF168 cell line and AMO1-high RNF168 MM cell line, which served also as a positive control for marker of MM plasma cells, MUM1. To see wether bortezomib therapy

might affect the level of RNF168 in the cell line model, we included two additional AMO1 cell lines, AMO1 wild type (AMO1-WT) and the AMO1-BTZ, that has undergone continuous bortezomib exposure for > 12 months. Our preliminary data show that CD138 and MUM1 positivity of MM plasma cells correlates with heightened level of proteotoxic stress in 3 different samples. Furthermore, in all samples MUM1 abundance correlated with elevated E3 RNF168 (Figure 9.12 B, C).

Interestingly, the upregulation of RNF168 seems to be independent of the disease stage as it was identified in MM as well as in MGUS bone marrow samples. These findings suggest the RNF168 expression level might serve as a useful diagnostic marker of assessing drug sensitivity in multiple myeloma and monoclonal gammopathy of uknown significance.

In addition to this, results from Herrero and colleagues showing presence of altered-hyperactivated DSB repair pathways in MM cell lines might give us alternative explanation of elevated RNF168 present in patients diagnosed for multiple myeloma. Interpretation of our results in line with previously mentioned study, hyperactivated RNF168 driven NHEJ pathway in MM cells might contribute to the repair of endogenous DNA damage but also increase genome instability, resulting in disease progression and acquisition of drug resistance (Herrero et al., 2015).

However, our preliminary data need to be analysed further and extended by more samples from MM patients with different diagnosis and therapy to substantiate the biological importance of studied phenomenon and validate the increased level of RNF168 as a new diagnostic feature of MM plasma cells or possible biomarker of responsiveness to bortezomib therapy.

A

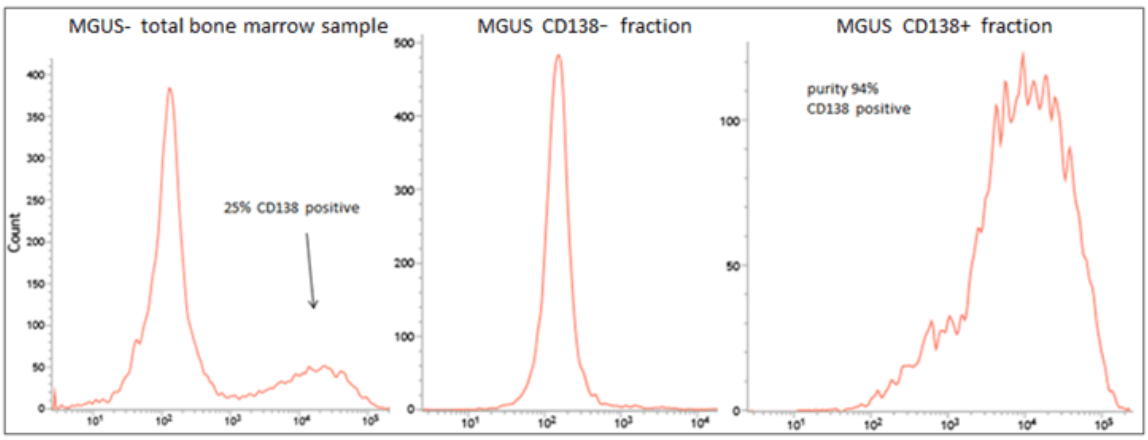

Figure 9.10 continues on the next page

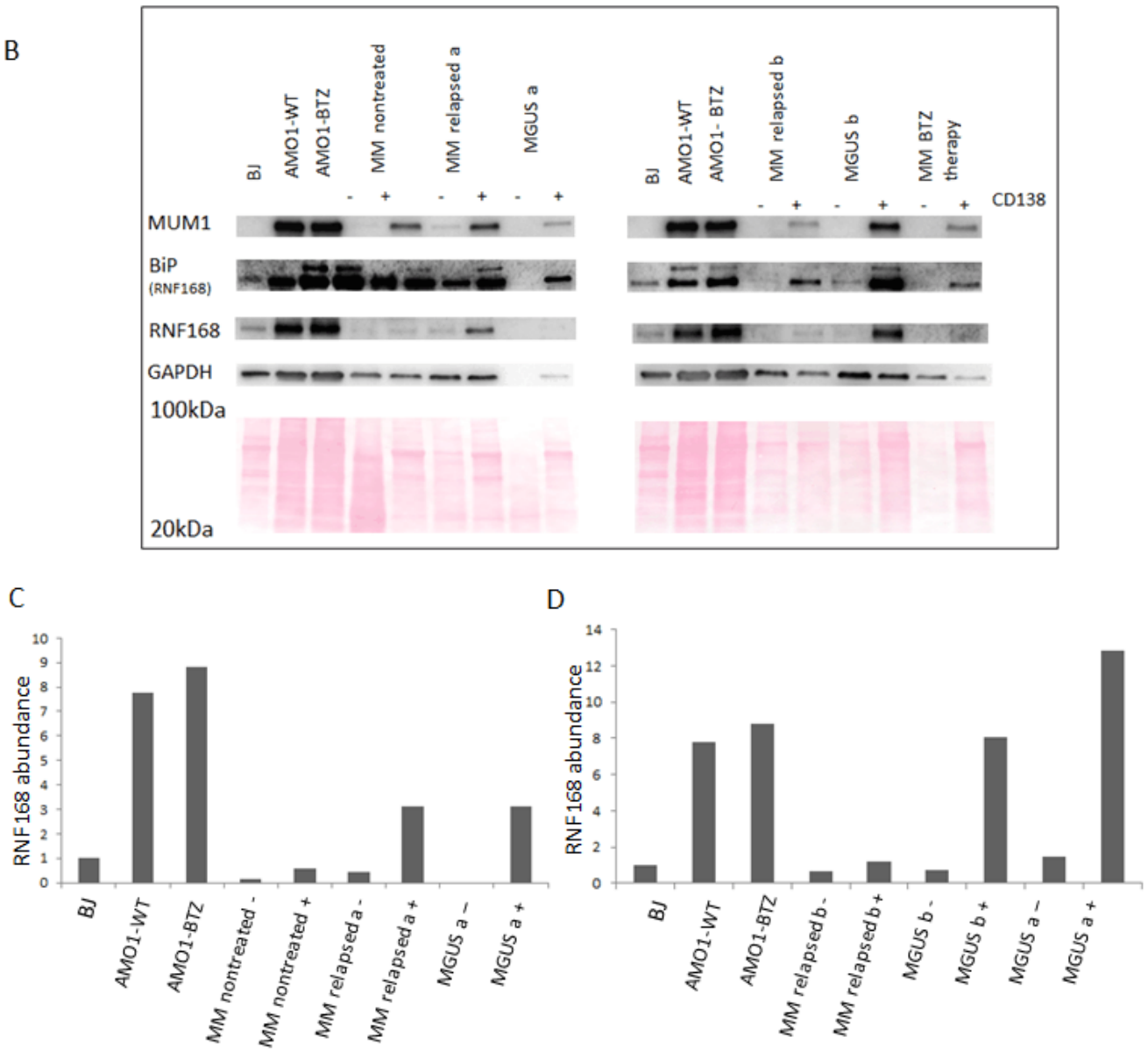

Figure 9.10: CD138 positive plasma cells from 6 patients with MM and MGUS exhibit increased level of RNF168

(a) Starting bone marrow fraction, isolated CD138+ plasma cells and CD138- cells were tested for CD138 positivity by FACS using CD138-PE antibody.(b) Lysates prepared from isolated CD138+ and CD138- cells from bone marrow of 6 patients were probed for PCs marker-MUM, endogenous proteotoxic stress-BiP and abundance of RNF168 by immunobloting. (c) RNF168 band intensity was quantified and normalized according to the total protein levels in the indicated lines.

From a broader perspective, our present study contributes to better understanding of genome integrity maintenance and points to previously unrecognized wide occurrence and impact of aberrant ubiquitin-mediated signaling of DNA damage under proteotoxic stress, with the ensuing consequences for genomic instability and responses to cancer treatment. Our results suggest that human tumors can be widely categorized into two subsets, featuring 'standard' and 'proteotoxic stress-resistant' responses to DNA breakage, respectively. The latter tumor category, discovered and characterized here, may represent an adaptive scenario of 'conditional/secondary' rather than 'genetically caused/primary' HR deficiency, with implications for genomic instability and selective advantages, but also potential vulnerabilities of such cancers.

Our findings further show that attenuation of DSB signaling because of proteotoxic stress might be circumvented by upregulation of one or more key ubiquitin ligases involved in the DDR, particularly RNF168. Importantly, this concept was supported by observation of the proteotoxic stress-resistant DSB response in multiple myeloma cells, an established model of cancer-related proteotoxic stress. It has been also reported that breast cancers exhibit elevated levels of some E2 ubiquitin conjugating enzymes (Chen and Madura, 2005). Taken together, this implies that upregulation of some ubiquitin-mediated cellular processes might represent a more general strategy to overcome adverse effects of cancer- associated proteotoxic stress. UPS has a major role in the regulation of several key tumorigenesis driving processes, such as cellular proliferation, apoptosis and stress tolerance (Deshaies, 2014; Velimezi et al., 2013). Hence, it is likely that these pathways are sensitive to proteotoxic stress and tumor cells have evolved compensatory mechanisms such as the upregulation of specific enzymes of the UPS. In terms of potential selective advantages during tumorigenesis, the acquired overabundance of RNF168 can help enhance survival of cancer cells under combined proteotoxic and replication stresses, fuel error-prone DNA repair, genomic instability and thereby intratumor heterogeneity (Figure 9.11), all features likely to promote tumor progression and aggressivity.

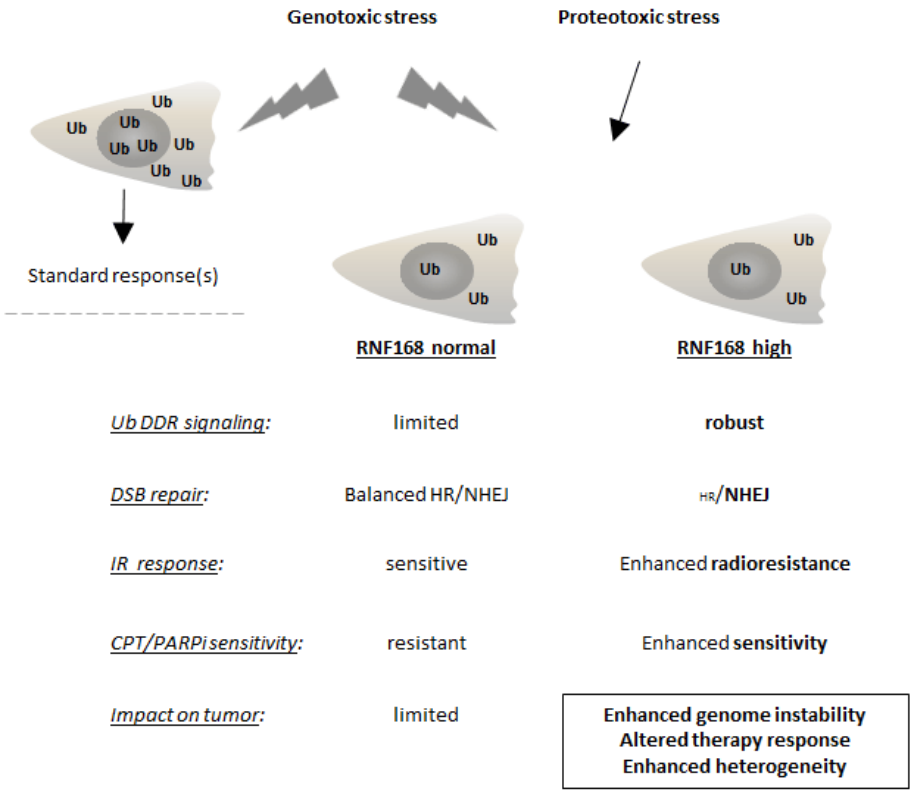

Figure 9.11: Model summarizing the proteotoxic stress-resistant DSB response and its impact on cancer cells. Changes in chromosome or gene copy number and transcription (de)regulation in cancer cells result in protein overproduction that overwhelms the cellular protein quality control, causing chronic proteotoxic stress and diminishing levels of free ubiquitin. The limited free ubiquitin supply has to be shared by diverse ubiquitin-dependent processes whose efficiency, including that of DSB signaling, is impaired. This is manifested by increased radiosensitivity. Overexpression of RNF168 (and other key DSB response ubiquitin-related enzymes) in the proteotoxic stress-resistant cells shifts the free ubiquitin equilibrium toward DSB signaling thus increasing radioresistance. Overexpression of RNF168 and concomitant robust 53BP1 recruitment promotes mutNHEJ at the expense of HR repair, rendering the cells sensitive to topoisomerase and PARPis, and leading to enhanced genomic instability. Such changes collectively impact tumor heterogeneity, progression and responses to therapy.

10 SUMMARY

Chromatin DNA damage response (DDR) is orchestrated by the E3 ubiquitin ligase ring finger protein 168 (RNF168), resulting in ubiquitin-dependent recruitment of DDR factors and tumor suppressors breast cancer 1 (BRCA1) and p53 binding protein 1 (53BP1).This ubiquitin signaling regulates pathway choice for repair of DNA double-strand breaks (DSBs), toxic lesions whose frequency increases during tumorigenesis. Recruitment of 53BP1 curbs DNA end resection, thereby limiting homologous recombination (HR) and directing DSB repair toward error-prone non-homologous end joining (NHEJ). Under cancer-associated ubiquitin starvation conditions reflecting endogenous or treatment-evoked proteotoxic stress, the ubiquitin-dependent accrual of 53BP1 and BRCA1 at the DNA damage sites is attenuated or lost. Challenging this current paradigm, we identified diverse human cancer cell lines that display 53BP1 recruitment to DSB sites even under proteasome inhibitor-induced proteotoxic stress, that is, under substantial depletion of free ubiquitin. We show that central to this unexpected phenotype is overabundance of RNF168 that enables more efficient exploitation of the residual-free ubiquitin. Cells with elevated RNF168 are more resistant to combined treatment by ionizing radiation and proteasome inhibition, suggesting that such aberrant RNF168-mediated signaling might reflect adaptation to chronic proteotoxic and genotoxic stresses experienced by tumor cells. Moreover, the overabundant RNF168 and the ensuing unorthodox recruitment patterns of 53BP1, RIF1 and REV7 (monitored on laser micro-irradiation-induced DNA damage) shift the DSB repair balance from HR toward NHEJ, a scenario accompanied by enhanced chromosomal instability/micronuclei formation and sensitivity under replication stress-inducing treatments with camptothecin or poly(ADP-ribose) polymerase (PARP) inhibitor. Overall, our data suggest that the deregulated RNF168/53BP1 pathway could promote tumorigenesis by selecting for a more robust, better stress-adapted cancer cell phenotype, through altered DNA repair, fueling genomic instability and tumor heterogeneity. Apart from providing insights into cancer (patho)biology, the elevated RNF168, documented here also in clinical bone marrow tumor specimens may provide a new plausible diagnostic or even prognostic biomarker of responses to standard-of-care and some emerging targeted therapies for multiple myeloma.

11 SÚHRN

Odpoveď na DNA poškodenie na úrovni chromatínu je regulovaná prostredníctvom E3 ubiquitín ligázy ring finger proteínu 168 (RNF168), ktorej výsledkom je ubiquitín-závislá väzba DDR faktorov a tumorsupresorov BRCA1 a 53BP1. Táto ubiquitín-závislá signalizácia usmerňuje výber vhodnej opravnej dráhy dvojvláknových zlomov DNA (DSBs), toxických poškodení, ktorých početnosť v priebehu tumorigenézy narastá. Väzobná aktivita 53BP1 limituje proces resekcie DNA, tým pádom aj opravu DSBs homologickou rekombináciou (HR) a spúšťa chybovú opravnú dráhu DSBs-nehomologické spájanie koncov (NHEJ). Za podmienok endogénneho alebo indukovaného deficitu ubiquitínu, ktorý je bežný v bunkách nádorov, dochádza k poklesu ubiquitín zavislej väzby alebo úplnej strate proteínov 53BP1 a BRCA1 v miestach poškodenia DNA.

Napriek tomuto všeobecne akceptovanému modelu sa nám podarilo identifikovať niekoľko nádorových bunkových línií schopných uskutočniť väbu proteínu 53BP1 do miest DSB aj v podmienkach inhibítorom indukovaného proteotoxického stresu a deficitu ubiquitínu. Predovšetkým poukazujeme na kľúčový menovateľ pre daný fenotyp, ktorým je zvýšená hladina E3 ubiquitín ligázy RNF168 umožňujúca efektívne využitie reziduálneho ubiquitínu prítomného v bunke. Bunky so zvýšenou hladinou RNF168 sú rezistentnejšie na kombinovanú terapiu gamma žiarením a inhibítorom proteazómu, čo naznačuje možnú spojitosť deregulácie RNF168 s adaptáciou danej rakovinovej bunky na endogénny proteotoxický stres, ktorému je takáto bunka prirodzene vystavená. Zvýšená hladina RNF168 podmieňujúca špecifickú väzbu 53BP1, RIF1 a REV7 (monitorovaná prostredníctvom laserom-indukovaného poškodenia DNA) má za následok posun rovnováhy opravných dráh k prevahe NHEJ, sprevádzanej zvýšenou nestabilitou chromozómov/zvýšeným počtom mikrojadierok. Takto vzniknutá nerovnováha môže mať za následok zvýšenú citlivosť buniek k induktorom replikačného stresu akými sú inhibítory: poly (ADP-ribóza) polymerázy (PARP) a topoizomeráz. Na základe získaných výsledkov možno konštatovať potenciálnu úlohu hyperaktivovanej RNF168/53BP1 signálnej dráhy v procese tumorigenézy. Cez navrhovanú pozmenenú kapacitu opravy DNA, následnú nestabilitu genómu a heterogenitu nádoru môže dochádzať k bunkovej selekcii rezistentného a na stres adaptovaného nádorového fenotypu.

Vedeckým prínosom predkladanej práce je nielem detailný náhľad do (pato)biológie nádorovej bunky, ale aj nájdená zvýšená hladina proteínu RNF168 v klinických vzorkách materiálu získaného z nádoru kostnej drene. Tento objav môže viesť k zavedeniu nového diagnostického ako aj prognostického markeru odpovede na štandardnú a novovznikajúcu liečbu nádorového ochorenia-mnohopočetný myelóm.

12 REFERENCES

Abraham, R.T. (2001). Cell cycle checkpoint signaling through the ATM and ATR kinases. Genes Dev. *15*, 2177–2196.

Acs, K., Luijsterburg, M.S., Ackermann, L., Salomons, F.A., Hoppe, T., and Dantuma, N.P. (2011). The AAA-ATPase VCP/p97 promotes 53BP1 recruitment by removing L3MBTL1 from DNA double-strand breaks. Nat. Struct. Mol. Biol. *18*, 1345–1350.

Adamo, A., Collis, S.J., Adelman, C.A., Silva, N., Horejsi, Z., Ward, J.D., Martinez-Perez, E., Boulton, S.J., and La Volpe, A. (2010). Preventing nonhomologous end joining suppresses DNA repair defects of Fanconi anemia. Mol. Cell *39*, 25–35.

Ahnesorg, P., Smith, P., and Jackson, S.P. (2006). XLF interacts with the XRCC4-DNA ligase IV complex to promote DNA nonhomologous end-joining. Cell *124*, 301–313.

Alt, F.W., Zhang, Y., Meng, F.-L., Guo, C., and Schwer, B. (2013). Mechanisms of programmed DNA lesions and genomic instability in the immune system. Cell *152*, 417–429.

Anderson, K.C. (2016). Progress and Paradigms in Multiple Myeloma. Clin. Cancer Res. *22*, 5419–5427.

Audebert, M., Salles, B., and Calsou, P. (2004). Involvement of poly(ADP-ribose) polymerase-1 and XRCC1/DNA ligase III in an alternative route for DNA double-strand breaks rejoining. J. Biol. Chem. *279*, 55117–55126.

Baker, R.T., and Board, P.G. (1987). The human ubiquitin gene family: structure of a gene and pseudogenes from the Ub B subfamily. Nucleic Acids Res. *15*, 443–463.

Balch, W.E., Morimoto, R.I., Dillin, A., and Kelly, J.W. (2008). Adapting proteostasis for disease intervention. Science *319*, 916–919.

Bao, Y. (2011). Chromatin response to DNA double-strand break damage. Epigenomics *3*, 307–321.

Barnes, D.E., and Lindahl, T. (2004). Repair and genetic consequences of endogenous DNA base damage in mammalian cells. Annu. Rev. Genet. *38*, 445–476.

Barnes, P.J., and Karin, M. (1997). Nuclear factor-kappaB: a pivotal transcription factor in chronic inflammatory diseases. N. Engl. J. Med. *336*, 1066–1071.

Bartek, J., and Lukas, J. (2003). Chk1 and Chk2 kinases in checkpoint control and cancer. Cancer Cell *3*, 421–429.

Bartek, J., and Lukas, J. (2007). DNA damage checkpoints: from initiation to recovery or adaptation. Curr. Opin. Cell Biol. *19*, 238–245.

Bartek, J., Lukas, C., and Lukas, J. (2004). Checking on DNA damage in S phase. Nat. Rev. Mol. Cell Biol. *5*, 792–804.

Bartek, J., Bartkova, J., and Lukas, J. (2007). DNA damage signalling guards against activated oncogenes and tumour progression. Oncogene *26*, 7773–7779.

Bartkova, J., Horejsí, Z., Koed, K., Krämer, A., Tort, F., Zieger, K., Guldberg, P., Sehested, M., Nesland, J.M., Lukas, C., et al. (2005). DNA damage response as a candidate anti-cancer barrier in early human tumorigenesis. Nature *434*, 864–870.

Bartkova, J., Rezaei, N., Liontos, M., Karakaidos, P., Kletsas, D., Issaeva, N., Vassiliou, L.-V.F., Kolettas, E., Niforou, K., Zoumpourlis, V.C., et al. (2006). Oncogene-induced senescence is part of the tumorigenesis barrier imposed by DNA damage checkpoints. Nature *444*, 633–637.

Basu, B., Yap, T.A., Molife, L.R., and de Bono, J.S. (2012). Targeting the DNA damage response in oncology: past, present and future perspectives. Curr Opin Oncol *24*, 316–324.

Beckerman, R., and Prives, C. (2010). Transcriptional regulation by p53. Cold Spring Harb Perspect Biol *2*, a000935.

Bekker-Jensen, S., and Mailand, N. (2010). Assembly and function of DNA double-strand break repair foci in mammalian cells. DNA Repair (Amst.) *9*, 1219–1228.

Bekker-Jensen, S., Rendtlew Danielsen, J., Fugger, K., Gromova, I., Nerstedt, A., Lukas, C., Bartek, J., Lukas, J., and Mailand, N. (2010). HERC2 coordinates ubiquitin-dependent assembly of DNA repair factors on damaged chromosomes. Nat. Cell Biol. *12*, 80-86-12.

Ben-Aroya, S., Agmon, N., Yuen, K., Kwok, T., McManus, K., Kupiec, M., and Hieter, P. (2010). Proteasome nuclear activity affects chromosome stability by controlling the turnover of Mms22, a protein important for DNA repair. PLoS Genet. *6*, e1000852.

Berger, A.H., Knudson, A.G., and Pandolfi, P.P. (2011). A continuum model for tumour suppression. Nature *476*, 163–169.

Bergsagel, P.L., and Kuehl, W.M. (2005). Molecular pathogenesis and a consequent classification of multiple myeloma. J. Clin. Oncol. *23*, 6333–6338.

Berndsen, C.E., and Wolberger, C. (2014). New insights into ubiquitin E3 ligase mechanism. Nat. Struct. Mol. Biol. *21*, 301–307.

Bernstein, E., and Hake, S.B. (2006). The nucleosome: a little variation goes a long way. Biochem. Cell Biol. *84*, 505–517.

Bertocci, B., De Smet, A., Weill, J.-C., and Reynaud, C.-A. (2006). Nonoverlapping functions of DNA polymerases mu, lambda, and terminal deoxynucleotidyltransferase during immunoglobulin V(D)J recombination in vivo. Immunity *25*, 31–41.

Bhattacharyya, A., Ear, U.S., Koller, B.H., Weichselbaum, R.R., and Bishop, D.K. (2000). The breast cancer susceptibility gene BRCA1 is required for subnuclear assembly of Rad51 and survival following treatment with the DNA cross-linking agent cisplatin. J. Biol. Chem. *275*, 23899–23903.

Bienko, M., Green, C.M., Crosetto, N., Rudolf, F., Zapart, G., Coull, B., Kannouche, P., Wider, G., Peter, M., Lehmann, A.R., et al. (2005). Ubiquitin-binding domains in Y-family polymerases regulate translesion synthesis. Science *310*, 1821–1824.

Blunt, T., Finnie, N.J., Taccioli, G.E., Smith, G.C., Demengeot, J., Gottlieb, T.M., Mizuta, R., Varghese, A.J., Alt, F.W., Jeggo, P.A., et al. (1995). Defective DNA-dependent protein kinase activity is linked to V(D)J recombination and DNA repair defects associated with the murine scid mutation. Cell *80*, 813–823.

Boersma, V., Moatti, N., Segura-Bayona, S., Peuscher, M.H., van der Torre, J., Wevers, B.A., Orthwein, A., Durocher, D., and Jacobs, J.J.L. (2015). MAD2L2 controls DNA repair at telomeres and DNA breaks by inhibiting 5' end resection. Nature *521*, 537–540.

Bohgaki, M., Bohgaki, T., El Ghamrasni, S., Srikumar, T., Maire, G., Panier, S., Fradet-Turcotte, A., Stewart, G.S., Raught, B., Hakem, A., et al. (2013). RNF168 ubiquitylates 53BP1 and controls its response to DNA double-strand breaks. Proc. Natl. Acad. Sci. U.S.A. *110*, 20982–20987.

Botuyan, M.V., Lee, J., Ward, I.M., Kim, J.-E., Thompson, J.R., Chen, J., and Mer, G. (2006). Structural basis for the methylation state-specific recognition of histone H4-K20 by 53BP1 and Crb2 in DNA repair. Cell *127*, 1361–1373.

Bouwman, P., Aly, A., Escandell, J.M., Pieterse, M., Bartkova, J., van der Gulden, H., Hiddingh, S., Thanasoula, M., Kulkarni, A., Yang, Q., et al. (2010). 53BP1 loss rescues BRCA1 deficiency and is associated with triple-negative and BRCA-mutated breast cancers. Nat. Struct. Mol. Biol. *17*, 688–695.

Bramson, J., Prévost, J., Malapetsa, A., Noë, A.J., Poirier, G.G., DesNoyers, S., Alaoui-Jamali, M., and Panasci, L. (1993). Poly(ADP-ribose) polymerase can bind melphalan damaged DNA. Cancer Res. *53*, 5370–5373.

Britton, S., Coates, J., and Jackson, S.P. (2013). A new method for high-resolution imaging of Ku foci to decipher mechanisms of DNA double-strand break repair. J. Cell Biol. *202*, 579–595.

Bryant, H.E., Schultz, N., Thomas, H.D., Parker, K.M., Flower, D., Lopez, E., Kyle, S., Meuth, M., Curtin, N.J., and Helleday, T. (2005). Specific killing of BRCA2-deficient tumours with inhibitors of poly(ADP-ribose) polymerase. Nature *434*, 913–917.

Brzovic, P.S., Keeffe, J.R., Nishikawa, H., Miyamoto, K., Fox, D., Fukuda, M., Ohta, T., and Klevit, R. (2003). Binding and recognition in the assembly of an active BRCA1/BARD1 ubiquitin-ligase complex. Proc. Natl. Acad. Sci. U.S.A. *100*, 5646–5651.

Bunting, S.F., Callén, E., Wong, N., Chen, H.-T., Polato, F., Gunn, A., Bothmer, A., Feldhahn, N., Fernandez-Capetillo, O., Cao, L., et al. (2010). 53BP1 inhibits homologous recombination in Brca1-deficient cells by blocking resection of DNA breaks. Cell *141*, 243–254.

Bunting, S.F., Callén, E., Kozak, M.L., Kim, J.M., Wong, N., López-Contreras, A.J., Ludwig, T., Baer, R., Faryabi, R.B., Malhowski, A., et al. (2012). BRCA1 functions independently of homologous recombination in DNA interstrand crosslink repair. Mol. Cell *46*, 125–135.

van der Burg, M., Ijspeert, H., Verkaik, N.S., Turul, T., Wiegant, W.W., Morotomi-Yano, K., Mari, P.-O., Tezcan, I., Chen, D.J., Zdzienicka, M.Z., et al. (2009). A DNA-PKcs mutation in a radiosensitive T-B- SCID patient inhibits Artemis activation and nonhomologous end-joining. J. Clin. Invest. *119*, 91–98.

Burrell, R.A., McClelland, S.E., Endesfelder, D., Groth, P., Weller, M.-C., Shaikh, N., Domingo, E., Kanu, N., Dewhurst, S.M., Gronroos, E., et al. (2013). Replication stress links structural and numerical cancer chromosomal instability. Nature *494*, 492–496.

Butler, L.R., Densham, R.M., Jia, J., Garvin, A.J., Stone, H.R., Shah, V., Weekes, D., Festy, F., Beesley, J., and Morris, J.R. (2012). The proteasomal de-ubiquitinating enzyme POH1 promotes the double-strand DNA break response. EMBO J. *31*, 3918–3934.

Callebaut, I., and Mornon, J.P. (1997). From BRCA1 to RAP1: a widespread BRCT module closely associated with DNA repair. FEBS Lett. *400*, 25–30.

Callén, E., Nussenzweig, M.C., and Nussenzweig, A. (2007). Breaking down cell cycle checkpoints and DNA repair during antigen receptor gene assembly. Oncogene *26*, 7759–7764.

Callen, E., Di Virgilio, M., Kruhlak, M.J., Nieto-Soler, M., Wong, N., Chen, H.-T., Faryabi, R.B., Polato, F., Santos, M., Starnes, L.M., et al. (2013). 53BP1 mediates productive and mutagenic DNA repair through distinct phosphoprotein interactions. Cell *153*, 1266–1280.

Cao, L., Xu, X., Bunting, S.F., Liu, J., Wang, R.-H., Cao, L.L., Wu, J.J., Peng, T.-N., Chen, J., Nussenzweig, A., et al. (2009). A selective requirement for 53BP1 in the biological response to genomic instability induced by Brca1 deficiency. Mol. Cell *35*, 534–541.

Cary, R.B., Peterson, S.R., Wang, J., Bear, D.G., Bradbury, E.M., and Chen, D.J. (1997). DNA looping by Ku and the DNA-dependent protein kinase. Proc. Natl. Acad. Sci. U.S.A. *94*, 4267–4272.

Caspari, T. (2000). How to activate p53. Curr. Biol. *10*, R315-317.

Ceccaldi, R., Rondinelli, B., and D'Andrea, A.D. (2016). Repair Pathway Choices and Consequences at the Double-Strand Break. Trends Cell Biol. *26*, 52–64.

Certo, M.T., Ryu, B.Y., Annis, J.E., Garibov, M., Jarjour, J., Rawlings, D.J., and Scharenberg, A.M. (2011). Tracking genome engineering outcome at individual DNA breakpoints. Nat. Methods *8*, 671–676.

Chapman, J.R., Taylor, M.R.G., and Boulton, S.J. (2012a). Playing the end game: DNA double-strand break repair pathway choice. Mol. Cell *47*, 497–510.

Chapman, J.R., Sossick, A.J., Boulton, S.J., and Jackson, S.P. (2012b). BRCA1-associated exclusion of 53BP1 from DNA damage sites underlies temporal control of DNA repair. J. Cell. Sci. *125*, 3529–3534.

Chapman, J.R., Barral, P., Vannier, J.-B., Borel, V., Steger, M., Tomas-Loba, A., Sartori, A.A., Adams, I.R., Batista, F.D., and Boulton, S.J. (2013). RIF1 is essential for 53BP1-dependent nonhomologous end joining and suppression of DNA double-strand break resection. Mol. Cell *49*, 858–871.

Chapman, M.A., Lawrence, M.S., Keats, J.J., Cibulskis, K., Sougnez, C., Schinzel, A.C., Harview, C.L., Brunet, J.-P., Ahmann, G.J., Adli, M., et al. (2011). Initial genome sequencing and analysis of multiple myeloma. Nature *471*, 467–472.

Chauhan, D., Hideshima, T., and Anderson, K.C. (2005). Proteasome inhibition in multiple myeloma: therapeutic implication. Annu. Rev. Pharmacol. Toxicol. *45*, 465–476.

Chen, L., and Madura, K. (2005). Increased proteasome activity, ubiquitin-conjugating enzymes, and eEF1A translation factor detected in breast cancer tissue. Cancer Res. *65*, 5599–5606.

Chen, Z.J., and Sun, L.J. (2009). Nonproteolytic functions of ubiquitin in cell signaling. Mol. Cell *33*, 275–286.

Chen, D., Frezza, M., Schmitt, S., Kanwar, J., and Dou, Q.P. (2011). Bortezomib as the First Proteasome Inhibitor Anticancer Drug: Current Status and Future Perspectives. Curr Cancer Drug Targets *11*, 239–253.

Chen, L., Trujillo, K., Sung, P., and Tomkinson, A.E. (2000). Interactions of the DNA ligase IV-XRCC4 complex with DNA ends and the DNA-dependent protein kinase. J. Biol. Chem. *275*, 26196–26205.

Ciccia, A., and Elledge, S.J. (2010). The DNA damage response: making it safe to play with knives. Mol. Cell *40*, 179–204.

Ciechanover, A., Elias, S., Heller, H., and Hershko, A. (1982). “Covalent affinity” purification of ubiquitin-activating enzyme. J. Biol. Chem. *257*, 2537–2542.

Ciehanover, A., Hod, Y., and Hershko, A. (1978). A heat-stable polypeptide component of an ATP-dependent proteolytic system from reticulocytes. Biochem. Biophys. Res. Commun. *81*, 1100–1105.

Cimprich, K.A., and Cortez, D. (2008). ATR: an essential regulator of genome integrity. Nat. Rev. Mol. Cell Biol. *9*, 616–627.

Clapier, C.R., and Cairns, B.R. (2009). The biology of chromatin remodeling complexes. Annu. Rev. Biochem. *78*, 273–304.

Coleman, K.A., and Greenberg, R.A. (2011). The BRCA1-RAP80 complex regulates DNA repair mechanism utilization by restricting end resection. J. Biol. Chem. *286*, 13669–13680.

Cooper, E.M., Cutcliffe, C., Kristiansen, T.Z., Pandey, A., Pickart, C.M., and Cohen, R.E. (2009). K63-specific deubiquitination by two JAMM/MPN+ complexes: BRISC-associated Brcc36 and proteasomal Poh1. EMBO J. *28*, 621–631.

Costantini, S., Woodbine, L., Andreoli, L., Jeggo, P.A., and Vindigni, A. (2007). Interaction of the Ku heterodimer with the DNA ligase IV/Xrcc4 complex and its regulation by DNA-PK. DNA Repair (Amst.) *6*, 712–722.

Costanzo, V., and Gautier, J. (2003). Single-strand DNA gaps trigger an ATR- and Cdc7-dependent checkpoint. Cell Cycle *2*, 17.

Coster, G., and Goldberg, M. (2010). The cellular response to DNA damage: a focus on MDC1 and its interacting proteins. Nucleus *1*, 166–178.

Cromie, G.A., Connelly, J.C., and Leach, D.R. (2001). Recombination at double-strand breaks and DNA ends: conserved mechanisms from phage to humans. Mol. Cell *8*, 1163–1174.

Curtin, N.J. (2012). DNA repair dysregulation from cancer driver to therapeutic target. Nat. Rev. Cancer *12*, 801–817.

Danielsen, J.R., Povlsen, L.K., Villumsen, B.H., Streicher, W., Nilsson, J., Wikström, M., Bekker-Jensen, S., and Mailand, N. (2012). DNA damage-inducible SUMOylation of HERC2 promotes RNF8 binding via a novel SUMO-binding Zinc finger. J. Cell Biol. *197*, 179–187.

Dantuma, N.P., Groothuis, T.A.M., Salomons, F.A., and Neefjes, J. (2006). A dynamic ubiquitin equilibrium couples proteasomal activity to chromatin remodeling. J. Cell Biol. *173*, 19–26.

Dantzer, F., Schreiber, V., Niedergang, C., Trucco, C., Flatter, E., De La Rubia, G., Oliver, J., Rolli, V., Ménissier-de Murcia, J., and de Murcia, G. (1999). Involvement of poly(ADP-ribose) polymerase in base excision repair. Biochimie *81*, 69–75.

De Vos, M., Schreiber, V., and Dantzer, F. (2012). The diverse roles and clinical relevance of PARPs in DNA damage repair: current state of the art. Biochem. Pharmacol. *84*, 137–146.

Deng, L., Wang, C., Spencer, E., Yang, L., Braun, A., You, J., Slaughter, C., Pickart, C., and Chen, Z.J. (2000). Activation of the IkappaB kinase complex by TRAF6 requires a dimeric ubiquitin-conjugating enzyme complex and a unique polyubiquitin chain. Cell *103*, 351–361.

Densham, R.M., Garvin, A.J., Stone, H.R., Strachan, J., Baldock, R.A., Daza-Martin, M., Fletcher, A., Blair-Reid, S., Beesley, J., Johal, B., et al. (2016). Human BRCA1-BARD1 ubiquitin ligase activity counteracts chromatin barriers to DNA resection. Nat. Struct. Mol. Biol. *23*, 647–655.

Dephoure, N., Hwang, S., O'Sullivan, C., Dodgson, S.E., Gygi, S.P., Amon, A., and Torres, E.M. (2014). Quantitative proteomic analysis reveals posttranslational responses to aneuploidy in yeast. Elife *3*, e03023.

Deshaies, R.J. (2014). Proteotoxic crisis, the ubiquitin-proteasome system, and cancer therapy. BMC Biol. *12*, 94.

Deshaies, R.J., and Joazeiro, C.A.P. (2009). RING domain E3 ubiquitin ligases. Annu. Rev. Biochem. *78*, 399–434.

Di Micco, R., Fumagalli, M., Cicalese, A., Piccinin, S., Gasparini, P., Luise, C., Schurra, C., Garre', M., Nuciforo, P.G., Bensimon, A., et al. (2006). Oncogene-induced senescence is a DNA damage response triggered by DNA hyper-replication. Nature *444*, 638–642.

Di Virgilio, M., Callen, E., Yamane, A., Zhang, W., Jankovic, M., Gitlin, A.D., Feldhahn, N., Resch, W., Oliveira, T.Y., Chait, B.T., et al. (2013). Rif1 prevents resection of DNA breaks and promotes immunoglobulin class switching. Science *339*, 711–715.

Doil, C., Mailand, N., Bekker-Jensen, S., Menard, P., Larsen, D.H., Pepperkok, R., Ellenberg, J., Panier, S., Durocher, D., Bartek, J., et al. (2009). RNF168 binds and amplifies ubiquitin conjugates on damaged chromosomes to allow accumulation of repair proteins. Cell *136*, 435–446.

Dolganov, G.M., Maser, R.S., Novikov, A., Tosto, L., Chong, S., Bressan, D.A., and Petrini, J.H. (1996). Human Rad50 is physically associated with human Mre11: identification of a conserved multiprotein complex implicated in recombinational DNA repair. Mol. Cell. Biol. *16*, 4832–4841.

D'Silva, I., Pelletier, J.D., Lagueux, J., D'Amours, D., Chaudhry, M.A., Weinfeld, M., Lees-Miller, S.P., and Poirier, G.G. (1999). Relative affinities of poly(ADP-ribose) polymerase and DNA-dependent protein kinase for DNA strand interruptions. Biochim. Biophys. Acta *1430*, 119–126.

Dye, B.T., and Schulman, B.A. (2007). Structural mechanisms underlying posttranslational modification by ubiquitin-like proteins. Annu Rev Biophys Biomol Struct *36*, 131–150.

Dynan, W.S., and Yoo, S. (1998). Interaction of Ku protein and DNA-dependent protein kinase catalytic subunit with nucleic acids. Nucleic Acids Res. *26*, 1551–1559.

El-Khamisy, S.F., Masutani, M., Suzuki, H., and Caldecott, K.W. (2003). A requirement for PARP-1 for the assembly or stability of XRCC1 nuclear foci at sites of oxidative DNA damage. Nucleic Acids Res. *31*, 5526–5533.

Escribano-Díaz, C., Orthwein, A., Fradet-Turcotte, A., Xing, M., Young, J.T.F., Tkáč, J., Cook, M.A., Rosebrock, A.P., Munro, M., Canny, M.D., et al. (2013). A cell cycle-dependent regulatory circuit composed of 53BP1-RIF1 and BRCA1-CtIP controls DNA repair pathway choice. Mol. Cell *49*, 872–883.

Essers, J., van Steeg, H., de Wit, J., Swagemakers, S.M., Vermeij, M., Hoeijmakers, J.H., and Kanaar, R. (2000). Homologous and non-homologous recombination differentially affect DNA damage repair in mice. EMBO J. *19*, 1703–1710.

d'Adda di Fagagna, F., Hande, M.P., Tong, W.M., Roth, D., Lansdorp, P.M., Wang, Z.Q., and Jackson, S.P. (2001). Effects of DNA nonhomologous end-joining factors on telomere length and chromosomal stability in mammalian cells. Curr. Biol. *11*, 1192–1196.

Falck, J., Coates, J., and Jackson, S.P. (2005). Conserved modes of recruitment of ATM, ATR and DNA-PKcs to sites of DNA damage. Nature *434*, 605–611.

Farmer, H., McCabe, N., Lord, C.J., Tutt, A.N.J., Johnson, D.A., Richardson, T.B., Santarosa, M., Dillon, K.J., Hickson, I., Knights, C., et al. (2005). Targeting the DNA repair defect in BRCA mutant cells as a therapeutic strategy. Nature *434*, 917–921.

Feng, L., Fong, K.-W., Wang, J., Wang, W., and Chen, J. (2013). RIF1 counteracts BRCA1-mediated end resection during DNA repair. J. Biol. Chem. *288*, 11135–11143.

Finley, D. (2009). Recognition and processing of ubiquitin-protein conjugates by the proteasome. Annu. Rev. Biochem. *78*, 477–513.

Finnie, N.J., Gottlieb, T.M., Blunt, T., Jeggo, P.A., and Jackson, S.P. (1995). DNA-dependent protein kinase activity is absent in xrs-6 cells: implications for site-specific recombination and DNA double-strand break repair. Proc. Natl. Acad. Sci. U.S.A. *92*, 320–324.

Fonseca, R., Bergsagel, P.L., Drach, J., Shaughnessy, J., Gutierrez, N., Stewart, A.K., Morgan, G., Van Ness, B., Chesi, M., Minvielle, S., et al. (2009). International Myeloma Working Group molecular classification of multiple myeloma: spotlight review. Leukemia *23*, 2210–2221.

Fradet-Turcotte, A., Canny, M.D., Escribano-Díaz, C., Orthwein, A., Leung, C.C.Y., Huang, H., Landry, M.-C., Kitevski-LeBlanc, J., Noordermeer, S.M., Sicheri, F., et al. (2013). 53BP1 is a reader of the DNA-damage-induced H2A Lys 15 ubiquitin mark. Nature *499*, 50–54.

Franz, A., Orth, M., Pirson, P.A., Sonneville, R., Blow, J.J., Gartner, A., Stemmann, O., and Hoppe, T. (2011). CDC-48/p97 coordinates CDT-1 degradation with GINS chromatin dissociation to ensure faithful DNA replication. Mol. Cell *44*, 85–96.

Freedman, D.A., Wu, L., and Levine, A.J. (1999). Functions of the MDM2 oncoprotein. Cell. Mol. Life Sci. *55*, 96–107.

Furgason, J.M., and Bahassi, E.M. (2013). Targeting DNA repair mechanisms in cancer. Pharmacol. Ther. *137*, 298–308.

Gething, M.J. (1999). Role and regulation of the ER chaperone BiP. Semin. Cell Dev. Biol. *10*, 465–472.

Giles, J. (2004). Chemistry Nobel for trio who revealed molecular death-tag. Nature *431*, 729.

Gorgoulis, V.G., Vassiliou, L.-V.F., Karakaidos, P., Zacharatos, P., Kotsinas, A., Liloglou, T., Venere, M., Ditullio, R.A., Kastrinakis, N.G., Levy, B., et al. (2005). Activation of the DNA damage checkpoint and genomic instability in human precancerous lesions. Nature *434*, 907–913.

Gottlieb, T.M., and Jackson, S.P. (1993). The DNA-dependent protein kinase: requirement for DNA ends and association with Ku antigen. Cell *72*, 131–142.

Greenlee, R.T., Murray, T., Bolden, S., and Wingo, P.A. (2000). Cancer statistics, 2000. CA Cancer J Clin *50*, 7–33.

Greer, E.L., and Brunet, A. (2005). FOXO transcription factors at the interface between longevity and tumor suppression. Oncogene *24*, 7410–7425.

Griffith, A.J., Blier, P.R., Mimori, T., and Hardin, J.A. (1992). Ku polypeptides synthesized in vitro assemble into complexes which recognize ends of double-stranded DNA. J. Biol. Chem. *267*, 331–338.

Gu, J., Lu, H., Tsai, A.G., Schwarz, K., and Lieber, M.R. (2007a). Single-stranded DNA ligation and XLF-stimulated incompatible DNA end ligation by the XRCC4-DNA ligase IV complex: influence of terminal DNA sequence. Nucleic Acids Res. *35*, 5755–5762.

Gu, J., Lu, H., Tippin, B., Shimazaki, N., Goodman, M.F., and Lieber, M.R. (2007b). XRCC4:DNA ligase IV can ligate incompatible DNA ends and can ligate across gaps. EMBO J. *26*, 1010–1023.

Gudjonsson, T., Altmeyer, M., Savic, V., Toledo, L., Dinant, C., Grøfte, M., Bartkova, J., Poulsen, M., Oka, Y., Bekker-Jensen, S., et al. (2012). TRIP12 and UBR5 suppress spreading of chromatin ubiquitylation at damaged chromosomes. Cell *150*, 697–709.

Gudmundsdottir, K., Lord, C.J., and Ashworth, A. (2007). The proteasome is involved in determining differential utilization of double-strand break repair pathways. Oncogene *26*, 7601–7606.

Guo, J.Y., Xia, B., and White, E. (2013). Autophagy-mediated tumor promotion. Cell *155*, 1216–1219.

Haber, J.E. (2000). Partners and pathwaysrepairing a double-strand break. Trends Genet. *16*, 259–264.

Halazonetis, T.D., Gorgoulis, V.G., and Bartek, J. (2008). An oncogene-induced DNA damage model for cancer development. Science *319*, 1352–1355.

Hanahan, D., and Weinberg, R.A. (2000). The hallmarks of cancer. Cell *100*, 57–70.

Hastings, P.J., Lupski, J.R., Rosenberg, S.M., and Ira, G. (2009). Mechanisms of change in gene copy number. Nat. Rev. Genet. *10*, 551–564.

Herrero, A.B., San Miguel, J., and Gutierrez, N.C. (2015). Deregulation of DNA double-strand break repair in multiple myeloma: implications for genome stability. PLoS ONE *10*, e0121581.

Hershko, A., and Ciechanover, A. (1998). The ubiquitin system. Annu. Rev. Biochem. *67*, 425–479.

Hershko, A., Heller, H., Elias, S., and Ciechanover, A. (1983). Components of ubiquitin-protein ligase system. Resolution, affinity purification, and role in protein breakdown. J. Biol. Chem. *258*, 8206–8214.

Heyer, W.-D., Ehmsen, K.T., and Liu, J. (2010). Regulation of homologous recombination in eukaryotes. Annu. Rev. Genet. *44*, 113–139.

Hideshima, T., Richardson, P., Chauhan, D., Palombella, V.J., Elliott, P.J., Adams, J., and Anderson, K.C. (2001). The proteasome inhibitor PS-341 inhibits growth, induces apoptosis, and overcomes drug resistance in human multiple myeloma cells. Cancer Res. *61*, 3071–3076.

Hideshima, T., Bradner, J.E., Wong, J., Chauhan, D., Richardson, P., Schreiber, S.L., and Anderson, K.C. (2005). Small-molecule inhibition of proteasome and aggresome function induces synergistic antitumor activity in multiple myeloma. Proc. Natl. Acad. Sci. U.S.A. *102*, 8567–8572.

Hjerpe, R., Thomas, Y., Chen, J., Zemla, A., Curran, S., Shpiro, N., Dick, L.R., and Kurz, T. (2012). Changes in the ratio of free NEDD8 to ubiquitin triggers NEDDylation by ubiquitin enzymes. Biochem. J. *441*, 927–936.

Hoeijmakers, J.H. (2001). Genome maintenance mechanisms for preventing cancer. Nature *411*, 366–374.

Hoffmann, S., Smedegaard, S., Nakamura, K., Mortuza, G.B., Räschle, M., Ibañez de Opakua, A., Oka, Y., Feng, Y., Blanco, F.J., Mann, M., et al. (2016). TRAIP is a PCNA-binding ubiquitin ligase that protects genome stability after replication stress. J. Cell Biol. *212*, 63–75.

Hsu, F.-M., Zhang, S., and Chen, B.P.C. (2012). Role of DNA-dependent protein kinase catalytic subunit in cancer development and treatment. Transl Cancer Res *1*, 22–34.

Hsu, H.L., Yannone, S.M., and Chen, D.J. (2002). Defining interactions between DNA-PK and ligase IV/XRCC4. DNA Repair (Amst.) *1*, 225–235.

Hu, Y., Scully, R., Sobhian, B., Xie, A., Shestakova, E., and Livingston, D.M. (2011). RAP80-directed tuning of BRCA1 homologous recombination function at ionizing radiation-induced nuclear foci. Genes Dev. *25*, 685–700.

Huang, D.T., Miller, D.W., Mathew, R., Cassell, R., Holton, J.M., Roussel, M.F., and Schulman, B.A. (2004). A unique E1-E2 interaction required for optimal conjugation of the ubiquitin-like protein NEDD8. Nat. Struct. Mol. Biol. *11*, 927–935.

Huber, L.J., Yang, T.W., Sarkisian, C.J., Master, S.R., Deng, C.X., and Chodosh, L.A. (2001). Impaired DNA damage response in cells expressing an exon 11-deleted murine Brca1 variant that localizes to nuclear foci. Mol. Cell. Biol. *21*, 4005–4015.

Huen, M.S.Y., Grant, R., Manke, I., Minn, K., Yu, X., Yaffe, M.B., and Chen, J. (2007). RNF8 transduces the DNA-damage signal via histone ubiquitylation and checkpoint protein assembly. Cell *131*, 901–914.

Inbar-Rozensal, D., Castiel, A., Visochek, L., Castel, D., Dantzer, F., Izraeli, S., and Cohen-Armon, M. (2009). A selective eradication of human nonhereditary breast cancer cells by phenanthridine-derived polyADP-ribose polymerase inhibitors. Breast Cancer Res. *11*, R78.

Jackson, S.P. (2002). Sensing and repairing DNA double-strand breaks. Carcinogenesis *23*, 687–696.

Jackson, S.P., and Bartek, J. (2009). The DNA-damage response in human biology and disease. Nature *461*, 1071–1078.

Jacquemont, C., and Taniguchi, T. (2007). Proteasome function is required for DNA damage response and fanconi anemia pathway activation. Cancer Res. *67*, 7395–7405.

de Jager, M., Dronkert, M.L., Modesti, M., Beerens, C.E., Kanaar, R., and van Gent, D.C. (2001). DNA-binding and strand-annealing activities of human Mre11: implications for its roles in DNA double-strand break repair pathways. Nucleic Acids Res. *29*, 1317–1325.

Jazayeri, A., Falck, J., Lukas, C., Bartek, J., Smith, G.C.M., Lukas, J., and Jackson, S.P. (2006). ATM- and cell cycle-dependent regulation of ATR in response to DNA double-strand breaks. Nat. Cell Biol. *8*, 37–45.

Jeggo, P.A., and Löbrich, M. (2007). DNA double-strand breaks: their cellular and clinical impact? Oncogene *26*, 7717–7719.

Jiang, Q., and Greenberg, R.A. (2015). Deciphering the BRCA1 Tumor Suppressor Network. J. Biol. Chem. *290*, 17724–17732.

Johnson, E.S., Ma, P.C., Ota, I.M., and Varshavsky, A. (1995). A proteolytic pathway that recognizes ubiquitin as a degradation signal. J. Biol. Chem. *270*, 17442–17456.

Juven-Gershon, T., and Oren, M. (1999). Mdm2: the ups and downs. Mol. Med. *5*, 71–83.

Kakarougkas, A., Ismail, A., Katsuki, Y., Freire, R., Shibata, A., and Jeggo, P.A. (2013). Co-operation of BRCA1 and POH1 relieves the barriers posed by 53BP1 and RAP80 to resection. Nucleic Acids Res. *41*, 10298–10311.

Kane, R.C., Farrell, A.T., Sridhara, R., and Pazdur, R. (2006). United States Food and Drug Administration approval summary: bortezomib for the treatment of progressive multiple myeloma after one prior therapy. Clin. Cancer Res. *12*, 2955–2960.

Kane, R.C., Dagher, R., Farrell, A., Ko, C.-W., Sridhara, R., Justice, R., and Pazdur, R. (2007). Bortezomib for the treatment of mantle cell lymphoma. Clin. Cancer Res. *13*, 5291–5294.

Kim, H.C., and Huibregtse, J.M. (2009). Polyubiquitination by HECT E3s and the determinants of chain type specificity. Mol. Cell. Biol. *29*, 3307–3318.

Kim, H., Chen, J., and Yu, X. (2007). Ubiquitin-binding protein RAP80 mediates BRCA1-dependent DNA damage response. Science *316*, 1202–1205.

Kim, M.Y., Mauro, S., Gévry, N., Lis, J.T., and Kraus, W.L. (2004). NAD+-dependent modulation of chromatin structure and transcription by nucleosome binding properties of PARP-1. Cell *119*, 803–814.

Kojic, M., Zhou, Q., Lisby, M., and Holloman, W.K. (2005). Brh2-Dss1 interplay enables properly controlled recombination in Ustilago maydis. Mol. Cell. Biol. *25*, 2547–2557.

Kolas, N.K., Chapman, J.R., Nakada, S., Ylanko, J., Chahwan, R., Sweeney, F.D., Panier, S., Mendez, M., Wildenhain, J., Thomson, T.M., et al. (2007). Orchestration of the DNA-damage response by the RNF8 ubiquitin ligase. Science *318*, 1637–1640.

Komander, D. (2009). The emerging complexity of protein ubiquitination. Biochem. Soc. Trans. *37*, 937–953.

Kornberg, R.D. (1977). Structure of chromatin. Annu. Rev. Biochem. *46*, 931–954.

Kouzarides, T. (2007). Chromatin modifications and their function. Cell *128*, 693–705.

Kovarova, L., Buresova, I., Buchler, T., Suska, R., Pour, L., Zahradova, L., Penka, M., and Hajek, R. (2009). Phenotype of plasma cells in multiple myeloma and monoclonal gammopathy of undetermined significance. Neoplasma *56*, 526–532.

Kracker, S., and Durandy, A. (2011). Insights into the B cell specific process of immunoglobulin class switch recombination. Immunol. Lett. *138*, 97–103.

Kristensen, C.N., Bystol, K.M., Li, B., Serrano, L., and Brenneman, M.A. (2010). Depletion of DSS1 protein disables homologous recombinational repair in human cells. Mutat. Res. *694*, 60–64.

Krogan, N.J., Lam, M.H.Y., Fillingham, J., Keogh, M.-C., Gebbia, M., Li, J., Datta, N., Cagney, G., Buratowski, S., Emili, A., et al. (2004). Proteasome involvement in the repair of DNA double-strand breaks. Mol. Cell *16*, 1027–1034.

Kulis, M., and Esteller, M. (2010). DNA methylation and cancer. Adv. Genet. *70*, 27–56.

Kurimasa, A., Kumano, S., Boubnov, N.V., Story, M.D., Tung, C.S., Peterson, S.R., and Chen, D.J. (1999). Requirement for the kinase activity of human DNA-dependent protein kinase catalytic subunit in DNA strand break rejoining. Mol. Cell. Biol. *19*, 3877–3884.

Kyle, R.A., Gertz, M.A., Witzig, T.E., Lust, J.A., Lacy, M.Q., Dispenzieri, A., Fonseca, R., Rajkumar, S.V., Offord, J.R., Larson, D.R., et al. (2003). Review of 1027 patients with newly diagnosed multiple myeloma. Mayo Clin. Proc. *78*, 21–33.

Lavin, M.F., and Kozlov, S. (2007). ATM activation and DNA damage response. Cell Cycle *6*, 931–942.

Leung-Hagesteijn, C., Erdmann, N., Cheung, G., Keats, J.J., Stewart, A.K., Reece, D.E., Chung, K.C., and Tiedemann, R.E. (2013). Xbp1s-negative tumor B cells and pre-plasmablasts mediate therapeutic proteasome inhibitor resistance in multiple myeloma. Cancer Cell *24*, 289–304.

Lieber, M.R. (2010). The mechanism of double-strand DNA break repair by the nonhomologous DNA end-joining pathway. Annu. Rev. Biochem. *79*, 181–211.

Lim, D.S., and Hasty, P. (1996). A mutation in mouse rad51 results in an early embryonic lethal that is suppressed by a mutation in p53. Mol. Cell. Biol. *16*, 7133–7143.

Lin, P., Owens, R., Tricot, G., and Wilson, C.S. (2004). Flow cytometric immunophenotypic analysis of 306 cases of multiple myeloma. Am. J. Clin. Pathol. *121*, 482–488.

Lindahl, T., and Barnes, D.E. (2000). Repair of endogenous DNA damage. Cold Spring Harb. Symp. Quant. Biol. *65*, 127–133.

Lindahl, T., Satoh, M.S., Poirier, G.G., and Klungland, A. (1995). Post-translational modification of poly(ADP-ribose) polymerase induced by DNA strand breaks. Trends Biochem. Sci. *20*, 405–411.

Liu, J., Doty, T., Gibson, B., and Heyer, W.-D. (2010). Human BRCA2 protein promotes RAD51 filament formation on RPA-covered single-stranded DNA. Nat. Struct. Mol. Biol. *17*, 1260–1262.

Livraghi, L., and Garber, J.E. (2015). PARP inhibitors in the management of breast cancer: current data and future prospects. BMC Med *13*, 188.

Long, D.T., and Walter, J.C. (2012). A novel function for BRCA1 in crosslink repair. Mol. Cell *46*, 111–112.

Lopez-Girona, A., Furnari, B., Mondesert, O., and Russell, P. (1999). Nuclear localization of Cdc25 is regulated by DNA damage and a 14-3-3 protein. Nature *397*, 172–175.

Luger, K., Mäder, A.W., Richmond, R.K., Sargent, D.F., and Richmond, T.J. (1997). Crystal structure of the nucleosome core particle at 2.8 A resolution. Nature *389*, 251–260.

Luijsterburg, M.S., and van Attikum, H. (2011). Chromatin and the DNA damage response: the cancer connection. Mol Oncol *5*, 349–367.

Lukas, J., and Bartek, J. (2004). Watching the DNA repair ensemble dance. Cell *118*, 666–668.

Lukas, J., Lukas, C., and Bartek, J. (2011). More than just a focus: The chromatin response to DNA damage and its role in genome integrity maintenance. Nat. Cell Biol. *13*, 1161–1169.

Luo, G., Yao, M.S., Bender, C.F., Mills, M., Bladl, A.R., Bradley, A., and Petrini, J.H. (1999). Disruption of mRad50 causes embryonic stem cell lethality, abnormal embryonic development, and sensitivity to ionizing radiation. Proc. Natl. Acad. Sci. U.S.A. *96*, 7376–7381.

Luo, J., Solimini, N.L., and Elledge, S.J. (2009). Principles of cancer therapy: oncogene and non-oncogene addiction. Cell *136*, 823–837.

Ma, T., Chen, Y., Zhang, F., Yang, C.-Y., Wang, S., and Yu, X. (2013). RNF111-dependent neddylation activates DNA damage-induced ubiquitination. Mol. Cell *49*, 897–907.

Ma, Y., Pannicke, U., Schwarz, K., and Lieber, M.R. (2002). Hairpin opening and overhang processing by an Artemis/DNA-dependent protein kinase complex in nonhomologous end joining and V(D)J recombination. Cell *108*, 781–794.

Ma, Y., Lu, H., Tippin, B., Goodman, M.F., Shimazaki, N., Koiwai, O., Hsieh, C.-L., Schwarz, K., and Lieber, M.R. (2004). A biochemically defined system for mammalian nonhomologous DNA end joining. Mol. Cell *16*, 701–713.

Ma, Y., Schwarz, K., and Lieber, M.R. (2005). The Artemis:DNA-PKcs endonuclease cleaves DNA loops, flaps, and gaps. DNA Repair (Amst.) *4*, 845–851.

Magrangeas, F., Avet-Loiseau, H., Munshi, N.C., and Minvielle, S. (2011). Chromothripsis identifies a rare and aggressive entity among newly diagnosed multiple myeloma patients. Blood *118*, 675–678.

Mailand, N., Bekker-Jensen, S., Faustrup, H., Melander, F., Bartek, J., Lukas, C., and Lukas, J. (2007). RNF8 ubiquitylates histones at DNA double-strand breaks and promotes assembly of repair proteins. Cell *131*, 887–900.

Mallette, F.A., and Richard, S. (2012). K48-linked ubiquitination and protein degradation regulate 53BP1 recruitment at DNA damage sites. Cell Res. *22*, 1221–1223.

Mallette, F.A., Gaumont-Leclerc, M.-F., and Ferbeyre, G. (2007). The DNA damage signaling pathway is a critical mediator of oncogene-induced senescence. Genes Dev. *21*, 43–48.

Mari, P.-O., Florea, B.I., Persengiev, S.P., Verkaik, N.S., Brüggenwirth, H.T., Modesti, M., Giglia-Mari, G., Bezstarosti, K., Demmers, J.A.A., Luider, T.M., et al. (2006). Dynamic assembly of end-joining complexes requires interaction between Ku70/80 and XRCC4. Proc. Natl. Acad. Sci. U.S.A. *103*, 18597–18602.

Marín, I., Lucas, J.I., Gradilla, A.-C., and Ferrús, A. (2004). Parkin and relatives: the RBR family of ubiquitin ligases. Physiol. Genomics *17*, 253–263.

de Massy, B. (2013). Initiation of meiotic recombination: how and where? Conservation and specificities among eukaryotes. Annu. Rev. Genet. *47*, 563–599.

Matilla, A., Gorbea, C., Einum, D.D., Townsend, J., Michalik, A., van Broeckhoven, C., Jensen, C.C., Murphy, K.J., Ptácek, L.J., and Fu, Y.H. (2001). Association of ataxin-7 with the proteasome subunit S4 of the 19S regulatory complex. Hum. Mol. Genet. *10*, 2821–2831.

Matsuoka, S., Huang, M., and Elledge, S.J. (1998). Linkage of ATM to cell cycle regulation by the Chk2 protein kinase. Science *282*, 1893–1897.

Matsuoka, S., Ballif, B.A., Smogorzewska, A., McDonald, E.R., Hurov, K.E., Luo, J., Bakalarski, C.E., Zhao, Z., Solimini, N., Lerenthal, Y., et al. (2007). ATM and ATR substrate analysis reveals extensive protein networks responsive to DNA damage. Science *316*, 1160–1166.

Mattiroli, F., and Sixma, T.K. (2014). Lysine-targeting specificity in ubiquitin and ubiquitin-like modification pathways. Nat. Struct. Mol. Biol. *21*, 308–316.

Mattiroli, F., Vissers, J.H.A., van Dijk, W.J., Ikpa, P., Citterio, E., Vermeulen, W., Marteijn, J.A., and Sixma, T.K. (2012). RNF168 ubiquitinates K13-15 on H2A/H2AX to drive DNA damage signaling. Cell *150*, 1182–1195.

Mayer-Kuckuk, P., Ullrich, O., Ziegler, M., Grune, T., and Schweiger, M. (1999). Functional interaction of poly(ADP-ribose) with the 20S proteasome in vitro. Biochem. Biophys. Res. Commun. *259*, 576–581.

McCabe, N., Turner, N.C., Lord, C.J., Kluzek, K., Bialkowska, A., Swift, S., Giavara, S., O'Connor, M.J., Tutt, A.N., Zdzienicka, M.Z., et al. (2006). Deficiency in the repair of DNA damage by homologous recombination and sensitivity to poly(ADP-ribose) polymerase inhibition. Cancer Res. *66*, 8109–8115.

McKinnon, P.J., and Caldecott, K.W. (2007). DNA strand break repair and human genetic disease. Annu Rev Genomics Hum Genet *8*, 37–55.

Meerang, M., Ritz, D., Paliwal, S., Garajova, Z., Bosshard, M., Mailand, N., Janscak, P., Hübscher, U., Meyer, H., and Ramadan, K. (2011). The ubiquitin-selective segregase VCP/p97 orchestrates the response to DNA double-strand breaks. Nat. Cell Biol. *13*, 1376–1382.

Mehta, A., and Haber, J.E. (2014). Sources of DNA double-strand breaks and models of recombinational DNA repair. Cold Spring Harb Perspect Biol *6*, a016428.

Meister, S., Schubert, U., Neubert, K., Herrmann, K., Burger, R., Gramatzki, M., Hahn, S., Schreiber, S., Wilhelm, S., Herrmann, M., et al. (2007). Extensive immunoglobulin production sensitizes myeloma cells for proteasome inhibition. Cancer Res. *67*, 1783–1792.

Miki, Y., Swensen, J., Shattuck-Eidens, D., Futreal, P.A., Harshman, K., Tavtigian, S., Liu, Q., Cochran, C., Bennett, L.M., and Ding, W. (1994). A strong candidate for the breast and ovarian cancer susceptibility gene BRCA1. Science *266*, 66–71.

Mimori, T., Hardin, J.A., and Steitz, J.A. (1986). Characterization of the DNA-binding protein antigen Ku recognized by autoantibodies from patients with rheumatic disorders. J. Biol. Chem. *261*, 2274–2278.

Mitelman, F., Johansson, B., and Mertens, F. (2007). The impact of translocations and gene fusions on cancer causation. Nat. Rev. Cancer *7*, 233–245.

Mortusewicz, O., Rothbauer, U., Cardoso, M.C., and Leonhardt, H. (2006). Differential recruitment of DNA Ligase I and III to DNA repair sites. Nucleic Acids Res. *34*, 3523–3532.

Mosbech, A., Lukas, C., Bekker-Jensen, S., and Mailand, N. (2013). The deubiquitylating enzyme USP44 counteracts the DNA double-strand break response mediated by the RNF8 and RNF168 ubiquitin ligases. J. Biol. Chem. *288*, 16579–16587.

Mukhopadhyay, D., and Riezman, H. (2007). Proteasome-independent functions of ubiquitin in endocytosis and signaling. Science *315*, 201–205.

Muñoz, M.C., Laulier, C., Gunn, A., Cheng, A., Robbiani, D.F., Nussenzweig, A., and Stark, J.M. (2012). RING finger nuclear factor RNF168 is important for defects in homologous recombination caused by loss of the breast cancer susceptibility factor BRCA1. J. Biol. Chem. *287*, 40618–40628.

Muñoz, M.C., Yanez, D.A., and Stark, J.M. (2014). An RNF168 fragment defective for focal accumulation at DNA damage is proficient for inhibition of homologous recombination in BRCA1 deficient cells. Nucleic Acids Res. *42*, 7720–7733.

Murai, J., Yang, K., Dejsuphong, D., Hirota, K., Takeda, S., and D'Andrea, A.D. (2011). The USP1/UAF1 complex promotes double-strand break repair through homologous recombination. Mol. Cell. Biol. *31*, 2462–2469.

Murakawa, Y., Sonoda, E., Barber, L.J., Zeng, W., Yokomori, K., Kimura, H., Niimi, A., Lehmann, A., Zhao, G.Y., Hochegger, H., et al. (2007). Inhibitors of the proteasome suppress homologous DNA recombination in mammalian cells. Cancer Res. *67*, 8536–8543.

Nakada, S., Tai, I., Panier, S., Al-Hakim, A., Iemura, S.-I., Juang, Y.-C., O'Donnell, L., Kumakubo, A., Munro, M., Sicheri, F., et al. (2010). Non-canonical inhibition of DNA damage-dependent ubiquitination by OTUB1. Nature *466*, 941–946.

Nam, E.A., and Cortez, D. (2011). ATR signalling: more than meeting at the fork. Biochem. J. *436*, 527–536.

Nick McElhinny, S.A., Snowden, C.M., McCarville, J., and Ramsden, D.A. (2000). Ku recruits the XRCC4-ligase IV complex to DNA ends. Mol. Cell. Biol. *20*, 2996–3003.

Nyberg, K.A., Michelson, R.J., Putnam, C.W., and Weinert, T.A. (2002). Toward maintaining the genome: DNA damage and replication checkpoints. Annu. Rev. Genet. *36*, 617–656.

Obeng, E.A., Carlson, L.M., Gutman, D.M., Harrington, W.J., Lee, K.P., and Boise, L.H. (2006). Proteasome inhibitors induce a terminal unfolded protein response in multiple myeloma cells. Blood *107*, 4907–4916.

Ochi, T., Blackford, A.N., Coates, J., Jhujh, S., Mehmood, S., Tamura, N., Travers, J., Wu, Q., Draviam, V.M., Robinson, C.V., et al. (2015). DNA repair. PAXX, a paralog of XRCC4 and XLF, interacts with Ku to promote DNA double-strand break repair. Science *347*, 185–188.

Ochs, F., Somyajit, K., Altmeyer, M., Rask, M.-B., Lukas, J., and Lukas, C. (2016). 53BP1 fosters fidelity of homology-directed DNA repair. Nat. Struct. Mol. Biol. *23*, 714–721.

O'Connor, M.J. (2015). Targeting the DNA Damage Response in Cancer. Mol. Cell *60*, 547–560.

Ogawa, H., Johzuka, K., Nakagawa, T., Leem, S.H., and Hagihara, A.H. (1995). Functions of the yeast meiotic recombination genes, MRE11 and MRE2. Adv. Biophys. *31*, 67–76.

Orthwein, A., Fradet-Turcotte, A., Noordermeer, S.M., Canny, M.D., Brun, C.M., Strecker, J., Escribano-Diaz, C., and Durocher, D. (2014). Mitosis inhibits DNA double-strand break repair to guard against telomere fusions. Science *344*, 189–193.

Ozkaynak, E., Finley, D., Solomon, M.J., and Varshavsky, A. (1987). The yeast ubiquitin genes: a family of natural gene fusions. EMBO J. *6*, 1429–1439.

Pace, P., Mosedale, G., Hodskinson, M.R., Rosado, I.V., Sivasubramaniam, M., and Patel, K.J. (2010). Ku70 corrupts DNA repair in the absence of the Fanconi anemia pathway. Science *329*, 219–223.

Palombella, V.J., Rando, O.J., Goldberg, A.L., and Maniatis, T. (1994). The ubiquitin-proteasome pathway is required for processing the NF-kappa B1 precursor protein and the activation of NF-kappa B. Cell *78*, 773–785.

Panier, S., and Boulton, S.J. (2014). Double-strand break repair: 53BP1 comes into focus. Nat. Rev. Mol. Cell Biol. *15*, 7–18.

Panier, S., and Durocher, D. (2009). Regulatory ubiquitylation in response to DNA double-strand breaks. DNA Repair (Amst.) *8*, 436–443.

Panier, S., Ichijima, Y., Fradet-Turcotte, A., Leung, C.C.Y., Kaustov, L., Arrowsmith, C.H., and Durocher, D. (2012). Tandem protein interaction modules organize the ubiquitin-dependent response to DNA double-strand breaks. Mol. Cell *47*, 383–395.

Pardo, B., Gómez-González, B., and Aguilera, A. (2009). DNA repair in mammalian cells: DNA double-strand break repair: how to fix a broken relationship. Cell. Mol. Life Sci. *66*, 1039–1056.

Patel, A.G., Sarkaria, J.N., and Kaufmann, S.H. (2011). Nonhomologous end joining drives poly(ADP-ribose) polymerase (PARP) inhibitor lethality in homologous recombination-deficient cells. Proc. Natl. Acad. Sci. U.S.A. *108*, 3406–3411.

Paull, T.T., and Gellert, M. (1998). The 3' to 5' exonuclease activity of Mre 11 facilitates repair of DNA double-strand breaks. Mol. Cell *1*, 969–979.

Paull, T.T., and Gellert, M. (1999). Nbs1 potentiates ATP-driven DNA unwinding and endonuclease cleavage by the Mre11/Rad50 complex. Genes Dev. *13*, 1276–1288.

Paull, T.T., and Lee, J.-H. (2005). The Mre11/Rad50/Nbs1 complex and its role as a DNA double-strand break sensor for ATM. Cell Cycle *4*, 737–740.

Peth, A., Besche, H.C., and Goldberg, A.L. (2009). Ubiquitinated proteins activate the proteasome by binding to Usp14/Ubp6, which causes 20S gate opening. Mol. Cell *36*, 794–804.

Peth, A., Uchiki, T., and Goldberg, A.L. (2010). ATP-dependent steps in the binding of ubiquitin conjugates to the 26S proteasome that commit to degradation. Mol. Cell *40*, 671–681.

Peuscher, M.H., and Jacobs, J.J.L. (2011). DNA-damage response and repair activities at uncapped telomeres depend on RNF8. Nat. Cell Biol. *13*, 1139–1145.

Pickart, C.M. (2001). Mechanisms underlying ubiquitination. Annu. Rev. Biochem. *70*, 503–533.

Pinato, S., Gatti, M., Scandiuzzi, C., Confalonieri, S., and Penengo, L. (2011). UMI, a novel RNF168 ubiquitin binding domain involved in the DNA damage signaling pathway. Mol. Cell. Biol. *31*, 118–126.

Pinder, J.B., Attwood, K.M., and Dellaire, G. (2013). Reading, writing, and repair: the role of ubiquitin and the ubiquitin-like proteins in DNA damage signaling and repair. Front Genet *4*, 45.

Plechanovová, A., Jaffray, E.G., Tatham, M.H., Naismith, J.H., and Hay, R.T. (2012). Structure of a RING E3 ligase and ubiquitin-loaded E2 primed for catalysis. Nature *489*, 115–120.

Polo, S.E., and Jackson, S.P. (2011). Dynamics of DNA damage response proteins at DNA breaks: a focus on protein modifications. Genes Dev. *25*, 409–433.

Poulsen, M., Lukas, C., Lukas, J., Bekker-Jensen, S., and Mailand, N. (2012). Human RNF169 is a negative regulator of the ubiquitin-dependent response to DNA double-strand breaks. J. Cell Biol. *197*, 189–199.

Prakash, R., Zhang, Y., Feng, W., and Jasin, M. (2015). Homologous recombination and human health: the roles of BRCA1, BRCA2, and associated proteins. Cold Spring Harb Perspect Biol *7*, a016600.

Rai, R., Li, J.-M., Zheng, H., Lok, G.T.-M., Deng, Y., Huen, M.S.-Y., Chen, J., Jin, J., and Chang, S. (2011). The E3 ubiquitin ligase Rnf8 stabilizes Tpp1 to promote telomere end protection. Nat. Struct. Mol. Biol. *18*, 1400–1407.

Raman, M., Havens, C.G., Walter, J.C., and Harper, J.W. (2011). A genome-wide screen identifies p97 as an essential regulator of DNA damage-dependent CDT1 destruction. Mol. Cell *44*, 72–84.

Ramsden, D.A., and Gellert, M. (1998). Ku protein stimulates DNA end joining by mammalian DNA ligases: a direct role for Ku in repair of DNA double-strand breaks. EMBO J. *17*, 609–614.

Rich, T., Allen, R.L., and Wyllie, A.H. (2000). Defying death after DNA damage. Nature *407*, 777–783.

Richly, H., Rape, M., Braun, S., Rumpf, S., Hoege, C., and Jentsch, S. (2005). A series of ubiquitin binding factors connects CDC48/p97 to substrate multiubiquitylation and proteasomal targeting. Cell *120*, 73–84.

Rieser, E., Cordier, S.M., and Walczak, H. (2013). Linear ubiquitination: a newly discovered regulator of cell signalling. Trends Biochem. Sci. *38*, 94–102.

Rodgers, K., and McVey, M. (2016). Error-Prone Repair of DNA Double-Strand Breaks. J. Cell. Physiol. *231*, 15–24.

Rogakou, E.P., Pilch, D.R., Orr, A.H., Ivanova, V.S., and Bonner, W.M. (1998). DNA double-stranded breaks induce histone H2AX phosphorylation on serine 139. J. Biol. Chem. *273*, 5858–5868.

Rotin, D., and Kumar, S. (2009). Physiological functions of the HECT family of ubiquitin ligases. Nat. Rev. Mol. Cell Biol. *10*, 398–409.

Rouse, J., and Jackson, S.P. (2002). Interfaces between the detection, signaling, and repair of DNA damage. Science *297*, 547–551.

Roy, R., Chun, J., and Powell, S.N. (2011). BRCA1 and BRCA2: different roles in a common pathway of genome protection. Nat. Rev. Cancer *12*, 68–78.

Saha, P., Eichbaum, Q., Silberman, E.D., Mayer, B.J., and Dutta, A. (1997). p21CIP1 and Cdc25A: competition between an inhibitor and an activator of cyclin-dependent kinases. Mol. Cell. Biol. *17*, 4338–4345.

San Miguel, J.F., Gutiérrez, N.C., Mateo, G., and Orfao, A. (2006). Conventional diagnostics in multiple myeloma. Eur. J. Cancer *42*, 1510–1519.

Sartori, A.A., Lukas, C., Coates, J., Mistrik, M., Fu, S., Bartek, J., Baer, R., Lukas, J., and Jackson, S.P. (2007). Human CtIP promotes DNA end resection. Nature *450*, 509–514.

Satoh, M.S., and Lindahl, T. (1992). Role of poly(ADP-ribose) formation in DNA repair. Nature *356*, 356–358.

Schlacher, K., Wu, H., and Jasin, M. (2012). A distinct replication fork protection pathway connects Fanconi anemia tumor suppressors to RAD51-BRCA1/2. Cancer Cell *22*, 106–116.

Schlegel, B.P., Jodelka, F.M., and Nunez, R. (2006). BRCA1 promotes induction of ssDNA by ionizing radiation. Cancer Res. *66*, 5181–5189.

Schulman, B.A., and Harper, J.W. (2009). Ubiquitin-like protein activation by E1 enzymes: the apex for downstream signalling pathways. Nat. Rev. Mol. Cell Biol. *10*, 319–331.

Shanbhag, N.M., Rafalska-Metcalf, I.U., Balane-Bolivar, C., Janicki, S.M., and Greenberg, R.A. (2010). ATM-dependent chromatin changes silence transcription in cis to DNA double-strand breaks. Cell *141*, 970–981.

Sharan, S.K., Morimatsu, M., Albrecht, U., Lim, D.S., Regel, E., Dinh, C., Sands, A., Eichele, G., Hasty, P., and Bradley, A. (1997). Embryonic lethality and radiation hypersensitivity mediated by Rad51 in mice lacking Brca2. Nature *386*, 804–810.

Shen, S.X., Weaver, Z., Xu, X., Li, C., Weinstein, M., Chen, L., Guan, X.Y., Ried, T., and Deng, C.X. (1998). A targeted disruption of the murine Brca1 gene causes gamma-irradiation hypersensitivity and genetic instability. Oncogene *17*, 3115–3124.

Shi, W., Ma, Z., Willers, H., Akhtar, K., Scott, S.P., Zhang, J., Powell, S., and Zhang, J. (2008). Disassembly of MDC1 foci is controlled by ubiquitin-proteasome-dependent degradation. J. Biol. Chem. *283*, 31608–31616.

Shiloh, Y., and Kastan, M.B. (2001). ATM: genome stability, neuronal development, and cancer cross paths. Adv. Cancer Res. *83*, 209–254.

Shrivastav, M., De Haro, L.P., and Nickoloff, J.A. (2008). Regulation of DNA double-strand break repair pathway choice. Cell Res. *18*, 134–147.

Smeenk, G., and Mailand, N. (2016). Writers, Readers, and Erasers of Histone Ubiquitylation in DNA Double-Strand Break Repair. Front Genet *7*, 122.

Smider, V., Rathmell, W.K., Lieber, M.R., and Chu, G. (1994). Restoration of X-ray resistance and V(D)J recombination in mutant cells by Ku cDNA. Science *266*, 288–291.

Smit, J.J., Monteferrario, D., Noordermeer, S.M., van Dijk, W.J., van der Reijden, B.A., and Sixma, T.K. (2012). The E3 ligase HOIP specifies linear ubiquitin chain assembly through its RING-IBR-RING domain and the unique LDD extension. EMBO J. *31*, 3833–3844.

Smith, G.C., and Jackson, S.P. (1999). The DNA-dependent protein kinase. Genes Dev. *13*, 916–934.

Sobhian, B., Shao, G., Lilli, D.R., Culhane, A.C., Moreau, L.A., Xia, B., Livingston, D.M., and Greenberg, R.A. (2007). RAP80 targets BRCA1 to specific ubiquitin structures at DNA damage sites. Science *316*, 1198–1202.

Sonoda, E., Sasaki, M.S., Buerstedde, J.M., Bezzubova, O., Shinohara, A., Ogawa, H., Takata, M., Yamaguchi-Iwai, Y., and Takeda, S. (1998). Rad51-deficient vertebrate cells accumulate chromosomal breaks prior to cell death. EMBO J. *17*, 598–608.

Stephens, P.J., Greenman, C.D., Fu, B., Yang, F., Bignell, G.R., Mudie, L.J., Pleasance, E.D., Lau, K.W., Beare, D., Stebbings, L.A., et al. (2011). Massive genomic rearrangement acquired in a single catastrophic event during cancer development. Cell *144*, 27–40.

Stewart, G.S., Panier, S., Townsend, K., Al-Hakim, A.K., Kolas, N.K., Miller, E.S., Nakada, S., Ylanko, J., Olivarius, S., Mendez, M., et al. (2009). The RIDDLE syndrome protein mediates a ubiquitin-dependent signaling cascade at sites of DNA damage. Cell *136*, 420–434.

Stieglitz, B., Morris-Davies, A.C., Koliopoulos, M.G., Christodoulou, E., and Rittinger, K. (2012). LUBAC synthesizes linear ubiquitin chains via a thioester intermediate. EMBO Rep. *13*, 840–846.

Stiff, T., Walker, S.A., Cerosaletti, K., Goodarzi, A.A., Petermann, E., Concannon, P., O'Driscoll, M., and Jeggo, P.A. (2006). ATR-dependent phosphorylation and activation of ATM in response to UV treatment or replication fork stalling. EMBO J *25*, 5775–5782.

Stucki, M., Clapperton, J.A., Mohammad, D., Yaffe, M.B., Smerdon, S.J., and Jackson, S.P. (2005). MDC1 directly binds phosphorylated histone H2AX to regulate cellular responses to DNA double-strand breaks. Cell *123*, 1213–1226.

Sugiyama, T., Zaitseva, E.M., and Kowalczykowski, S.C. (1997). A single-stranded DNA-binding protein is needed for efficient presynaptic complex formation by the Saccharomyces cerevisiae Rad51 protein. J. Biol. Chem. *272*, 7940–7945.

Symington, L.S. (2014). End resection at double-strand breaks: mechanism and regulation. Cold Spring Harb Perspect Biol *6*.

Symington, L.S., and Gautier, J. (2011). Double-strand break end resection and repair pathway choice. Annu. Rev. Genet. *45*, 247–271.

Taccioli, G.E., Gottlieb, T.M., Blunt, T., Priestley, A., Demengeot, J., Mizuta, R., Lehmann, A.R., Alt, F.W., Jackson, S.P., and Jeggo, P.A. (1994). Ku80: product of the XRCC5 gene and its role in DNA repair and V(D)J recombination. Science *265*, 1442–1445.

Takata, M., Sasaki, M.S., Sonoda, E., Morrison, C., Hashimoto, M., Utsumi, H., Yamaguchi-Iwai, Y., Shinohara, A., and Takeda, S. (1998). Homologous recombination and non-homologous end-joining pathways of DNA double-strand break repair have overlapping roles in the maintenance of chromosomal integrity in vertebrate cells. EMBO J. *17*, 5497–5508.

Tang, J., Cho, N.W., Cui, G., Manion, E.M., Shanbhag, N.M., Botuyan, M.V., Mer, G., and Greenberg, R.A. (2013). Acetylation limits 53BP1 association with damaged chromatin to promote homologous recombination. Nat. Struct. Mol. Biol. *20*, 317–325.

Thorslund, T., Ripplinger, A., Hoffmann, S., Wild, T., Uckelmann, M., Villumsen, B., Narita, T., Sixma, T.K., Choudhary, C., Bekker-Jensen, S., et al. (2015). Histone H1 couples initiation and amplification of ubiquitin signalling after DNA damage. Nature *527*, 389–393.

Tiscornia, G., Singer, O., and Verma, I.M. (2006). Production and purification of lentiviral vectors. Nat Protoc *1*, 241–245.

Torres, E.M., Dephoure, N., Panneerselvam, A., Tucker, C.M., Whittaker, C.A., Gygi, S.P., Dunham, M.J., and Amon, A. (2010). Identification of aneuploidy-tolerating mutations. Cell *143*, 71–83.

Tran, H., Brunet, A., Grenier, J.M., Datta, S.R., Fornace, A.J., DiStefano, P.S., Chiang, L.W., and Greenberg, M.E. (2002). DNA repair pathway stimulated by the forkhead transcription factor FOXO3a through the Gadd45 protein. Science *296*, 530–534.

Trujillo, K.M., Yuan, S.S., Lee, E.Y., and Sung, P. (1998). Nuclease activities in a complex of human recombination and DNA repair factors Rad50, Mre11, and p95. J. Biol. Chem. *273*, 21447–21450.

Tsuzuki, T., Fujii, Y., Sakumi, K., Tominaga, Y., Nakao, K., Sekiguchi, M., Matsushiro, A., Yoshimura, Y., and MoritaT, null (1996). Targeted disruption of the Rad51 gene leads to lethality in embryonic mice. Proc. Natl. Acad. Sci. U.S.A. *93*, 6236–6240.

Typas, D., Luijsterburg, M.S., Wiegant, W.W., Diakatou, M., Helfricht, A., Thijssen, P.E., van den Broek, B., Mullenders, L.H., and van Attikum, H. (2016). The de-ubiquitylating enzymes USP26 and USP37 regulate homologous recombination by counteracting RAP80. Nucleic Acids Res. *44*, 2976.

Uematsu, N., Weterings, E., Yano, K., Morotomi-Yano, K., Jakob, B., Taucher-Scholz, G., Mari, P.-O., van Gent, D.C., Chen, B.P.C., and Chen, D.J. (2007). Autophosphorylation of DNA-PKCS regulates its dynamics at DNA double-strand breaks. J. Cell Biol. *177*, 219–229.

Ullrich, O., Reinheckel, T., Sitte, N., Hass, R., Grune, T., and Davies, K.J. (1999). Poly-ADP ribose polymerase activates nuclear proteasome to degrade oxidatively damaged histones. Proc. Natl. Acad. Sci. U.S.A. *96*, 6223–6228.

Usui, T., Ohta, T., Oshiumi, H., Tomizawa, J., Ogawa, H., and Ogawa, T. (1998). Complex formation and functional versatility of Mre11 of budding yeast in recombination. Cell *95*, 705–716.

Uziel, T., Lerenthal, Y., Moyal, L., Andegeko, Y., Mittelman, L., and Shiloh, Y. (2003). Requirement of the MRN complex for ATM activation by DNA damage. EMBO J. *22*, 5612–5621.

Velimezi, G., Liontos, M., Vougas, K., Roumeliotis, T., Bartkova, J., Sideridou, M., Dereli-Oz, A., Kocylowski, M., Pateras, I.S., Evangelou, K., et al. (2013). Functional interplay between the DNA-damage-response kinase ATM and ARF tumour suppressor protein in human cancer. Nat. Cell Biol. *15*, 967–977.

Verma, R., Oania, R., Fang, R., Smith, G.T., and Deshaies, R.J. (2011). Cdc48/p97 mediates UV-dependent turnover of RNA Pol II. Mol. Cell *41*, 82–92.

Vogelstein, B., Papadopoulos, N., Velculescu, V.E., Zhou, S., Diaz, L.A., and Kinzler, K.W. (2013). Cancer genome landscapes. Science *339*, 1546–1558.

de Vries, E., van Driel, W., Bergsma, W.G., Arnberg, A.C., and van der Vliet, P.C. (1989). HeLa nuclear protein recognizing DNA termini and translocating on DNA forming a regular DNA-multimeric protein complex. J. Mol. Biol. *208*, 65–78.

Wang, B., and Elledge, S.J. (2007). Ubc13/Rnf8 ubiquitin ligases control foci formation of the Rap80/Abraxas/Brca1/Brcc36 complex in response to DNA damage. Proc. Natl. Acad. Sci. U.S.A. *104*, 20759–20763.

Wang, B., Matsuoka, S., Ballif, B.A., Zhang, D., Smogorzewska, A., Gygi, S.P., and Elledge, S.J. (2007). Abraxas and RAP80 form a BRCA1 protein complex required for the DNA damage response. Science *316*, 1194–1198.

Wang, J., Aroumougame, A., Lobrich, M., Li, Y., Chen, D., Chen, J., and Gong, Z. (2014). PTIP associates with Artemis to dictate DNA repair pathway choice. Genes Dev. *28*, 2693–2698.

Wang, M., Wu, W., Wu, W., Rosidi, B., Zhang, L., Wang, H., and Iliakis, G. (2006). PARP-1 and Ku compete for repair of DNA double strand breaks by distinct NHEJ pathways. Nucleic Acids Res. *34*, 6170–6182.

Warner, J.R., Mitra, G., Schwindinger, W.F., Studeny, M., and Fried, H.M. (1985). Saccharomyces cerevisiae coordinates accumulation of yeast ribosomal proteins by modulating mRNA splicing, translational initiation, and protein turnover. Mol. Cell. Biol. *5*, 1512–1521.

Wee, S., Wiederschain, D., Maira, S.-M., Loo, A., Miller, C., deBeaumont, R., Stegmeier, F., Yao, Y.-M., and Lengauer, C. (2008). PTEN-deficient cancers depend on PIK3CB. Proc. Natl. Acad. Sci. U.S.A. *105*, 13057–13062.

Wenzel, D.M., Lissounov, A., Brzovic, P.S., and Klevit, R.E. (2011). UBCH7 reactivity profile reveals parkin and HHARI to be RING/HECT hybrids. Nature *474*, 105–108.

Weston, V.J., Oldreive, C.E., Skowronska, A., Oscier, D.G., Pratt, G., Dyer, M.J.S., Smith, G., Powell, J.E., Rudzki, Z., Kearns, P., et al. (2010). The PARP inhibitor olaparib induces significant killing of ATM-deficient lymphoid tumor cells in vitro and in vivo. Blood *116*, 4578–4587.

Whitesell, L., and Lindquist, S.L. (2005). HSP90 and the chaperoning of cancer. Nat. Rev. Cancer *5*, 761–772.

Wiborg, O., Pedersen, M.S., Wind, A., Berglund, L.E., Marcker, K.A., and Vuust, J. (1985). The human ubiquitin multigene family: some genes contain multiple directly repeated ubiquitin coding sequences. EMBO J. *4*, 755–759.

Wiederschain, D., Wee, S., Chen, L., Loo, A., Yang, G., Huang, A., Chen, Y., Caponigro, G., Yao, Y.-M., Lengauer, C., et al. (2009). Single-vector inducible lentiviral RNAi system for oncology target validation. Cell Cycle *8*, 498–504.

van Wijk, S.J.L., and Timmers, H.T.M. (2010). The family of ubiquitin-conjugating enzymes (E2s): deciding between life and death of proteins. FASEB J. *24*, 981–993.

Williams, B.R., and Amon, A. (2009). Aneuploidy: cancer's fatal flaw? Cancer Res. *69*, 5289–5291.

Williams, B.R., Prabhu, V.R., Hunter, K.E., Glazier, C.M., Whittaker, C.A., Housman, D.E., and Amon, A. (2008). Aneuploidy affects proliferation and spontaneous immortalization in mammalian cells. Science *322*, 703–709.

Williamson, C.T., Muzik, H., Turhan, A.G., Zamò, A., O'Connor, M.J., Bebb, D.G., and Lees-Miller, S.P. (2010). ATM deficiency sensitizes mantle cell lymphoma cells to poly(ADP-ribose) polymerase-1 inhibitors. Mol. Cancer Ther. *9*, 347–357.

Williamson, C.T., Kubota, E., Hamill, J.D., Klimowicz, A., Ye, R., Muzik, H., Dean, M., Tu, L., Gilley, D., Magliocco, A.M., et al. (2012). Enhanced cytotoxicity of PARP inhibition in mantle cell lymphoma harbouring mutations in both ATM and p53. EMBO Mol Med *4*, 515–527.

Wilson, T.E., and Lieber, M.R. (1999). Efficient processing of DNA ends during yeast nonhomologous end joining. Evidence for a DNA polymerase beta (Pol4)-dependent pathway. J. Biol. Chem. *274*, 23599–23609.

Wilson, M.D., Benlekbir, S., Fradet-Turcotte, A., Sherker, A., Julien, J.-P., McEwan, A., Noordermeer, S.M., Sicheri, F., Rubinstein, J.L., and Durocher, D. (2016). The structural basis of modified nucleosome recognition by 53BP1. Nature *536*, 100–103.

Wu, L.C., Wang, Z.W., Tsan, J.T., Spillman, M.A., Phung, A., Xu, X.L., Yang, M.C., Hwang, L.Y., Bowcock, A.M., and Baer, R. (1996). Identification of a RING protein that can interact in vivo with the BRCA1 gene product. Nat. Genet. *14*, 430–440.

Wyman, C., and Kanaar, R. (2006). DNA double-strand break repair: all's well that ends well. Annu. Rev. Genet. *40*, 363–383.

Xia, B., Dorsman, J.C., Ameziane, N., de Vries, Y., Rooimans, M.A., Sheng, Q., Pals, G., Errami, A., Gluckman, E., Llera, J., et al. (2007). Fanconi anemia is associated with a defect in the BRCA2 partner PALB2. Nat. Genet. *39*, 159–161.

Xiao, Y., and Weaver, D.T. (1997). Conditional gene targeted deletion by Cre recombinase demonstrates the requirement for the double-strand break repair Mre11 protein in murine embryonic stem cells. Nucleic Acids Res. *25*, 2985–2991.

Xing, M., Yang, M., Huo, W., Feng, F., Wei, L., Jiang, W., Ning, S., Yan, Z., Li, W., Wang, Q., et al. (2015). Interactome analysis identifies a new paralogue of XRCC4 in non-homologous end joining DNA repair pathway. Nat Commun *6*, 6233.

Xu, B., Kim, S.-T., Lim, D.-S., and Kastan, M.B. (2002). Two molecularly distinct G(2)/M checkpoints are induced by ionizing irradiation. Mol. Cell. Biol. *22*, 1049–1059.

Xu, G., Chapman, J.R., Brandsma, I., Yuan, J., Mistrik, M., Bouwman, P., Bartkova, J., Gogola, E., Warmerdam, D., Barazas, M., et al. (2015). REV7 counteracts DNA double-strand break resection and affects PARP inhibition. Nature *521*, 541–544.

Xu, P., Duong, D.M., Seyfried, N.T., Cheng, D., Xie, Y., Robert, J., Rush, J., Hochstrasser, M., Finley, D., and Peng, J. (2009). Quantitative proteomics reveals the function of unconventional ubiquitin chains in proteasomal degradation. Cell *137*, 133–145.

Yamaguchi-Iwai, Y., Sonoda, E., Sasaki, M.S., Morrison, C., Haraguchi, T., Hiraoka, Y., Yamashita, Y.M., Yagi, T., Takata, M., Price, C., et al. (1999). Mre11 is essential for the maintenance of chromosomal DNA in vertebrate cells. EMBO J. *18*, 6619–6629.

Yaneva, M., Kowalewski, T., and Lieber, M.R. (1997). Interaction of DNA-dependent protein kinase with DNA and with Ku: biochemical and atomic-force microscopy studies. EMBO J. *16*, 5098–5112.

Yannone, S.M., Khan, I.S., Zhou, R.-Z., Zhou, T., Valerie, K., and Povirk, L.F. (2008). Coordinate 5' and 3' endonucleolytic trimming of terminally blocked blunt DNA double-strand break ends by Artemis nuclease and DNA-dependent protein kinase. Nucleic Acids Res. *36*, 3354–3365.

Yano, K., Morotomi-Yano, K., Wang, S.-Y., Uematsu, N., Lee, K.-J., Asaithamby, A., Weterings, E., and Chen, D.J. (2008). Ku recruits XLF to DNA double-strand breaks. EMBO Rep. *9*, 91–96.

Yun, M.H., and Hiom, K. (2009). CtIP-BRCA1 modulates the choice of DNA double-strand-break repair pathway throughout the cell cycle. Nature *459*, 460–463.

Zhang, F., Fan, Q., Ren, K., and Andreassen, P.R. (2009). PALB2 functionally connects the breast cancer susceptibility proteins BRCA1 and BRCA2. Mol. Cancer Res. *7*, 1110–1118.

Zhivotovsky, B., and Kroemer, G. (2004). Apoptosis and genomic instability. Nat. Rev. Mol. Cell Biol. *5*, 752–762.

Zhou, B.B., and Elledge, S.J. (2000). The DNA damage response: putting checkpoints in perspective. Nature *408*, 433–439.

Zhou, Q., Kojic, M., Cao, Z., Lisby, M., Mazloum, N.A., and Holloman, W.K. (2007). Dss1 interaction with Brh2 as a regulatory mechanism for recombinational repair. Mol. Cell. Biol. *27*, 2512–2526.

Zhu, J., Petersen, S., Tessarollo, L., and Nussenzweig, A. (2001). Targeted disruption of the Nijmegen breakage syndrome gene NBS1 leads to early embryonic lethality in mice. Curr. Biol. *11*, 105–109.

Zimmermann, M., Lottersberger, F., Buonomo, S.B., Sfeir, A., and de Lange, T. (2013). 53BP1 regulates DSB repair using Rif1 to control 5' end resection. Science *339*, 700–704.

Ziv, Y., Bar-Shira, A., Pecker, I., Russell, P., Jorgensen, T.J., Tsarfati, I., and Shiloh, Y. (1997). Recombinant ATM protein complements the cellular A-T phenotype. Oncogene *15*, 159–167.

Zong, D., Callén, E., Pegoraro, G., Lukas, C., Lukas, J., and Nussenzweig, A. (2015). Ectopic expression of RNF168 and 53BP1 increases mutagenic but not physiological non-homologous end joining. Nucleic Acids Res. *43*, 4950–4961.

Zou, L., and Elledge, S.J. (2003). Sensing DNA damage through ATRIP recognition of RPA-ssDNA complexes. Science *300*, 1542–1548.

13 ABBREVIATIONS

53BP1/TP53BP1	(tumor protein) p53 binding protein 1
A-T	Ataxia Talengiactasia
ATM	Ataxia-Talangiectasia Mutated
ATP	Adenosine TriPhosphate
ATR	Ataxia-Talangiecstasia mutated and Rad3 related
ATRIP	ATR Interacting Protein
BER	Base Excision Repair
BiP	Binding Immunoglobulin Protein
BLM	Bloom DNA helicase
BRCA1	Breast Cancer susceptibility protein 1
BRCA2	Breast Cancer susceptibility protein 2
BRCT	BRCA1 Carboxy Terminal domain
BTZ	Bortezomib
BrdU	5-bromo-2'-deoxyuridine
CDK1	Cyclin-Dependent Kinase 1
CD138 (SCD1)	Syndecan 1
CHK1/CHK2	Checkpoint proteins 1 and 2
CPT	Camptothecin
CSR	Class Switch Recombination
CTIP/RBBP8	C Terminal binding protein Interacing Protein/ Retinoblastoma Binding protein
DAPI	4',6-diamidino-2-phenylindole
DDR	DNA Damage Response
DNA	deoxyribonucleic acid
DNA-PK	DNA-dependent protein kinase
DNA-PKcs	catalytic subunit of DNA-dependent protein kinase
DSB	Double-Strand Break
Dox	Doxycycline
DUB	DeUBiquitylating enzyme/deubiquitylase

E1	Ubiquitin- activating enzyme
E2	Ubiquitin-conjugating enzyme
E3	Ubiquitin ligase
ECL	Enhanced Chemiluminiscence (detection)
FACS	Fluorescence Associated Cell Sorting
FHA	ForkHead-Associated domain
FK2	Mono- and polyubiquitylated protein conjugates in DDR
GAPDH	GlycerAldehyde 3-Phosphate DeHydrogenase
GFP	Green Fluorescent Protein
Gy	Gray
yH2AX	Histone variant H2A.X phosphorylated at serine-139
H2AK15ub	ubiquitylated histone H2A on lysine 15
H4K20me2	dimethylated histone H4 on lysine 20
HC	Heterochromatin
HECT	Homology to E6AP Carboxyl-Terminus
IRIF	Ionizing Radiation Induced Immunofluorescent Foci
JMJD2A	JuMonJi Domain 2 protein A
K48	lysine number 48
K63	lysine number 63
L3MBTL1	Lethal (3) Malignant Brain Tumor-Like protein 1
MDC1	Mediator of DNA damage Checkpoint protein 1
MGUS	Monoclonal Gammopathy of Uknown Significance
MM	Multiple Myeloma
MMR	Mismatch Repair
MRE11	Meiotic Recombination protein 11
NBS1	Nijmengen Breakage Syndrome protein 1
NER	Nucleotide Excision Eepair
NHEJ	Non-Homologous End Joining
aNHEJ	alternativej Non-Homologous End Joining
cNHEJ	classic Non-Homologous End Joining
mutNHEJ	mutagenic Non-Homologous End Joining

P53/TP53	Tumor Protein p53
PALB2	Partner And Localizer of BRCA2
PAR	Poly- (ADP Ribose)
PARP1	Poly-(ADP Ribose) Polymerase 1
PARP2	Poly-(ADP Ribose) Polymerase 2
PARPi	Poly (ADP-Ribose) Polymerase inhibitor
PAXX	PAralog of XRCC4 and XLF
PIs	Proteasome Inhibitors
PBS	Phosphate-Buffered Saline
PCNA	Proliferating Cell Nuclear Antigen
PCs	Plasma Cells
PTIP	PAX transcription activation domain interacting protein
PTM	Post-Translational Modification
PIKK	Phosphatidylinositol 3-kinase-related kinase
RAD50	DNA repair protein RAD50
RAD51	RAD51 recombinase
RBR	Ring Between Ring
RIDDLE	Radiosensitivity, Immunodeficiency, Dysmorphic features and Learning difficulties
RIF1	Replication timing regulatory factor 1
RING	Really Interesting New Gene
RNF8	RiNg Finger protein 8
RNF168	RiNg Finger protein 168
RPA	Replication Protein A
SCID	Severe Combined ImmunoDeficiency
shRNA	Short Hairpin RNA
SMC1	Structural Maintenance of Chromosomes protein 1
siRNA	Small Interfered RNA
SSB	Single-Strand Break
ssDNA	single-stranded DNA
TLS	Translesion Synthesis

TOPBP1	Topoisomerase Binding Protein 1
TRIP12	Thyroid hormone Receptor Interactor Protein 12
TT	Tandem Tudor domain
Ub	Ubiquitin
UBC13/UBE2N	UBiquitin Conjugating enzyme 13
UBR5	Ubiquitin protein ligase E3 component n-recognin 5
UDR	Ubiquitin Damage Response domain
UPR	Ubiquitin-Proteasome Response
USP26	Ubiquitin Specific peptidase 26
USP37	Ubiquitin Specific Peptidase 37
UV	Ultraviolet light
XRCC4	X-ray Cross-Complementation group 4

14 BIBLIOGRAPHY

14.1 ORIGINAL ARTICLES AND REVIEWS

K Chroma, M Mistrik, P Moudry, J Gursky, M Liptay, R Strauss, Z Skrott, R Vrtel, J Bartkova, J Kramara, J Bartek. Tumors overexpressing RNF168 show altered DNA repair and responses to genotoxic treatments, genomic instability and resistance to proteotoxic stress. Oncogene 2016 Nov 14., IF (2016): 7.932

K Chroma, J Kramara , P Moudry , M Mistrik , J Bartek . Sustained DNA damage response in proteasome inhibitor treated cancer cell lines. Zborník prednášok- Súťaž mladých onkológov 2014, NADÁCIA VÝSKUM RAKOVINY A ÚSTAV EXPERIMENTÁLNEJ ONKOLÓGIE SAV BA, ISBN 978 -80 -971621-0-8. No IF

L Beresova, E Vesela, I Chamrád, J Voller, M Yamada, T Furst, R Lenobel, **K Chroma**, J Gursky, K Krizova, M Mistrik, and J Bartek, Role of DNA repair factor XPC in response to replication stress, revealed by DNA fragile site affinity chromatography and quantitative proteomics. J. Proteome Res. 2016 October 30., IF (2016): 4.173

E Vesela, **K Chroma**, Z Turi, M Mistrik. Common Chemical Inductors of Replication Stress: Focus on Cell-Based Studies. Biomolecules 2017 February 21., IF (2017) not defined yet

14.2 CONFERENCE LECTURES AND POSTER PRESENTATIONS

ORAL TALKS:

K Chroma, J Kramara , P Moudry , M Mistrik , J Bartek . Sustained DNA damage response in proteasome inhibitor treated cancer cell lines, Súťaž mladých onkológov o najlepšiu prácu v oblasti onkologického výzkumu, Bratislava, 2014.

K Chroma , J Kramara , P Moudry , M Mistrik , J Bartek . Sustained DNA damage response in proteasome inhibitor treated cancer cell lines. IX. Diagnostic, Predictive and Experimental Oncology days, Olomouc, 2013.

K Chroma , J Kramara , P Moudry , M Mistrik , J Bartek. Sustained DNA damage response in proteasome inhibitor treated cancer cell lines. XIV Mezioborovom setkání mladých biologu, biochemiku a chemiku, hotel Devět Skal Milovy, 2014.

K Chroma, M Mistrik, P Moudry, J Gursky, M Liptay, R Strauss, Z Skrott, R Vrtel, J Bartkova, J Kramara, J Bartek. Tumors overexpressing RNF168 show altered DNA repair and responses to genotoxic treatments, genomic instability and resistance to proteotoxic stress. XII. Diagnostic Predictive and Experimental Oncology Days, Olomouc, 2016.

POSTER PRESENTATIONS:

K Chroma , J Kramara , P Moudry , J Gursky , R Strauss , M Mistrik , J Bartek. Sustained DNA damage response in proteasome inhibitor treated cancer cell lines. The 2015 IMB Conference- DNA repair and genome stability within chromatin environment, Mainz, 2015.

K Chroma , J Kramara , P Moudry , J Gursky , R Strauss , M Mistrik , J Bartek. Upregulated expression of the RNF168 E3 ubiquitin ligase enables sustained DNA Damage Response under proteotoxic stress, The Biomania Student Scientific Meeting 2015, Brno, 2015.

K Chroma , J Kramara , P Moudry , J Gursky , R Strauss , M Mistrik , J Bartek. Cancer-associated overexpression of RNF168 ubiquitin ligase alters DNA repair and response to PARP inhibitors under proteotoxic stress. XI Diagnostic, Predictive and Experimental Oncology Days, Olomouc 2015

K Chroma, P Moudry, M Mistrik, J Gursky, M Liptay, R Strauss, Z Skrott, R Vrtel, J Kramara , J Bartek . Proteotoxic stress-associated overexpression of RNF168 ubiquitin ligase alters DNA repair pathway choice, genomic instability and responses to genotoxic treatments

in subsets of human cancer. 10th Quinquennial Conference on Response to DNA damage: from molecule to disease. Egmond aan Zee, The Netherlands, 2016

K Chroma, P Moudry, M Mistrik, J Gursky, M Liptay, R Strauss, Z Skrott, R Vrtel, J Kramara , J Bartek. Overexpression of RNF168 ubiquitin ligase marks a subset of human tumors with aberrant stress responses, altered DNA repair and genomic instability. 7th DNA Repair Workshop, Smolenice, 2016.

15 APPENDIX- FULL TEXT PUBLICATIONS RELATED TO THE THESIS

15.1 APPENDIX A

K Chroma, M Mistrik, P Moudry, J Gursky, M Liptay, R Strauss, Z Skrott, R Vrtel, J Bartkova, J Kramara, J Bartek. Tumors overexpressing RNF168 show altered DNA repair and responses to genotoxic treatments, genomic instability and resistance to proteotoxic stress. Oncogene 2016 Nov 14, IF (2016): 7.932

Oncogene (2016), 1–18

www.nature.com/onc

ORIGINAL ARTICLE

Tumors overexpressing RNF168 show altered DNA repair and responses to genotoxic treatments, genomic instability and resistance to proteotoxic stress

K Chroma[1], M Mistrik[1,5], P Moudry[1,2,5], J Gursky[1], M Liptay[1], R Strauss[2], Z Skrott[1], R Vrtel[3], J Bartkova[2,4], J Kramara[1] and J Bartek[1,2,4]

Chromatin DNA damage response (DDR) is orchestrated by the E3 ubiquitin ligase ring finger protein 168 (RNF168), resulting in ubiquitin-dependent recruitment of DDR factors and tumor suppressors breast cancer 1 (BRCA1) and p53 binding protein 1 (53BP1). This ubiquitin signaling regulates pathway choice for repair of DNA double-strand breaks (DSB), toxic lesions whose frequency increases during tumorigenesis. Recruitment of 53BP1 curbs DNA end resection, thereby limiting homologous recombination (HR) and directing DSB repair toward error-prone non-homologous end joining (NHEJ). Under cancer-associated ubiquitin starvation conditions reflecting endogenous or treatment-evoked proteotoxic stress, the ubiquitin-dependent accrual of 53BP1 and BRCA1 at the DNA damage sites is attenuated or lost. Challenging this current paradigm, here we identified diverse human cancer cell lines that display 53BP1 recruitment to DSB sites even under proteasome inhibitor-induced proteotoxic stress, that is, under substantial depletion of free ubiquitin. We show that central to this unexpected phenotype is overabundance of RNF168 that enables more efficient exploitation of the residual-free ubiquitin. Cells with elevated RNF168 are more resistant to combined treatment by ionizing radiation and proteasome inhibition, suggesting that such aberrant RNF168-mediated signaling might reflect adaptation to chronic proteotoxic and genotoxic stresses experienced by tumor cells. Moreover, the overabundant RNF168 and the ensuing unorthodox recruitment patterns of 53BP1, RIF1 and REV7 (monitored on laser micro-irradiation-induced DNA damage) shift the DSB repair balance from HR toward NHEJ, a scenario accompanied by enhanced chromosomal instability/micronuclei formation and sensitivity under replication stress-inducing treatments with camptothecin or poly(ADP-ribose) polymerase (PARP) inhibitor. Overall, our data suggest that the deregulated RNF168/53BP1 pathway could promote tumorigenesis by selecting for a more robust, better stress-adapted cancer cell phenotype, through altered DNA repair, fueling genomic instability and tumor heterogeneity. Apart from providing insights into cancer (patho)biology, the elevated RNF168, documented here also by immunohistochemistry on human clinical tumor specimens, may impact responses to standard-of-care and some emerging targeted cancer therapies.

Oncogene advance online publication, 14 November 2016; doi:10.1038/onc.2016.392

INTRODUCTION

Reflecting the process of oncogenic transformation and the ensuing biological consequences, cancer cells are generally exposed to enhanced endogenous stresses such as replication stress/DNA damage and proteotoxic stress. Such environment provides selective pressures for tumors to adapt, through selection of features that allow cancer cell survival and proliferation at the expense of genomic instability and potential vulnerabilities in the form of dependencies on various stress-support pathways.[1–3] For example, nascent tumor cells in early stages of tumorigenesis experience increased replication stress and incidence of DNA lesions including the highly toxic DNA double-strand breaks (DSBs), and such DNA damage is sensed and acted upon by the cell's DNA damage response (DDR) machinery.[2,4,5] Although such checkpoint response provides a biological anticancer barrier capable of preventing tumor growth through induction of cellular senescence or cell death,[6–8] some tumors escape the barriers and progress to aggressive malignancy. One way how cancers breach the DDR barrier is through selection of mutations in the ataxia telangiectasia mutated (ATM)-Chk2-p53 pathway,[4,6] however, in many cases the adaptation mechanisms that help cancer cells cope with diverse stresses and thereby support tumor progression remain poorly understood.

Given that tumor cells are exposed to higher loads of DSBs, because of both endogenous replication stress and impact of standard-of-care treatments including radiotherapy and multiple chemotherapeutic drugs, cancer cell responses to DSBs are crucial for cancer development and treatment response. Mammalian cells respond to DSBs by activating a multi-component signaling cascade that relies on several protein posttranslational modifications including phosphorylation, ubiquitination, methylation, sumoylation and poly(ADP ribosylation) to orchestrate the DSB

[1]Institute of Molecular and Translational Medicine, Faculty of Medicine and Dentistry, Palacky University, Olomouc, Czech Republic; [2]Genome Integrity Unit, Danish Cancer Society Research Center, Copenhagen, Denmark; [3]Department of Clinical Genetics, University Hospital Olomouc, Olomouc, Czech Republic and [4]Department of Medical Biochemistry and Biophysics, Science For Life Laboratory, Division of Translational Medicine and Chemical Biology, Karolinska Institute, Solna, Sweden. Correspondence: Dr J Kramara, Institute of Molecular and Translational Medicine, Faculty of Medicine and Dentistry, Palacky University, Hnevotinska 5, Olomouc 775 15, Czech Republic or Professor J Bartek, Genome Integrity Unit, Danish Cancer Society Research Center, Strandboulevarden 49, Copenhagen DK-2100, Denmark.
E-mail: juraj.kramara@upol.cz or jb@cancer.dk
[5]These authors contributed equally to this work.
Received 6 June 2016; revised 14 August 2016; accepted 12 September 2016

signaling and repair.[9] Closely linked with DSB-induced phosphorylation signaling by the ATM kinase, ubiquitination of diverse proteins on damaged chromatin, mediated by E3 ubiquitin ligases ring finger protein 8 (RNF8) and ring finger protein 168 (RNF168), is critical for proper cellular response to DSBs.[10] RNF8 is recruited to DSB sites through binding to phosphorylated mediator of DNA damage checkpoint 1 (MDC1), an adaptor protein that recognizes the initial DSB signal—the ATM-phosphorylated histone variant H2A.X[11] (γH2AX). RNF8 catalyzes lysine K63-linked ubiquitination of histone H1, which promotes recruitment of the other key E3 ligase, RNF168.[12] The RNF8/RNF168-driven ubiquitinations create a platform for binding of two essential effectors (and tumor suppressors) to the DSB site: p53 binding protein 1 (53BP1) and breast cancer 1 (BRCA1).[13,14] These two proteins control the DSB repair pathway choice: 53BP1 promotes repair by the non-homologous end joining (NHEJ) pathway, whereas BRCA1 may oppose or facilitate (depending on distinct protein complexes of BRCA1) the homologous recombination (HR) repair. Both BRCA1 and 53BP1 exert their control over the repair pathway choice by regulating DSB end resection. Although 53BP1 licenses NHEJ by limiting resection and dominates in G1 phase, some BRCA1 complexes counteract 53BP1 by removing it from the sites of damage in S phase thereby enabling DNA resection and HR initiation.[15–17] The exact mechanism of resection inhibition by 53BP1 remains enigmatic, however several 53BP1 interacting factors have been identified recently that have been implicated in resection control, including RIF1 and REV7.[18–21] Upregulated 53BP1 recruitment in S phase because of absence of functional BRCA1 precludes the error-free HR and licenses inappropriate mutagenic NHEJ at replication-associated DSBs instead, resulting in enhanced chromosomal instability.[22] Hence, cells with aberrant S-phase recruitment of 53BP1, such as BRCA1-deficient tumors, exhibit sensitivity toward chemotherapeutic agents that cause damage of replicating DNA, including poly(ADP-ribose) polymerase (PARP) inhibitors (PARPis).[15]

The exact nature of 53BP1 recruitment to the DNA damage sites has been elucidated only recently. It has been shown that along with the dimethylated histone H4K20, 53BP1 also reads H2AK15 monoubiquitination catalyzed by RNF168 upon DNA damage.[23,24] Another layer of regulation represent proteins that compete for the H4K20 mark with 53BP1 and thus oppose 53BP1's recruitment to chromatin. Three such proteins have been reported, the JMJD2A and JMJD2B demethylases and the polycomb protein L3MBTL. All are removed from chromatin upon DNA damage by the ubiquitin–proteasome system (UPS) in an RNF168-dependent manner. Clearance of the competing proteins exposes the H4K20 mark and allows 53BP1 binding to chromatin.[25,26] Collectively, RNF168 appears to be crucial for both recruitment modes of 53BP1 and thereby for shifting the DSB repair balance toward NHEJ. The central role of RNF168 in DSB signaling is also consistent with the clinical phenotype of its homozygous inactivating mutation, leading to a grave human disease highly reminiscent of the ATM kinase deficiency-associated neurodegeneration, immunodeficiency and cancer-prone syndrome of Ataxia Telangectasia.[27] As a powerful signal amplifier at damaged chromatin, RNF168 requires a careful control over its abundance and function, a requirement documented by negative regulation of RNF168 by two ubiquitin ligases—TRIP12 and UBR5 that target RNF168 for proteasomal degradation.[28] Depletion of these proteins causes, in an additive manner, accumulation of RNF168 to supraphysiological levels and enhances the accrual of 53BP1 and other genome caretakers on chromatin.[28]

According to current understanding in the field, depletion of the cellular-free ubiquitin pool that occurs as a consequence of proteotoxic stress abrogates the ubiquitin-dependent aspects of DSB response such as recruitment of 53BP1.[29,30] Under proteotoxic stress, ubiquitin is redistributed within the cell, the bulk being trapped in cytoplasmic protein conjugates because of the limited recycling capacity of the proteasome. Consequently, the free ubiquitin level in the nucleus is depleted and ubiquitin-dependent nuclear processes such as the DSB signaling are attenuated.[29] A typical phenotypic manifestation of DDR attenuation under ubiquitin depletion conditions is a failure to recruit the 53BP1 and BRCA1 proteins to the sites of damage.[30] As mentioned above, most tumors experience at least partly enhanced endogenous proteotoxic stress, a scenario most prominent in multiple myeloma.[1] The endogenous proteotoxic stress is a consequence of cancer-related gross changes in chromosome number, gene copy number, aberrant protein overproduction exemplified by the immunoglobulin-producing myelomas and/or transcription variants that boost the production of aberrant proteins thus overloading the UPS.[1] Hence, proteotoxic stress seems to be intimately linked to cancer and has been listed as one of the emerging cancer hallmarks.[3] Exacerbating the endogenous proteotoxic stress by proteasome inhibitors has proven to be a viable strategy in treatment of multiple myeloma and it may be applicable also to other cancers.[1] Nevertheless, a broader use of proteasome inhibitors in cancer treatment has so far been hampered by limited efficiency of proteasome inhibition *in vivo* and frequent emergence of resistance.[1]

While analyzing responses to diverse stresses among a range of human cell types, we identified a subset of cancer cell lines that did not follow the established pattern of limited DSB response under enhanced proteotoxic stress. Through a combination of functional DDR-related, biochemical and cell biology approaches, we pinpointed aberrant ubiquitin signaling centered around overabundance of RNF168 as the mechanistic basis of this paradigm-shifting cancer-associated phenotype. These results, as well as implications of these findings for our understanding of tumorigenesis and responses of cancer cells to diverse treatments are presented below.

RESULTS

53BP1 is recruited to DNA damage sites despite proteotoxic stress in MDA-MB-231 cells

In an attempt to identify vulnerabilities of triple-negative carcinomas, a subset of breast tumors with poor prognosis, often aberrant DSB repair and currently lacking any targeted treatment option, we examined diverse aspects of the DDR machinery in the human triple-negative breast cancer model cell line MDA-MB-231. In sharp contrast to the current consensus in the field, inhibition of proteasome activity that depletes the pool of free cellular ubiquitin did not abrogate recruitment of the 53BP1 protein to ionizing radiation induced foci (IRIF). Indeed, in the MDA-MB-231 cell line exposed to IR after a 2-h pre-treatment with the proteasome inhibitor MG132 formation of 53BP1-positive IRIF was not diminished compared with controls with active proteasome, as over 40 % of cells formed >5 53BP1 IRIFs (Figures 1a and b). In contrast, in the control U2OS sarcoma cell line, the same treatment abrogated 53BP1 IRIF formation completely (Figures 1a and b). Another control cell type, a primary diploid human fibroblast strain (BJ) responded in the same manner as the U2OS cells (Figures 1a and b). Collectively, these results indicated that in the MDA-MB-231 cells, the 53BP1 DSB response pathway displays an exceptional resistance to depletion of free ubiquitin.

Unorthodox DSB response in MDA-MB-231 cells is limited to downstream steps of the pathway

We reasoned that the MDA-MB-231 cells might exhibit a non-standard response to core proteasome inhibition resulting in a less pronounced drop in free ubiquitin levels thus enabling sustained 53BP1 IRIF formation. Nevertheless, immunoblotting analysis of total ubiquitin showed accumulation of high-molecular weight ubiquitin conjugates and depletion of free ubiquitin in both

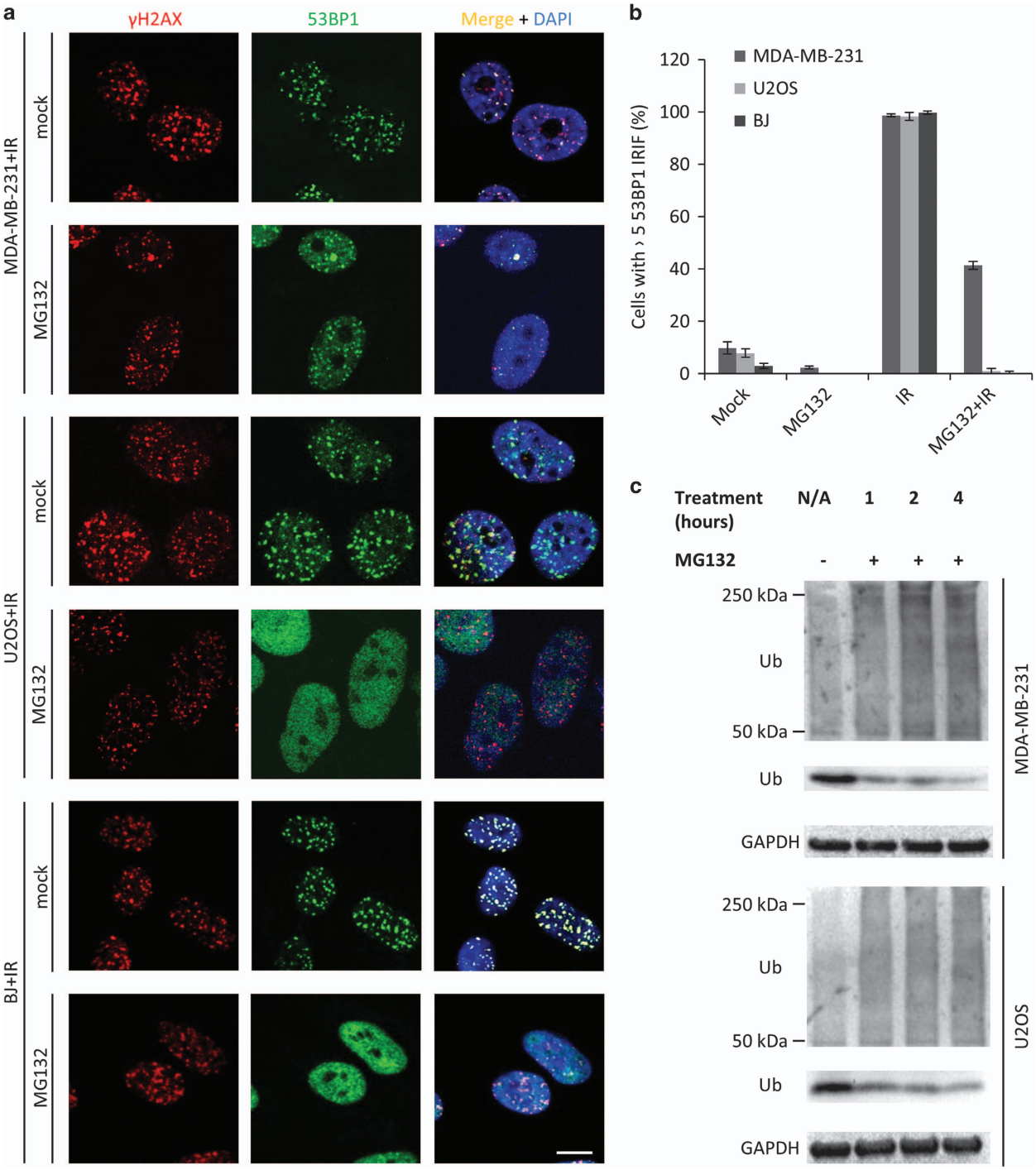

Figure 1. 53BP1 is recruited to DNA damage sites despite proteotoxic stress in MDA-MB-231 cells. (**a**) MDA-MB-231, U2OS and BJ cells were mock- or MG132 (5 μM) treated for 2 h and subsequently irradiated with 2 Gy. One hour post-irradiation, the cells were fixed and immunostained for γH2AX and 53BP1. Scale 10 μM. (**b**) Cells with >5 53BP1 IRIFs were scored for all three lines after mock, MG132 or either of the treatments combined with irradiation (2 Gy). (**c**) MDA-MB-231 and U2OS cells were mock and MG132 treated, lysed at various time points and subsequently probed for free ubiquitin and ubiquitin conjugate levels using immunoblotting. In (**b**), results are mean ± s.d. of three independent experiments.

MDA-MB-231 and U2OS control upon MG132 treatment (Figure 1c). Along with free ubiquitin depletion, accumulation of such protein–ubiquitin conjugates is a sign of proteasome inhibition, indicating that altered sensitivity to proteasome inhibitors is unlikely to cause the observed MDA-MB-231 phenotype.

Analogous to the known response in U2OS cells,[13] the MG132-treated MDA-MB-231 cells also displayed the disappearance of ubiquitin conjugates (detected by the FK2 antibody) at sites of IR-inflicted DNA damage (Figures 2a and b). It has been shown that upon proteasome inhibition, ubiquitin is largely lost from histones and other nuclear proteins and shuttled to cytoplasmic proteins

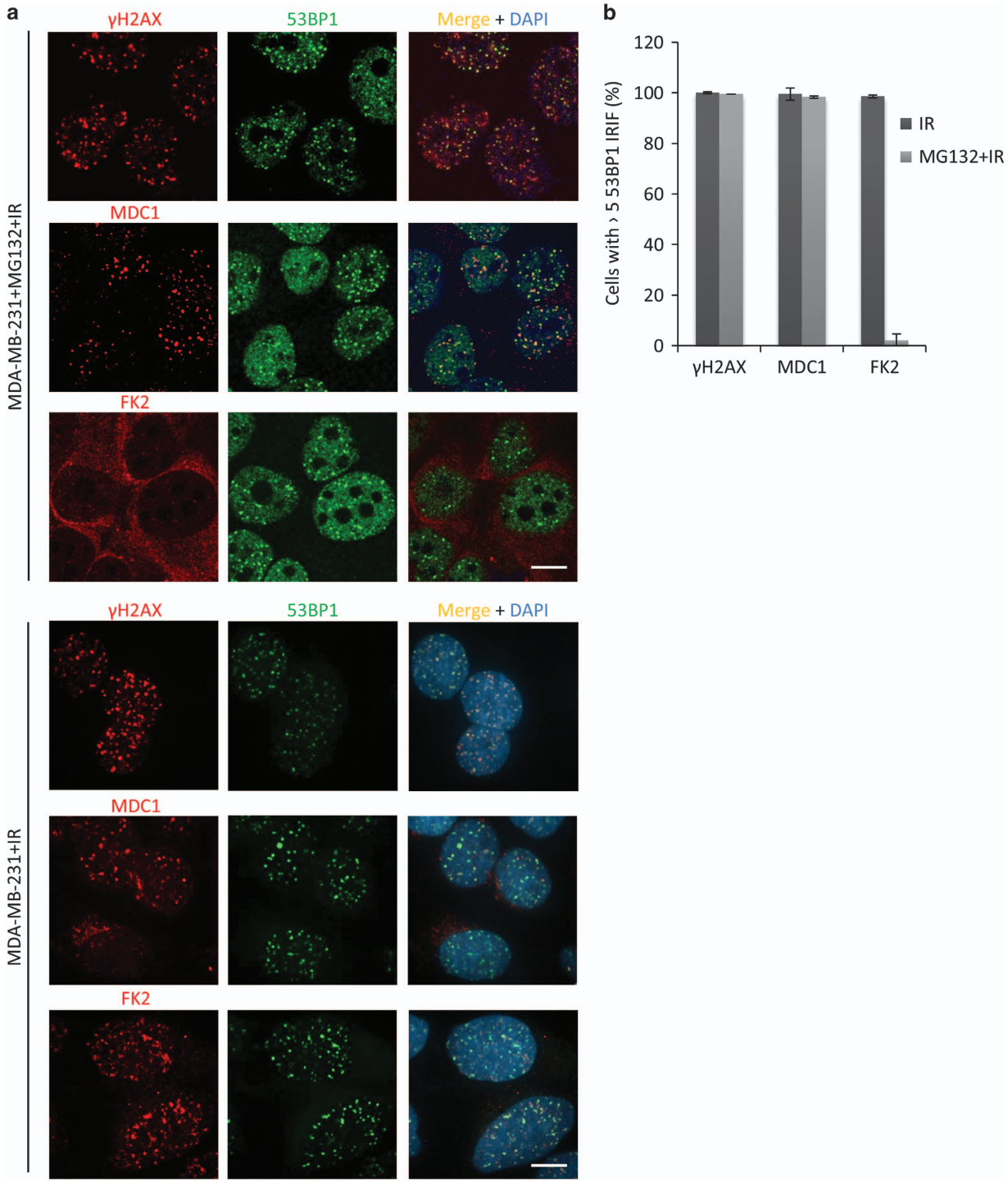

Figure 2. Probing DSB response upstream of 53BP1 in MG132-treated MDA-MB-231 and U2OS cells. (**a**) MDA-MB-231 cells were pretreated with MG132 for 2 h, irradiated with 2 Gy and 1h post-irradiation immunostained for the indicated proteins or protein modifications known to be present in IRIFs. Scale 10 μM. (**b**) Graphical summary of nuclei with >5 γH2AX, FK2 or MDC1 IRIFs, scored in cells bearing >5 53BP1 IRIFs. Results are mean $\pm$ s.d. of three independent experiments.

awaiting degradation in the proteasome complex.[29] This result again shows that MDA-MB-231 cells respond to proteasome inhibition in an apparently standard way leading to depletion of the free nuclear ubiquitin pool, without any obvious compensatory mechanism that would facilitate the sustained 53BP1 accrual at the sites of DNA damage.

Importantly, additional key DDR factors acting upstream of 53BP1 such as γH2AX and recruitment of MDC1 were observed in IRIFs (Figures 2a and b) in both mock-treated and proteasome inhibitor-treated cells. This suggested that the upstream steps of the DSB response pathway react to proteasome inhibition largely in a standard mode in MDA-MB-231 cells.

To further assess the chromatin DSB response pathway at the level of 53BP1 and its associated proteins in the proteasome-inhibited cells, we probed the MDA-MB-231 and the control U2OS cells for recruitment of two known 53BP1 effectors—RIF1[19,21] and

REV7,[20] to laser micro-irradiation induced DNA damage sites. In contrast to U2OS, MG132 pretreated MDA-MB-231 cells showing 53BP1 accumulation in laser-induced 'stripes' also displayed RIF1 and REV7 accrual at such sites of micro-irradiation (Figures 3a and b). These results imply that the upstream steps of the DSB response pathway operate normally, and the unorthodox DSB response in the MDA-MB-231 cells under proteotoxic stress is shared by 53BP1 and its downstream effectors.

UDR motif-mutated 53BP1 is not recruited to DSB sites under proteotoxic stress

53BP1 binds to two chromatin modifications at the DSBs—dimethylated histone H4 (H4K20) and ubiquitinated histone H2A (H2AK15Ub).[23,24] The H2AK15Ub mark is recognized by the ubiquitin damage response (UDR) domain at the C-terminal part of 53BP1.[24] We utilized a UDR motif-mutated 53BP1 incapable of binding the H2AK15Ub mark to test whether ubiquitin was indeed required for 53BP1 accumulation at DSBs under conditions of proteotoxic stress in the MDA-MB-231 line. Although a 53BP1 wild-type green fluorescent protein (GFP) fusion protein was recruited to IRIFs, cells expressing the GFP-tagged UDR mutant (L1619A)[24] did not form 53BP1 IRIFs (Figure 4). Furthermore, a GFP-tagged Tudor domain 53BP1 mutant (D1521R)[24] behaved similarly and was not recruited to IRIFs (Figure 4). Taken together, this implied that in the MDA-MB-231 cells, 53BP1 recruitment still depends on each of the two intact modules that recognize H4K20 and H2AK15Ub, respectively, even when levels of cellular-free ubiquitin become limiting.

The proteotoxic stress-resistant DSB response depends on ubiquitin signaling, particularly RNF168

As the DSB response in the MDA-MB-231 cells is still fueled by ubiquitin under proteotoxic stress, a mechanism should exist that provides sufficient amount of ubiquitin to sustain the process. One plausible way of bypassing an acute decrease in free ubiquitin levels is overexpression of the E2 and/or E3 ubiquitin conjugating enzymes/ligases. Elevated pool of an E2 conjugating enzyme that was charged with ubiquitin before the drop in free ubiquitin level might serve as a temporary reservoir for downstream processes. On the other hand, an overexpressed E3 ligase might outcompete other E3 ligases in the uptake of residual ubiquitin under conditions of proteotoxic stress. Hence, we examined the levels of the key DSB response related ubiquitin conjugating enzyme UBC13 (UBE2N) and E3 ligases RNF8 and RNF168 in the MDA-MB-231 cells. Strikingly, all three enzymes displayed elevated levels in this cell line (Figure 5a). When normalized to glyceraldehyde 3-phosphate dehydrogenase (GAPDH), both RNF8 and RNF168 showed more than twofold higher levels than those in the U2OS cells, whereas UBC13 level was even higher—more than fivefold above the U2OS cells (Figure 5b). The overabundance of these three enzymes was even more profound when the normal diploid BJ cells were compared with MDA-MB-231 cells: more than fourfold for UBC13, sixfold for RNF8 and more than eightfold in the case of RNF168 (Figure 5b). Importantly, the level of the 53BP1 protein was comparable in all three cell types (Figure 5b).

Quantitative PCR and cycloheximide chase experiments indicated that the overabundance of RNF168 in the MDA-MB-231 cells reflected transcriptional upregulation rather than increased protein stability (Supplementary Figures S1A and B). In addition to transcriptional upregulation, an increase in RNF168 translation efficiency and/or transcript stability likely contribute to the observed RNF168 protein overabundance in MDA-MB-231 cells as transcriptional upregulation alone (a 2.5-fold increase compared with U2OS, Supplementary Figure S1A) is unlikely to account for the high RNF168 protein levels given the faster protein turnover of RNF168 in these cells (deduced from the almost fourfold shorter RNF168 protein half-life in MDA-MB-231 compared with U2OS, Supplementary Figure S1B). Indeed, the accelerated turnover of RNF168 protein was consistent with overabundant TRIP12 and UBR5 (Supplementary Figure S1C), the two enzymes critical for ubiquitin/proteasome-mediated degradation of RNF168.[28] The elevated TRIP12 and UBR5 might reflect a fine-tuning mechanism in MDA-MB-231 cells, possibly providing a negative feedback loop to limit the overabundant RNF168 to levels that are not overly harmful to cells, a scenario that occurs upon experimental gross overexpression of RNF168.[28] Consistently, depletion of either TRIP12 or UBR5 in MDA-MB-231 led to an even more pronounced DSB response phenotype resistant to proteasome inhibition (Supplementary Figure S1D), possibly due to further increase in the abundance of RNF168. As to additional components of the ubiquitin-mediated DSB signaling, we found enhanced abundance of HERC2 (Supplementary Figure S1C), another ubiquitin ligase that promotes 53BP1 recruitment at DSBs,[31] whereas there was little if any alteration of the negative regulators JMJD2A, L3MBTL1 or RNF169 proteins[32] (negative data, not shown).

Overall, these results supported the functional significance of the RNF168-centered ubiquitin-mediated signaling pathway in the altered DSB response in MDA-MB-231 cells. This notion was further supported by functional experiments, in which small interfering RNA (siRNA)-mediated knockdown of UBC13, RNF8 or RNF168 completely abolished the proteotoxic stress-resistant DSB response phenotype in the proteasome inhibitor-treated MDA-MB-231 cells (Figures 5c and d).

Based on available mechanistic insights[28] and the pronounced clinical phenotype of RNF168 deficiency,[27] we hypothesized that the RNF168 ligase could be central to the unorthodox DSB response phenotype in MDA-MB-231 cells. Partial knockdown of RNF168 with increasing amounts of siRNA resulted in a gradual decrease of cells capable of forming >5 53BP1 IRIFs (Figure 6a). Importantly, this phenotype could be rescued by expression of siRNA-resistant WT, but not the mutant version of RNF168 (C16S, in the RING domain) that abolishes the enzymatic activity of the protein (Figure 6b).

If RNF168 has a central role in the studied DSB response phenotype, overexpression of the enzyme in a cell line incapable of sustaining DSB signaling under proteotoxic stress might mimic the situation seen in MDA-MB-231 cells. Indeed, an U2OS-derived cell line overexpressing a RNF168-GFP fusion protein exhibited 53BP1 IRIF formation in nearly all nuclei even after proteasome inhibition (Figures 6c–e). As in the case of MDA-MB-231 cells, the number of 53BP1 IRIF-positive cells correlated with the level of RNF168 (Supplementary Figure S2) and, consistent with the pathway hierarchy,[5,13] the phenotype was dependent on RNF8 (Supplementary Figure S3). Of note, changes in RNF8 levels had a less profound effect on the phenotype compared with the more marked impact of RNF168 abundance, thereby supporting the major role of RNF168 in the proteotoxic stress-resistant DSB response (Supplementary Figure S3). Furthermore, ectopic expression of the RNF168 (C16S) mutant in the U2OS cell line did not result in the proteotoxic stress-resistant phenotype (Supplementary Figure S4), as opposed to expression of the WT protein (Figures 6c and d and Supplementary Figure S4). These results also parallel the scenario seen in MDA-MB-231 cells, where the ectopic RNF168 C16S RING mutant was incapable of rescuing the loss of the phenotype caused by knockdown of endogenous RNF168. Overall, these data were consistent with the emerging key role of RNF168 abundance in the proteotoxic stress-resistant DSB response.

The proteotoxic stress-resistant DSB response cancer phenotype is more common

Next, we asked whether the emerging phenotype observed in the triple-negative breast cancer cells MDA-MB-231 is unique or more widespread, and tested a panel of proteasome inhibitor-treated

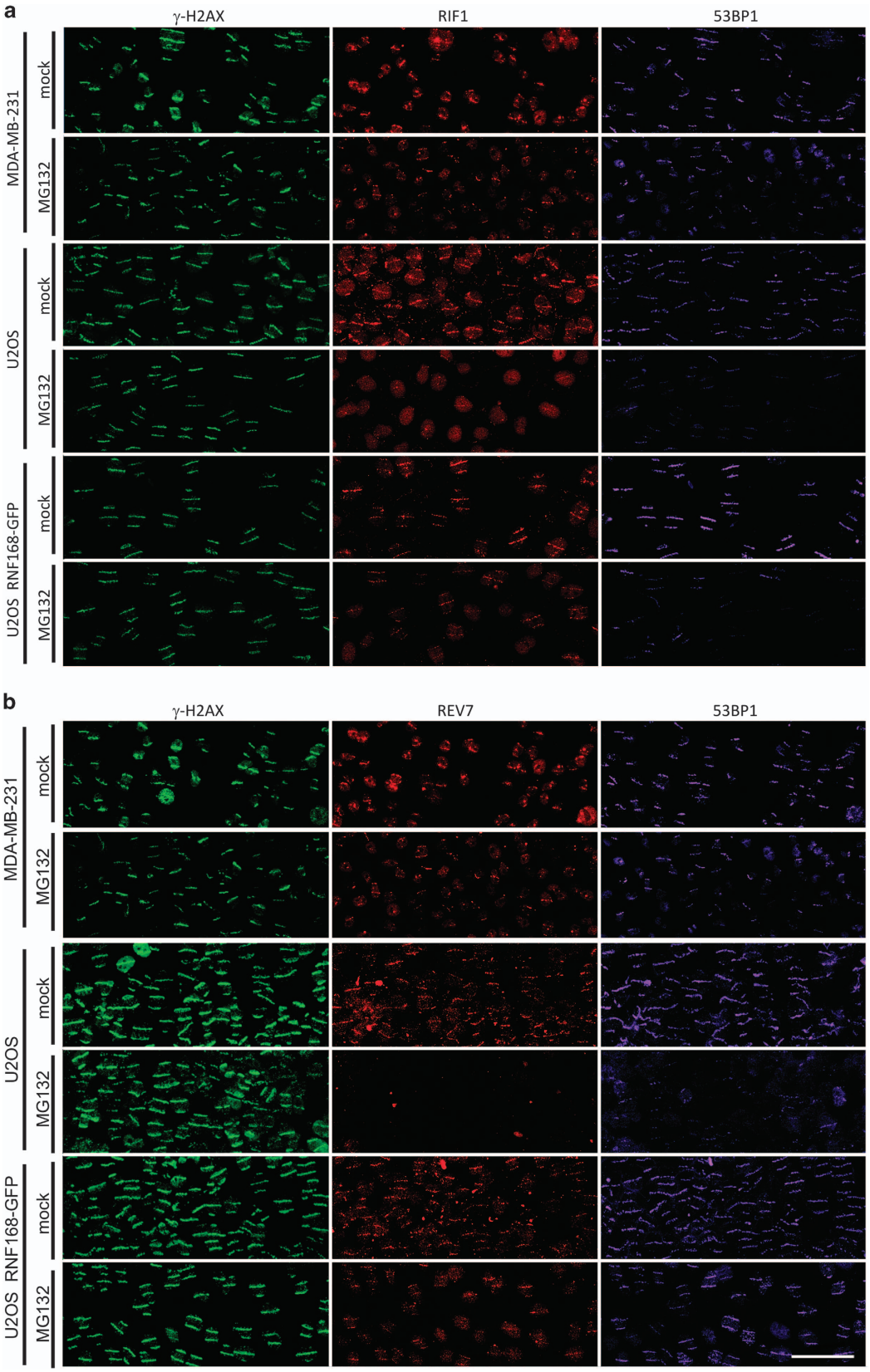

Figure 3. Probing DSB response downstream of 53BP1 in MG132-treated MDA-MB-231, U2OS and U2OS RNF168-GFP cells. (**a**) Mock or MG132-treated (5 μM, 2 h) MDA-MB-231, U2OS and U2OS RNF168-GFP cells were laser-microirradiated and immunostained for γH2AX, 53BP1 and RIF1. (**b**) As in (**a**), but staining for γH2AX, 53BP1 and REV7. Scale bar 50 μM.

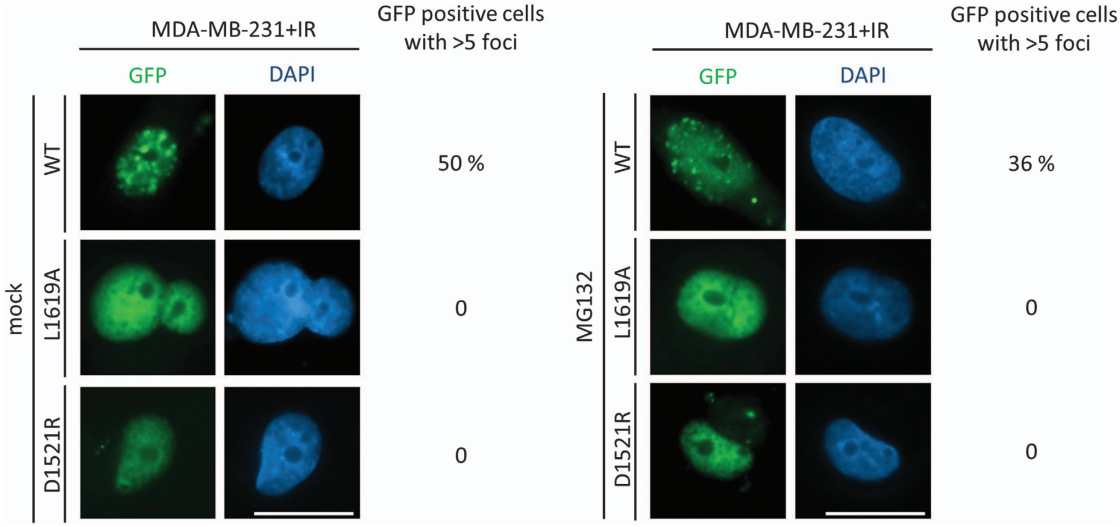

Figure 4. 53BP1 recruitment to sites of damage in MDA-MB-231 is methylation and ubiquitination dependent. MDA-MB-231 cells transfected with siRNA against 53BP1 and expression vectors for the indicated siRNA-resistant GFP-tagged versions of 53BP1 were mock or MG132 treated (2 h, 5 μM), irradiated with 2 Gy and after 1h processed for GFP imaging. Scale 20 μM. Results are mean of two independent experiments.

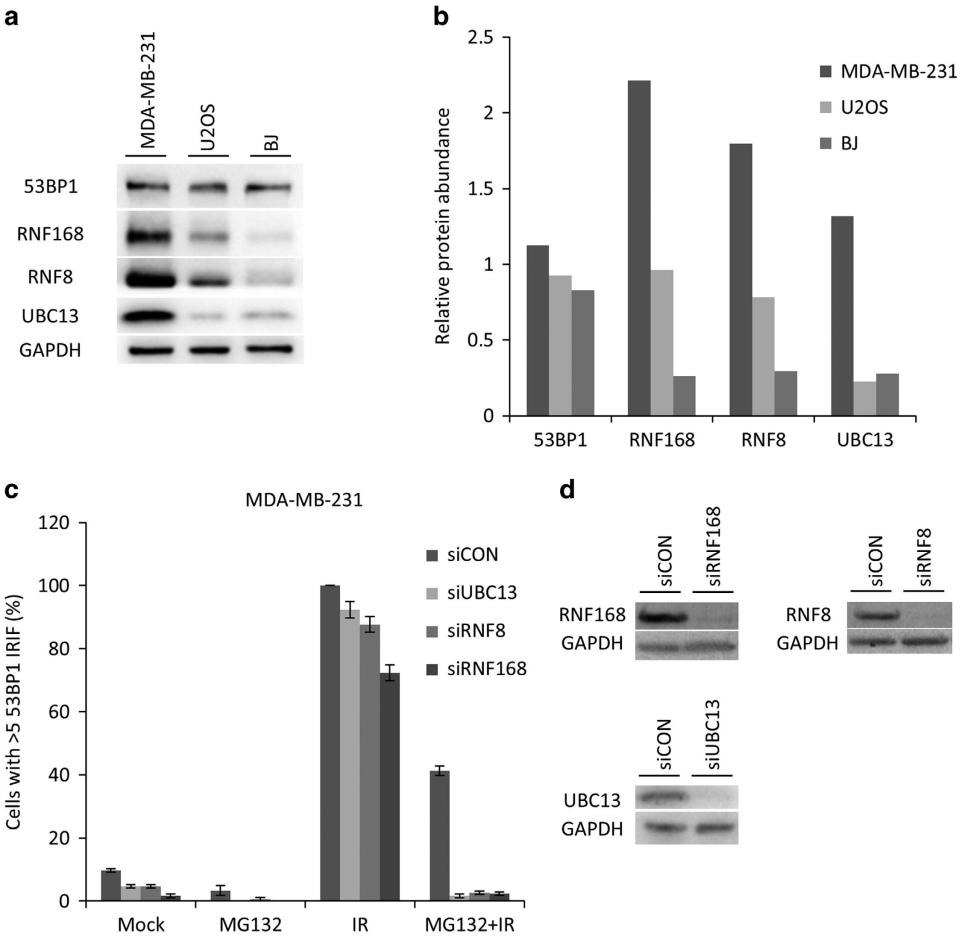

Figure 5. Elevated levels and impact of ubiquitin-mediated DSB signaling-related enzymes in MDA-MB-231 cells. (**a**) MDA-MB-231, U2OS and BJ cell lysates were analyzed by immunoblotting for abundance of 53BP1 and the major DSB ubiquitin signaling enzymes RNF8, RNF168 and UBC13. (**b**) Protein abundance was calculated using densitometric analysis of the immunoblot shown in **a**. Band intensities were normalized to corresponding GAPDH bands. (**c**) MDA-MB-231 cells were transfected with indicated siRNAs, mock and MG132 treated (2 h, 5 μM) with and without irradiation (2 Gy) and 1 h post-irradiation stained for 53BP1. Cells with >5 53BP1 IRIF were scored. Results are mean ± s.d. of three independent experiments (**d**) Knockdown efficiency in (**c**) was verified by probing corresponding cell lysates by immunobloting using indicated antibodies.

human cancer cell lines for occurrence of 53BP1 IRIF. Strikingly, we observed the proteotoxic stress-resistant DSB response analogous to MDA-MB-231 cells also in two other cell lines, the breast cancer-derived MCF7 cells and cervical cancer-derived HeLa cells, whereas MDA-MB-436, another breast cancer cell line, was phenotypically similar to the control U2OS cells (Figure 7a). Notably, all cell lines displaying the proteotoxic stress-resistant DSB response showed elevated RNF168 (Figures 7b and c). The protein levels of RNF8 and UBC13 in MCF7 and HeLa cells showed only a slight if any increase, in contrast to the more pronounced

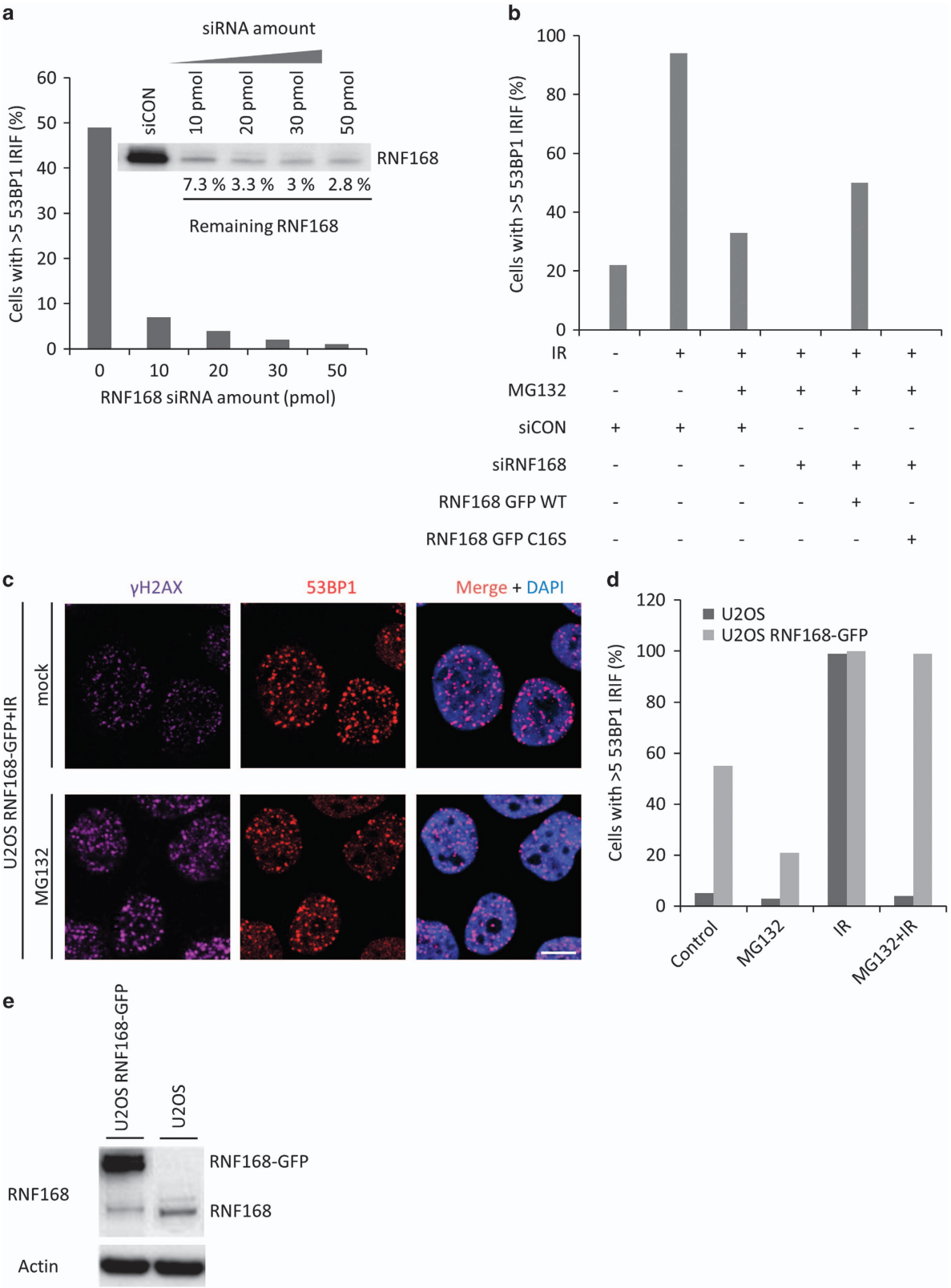

elevation of RNF168 (Figure 7b). The combination of enhanced RNF168 and 'normal' levels of RNF8 and UBC13 was therefore reminiscent of the scenario seen in the engineered RNF168-GFP overexpressing U2OS cell line (Figure 7b), which also shares the altered DSB response phenotype. Consistently, the selectively enhanced level of RNF168 in the RNF168-GFP overexpressing U2OS cell line also resulted in the recruitment to DSBs of the 53BP1-dependent RIF1 and REV7 proteins under conditions of proteasome inhibition (Figures 3a and b). Overall, these results further supported the central role of the RNF168 ligase in the altered DSB response phenotype.

Given the wider occurrence of the proteotoxic stress-resistant DSB response, we asked whether it might represent some kind of phenotypic adaptation beneficial for tumor cells. Cancer cells experience a higher load of intrinsic genotoxic stress including DSBs[2,4] and enhanced proteotoxic stress[1] that might possibly attenuate the ubiquitin-mediated DSB response pathway because of chronic limitation of free ubiquitin. We hypothesized that a proteotoxic stress-resistant DSB response may help to counteract the adverse effects of proteotoxic stress on DSB signaling and thereby support tumor cell viability. When four cell lines from our panel were treated with MG132 and subsequently irradiated, their survival positively correlated with their respective abilities to sustain the DSB response under such proteotoxic stress conditions. The cell lines MDA-MB-231 and MCF7 that display the proteotoxic stress-resistant DSB response showed significantly higher survival compared with the control U2OS and BJ cells (Figure 7e). Also, consistent with the above-mentioned hypothesis about the potential adaptive value of the proteotoxic stress-resistant DSB response during tumor progression, partial short hairpin RNA (shRNA)-mediated knockdown of RNF168 lowered the tolerance to combined proteasome inhibition and IR treatment in MDA-MB-231 cells (data not shown).

One of the most prominent signs of chronic proteotoxic stress is accumulation of ubiquitin-conjugated proteins because of cellular protein quality control and UPS overload. The accumulation is readily detectable by immunoblotting and immunostaining techniques using antibodies recognizing protein-conjugated ubiquitin. To examine whether the heightened resistance to combined irradiation and proteasome inhibition (Figure 7e) correlated with higher loads of endogenous proteotoxic stress, we compared the levels of conjugated ubiquitin in our panel of cell lines (Figure 7d) by immunoblotting using an antibody against K48 linked ubiquitin. Pronounced conjugate accumulation in both MDA-MB-231 and MCF7 cells was apparent compared with BJ and U2OS cells (Figure 7d). This finding was consistent with our hypothesis that the increased tolerance to simultaneous irradiation and proteasome inhibition in the MDA-MB-231 and MCF7 lines might reflect adaptation to chronic proteotoxic stress.

Proteasome inhibitors have been successfully used in the treatment of multiple myeloma and other hematological malignancies.[33] Besides pro-apoptotic effects, one of the proposed modes of action of these inhibitors is further exacerbation of the high intrinsic proteotoxic stress in the immunoglobulin-producing myeloma cells thus causing a lethal unfolded protein response.[1] Given the high endogenous levels of proteotoxic stress in myeloma cells, we asked whether myelomas show a similarly 'adapted' DSB response, reminiscent of some carcinoma cell lines such as MDA-MB-231. We therefore probed two human myeloma cell lines, AMO1 and MMS1, for their ability to form 53BP1 IRIFs after MG132 treatment. Strikingly, the proteotoxic stress-resistant DSB response phenotype in these myeloma cell lines was even more pronounced than in the MDA-MB-231 cells, as 60% and 90% of AMO1 and MMS1 myeloma cells, respectively, formed more than five 53BP1 IRIFs under proteasome inhibition conditions (Figures 8a and b). Similarly to MDA-MB-231 and other cancer cell lines that share the proteotoxic stress-resistant DSB response, the ability to sustain 53BP1 IRIF formation after MG132 treatment correlated with elevated RNF168. Protein levels of RNF168 in AMO1 and MMS1 cells exceeded not only those seen in BJ and U2OS cells, but even that in MDA-MB-231 cells (Figure 8c). As expected, both AMO1 and MMS1 cell lines showed grossly elevated levels of intrinsic proteoxic stress manifested by accumulation of poly-ubiqutinated proteins and the BiP protein —an established marker of proteotoxic stress and UPR activation (Figure 8c).[34] Taken together, these results further support the possibility that the proteotoxic stress-resistant DSB response indeed represents an adaptation to chronic proteotoxic stress experienced by tumors.

To validate the relevance of our findings obtained in experiments with cultured cell lines on clinical material, we performed an immunohistochemical analysis of the abundance of the central element of the pathway, RNF168 on archival paraffin sections from a cohort of carcinomas of the head and neck, uterine cervix and anus, and the corresponding normal human stratified epithelial tissues as matching controls. The rationale for using this material included the following main arguments: (i) the above tumor types often harbor human papillomavirus oncogenes and therefore match HeLa cells that we found positive for the proteotoxic stress-resistant DSB response phenotype; (ii) as normal breast epithelium contains only rare proliferating cells, the stratified epithelium provides a more rigorous control tissue as there are clearly defined layers of constantly proliferating cells, thereby avoiding a bias of comparing proliferating breast tumors (relevant to MDA-MB-231 and MCF7 cell lines in our panel) with largely nonproliferating normal breast tissue. As can be seen from the representative examples of the immunohistochemical staining patterns (Supplementary Figure S5), the abundance of RNF168 was clearly higher in the cancer tissues ($n = 25$) compared with normal epithelium ($n = 18$), whereas the expression of 53BP1, used as an internal control protein, was comparable in both cancerous and normal tissues (Supplementary Figure S5).

Overall, these results indicate that the observed proteotoxic stress-resistant DSB response phenotype is shared by a subset of human cancer cell lines, and its main feature—the overabundance of RNF168, is also observed in clinical tumor specimens.

Figure 6. The proteotoxic stress-resistant DSB response phenotype depends on RNF168. (**a**) MDA-MB-231 cells were transfected with increasing amounts of RNF168 siRNA, treated with 5 μM MG132 (2 h), irradiated (2 Gy) and 1h post-irradiation stained for 53BP1. Nuclei with >5 53BP1 IRIFs were scored. Inset—siRNA transfected MDA-MB-231 cells were lysed and analyzed by immunoblotting for remaining RNF168 level. (**b**) MDA-MB-231 cells were co-transfected with control or RNF168 siRNA and siRNA-resistant plasmids carrying GFP-tagged WT or the C16S RING mutant version of RNF168. Transfected cells were mock or MG132 treated (2 h, 5 μM), irradiated (2 Gy) and 1 h post-irradiation stained for 53BP1 and scored for nuclei with >5 53BP1 IRIFs. (**c**) U2OS RNF168-GFP cells were pre-treated with MG132 for 2 h, irradiated with 2 Gy and 1h post-irradiation immunostained for γH2AX and 53BP1. Scale bar 10 μM. (**d**) U2OS RNF168-GFP cells were mock or MG132 treated (2 h, 5 μM), irradiated (2 Gy) and 1 h post-irradiation stained for 53BP1 and scored for nuclei with >5 53BP1 IRIFs. The chart shows one of three consistent repeats. (**e**) U2OS and U2OS RNF168-GFP cells were lysed and probed for RNF168 levels by immunoblotting. The total level of RNF168 in U2OS RNF168-GFP is approximately fivefold higher than in U2OS. In (**a**, **b** and **d**), the charts show one out of three consistent experiments.

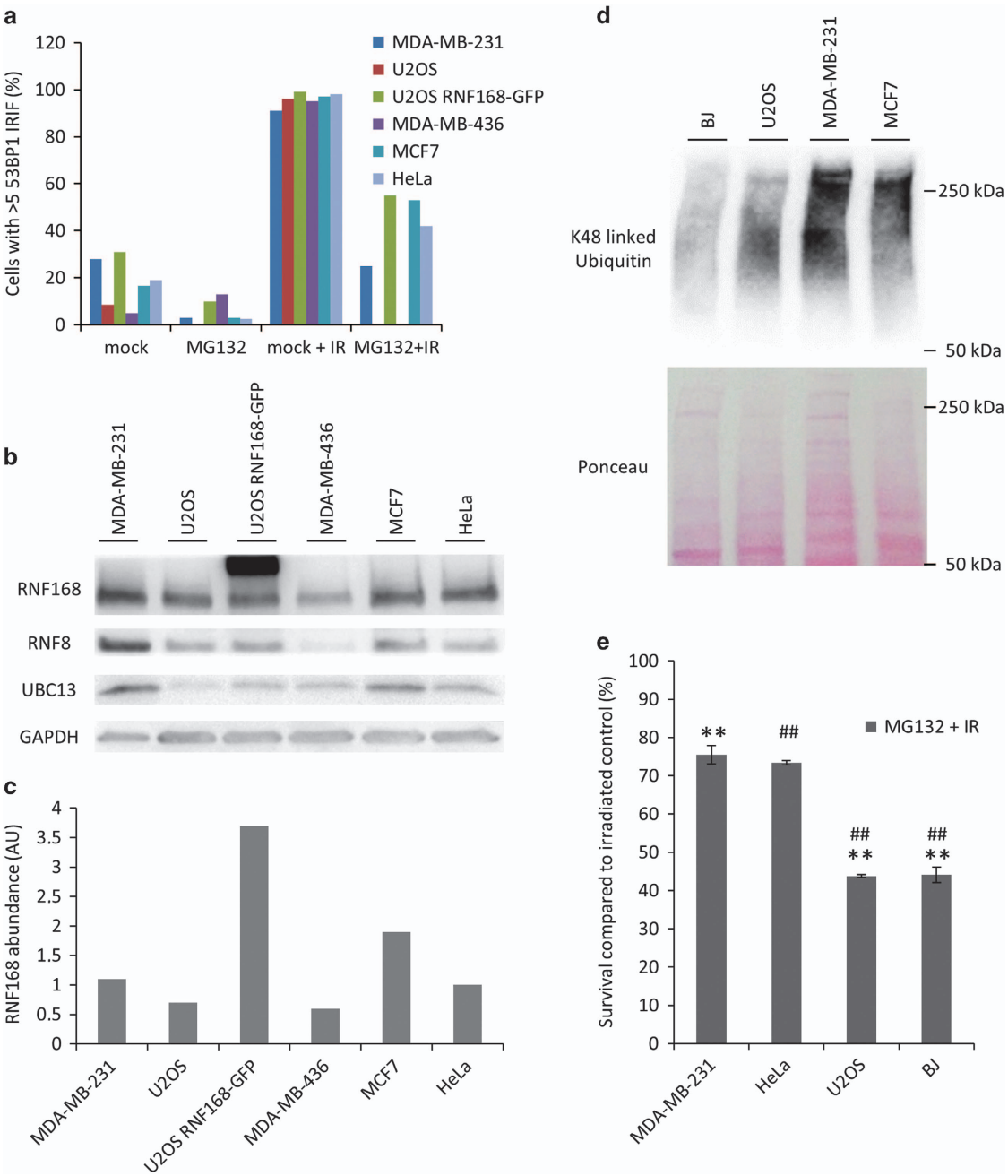

Figure 7. The proteotoxic stress-resistant DSB response phenotype is shared by other cancer cell lines. (**a**) Indicated cells lines were mock- and MG132 treated (2 h, 5 μM), either with or without irradiation (2 Gy) and 1 h post-irradiation stained for 53BP1. Nuclei with >5 53BP1 IRIFs were scored. (**b**) Lysates prepared from the lines in (**a**) were probed for RNF8, RNF168 and UBC13 levels by immunoblotting. (**c**) RNF168 band intensity was quantified and normalized according to the total protein levels in the indicated lines. (**d**) Indicated cell lines were probed for the level of conjugated K48 linked ubiquitin by immunoblotting. Equal protein amounts were loaded for all the cell lines. (**e**) Indicated cell lines displaying various levels of RNF168 expression were pretreated with 5 μM MG132 (2 h), irradiated with 2 Gy and 1 h post-treatment seeded to Petri dishes. Six days post-irradiation, the cells were trypsinized and counted using an automated cell counter. In (**a** and **e**), results are mean ± s.d. of three independent experiments. Statistical significance was determined with two-tailed unpaired Student's *t*-test; $^{**,\#\#}P < 0.005$.

Overabundant RNF168 shifts DSB repair toward NHEJ, enhances genomic instability and vulnerability to PARPis and camptothecin

The results obtained so far suggested that MDA-MB-231 and some other cancer cell lines capable of DSB signaling despite proteotoxic stress may deviate from normal cells and from other cancer cell lines in various aspects of their genome integrity control. To explore this emerging concept further, we first assessed the response of MDA-MB-231 cells to PARPi, a strategy that causes DNA damage mainly during S phase and which showed promise in treatment of a subset of triple-negative breast tumors in clinical trials.[35,36] Immunofluorescence analysis showed that while >60% of S-phase MDA-MB-231 cells treated by a PARPi displayed over 10 53BP1-positive foci per nucleus, in U2OS the fraction of such cells was significantly lower (Figures 9a and b). Given the similar cell cycle phase profiles of both cell lines (data not shown) and the fact that the DSBs caused by PARPi commonly occur during S phase and are preferentially repaired by HR the

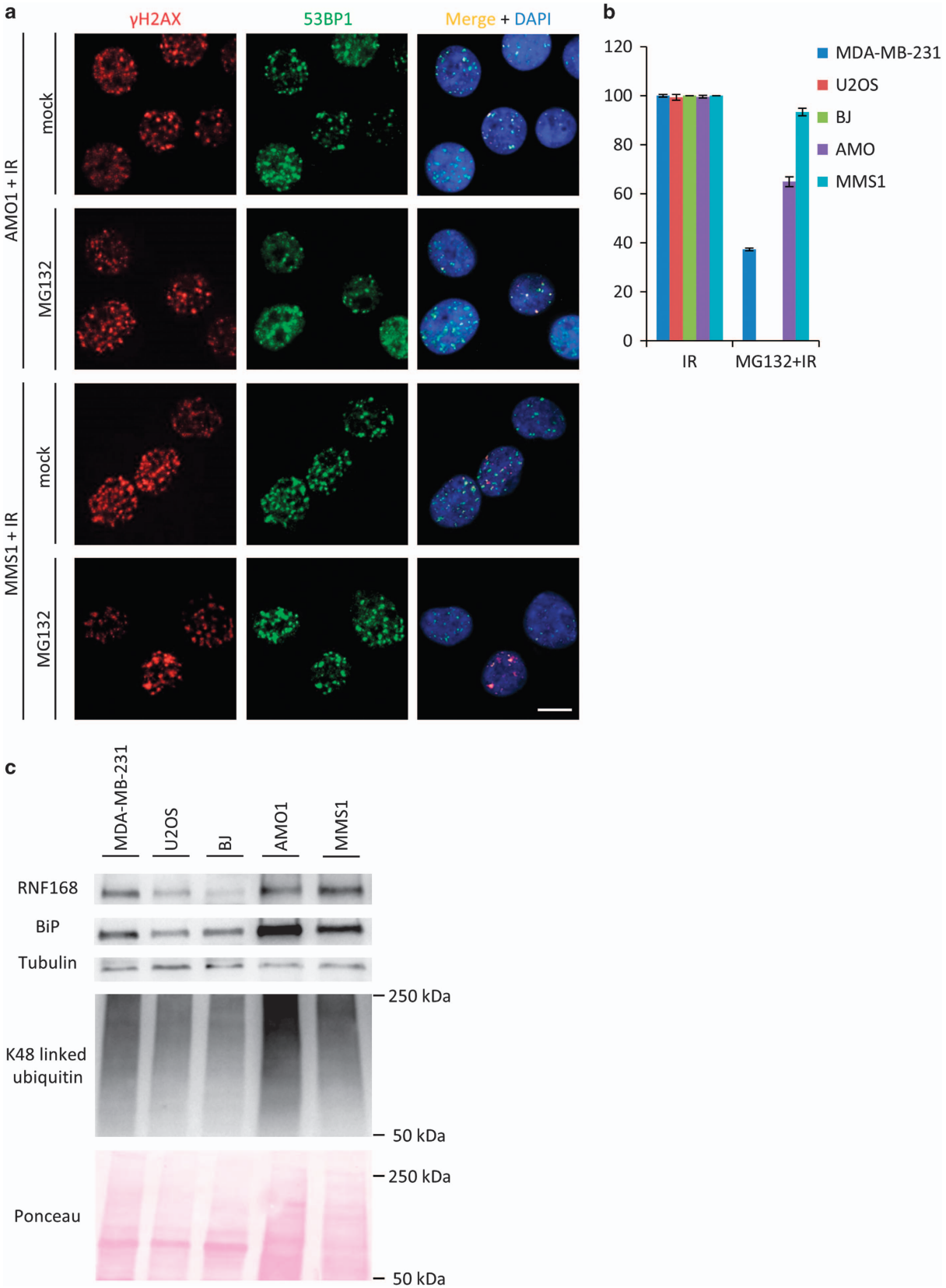

Figure 8. Multiple myeloma cell lines exhibit the RNF168-fueled proteotoxic stress-resistant DSB response. (**a** and **b**) AMO1 and MMS1 cell lines were mock- and MG132-treated (2 h, 5 μM), either with or without irradiation (2 Gy) and 1h post-irradiation stained for 53BP1. Nuclei with >5 53BP1 IRIFs were scored. Scale 10 μM. (**c**) Indicated cell lines were probed for the level of conjugated K48 linked ubiquitin, RNF168 and BiP by immunoblotting. Equal protein amounts were loaded for all the cell lines. In (**b**), results are mean ± s.d. of three independent experiments.

efficiency of which is affected by 53BP1 recruitment,[15,37] these results suggested that such unscheduled recruitment of 53BP1 might alter the balance between the major DSB repair pathways. The latter possibility would also be consistent with the ability of 53BP1 to promote mutagenic NHEJ (mutNHEJ) by blocking DSB end resection, resulting in hypersensitivity toward chemotherapeutic agents that damage DNA in S-phase cells, including PARPis and topoisomerase inhibitors.[15,37] To address such possibilities in a syngeneic system, we first generated clones of MDA-MB-231 cells expressing a doxycycline (DOX)-inducible shRNA against RNF168, and validated the partial knockdown of RNF168 in these models by immunoblotting (Figure 9c). Next, we assessed the ratio of mutNHEJ/HR repair modes by introducing into the RNF168-regulatable cell lines the so-called Traffic light

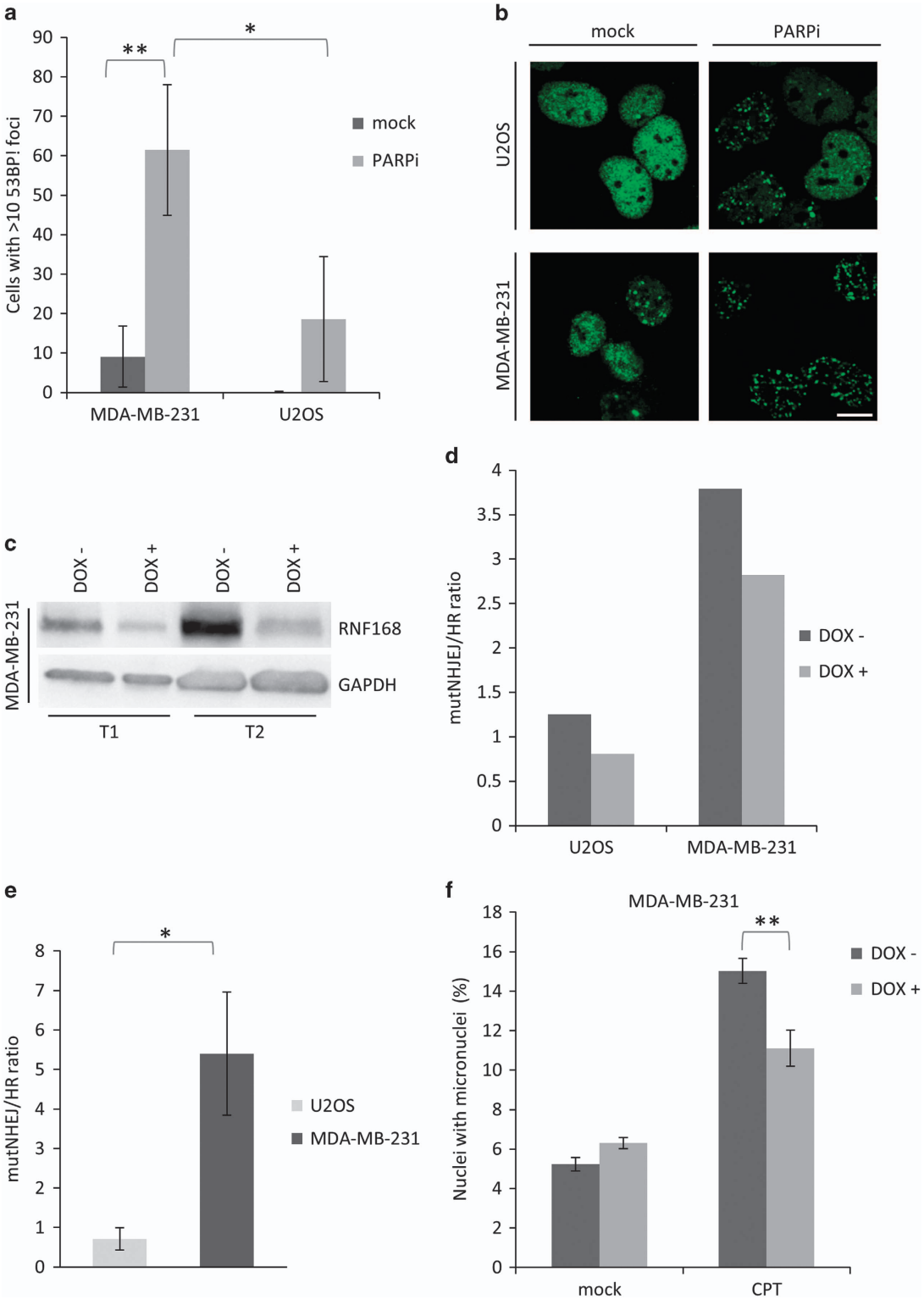

system,[38] a reporter that enables flow cytometric analysis of repair pathway choice at individual I-SceI induced DNA breaks. Quantification of red (mutNHEJ) and green (HR) events then provides information on the overall activity proportion of the two pathways in the analyzed cell population. A representative example of such experiment shown in Figure 9d indeed supports the RNF168-dependent repair shift, as the cells with DOX-induced partial RNF168 knockdown showed a lower mutNHEJ/HR ratio. Furthermore, consistent with the high and low levels of RNF168, respectively, the mutNHEJ/HR ratio was more than sixfold higher in the parental MDA-MB-231 cells compared with the parental U2OS cells (Figure 9e).

Excessive mutNHEJ leads to frequent chromosome aberrations and genome rearrangements that might contribute to tumor heterogeneity.[22,39] To examine whether the RNF168-driven upregulation of mutNHEJ makes the MDA-MB-231 line more prone to genome rearrangements, we used the DOX-inducible RNF168 knockdown model in MDA-MB-231 cells and compared numbers of micronuclei in DOX-induced and non-induced cells pretreated by a topoisomerase I inhibitory drug camptothecin (CPT). The number of micronuclei was indeed significantly lower in the DOX-induced cells with lowered RNF168 level and hence a more proficient HR repair because of less robust recruitment of 53BP1 (Figure 9f). These results support a plausible scenario that the aberrantly upregulated RNF168 protects cancer cells from adverse effects of proteotoxic stress on the DDR, however, only at the cost of increased genomic instability.

As the altered balance of DSB repair pathway choice toward higher mutNHEJ and the ensuing chromosomal instability can impact cell viability under exposure to S-phase genotoxic insults that require HR for efficient DNA repair,[22] we next tested sensitivity of the MDA-MB-231 cells with inducible RNF168 knockdown toward CPT. Strikingly, the DOX-induced cells with decreased RNF168 levels were significantly less sensitive to CPT (Figure 10a) than the non-induced counterpart cells. We interpret the observed decrease in CPT sensitivity upon RNF168 knockdown as further evidence for upregulation of NHEJ and the ensuing genomic instability in the MDA-MB-231 cells driven by RNF168 overabundance.

Surprisingly, the MDA-MB-231 knockdown cell line did not show a significant change in sensitivity toward PARP1 inhibition, which is also known to be particularly toxic to cells with deregulated NHEJ.[15] We reasoned that this might be caused by only moderate degree of RNF168 knockdown achieved in the MDA-MB-231 cells. To address this possibility, we also established and tested a MCF7-derived RNF168 knockdown cell line for sensitivity to CPT and the KU58948 PARP1 inhibitor. Indeed, MCF7 cells that share with MDA-MB-231 cells also the RNF168-fueled proteotoxic stress-resistant DSB response proved to be more amenable to the DOX-inducible RNF168 knockdown as the RNF168 level dropped >3.5-fold upon DOX treatment (Figure 10b). Another important reason for including MCF7 was the fact that, along with MDA-MB-231, MCF7 cells exhibited significant PARPi sensitivity, despite both these cell lines are BRCA1/BRCA2 proficient.[15] We hypothesized that the observed sensitivity to PARPi might be at least partly attributable to the RNF168 overabundance and the ensuing shift of the mutNHEJ/HR ratio, thereby creating a partial, relative 'HR deficiency' despite the proficient BRCA1/2 genes. Consistent with such possibility, the MCF7 cells showed significantly decreased sensitivity toward both CPT and the PARPi upon induction of RNF168 knockdown (Figure 10c). Thus, apart from providing another piece of evidence for aberrant upregulation of NHEJ in these cell lines, this result might also represent an important clue for better understanding of PARPi sensitivity in BRCA1/2-proficient tumors.

DISCUSSION

From a broader perspective, our present study contributes to better understanding of genome integrity maintenance and points to previously unrecognized wide occurrence and impact of aberrant ubiquitin-mediated signaling of DNA damage under proteotoxic stress, with the ensuing consequences for genomic instability and responses to cancer treatment. Our results suggest that human tumors can be widely categorized into two subsets, featuring 'standard' and 'proteotoxic stress-resistant' responses to DNA breakage, respectively. The latter tumor category, discovered and characterized here, may represent an adaptive scenario of 'conditional/secondary' rather than 'genetically caused/primary' HR deficiency, with implications for genomic instability and selective advantages, but also potential vulnerabilities of such cancers.

First, from the mechanistic point of view of the chromatin response to DSB, we show that overabundance of the RNF168 ubiquitin ligase, sometimes accompanied by enhanced levels of additional E2/E3 enzymes, renders the DSB signaling insensitive to depletion of free ubiquitin levels resulting from proteotoxic stress. According to the current paradigm scenario typical for normal cells and some cancers, exemplified by the widely used human U2OS sarcoma cell line model, DSB signaling is grossly attenuated when free ubiquitin levels become limiting upon proteasome inhibition-induced proteotoxic stress. Therefore, it seemed counterintuitive that we could observe sustained recruitment of 53BP1 and its partner proteins REV7 and RIF1 after proteasome inhibition. Although 53BP1 recruitment is regulated also by other modifications including NEDDylation and acetylation[40,41] and NEDDylation was suggested to compensate for ubiquitination when proteasome is inhibited[42] our own experiments using inhibitors of NEDD conjugation and deacetylation did not support this possibility (our unpublished data). Based on our results, we propose a model whereby ubiquitin is still used under proteotoxic stress to relay the DSB chromatin signaling, provided that the RNF168 E3 ligase is overabundant and hence can preferentially channel the remaining available ubiquitin to the RNF168-mediated pathway (Figure 11). Notably, whereas experimentally

Figure 9. Overabundant RNF168 causes unscheduled 53BP1 recruitment, increased mutNHEJ pathway activity and micronuclei formation. (**a**) MDA-MB-231 and U2OS cells were mock or PARPi (10 μM, 24 h) treated, immunostained for 53BP1 and cyclin A. Cyclin A-positive cells with >10 53BP1 foci were scored. (**b**) Representative images of 53BP1 immunostained cells from (**a**). Scale 10 μM. (**c**) The MDA-MB-231 DOX-inducible knockdown cells were pretreated with DOX (DOX, 100 ng/ml; 72 h: T1 or 96 h: T2), lysed and probed for RNF168. After the 72 h pre-treatment, the RNF168 levels were >2.5 times lower in the DOX-treated cells compared with controls (T1). The endpoint (96-h knockdown) RNF168 levels are shown in the T2 panel. (**d**) The effect of RNF168 level on the mutNHEJ/HR ratio was assessed in the MDA-MB-231 and U2OS cell lines bearing the DOX-inducible RNF168 knockdown and the Traffic light reporter. Stable reporter cell lines were pretreated with DOX as in (**a**) and subsequently transduced with a lentivirus carrying an HR repair template and an I-SceI gene. Five days post-transduction, cells were examined by flow cytometry for mCherry and GFP signal. The NHEJ/HR ratio was calculated by correlating the numbers of red (NHEJ) and green (HR). (**e**) Analogous to (**d**), assessed in the parental U2OS and MDA-MB-231 cell lines only. (**f**) MDA-MB-231 cells were pretreated with DOX as above, then mock or CPT treated (10 nM. 24 h) and nuclei/micronuclei were counterstained with DAPI. Fraction of micronuclei in the DAPI-stained objects was determined. In (**a**, **e** and **f**), results are mean ± s.d. of three independent experiments. Statistical significance was determined with two-tailed unpaired Student's *t*-test; $*P < 0.05$; $**P < 0.005$.

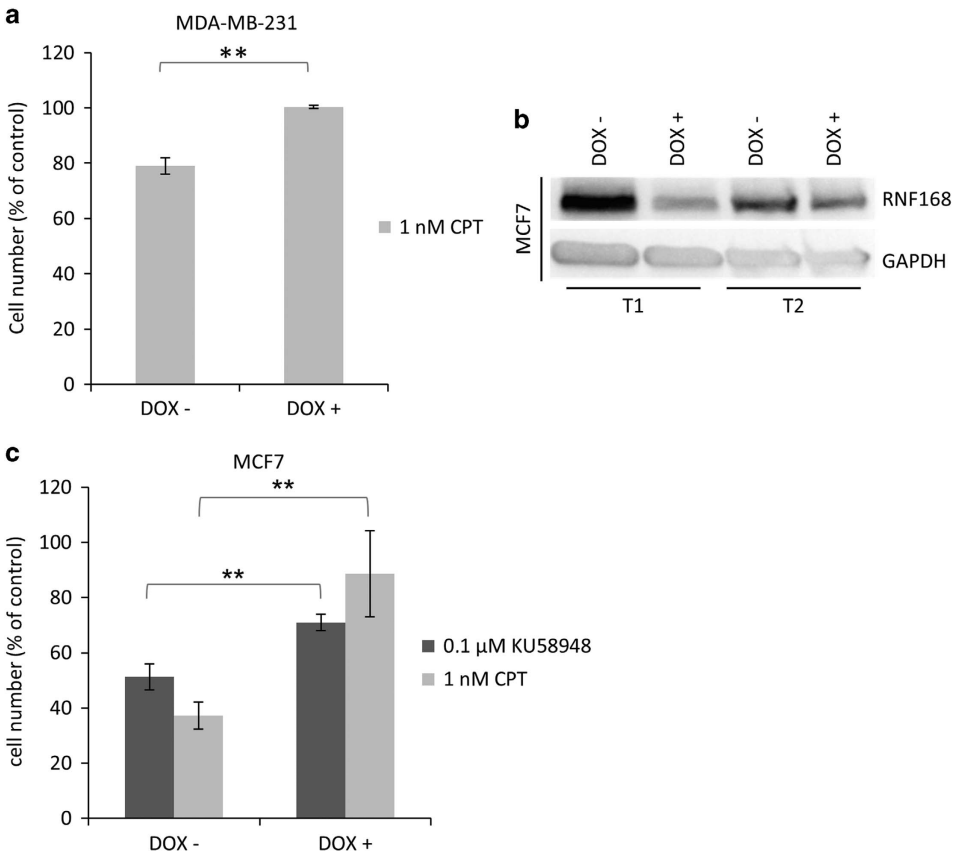

Figure 10. RNF168 overabundance sensitizes MDA-MB-231 and MCF7 cells to CPT and PARPi. (**a**) Sensitivity of the MDA-MB-231 RNF168 knockdown cells toward CPT was assessed by a cell survival assay. The cells were pretreated with DOX as above and then treated with 1 nM CPT. After 6 days, the cells were trypsinized and counted using an automated cell counter. (**b**) The MCF7 DOX-inducible knockdown cell line was pretreated with DOX (DOX, 100 ng/ml; 72 h: T1 or 96 h: T2), lysed and probed by immunoblotting for RNF168. After the 72 h pre-treatment, the RNF168 levels were >3.5-fold lower in the DOX-induced cells than in the non-treated control cells (T1). (**c**) Sensitivity of the MCF7 RNF168 knockdown cells toward CPT and KU58948 was assessed as in (**a**). In (**a** and **c**), results are mean $\pm$ s.d. of three independent experiments. Statistical significance was determined with two-tailed unpaired Student's *t*-test; $^{**}P < 0.005$.

induced ectopic overexpression of RNF168 can rescue the otherwise abolished DSB recruitment of 53BP1 (as well as recruitment of RIF1 and REV7) under proteotoxic stress in cells with moderate, physiological levels of endogenous RNF168 (Figures 6c and d, 3a and b), recruitment of the RAP80-BRCA1 complex to DSB lesions is not rescued under such circumstances (our unpublished results). This striking difference between the two branches of the chromatin response to DSBs further supports our recent report on a functional interplay between JMJD1C demethylase, RNF8 and the MDC1 scaffold protein as a selective mechanism required to recruit the RAP80-BRCA1 complex, but not 53BP1.[43] Considered in the context of our present study, the 'hyper-activity' of the overabundant RNF168 that is sufficient to rescue the 53BP1 recruitment under proteotoxic stress is not enough to allow recruitment of RAP80-BRCA1, as the latter branch of the DSB chromatin response critically depends on RNF8-mediated ubiquitination of MDC1, rather than histone ubiquitination by RNF168, as well as on additional protein modifications.[43] Such a dichotomy in ubiquitin-mediated recruitment of 53BP1 versus RAP80-BRCA1 is also consistent with the recent report from the Halazonetis laboratory that 53BP1 recruitment in proteasome inhibitor-treated cells may be partially rescued by fusing a bulky moiety to the H2AX histone.[44] This presumably opens up chromatin in the vicinity of DSBs and thus partially restores residual chromatin ubiquitination that in turn enables 53BP1 accrual at DNA lesions.[44] Analogous to the differential responses to overexpression of RNF168 in our present study, recruitment of the RAP80-BRCA1 complex to IRIFs under proteasome inhibition conditions was also not rescued by the chromatin opening strategy. Furthermore, our data are also consistent with the notion that the FK2 antibody detected ubiquitin conjugates at the DSB sites may reflect preferential reactivity with RNF8-mediated ubiquitination of MDC1, whereas the histone ubiquitin products catalyzed by RNF168 may not be accessible to antibodies because of nucleosome compaction.[43] Such interpretation can also help explain that upon replacement of endogenous RNF168 with a catalytically inactive RNF168 variant, the FK2 antibody foci remained detectable, whereas ubiquitination of histone H2AX was abolished.[45]

We suggest that our experiments can shed some light also on the competition based mode of 53BP1 recruitment that reportedly requires the two competing demethylases, JMJD2A and JMJD2B to be removed from chromatin flanking the DSBs and degraded in order to expose the H4K20me2 that can be subsequently bound by the 53BP1's tandem TUDOR domains.[26] As we have observed sustained 53BP1 recruitment under conditions of proteasome inhibition, it seems unlikely that the two demethylases have to be degraded to allow for 53BP1 recruitment to chromatin. We favor a model in which the clearance of the competing proteins from the DSB-flanking chromatin is sufficient and does not have to be accompanied by their degradation in order to permit 53BP1 recruitment. According to such modified model, the RNF168-mediated ubiquitination of JMJD2A and JMJD2B would serve primarily as a chromatin eviction signal and the subsequent

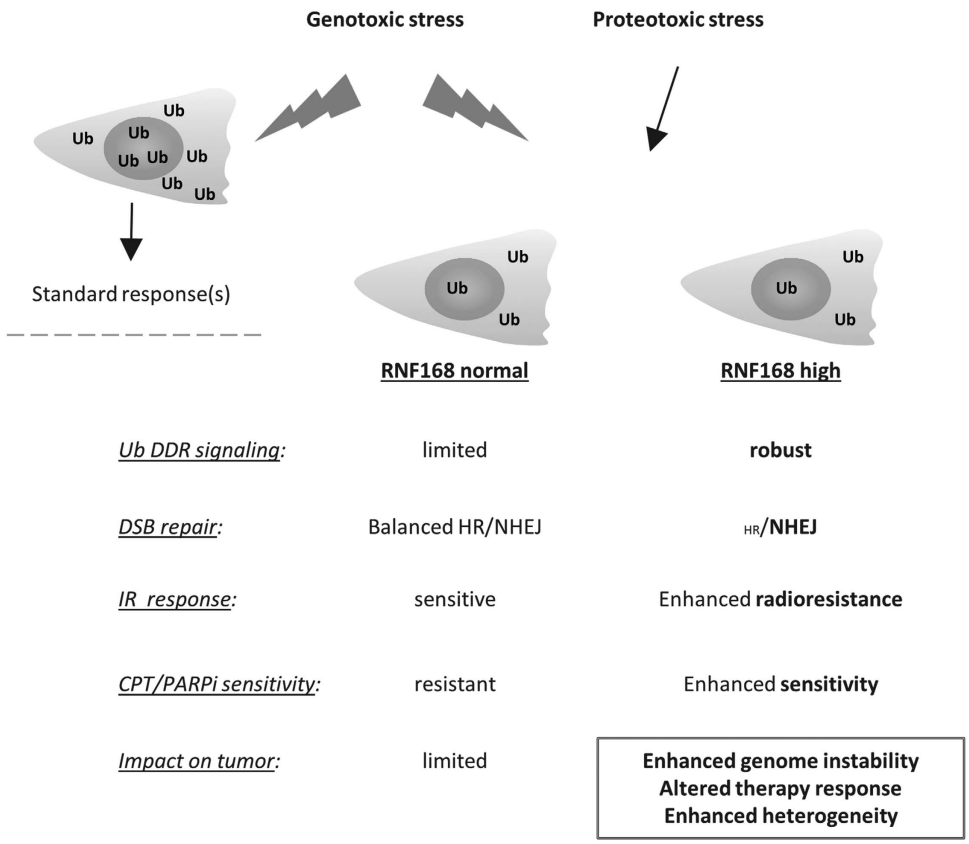

Figure 11. Model summarizing the proteotoxic stress-resistant DSB response and its impact on cancer cells. Changes in chromosome or gene copy number and transcription (de)regulation in cancer cells result in protein overproduction that overwhelms the cellular protein quality control, causing chronic proteotoxic stress and diminishing levels of free ubiquitin. The limited free ubiquitin supply has to be shared by diverse ubiquitin-dependent processes whose efficiency, including that of DSB signaling, is impaired. This is manifested by increased radiosensitivity. Overexpression of RNF168 (and other key DSB response ubiquitin-related enzymes) in the proteotoxic stress-resistant cells shifts the free ubiquitin equilibrium toward DSB signaling thus increasing radioresistance. Overexpression of RNF168 and concomitant robust 53BP1 recruitment promotes mutNHEJ at the expense of HR repair, rendering the cells sensitive to topoisomerase and PARPis, and leading to enhanced genomic instability. Such changes collectively impact tumor heterogeneity, progression and responses to therapy.

degradation of these demethylases is not essential for 53BP1 recruitment.

In the absence of BRCA1 that limits 53BP1 chromatin loading during S phase, the RNF168-driven 53BP1 recruitment precludes DSB end resection and thereby HR, whereas boosting DNA repair by the mutagenic NHEJ pathway.[22,46,47] Unexpectedly, our findings show that BRCA1-proficient cells bearing overabundant RNF168 mimic, at least to some extent, the BRCA1-deficient phenotype by displaying lower levels of HR at the expense of upregulated mutNHEJ. We show that this is most likely caused by aberrantly enhanced 53BP1 recruitment in S-phase cells that is fueled by the excess of RNF168. Albeit not tested in our present study, it is predictable based on the published work in mouse B cells and embryonic fibroblasts, which the overabundant RNF168 inhibits efficient DSB end resection and fuels DSB repair by the mutagenic NHEJ pathway.[22] The RNF168 overexpression seems to derail the physiological balance of the DSB repair pathways toward 53BP1 recruitment and mutNHEJ. We speculate that this imbalance leads to 'conditional HR deficiency' especially under chronic proteotoxic stress conditions, and might account for (or contribute to) the observed increased sensitivity of certain BRCA1-proficient (and principally also HR-proficient) tumors such as subsets of triple-negative breast carcinomas, toward PARPis.[35,48]

The unexpectedly wide occurrence of the proteotoxic stress-resistant DDR among different tumor cell lines raises a question whether it might represent a means of adaptation or provide some selective advantage(s) during tumorigenesis. Cancer cells suffer from increased endogenous proteotoxic stress that stems from such features as aneuploidy, mutation overload and hence accumulation of altered proteins, and variation of gene copy number and levels of transcription.[1,3] We propose that apart from placing a significant burden on the protein quality control mechanisms,[3] proteotoxic stress also impacts on DSB response via attenuating the ubiquitin driven signaling at damaged chromatin. Of note, the load of endogenous DSBs increases during cell transformation and tumor progression because of enhanced replication stress evoked by diverse oncogenes and loss of some tumor suppressors.[6,7,49–51] Given its pathophysiological significance, aberrations in the DSB ubiquitination signaling pathway might profoundly affect genome integrity of tumor cells. Our findings show that attenuation of DSB signaling because of proteotoxic stress might be circumvented by upregulation of one or more key ubiquitin ligases involved in the DDR, particularly RNF168. Importantly, this concept was further supported by observation of the proteotoxic stress-resistant DSB response in multiple myeloma cells, an established model of cancer-related proteotoxic stress. It has been also reported that breast cancers exhibit elevated levels of some E2 ubiquitin conjugating enzymes.[52] Taken together, this implies that upregulation of some ubiquitin-mediated cellular processes might represent a more general strategy to overcome adverse effects of cancer-

associated proteotoxic stress. UPS has a major role in the regulation of several key tumorigenesis driving processes, such as cellular proliferation, apoptosis and stress tolerance.[1,53] Hence, it is likely that these pathways are sensitive to proteotoxic stress and tumor cells have evolved compensatory mechanisms such as the upregulation of specific enzymes of the UPS. In terms of potential selective advantages during tumorigenesis, the acquired overabundance of RNF168 can help enhance survival of cancer cells under combined proteotoxic and replication stresses, fuel error-prone DNA repair, genomic instability and thereby intra-tumor heterogeneity (Figure 11), all features likely to promote tumor progression and aggressivity.

It remains to be elucidated how cancer cells acquire the elevated expression of RNF168 and/or other ubiquitin ligases and conjugating enzymes. Analogous to other tumor-associated changes in gene expression, the most likely candidates are mutations in gene regulatory sequences, genome rearrangements or transcription suppressor/activator mutations. One of the likely candidates that might drive the cancer-related RNF168 over-expression is the family of FOXO transcription factors known to regulate various stress response genes including components of the DDR machinery.[54,55] Dysregulation of the FOXO3a transcription factor occurs in both breast cancer and hematological malignancies,[54] which implies that this protein (and possibly other FOXO family members) might fuel the elevated RNF168 expression in tumors. Regardless of the molecular mechanism, it will also be conceptually interesting to find out when during tumor progression such overexpression of RNF168 occurs, relative to the reported activation of the DSB-responsive checkpoint anticancer barrier and its interplay with the ARF-p53 checkpoint pathway.[2,4,8,53]

Last but not least, our present results indicate that such possibly adaptive upregulation of RNF168 may have important implications for responses of tumors to standard-of-care as well as some emerging targeted treatments. On one hand, we show that tumor cells with the proteotoxic stress-resistant DSB response phenotype are more resistant to ionizing radiation under conditions of enhanced proteotoxic stress. At the same time, however, the altered balance among the DSB repair pathways appears to generate a kind of adaptive, conditional HR deficiency, and thereby unmask some potentially exploitable vulnerabilities to S-phase genotoxic drugs such as CPT or PARPis. In the light of our present findings, combined immunohistochemical detection of RNF168 and markers of proteotoxic stress such as conjugated ubiquitin or the BiP chaperone might be exploited as candidate biomarkers to identify the subsets of patients whose tumors may display the proteotoxic stress-resistant phenotype described here, and possibly help decisions about personalized cancer therapy in the future.

MATERIALS AND METHODS

Cell culture and generation of DSBs

Most cell lines used in this work were cultured in Dulbecco's modified Eagle's medium, supplemented with 10% fetal bovine serum (PAA, Pasching, Austria) and penicillin/streptomycin (Sigma-Aldrich, St Louis, MO, USA) in a humidified atmosphere of 5% CO_2 at 37 °C. For MCF7, AMO1 and MMS1 culturing, the standard cell culture medium was RPMI-1640 with the same supplements as above. All cell lines were purchased from ATCC (Manassas, VA, USA) with the exception of U2OS RNF168-GFP that was established previously.[13]

X-ray irradiation was done using the YXLON.SMART 160E/1.5 device (YXLON, Horsens, Denmark) at the following settings: 150 kV, 6 mA, 11 mGy/s.

Micro-irradiation

Laser micro-irradiation was performed on a Zeiss Axioimager Z.1 instrument equipped with a laser scanning LSM780 module (Zeiss, Oberkochen, Germany). A UV-A laser (355 nm 65 mW) was used to induce the DNA damage. BrDU presensitization and irradiation of the cells was done as described previously.[56] Subsequent immunofluorescent detection of recruited proteins was essentially done as in Xu *et al*.[20]

Plasmids and RNA interference

Most plasmids were transfected using the FuGENE 6 (Roche, Basel, Switzerland) reagent following the manufacturer's instructions. When required, plasmid DNA was transfected by nucleofection using the Neon (Life Technologies, Carlsbad, CA, USA) device at settings recommended by the manufacturer for the respective cell line. The pGFP-53BP1-FI-wt, pGFP-53BP1-FI-L1619A and pGFP-53BP1-FI-D1521 plasmids carrying the 53BP1 UDR and Tudor domains mutations were a gift from D Durocher (Samuel Lunenfeld Research Institute, Ontario, Canada). The pAcGFP-C1-RNF168 plasmids harboring the C16S RING and MIU mutations were described previously.[13] The Traffic light repair template, the I-SceI lentiviral constructs[38] as well as the lentivirus production plasmids pMD2.G and psPAX2 (D Trono, unpublished) were purchased from Addgene (Cambridge, MA, USA; plasmids no's 31476, 31482, 12259 and 12260). The inducible shRNA RNF168 knockdown lentiviral plasmids were constructed as described in Wiederschain *et al*.[57] using following oligonucleotides (5'–3'): shRNA RNF168 sense CCGGGGCGAAGAGCGATGGAGGACTCGAG TCCTCCATCGCTCTTCGCCTTTTT; shRNA RNF168 antisense AATTAAAAAGGC GAAGAGCGATGGAGGACTCGAGTCCTCCATCGCTCTTCGCC (Generi Biotech, Hradec Kralove, Czech Republic). The backbone pLKO-Tet-On Puro[57,58] plasmid was obtained from Addgene (plasmid no. 21915).

siRNA's were transfected with the Lipofectamine RNAiMAX (Invitrogen, Carlsbad, CA, USA) reagent following the manufacturer's instructions. siRNAs were purchased from Thermo Fisher Scientific (Waltham, MA, USA): siCON-negative control, siRNA#1 (ID#4390843), siRNF168 (ID #126171), siRNF8 (ID#17200) and from MWG Operon (Ebersberg, Germany): 53BP1DD2013 GAGAGCAGAUGAUCCUUUAtt (5'–3').

Oligonucleotides and quantitative PCR

The abundance of RNF168 mRNA level was probed by quantitative PCR using a Nano LightCycler (Roche) instrument and following oligos (5'–3'): RNF168qPCR_F1 CAGGGCAAGACACAGAAATAGA; RNF168qPCR_R1 GGCAC CACAGGCACATAA; RNF168qPCR_F2 CTCCCTACAGCCTAGCATTTC and RNF 168qPCR_R2 AGATCACAAAGCACTCCCTTTA (Generi Biotech). Following GAPDH, primers were used as an internal control: GAPDH—F GAAG ATGGTGATGGGATTTC; GAPDH—R GAAGGTGAAGGTCGGAGT (Generi Biotech) PCR product abundance was quantified using the LighCycler Nano software (Roche).

Chemicals and antibodies

The Bortezomib (PS-341), MG132 and CPT inhibitors were purchased from Sigma-Aldrich. The KU58948 PARP1 inhibitor was obtained from AstraZeneca (London, UK). Antibodies used in this study included following mouse monoclonal antibodies: γH2AX (Merck Millipore, Billerica, MA, USA), RNF8 (B-2) (Santa Cruz Biotechnology, Santa Cruz, CA, USA), Ubc13, JMJD2A (KDM4A) (Thermo Fisher Scientific, Waltham, MA, USA), HERC2 (BD Transduction Laboratories, San Jose, CA, USA), MDC1, USP34 (Abcam, Cambridge, UK), GAPDH (GT239) (GeneTex, Hsinchu, Taiwan), β-actin (Sigma-Aldrich) and polyclonal rabbit: 53BP1, BRCA1 (Santa Cruz Biotechnology), TRIP12 (Abcam), UBR5 (Sigma-Aldrich), FK2 (Enzo Life Sciences, Farmingdale, NY, USA), RIF1 (Bethyl Laboratories, Montgomery, TX, USA), REV7 (BD Transduction Laboratories). The rabbit polyclonal antibodies to RNF168 and RNF169 were a gift from N Mailand (Center for Protein Research, Copenhagen, Denmark).

Immunoblotting

Cells were lysed in Laemmli sample buffer and the whole-cell lysates were subsequently separated on a 10% sodium dodecyl sulfate–polyacrylamide gel electrophoresis gel and transferred to a nitrocellulose membrane (GE Healthcare, Little Chalfont, UK). The membrane was blocked in 5 % (w/v) skim milk in Tris-buffered saline supplemented with in 0.1% (v/v) Tween-20 and probed with a primary antibody. Subsequently, the membrane was incubated with horseradish peroxidase-labeled secondary anti-mouse or anti-rabbit antibodies (Santa Cruz Biotechnology) and the signals were visualized using ECL detection reagents (Thermo Fisher Scientific) and the ChemiDoc system (Bio-Rad, Hercules, CA, USA). Band intensity quantification was performed in the ImageJ software (http://imagej.nih.gov/ij/).

Immunofluorescence and micronuclei staining, microscopic analysis

Cells grown on 12-mm coverslips were fixed with 4% paraformaldehyde in phosphate-buffered saline (PBS) for 15 min and then permeabilized with PBS containing 0.2% (v/v) Triton X-100 for 5 min. Suspension cells were cytospinned onto microscopic slides before fixation using the Cyto-Tek Sakura instrument (Sakura Finetek, Torrance, CA, USA). Fixed cells were blocked with 5% (v/v) fetal bovine serum in PBS for 30 min and incubated overnight at 4 °C with primary antibodies (diluted in 5% (w/v) bovine serum albumin in PBS). Coverslips were washed three times in PBS supplemented with 0.1% (v/v) Tween-20, once with PBS and then incubated with an appropriate secondary goat anti-rabbit or goat anti-mouse Alexa Fluor 488 or Alexa Fluor 568 conjugated (Invitrogen) secondary antibody (diluted in in 5% (w/v) bovine serum albumin in PBS) for 60 min at room temperature. Slips were then washed as above and mounted onto slides using the 4,6-diamidino-2-phenylindole (DAPI) containing Vectashield mounting reagent (Vector Laboratories, Burlingame, CA, USA). Coverslips for micronuclei analysis were fixed and washed as above, stained with DAPI diluted in PBS and subsequently mounted with the Vectashield reagent (without DAPI).

Slides were visualized by the Axio Observer.Z1/Cell Observer Spinning Disc microscopic system (Yokogawa, Tokyo, Japan and Zeiss) equipped with an Evolve 512 (Photometrix, Tucson, AZ, USA) EMCCD camera. Zeiss Plan Apochromat 63x and 100x/1.40 NA objectives were used.

For quantitative image analysis, a series of random fields were recorded automatically using the ScanR imaging workstation (Olympus, Tokyo, Japan; with an EM charge-coupled device camera (C9100; Hamamatsu Photonics, Hamamatsu City, Japan), a U Plan S Apochromat 40 × /0.9 NA objective, and an image resolution of 200 × 200 nm/pixel). The number and intensity of micronuclei and IR-induced nuclear foci were quantified using the ScanR image analysis software (Olympus).

Generation of lentiviruses and lentiviral transduction

Lentiviruses were generated by co-transfecting 293T cells with 4 μg of pMD2.G, 7 μg of psPAX2 and 9 μg of a lentiviral plasmid of interest using the $CaPO_4$ precipitation method.[59] Six to eight hours post-transfection, the cells were washed briefly with pre-warmed PBS and medium was changed. Lentivirus containing supernatant was collected 48 h later. Target cells were transduced at multiplicity of infection of 1–10 with the supernatant supplemented with 4 μg/ml polybrene (Sigma-Aldrich). Twenty-four hours post-transduction, the medium was changed and when required, the cells were selected in 1 μg/ml puromycin.

Flow cytometric analysis of DNA repair pathway choice

Cells harboring the Traffic light reporter were seeded in a 12-well plate and 24-h later transduced with the I-SceI and GFP repair template containing construct using the procedure above. Seven days later, the cells were trypsinized, fixed with formaldehyde and analyzed by an Influx (BD Biosciences, San Jose, CA, USA) instrument. GFP was measured using a 488 nm laser for excitation and a 530/40 filter, whereas mCherry was excited using a 561 nm laser and acquired with a 610/20 filter. Data were analyzed using the FACS Sortware (BD Biosciences) software.

Cell cycle analysis

Cells were fixed in 70% ethanol and stained with propidium iodide for flow cytometric analysis. Fixed cells were analyzed on a FACS Verse instrument (BD Biosciences) and cell cycle distribution was assigned using the FACSuite software (BD Biosciences).

Long-term cell survival assay

In all, 1×10^5 cells were seeded in triplicate to ø 6 cm plates and left to attach overnight. Next day, the medium was replaced by inhibitor or dimethylsulfoxide (mock) containing medium. Seven days later, the cells were trypsinized and cell number was scored using a Vi-Cell XR Cell Viability Analyzer (Beckman Coulter, Brea, CA, USA) equipped with the ViCELL XR software (Beckman Coulter).

The IR resistance of proteotoxic stress DDR-resistant lines was assessed as above with following modifications: attached cells were pretreated with 5 μM MG132 or dimethylsulfoxide (mock) for 2 h and subsequently irradiated with 2 Gy. Then medium was changed and cell survival was assayed as above 7 days later.

Statistical analysis

Differences in DNA repair pathway efficiency and cell survival assays were analyzed by Student's *t*-test. Variability and reproducibility among repeated experiments subjected to quantitative evaluations, such as immunofluorescence IRIF counts or quantitative PCR products is indicated by mean ± s.d. and shown as error bars in graphical summaries in the relevant figures.

ABBREVIATIONS

53BP1, p53 binding protein 1; BRCA1, breast cancer 1; DDR, DNA damage response; DSB, double-strand break; HR, homologous recombination; IRIF, ionizing radiation induced foci; NHEJ, non-homologous end joining; PARP1, poly(ADP-ribose) polymerase 1; RNF168, ring finger protein 168.

CONFLICT OF INTEREST

The authors declare no conflict of interest.

ACKNOWLEDGEMENTS

We thank Jan Bouchal, Katerina Bouchalova and our colleagues from the Laboratory of Genome Integrity for technical assistance, suggestions and comments on the manuscript. This work was supported by grants from the following foundations: Grant Agency of the Czech Republic 13-17555S, Czech National Program of Sustainability LO1304, the Kellner Family Foundation, the Norwegian Financial Mechanism CZ09 (Project PHOSCAN 7F14061), MEYS CR (LM2015062 Czech-Biolmaging), the internal grant IGA-LF-2016-030, the EU operation program CZ.1.07/2.3.00/30.0004, the Danish National Research Foundation (DNRF125, project CARD), Danish Cancer Society, the Swedish Research Council, the Lundbeck Foundation, Cancer Fonden, and the Danish Council for Independent Research.

REFERENCES

1 Deshaies RJ. Proteotoxic crisis, the ubiquitin-proteasome system, and cancer therapy. *BMC Biol* 2014; **12**: 94.
2 Halazonetis TD, Gorgoulis VG, Bartek J. An oncogene-induced DNA damage model for cancer development. *Science* 2008; **319**: 1352–1355.
3 Luo J, Solimini NL, Elledge SJ. Principles of cancer therapy: oncogene and non-oncogene addiction. *Cell* 2009; **136**: 823–837.
4 Bartek J, Bartkova J, Lukas J. DNA damage signalling guards against activated oncogenes and tumour progression. *Oncogene* 2007; **26**: 7773–7779.
5 Jackson SP, Bartek J. The DNA-damage response in human biology and disease. *Nature* 2009; **461**: 1071–1078.
6 Bartkova J, Horejsi Z, Koed K, Kramer A, Tort F, Zieger K *et al.* DNA damage response as a candidate anti-cancer barrier in early human tumorigenesis. *Nature* 2005; **434**: 864–870.
7 Bartkova J, Rezaei N, Liontos M, Karakaidos P, Kletsas D, Issaeva N *et al.* Oncogene-induced senescence is part of the tumorigenesis barrier imposed by DNA damage checkpoints. *Nature* 2006; **444**: 633–637.
8 Evangelou K, Bartkova J, Kotsinas A, Pateras IS, Liontos M, Velimezi G *et al.* The DNA damage checkpoint precedes activation of ARF in response to escalating oncogenic stress during tumorigenesis. *Cell Death Differ* 2013; **20**: 1485–1497.
9 Zhao Y, Brickner JR, Majid MC, Mosammaparast N. Crosstalk between ubiquitin and other post-translational modifications on chromatin during double-strand break repair. *Trends Cell Biol* 2014; **24**: 426–434.
10 Lukas J, Lukas C, Bartek J. More than just a focus: the chromatin response to DNA damage and its role in genome integrity maintenance. *Nat Cell Biol* 2011; **13**: 1161–1169.
11 Reinhardt HC, Yaffe MB. Phospho-Ser/Thr-binding domains: navigating the cell cycle and DNA damage response. *Nat Rev Mol Cell Biol* 2013; **14**: 563–580.
12 Thorslund T, Ripplinger A, Hoffmann S, Wild T, Uckelmann M, Villumsen B *et al.* Histone H1 couples initiation and amplification of ubiquitin signalling after DNA damage. *Nature* 2015; **527**: 389–393.
13 Doil C, Mailand N, Bekker-Jensen S, Menard P, Larsen DH, Pepperkok R *et al.* RNF168 binds and amplifies ubiquitin conjugates on damaged chromosomes to allow accumulation of repair proteins. *Cell* 2009; **136**: 435–446.
14 Stewart GS, Panier S, Townsend K, Al-Hakim AK, Kolas NK, Miller ES *et al.* The RIDDLE syndrome protein mediates a ubiquitin-dependent signaling cascade at sites of DNA damage. *Cell* 2009; **136**: 420–434.
15 Bunting SF, Callen E, Wong N, Chen HT, Polato F, Gunn A *et al.* 53BP1 inhibits homologous recombination in Brca1-deficient cells by blocking resection of DNA breaks. *Cell* 2010; **141**: 243–254.

16 Daley JM, Sung P. 53BP1, BRCA1, and the choice between recombination and end joining at DNA double-strand breaks. *Mol Cell Biol* 2014; **34**: 1380–1388.
17 Densham RM, Garvin AJ, Stone HR, Strachan J, Baldock RA, Daza-Martin M *et al.* Human BRCA1-BARD1 ubiquitin ligase activity counteracts chromatin barriers to DNA resection. *Nat Struct Mol Biol* 2016; **23**: 647–655.
18 Callen E, Di Virgilio M, Kruhlak MJ, Nieto-Soler M, Wong N, Chen HT *et al.* 53BP1 mediates productive and mutagenic DNA repair through distinct phosphoprotein interactions. *Cell* 2013; **153**: 1266–1280.
19 Chapman JR, Barral P, Vannier JB, Borel V, Steger M, Tomas-Loba A *et al.* RIF1 is essential for 53BP1-dependent nonhomologous end joining and suppression of DNA double-strand break resection. *Mol Cell* 2013; **49**: 858–871.
20 Xu G, Chapman JR, Brandsma I, Yuan J, Mistrik M, Bouwman P *et al.* REV7 counteracts DNA double-strand break resection and affects PARP inhibition. *Nature* 2015; **521**: 541–544.
21 Zimmermann M, Lottersberger F, Buonomo SB, Sfeir A, de Lange T. 53BP1 regulates DSB repair using Rif1 to control 5' end resection. *Science* 2013; **339**: 700–704.
22 Zong D, Callen E, Pegoraro G, Lukas C, Lukas J, Nussenzweig A. Ectopic expression of RNF168 and 53BP1 increases mutagenic but not physiological non-homologous end joining. *Nucleic Acids Res* 2015; **43**: 4950–4961.
23 Botuyan MV, Lee J, Ward IM, Kim JE, Thompson JR, Chen J *et al.* Structural basis for the methylation state-specific recognition of histone H4-K20 by 53BP1 and Crb2 in DNA repair. *Cell* 2006; **127**: 1361–1373.
24 Fradet-Turcotte A, Canny MD, Escribano-Diaz C, Orthwein A, Leung CC, Huang H *et al.* 53BP1 is a reader of the DNA-damage-induced H2A Lys 15 ubiquitin mark. *Nature* 2013; **499**: 50–54.
25 Acs K, Luijsterburg MS, Ackermann L, Salomons FA, Hoppe T, Dantuma NP. The AAA-ATPase VCP/p97 promotes 53BP1 recruitment by removing L3MBTL1 from DNA double-strand breaks. *Nat Struct Mol Biol* 2011; **18**: 1345–1350.
26 Mallette FA, Mattiroli F, Cui G, Young LC, Hendzel MJ, Mer G *et al.* RNF8- and RNF168-dependent degradation of KDM4A/JMJD2A triggers 53BP1 recruitment to DNA damage sites. *EMBO J* 2012; **31**: 1865–1878.
27 Devgan SS, Sanal O, Doil C, Nakamura K, Nahas SA, Pettijohn K *et al.* Homozygous deficiency of ubiquitin-ligase ring-finger protein RNF168 mimics the radiosensitivity syndrome of ataxia-telangiectasia. *Cell Death Differ* 2011; **18**: 1500–1506.
28 Gudjonsson T, Altmeyer M, Savic V, Toledo L, Dinant C, Grofte M *et al.* TRIP12 and UBR5 suppress spreading of chromatin ubiquitylation at damaged chromosomes. *Cell* 2012; **150**: 697–709.
29 Dantuma NP, Groothuis TA, Salomons FA, Neefjes J. A dynamic ubiquitin equilibrium couples proteasomal activity to chromatin remodeling. *J Cell Biol* 2006; **173**: 19–26.
30 Jacquemont C, Taniguchi T. Proteasome function is required for DNA damage response and fanconi anemia pathway activation. *Cancer Res* 2007; **67**: 7395–7405.
31 Bekker-Jensen S, Rendtlew Danielsen J, Fugger K, Gromova I, Nerstedt A, Lukas C *et al.* HERC2 coordinates ubiquitin-dependent assembly of DNA repair factors on damaged chromosomes. *Nat Cell Biol* 2010; **12**: 80–86. sup pp 1-12.
32 Panier S, Boulton SJ. Double-strand break repair: 53BP1 comes into focus. *Nat Rev Mol Cell Biol* 2014; **15**: 7–18.
33 Chauhan D, Hideshima T, Anderson KC. Proteasome inhibition in multiple myeloma: therapeutic implication. *Annu Rev Pharmacol Toxicol* 2005; **45**: 465–476.
34 Gething MJ. Role and regulation of the ER chaperone BiP. *Semin Cell Dev Biol* 1999; **10**: 465–472.
35 Livraghi L, Garber JE. PARP inhibitors in the management of breast cancer: current data and future prospects. *BMC Med* 2015; **13**: 188.
36 Ricks TK, Chiu HJ, Ison G, Kim G, McKee AE, Kluetz P *et al.* Successes and challenges of PARP inhibitors in cancer therapy. *Front Oncol* 2015; **5**: 222.
37 Bouwman P, Aly A, Escandell JM, Pieterse M, Bartkova J, van der Gulden H *et al.* 53BP1 loss rescues BRCA1 deficiency and is associated with triple-negative and BRCA-mutated breast cancers. *Nat Struct Mol Biol* 2010, biology **17**: 688–695.
38 Certo MT, Ryu BY, Annis JE, Garibov M, Jarjour J, Rawlings DJ *et al.* Tracking genome engineering outcome at individual DNA breakpoints. *Nat Methods* 2011; **8**: 671–676.
39 Rodgers K, McVey M. Error-prone repair of DNA double-strand breaks. *J Cell Physiol* 2016; **231**: 15–24.
40 Ma T, Chen Y, Zhang F, Yang CY, Wang S, Yu X. RNF111-dependent neddylation activates DNA damage-induced ubiquitination. *Mol Cell* 2013; **49**: 897–907.
41 Tang J, Cho NW, Cui G, Manion EM, Shanbhag NM, Botuyan MV *et al.* Acetylation limits 53BP1 association with damaged chromatin to promote homologous recombination. *Nat Struct Mol Biol* 2013; **20**: 317–325.
42 Hjerpe R, Thomas Y, Chen J, Zemla A, Curran S, Shpiro N *et al.* Changes in the ratio of free NEDD8 to ubiquitin triggers NEDDylation by ubiquitin enzymes. *Biochem J* 2012; **441**: 927–936.
43 Watanabe S, Watanabe K, Akimov V, Bartkova J, Blagoev B, Lukas J *et al.* JMJD1C demethylates MDC1 to regulate the RNF8 and BRCA1-mediated chromatin response to DNA breaks. *Nat Struct Mol Biol* 2013; **20**: 1425–1433.
44 Kocylowski MK, Rey AJ, Stewart GS, Halazonetis TD. Ubiquitin-H2AX fusions render 53BP1 recruitment to DNA damage sites independent of RNF8 or RNF168. *Cell Cycle* 2015; **14**: 1748–1758.
45 Mattiroli F, Vissers JH, van Dijk WJ, Ikpa P, Citterio E, Vermeulen W *et al.* RNF168 ubiquitinates K13-15 on H2A/H2AX to drive DNA damage signaling. *Cell* 2012; **150**: 1182–1195.
46 Munoz MC, Laulier C, Gunn A, Cheng A, Robbiani DF, Nussenzweig A *et al.* RING finger nuclear factor RNF168 is important for defects in homologous recombination caused by loss of the breast cancer susceptibility factor BRCA1. *J Biol Chem* 2012; **287**: 40618–40628.
47 Munoz MC, Yanez DA, Stark JM. An RNF168 fragment defective for focal accumulation at DNA damage is proficient for inhibition of homologous recombination in BRCA1 deficient cells. *Nucleic Acids Res* 2014; **42**: 7720–7733.
48 Inbar-Rozensal D, Castiel A, Visochek L, Castel D, Dantzer F, Izraeli S *et al.* A selective eradication of human nonhereditary breast cancer cells by phenanthridine-derived polyADP-ribose polymerase inhibitors. *Breast Cancer Res* 2009; **11**: R78.
49 Burrell RA, McClelland SE, Endesfelder D, Groth P, Weller MC, Shaikh N *et al.* Replication stress links structural and numerical cancer chromosomal instability. *Nature* 2013; **494**: 492–496.
50 Di Micco R, Fumagalli M, Cicalese A, Piccinin S, Gasparini P, Luise C *et al.* Oncogene-induced senescence is a DNA damage response triggered by DNA hyper-replication. *Nature* 2006; **444**: 638–642.
51 Gorgoulis VG, Vassiliou LV, Karakaidos P, Zacharatos P, Kotsinas A, Liloglou T *et al.* Activation of the DNA damage checkpoint and genomic instability in human precancerous lesions. *Nature* 2005; **434**: 907–913.
52 Chen L, Madura K. Increased proteasome activity, ubiquitin-conjugating enzymes, and eEF1A translation factor detected in breast cancer tissue. *Cancer Res* 2005; **65**: 5599–5606.
53 Velimezi G, Liontos M, Vougas K, Roumeliotis T, Bartkova J, Sideridou M *et al.* Functional interplay between the DNA-damage-response kinase ATM and ARF tumour suppressor protein in human cancer. *Nat Cell Biol* 2013; **15**: 967–977.
54 Greer EL, Brunet A. FOXO transcription factors at the interface between longevity and tumor suppression. *Oncogene* 2005; **24**: 7410–7425.
55 Tran H, Brunet A, Grenier JM, Datta SR, Fornace AJ Jr., DiStefano PS *et al.* DNA repair pathway stimulated by the forkhead transcription factor FOXO3a through the Gadd45 protein. *Science* 2002; **296**: 530–534.
56 Mistrik M, Vesela E, Furst T, Hanzlikova H, Frydrych I, Gursky J *et al.* Cells and stripes: a novel quantitative photo-manipulation technique. *Sci Rep* 2016; **6**: 19567.
57 Wiederschain D, Wee S, Chen L, Loo A, Yang G, Huang A *et al.* Single-vector inducible lentiviral RNAi system for oncology target validation. *Cell Cycle* 2009; **8**: 498–504.
58 Wee S, Wiederschain D, Maira SM, Loo A, Miller C, deBeaumont R *et al.* PTEN-deficient cancers depend on PIK3CB. *Proc Natl Acad Sci USA* 2008; **105**: 13057–13062.
59 Tiscornia G, Singer O, Verma IM. Production and purification of lentiviral vectors. *Nat Protoc* 2006; **1**: 241–245.

Supplementary Information accompanies this paper on the Oncogene website (http://www.nature.com/onc)

15.2 APPENDIX B

K Chroma, J Kramara, P Moudry, M Mistrik, J Bartek. Sustained DNA damage response in proteasome inhibitor treated cancer cell lines. Zborník prednášok- Súťaž mladých onkológov 2014, NADÁCIA VÝSKUM RAKOVINY A ÚSTAV EXPERIMENTÁLNEJ ONKOLÓGIE SAV BA, ISBN 978 -80 -971621-0-8. No IF

Sustained DNA damage response in proteasoem inhibitor treated cancer cell lines

Chromá K.[1] , Kramara J.[1], Moudrý P.[2], Mistrík M.[1], Bártek J.[1,2]
[1]*Institute of Molecular and Translational Medicine, Olomouc, Czech Republic;*
[2] *Danish Cancer Society, Copenhagen, Denmark* 116

Introduction

The DNA-damage response (DDR) is a complex network pathway critical for maintenance of genome integrity by sensing a diverse group of DNA lesions [1]. It is regulated by several posttranslational modifications involving ubi uitination, sumoylation, acetylation, methylation and phosphorylation targeting histones and an extensive number of mediators and effectors performing DNA repair [2]. Of the many types of DNA lesions, DNA double-strand breaks (DSBs) are considered to be the most harmful. One left unrepaired is sufficient to trigger growth arrest, cell death or lead through gross chromosomal rearrangements in malignant transformation. Eukaryotic cells have two main repair pathways to deal with DSBs: non-homologous end-joining (NHEJ) and homologous recombination (HR). Important regulators in choice of DSB signalling pathway are the tumorsupressors 53BP1 promoting NHEJ and BRCA1 required for efficient HR [3,4]. Both are known to accumulate rapidly in the vicinity of DSBs. Their recruitment is dependent on a signalling cascade terminating with two E3 ubiquitin ligases- RNF8 and RNF168, which mark the DSB flanking chromatin with ubiquitin. 26S proteasome is a multisubunit complex performing degradation of misfolded and toxic proteins with an indirect role in the ubiquitin dependent DDR signalling. After treatment with proteasome core inhibitors, such as Bortezomib (PS341) or MG132, Ub molecules are captured in high molecular weight conjugates without compensation in increased level of Ub transcription. As a consequence the pool of free Ub is diminished and Ub conjugation events are prevented. The Ub shortage also affects the DDR sinalling, namely formation of Ub dependent nuclear foci of BRCA1 and 53BP1before or shortly after induction of DNA damage [5]. This is due to the inability of DNA repair ligases to ´fire´ under Ub starvation resulting in failure of the damage response to progress. However, we have identified several cancer cell lines exhibiting 53BP1 recruitment even after proteasome inhibition. In this work we demonstrate the importance of the E3 ubiquitin ligase RNF168 level in sustained DNA damage response and persistence of 53BP1foci under the condition of proteasome inhibition.

Key words: Proteasome inhibition, 53BP1 foci, E3 ubiquitin ligase RNF16

Material and Methods

Cell Culture and generation of DSBs
The human cell line MCF7 was cultured in RPMI 1640, cell lines MDA-MB-231, U2OS, MDA-MB-436, Cal51, Hela were cultured in Dulbecco's modified Eagle's medium, supplemented with 10% fetal bovine serum (PAA) and penicillin/streptomycin (Sigma) in a humidified atmosphere of 5% CO2 at 37°C. All lines except for U2OS GFP RNF168 have been purchased from ATCC. The RNF168 GFP fusion overexpressing U2OS line (Doil et al., 2009) was a gift from our sister laboratory at Danish Cancer Society, Copenhagen, Denmark. X-ray irradiation was done with a XYLON.SMART 160E/1.5 device (150 kV, 6 mA; YXLON. International A/S) delivering 11.8 mGy per second.

Plasmid transfection and RNA interference
Transfection of plasmid pAcGFP-C1-RNF168 siRNAr (Copenhagen) with the point mutation in the RING domain (*RING; C16S) was performed using FuGENE 6 (Roche) according to the manufacturer's instructions. siRNA transfection was performed using Lipofectamine RNAiMAX (Invitrogen). siRNAs were purchased from Ambion: siCON-negative control, siRNA #1 (ID#4390843), siRNF168 (ID #126171).

Chemicals and antibodies
Proteasome inhibitors Bortezomib (PS-341), MG-132 as well as inhibitor of UBA1 Pyr-41 were obtained from Sigma and used at 5μM concentration. Antibodies used in this study included mouse monoclonal antibodies γH2AX (Milipore), RNF8 (B-2) (Santa Cruz Biotechnology), Ubc13 (Zymed), HERC2 (BD Transduction Laboratories), USP34 (Abcam), JMJD2A (KDM4A) (Thermo), GAPDH (GT239) (GeneTex) and Polyclonal rabbit- KAP-1 (phospho S824) (Bethyl), antibody against 53BP1 (Santa Cruz Biotechnology), RNF169, RNF168 (N. Mailand, Copenhagen University)), TRIP12 (Abcam), Ubr5 (Sigma), RNF168 (Cph).

Immunoblotting
Cells were lysed with LSB buffer and whole cell lysates were separated by 10% SDS-PAGE and transferred to nitrocellulose membranes (GE Healthcare). The membranes were blocked with 5% (w/v) dry milk in 0.1% (v/v) Tween-20 in PBS and probed with the primary antibodies listed above, followed by HRP-labeled secondary antibodies (Vector Laboratories and Santa Cruz Biotechnology) and visualization using ECL detection reagents (GE Healthcare).

Immunofluorescence staining, microscopy analysis
Cells grown on 12-mm coverslips were fixed with 4% paraformaldehyde in PBS for 15 min and then permeabilized with PBS containing 0.2% Triton X-100 for 5 min. The fixed cells were blocked with 5% fetal bovine serum for 30 minutes and incubated overnight at 4 °C with primary antibodies (diluted in PBS containing 5% bovine serum albumin). Coverslips were washed 3 times in PBS+0,1% Tween 20, once with PBS and then incubated with an appropriate secondary antibody for 45 minutes at RT. Slips were then washed as above and mounted onto slides using the Vectashield mounting reagent containing DAPI (Vector Laboratories). A series of 117

random fields were recorded automatically using the ScanR imaging workstation (Olympus; with an EM charge-coupled device camera [C9100; Hamamatsu Photonics], a U Plan S Apochromat 40×/0.9 NA objective, and an image resolution of 200 × 200 nm/pixel). The number and intensity of IR-induced nuclear foci were quantified using the ScanR image analysis software (Olympus).

Results

Sustained DDR in MDA-MB-231 after proteasome inhibition.

In mammalian cells, inhibition of the proteasome abrogates the recruitment of multiple DDR players to sites of damage including the 53BP1 protein. However, our observation of persisting 53BP1 foci in the breast cancer cell line MDA-MB-231 after proteasome inhibition followed by gamma irradiation (Fig.1) contradicts this generally believed phenomenon. Firstly, we asked, whether some of upstream 53BP1 regulators is not up- or downregulated in the examined cell line thus affecting 53BP1 recruitment to the DNA damage sites.

We probed the levels of various 53BP1 positive and negative regulators which could affect the IR induced 53BP1 recruitment in the presence of proteasome inhibitor (Fig.2A). MDA-MB-231 protein levels were compared to those of the U2OS cell line, that does not exhibit persisting 53BP1 foci under the described conditions. Within the selected set of proteins there were several variations between the two cell lines. Our attention was drawn mainly by the extreme upregulation of the RNF168 protein in MDA-MB-231 as this E3 ubiquitin ligase is critical for this branch of the DDR (Fig.2B).

Crucial role of RNF168 in persistence of 53BP1 foci upon proteasome inhibition

Since the RNF168 E3 ubiqutin ligase is essential for 53BP1 accumulation at sites of DNA damage, we hypothesized that RNF168 knock down would reduce accumulation of 53BP1 after proteasome inhibition following DNA damage in the MDA MB 231 cell line. Performed siRNA mediated knock-down in MDA-MB-231 cell line using different concentrations of interfered RNA resulted in significant decrease in number of nuclei with 53BP1 foci (Fig.2B). To the same conclusion, and the essential role of RNF168 in this context led us U2OS cell line U2OS GFP RNF168 stable expressing about 10 times higher level of RNF168 (data not shown) restoring the DDR after treatment with MG132 and IR almost to the same level as just in case of DNA damage.

To understand the structural underpinnings of the RNF168 in this process we silenced endogenous RNF168 by siRNA, reintroduced into these cells 2 forms of GFP-tagged (and siRNA-resistant) RNF168, and tested their ability to accumulate at the DSB sites. Wild-type RNF168 in contrast to its variant bearing an inactivating mutation in the catalytic RING domain (*RING), regained the ability to generate ubiquitin conjugates at the DSB site and restored studied phenotype (IRIF 53BP1 foci) after proteasome inhibition.

Overall, we conclude from these results that execution of the DSB-induced chromatin response and retention of repair protein 53BP1 under condition of ubiquitin starvation is dependent on the catalytic activity and level of E3 ligase RNF168.

Level of E3 and E2 affects DNA damage response in proteasome inhibitor treated cancer cell line

To independently test our hypothesis about the emerging epistatic effect of RNF168 level on 53BP1 DSB association after loss of free ubiquitin we checked the described phenotype in several cancer cell lines in comparison to level of RNF168 as well as its upstream interplayers E3 RNF8 and E2 Ubc13 meassured by Western blotting (Fig. 3A, 3B). Our results indicate strong correlation between RNF168 upregulation and counted 53BP1comprised nuclei, with an additive role of its upstream enzymes. These data are consistent with a model in which Ubc13, RNF8 and RNF168 operate on a shared pathway that facilitates ubiquitination-dependent recruitment of DDR factors to DSB.

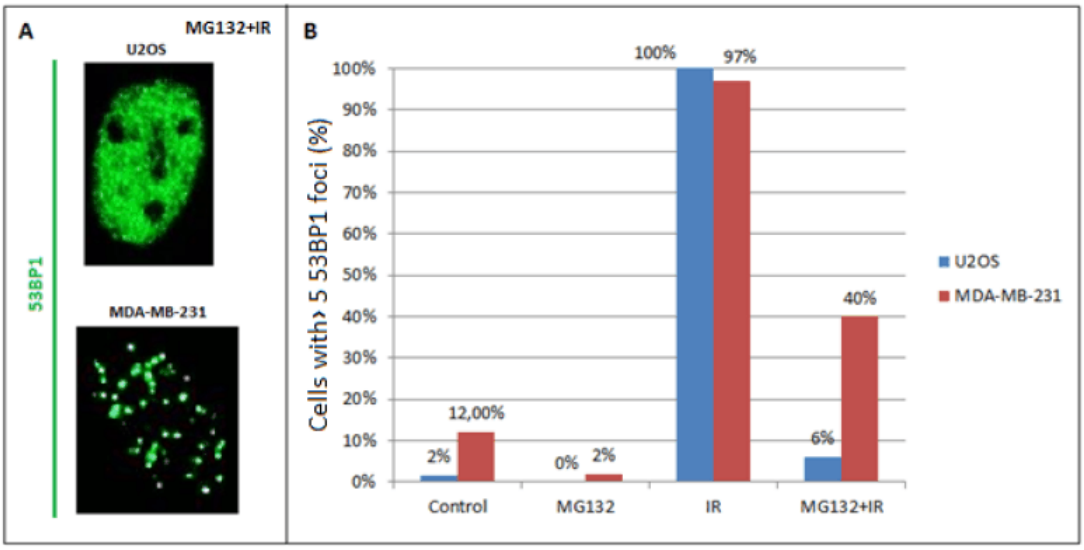

Figure 1. Persistence of 53BP1 foci in MDA-MB-231 after proteasome inhibition followed by induction of DNA damage. A) U2OS and MDA-MB-231 cells were treated with 5 μM MG132 2h before irradiation with 2 Gy and 1h later stained with 53BP1 antibody. Scale bar 10 μM. B) Quantification of images from (A). Cells with >5 53BP1 foci were counted. At least 200 cells were scored in each experiment.

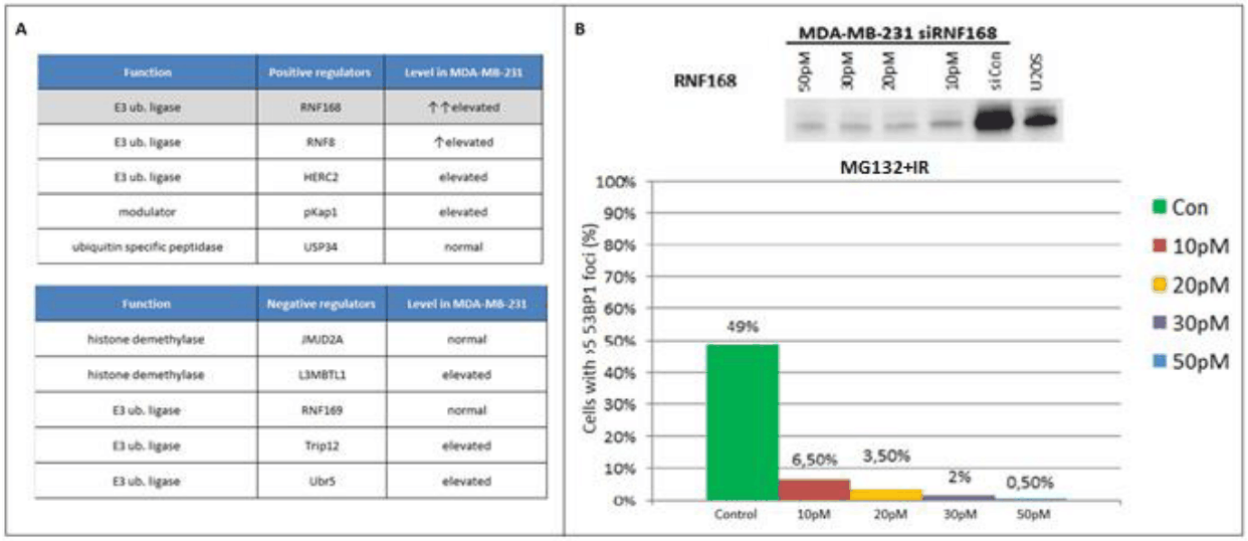

Function	Positive regulators	Level in MDA-MB-231
E3 ub. ligase	RNF168	↑↑elevated
E3 ub. ligase	RNF8	↑elevated
E3 ub. ligase	HERC2	elevated
modulator	pKap1	elevated
ubiquitin specific peptidase	USP34	normal

Function	Negative regulators	Level in MDA-MB-231
histone demethylase	JMJD2A	normal
histone demethylase	L3MBTL1	elevated
E3 ub. ligase	RNF169	normal
E3 ub. ligase	Trip12	elevated
E3 ub. ligase	Ubr5	elevated

Figure 2. A) Level of 53BP1 recruitment regulators in MDA-MB231 compared to U2OS. B) Knock-down of RNF 168 using different concentrations of siRNA impairs cellular response to DSB in MDA-MB-23. Cell lysates were analyzed by immunoblot.

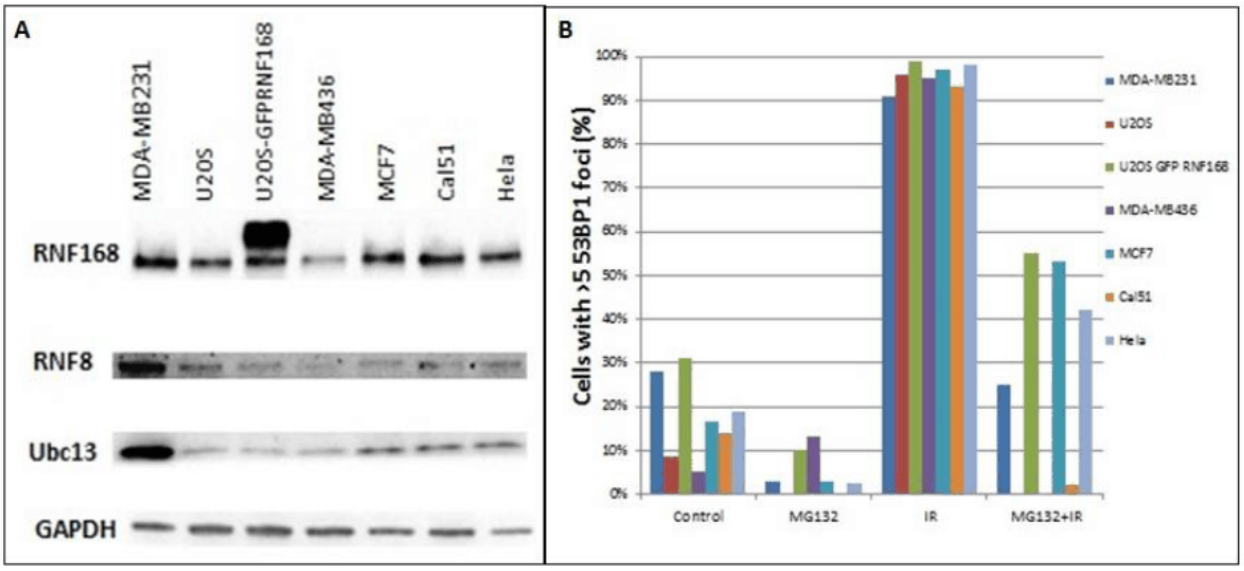

Figure 3. Level of E3 and E2 enzymes affects DNA damage response in proteasome inhibitor treated cancer cell lines A) Quantification of RNF168, RNF8 and Ubc13 protein level from total cell extracts by immunobloting. B) Indicated cells were treated with 5 μM MG132 2h before irradiation with 2 Gy and 1h later stained with 53BP1 antibody. Scale bar 10 μM. Cells with >5 53BP1 foci were counted. At least 200 cells were scored in each experiment.

Discussion

53BP1 is recruited to sites of damage via interaction of its tandem Tudor domains with methylated histones, in particular the H4K20me2. In addition, it is known, that the recruitment of 53BP1 also requires action of two E3 ubiquitin ligases- RNF8 and RNF168, raising a question of how a ubiquitin ligase promotes the accumulation of a methylated histone binding protein at sites of DNA damage. Current models of 53BP1 recruitment to DSB sites propose that 53BP1 is a bivalent histone reader

recognizing mononucleosomes containing dimethylated H4K20 (H4K20me2) and H2A ubiquitinated on the Lys15 (H2AK15ub), the latter being the product of RNF168 action on chromatin [6].
There are several possible scenarios in which RNF168 may promote 53BP1 DSB association even under conditions of ubiquitin starvation. First, it is possible that ubiquitin ligation in response to DNA damage is not completely perturbed and RN168 still monoubiquitinates H2AK15 thus forming efficient docking site for 53BP1. We think that elevated number of RNF168 molecules may efficiently compete for residual ubiquitin pool (after proteasome inhibition) and perform H2AK15 monoubiquitination sufficient for 53BP1 recruitment (provided that the H4K20 modification is present at the site of damage). This hypothesis could be verified in an experiment where effect of 53BP UDR (Ubiquitination dependent recruitment motif) mutant expression on the number of 53BP1 IRIFs in irradiated and proteasome inhibitor treated cells is examined. In a complementary experiment, one may transiently express GFP-tagged ubiquitin in the target proteasome inhibitor treated cells. Labelled Ub co-localisation with γH2AX at DNA damage sites following γ-irradiation would confirm the presence of the ubH2AK15 platform required for the 53BP1 DSB association.
In the second scenario, ubiquitin might be replaced by ubiquitin-like protein NEDD8 thus bypassing the proteasome inhibition induced ubiquitin starvation. NEDD8 bears an 80% homology with ubiquitin and was shown to be involved in certain pathways of DNA damage signalling [7]. Moreover, it has been shown that under accute Ub starvation ubiquitin-like molecules may also take over the canonical roles of Ub. Under such circumstances, ubiquitin ligases were shown to be capable of utilizing the NEDD8 ubiquitin like molecule [8]. Consequently, upon proteasome inhibition and subsequent Ub starvation, NEDD8 might become a substrate for the E2-E3 ligases involved in the 53BP1 recruitment and replace Ub in this pathway. Nevertheless, experiments using MLN4924, a novel inhibitor of NAE (NEDD8 activating enzyme), in combination with a proteasome inhibitor MG132 did not alter the 53BP1 persistence phenotype in MDA-MB-231 after gamma irradiation (data not shown) thus ruling out the possibility that NEDD8 mimicks Ub in DDR upon Ub starvation. This result was further corroborated by combined treatment with MG132 and PYR41, an inhibitor of the E1 ubiquitin activating enzyme UBA1 that is common for both ubiquitinylation and neddylation pathways. The treatment also did not abolish 53BP1 DSB accumulation indicating that NEDD8 is not involved in this phenotype (data not shown).
Intriguingly, under the same experimental setup, depletion of enzymes TRIP12 and UBR5 previously reported to control RNF168 accumulation, showed increased number of 53BP1 IRIF in MDA-MB-231, U2OS GFP RNF168 and some foci emerging in U2OS cell line. Gudjonsson et al. found, depletion of these two HECT domain ubiquitin E3 ligases allows accumulation of RNF168 to supraphysiological levels, followed by massive spreading of ubiquitin conjugates and hyperaccumulation of ubiquitin-regulated genome caretakers such as 53BP1 and BRCA1 [9]. However, in their hands, depletion of free ubiquitin by MG132 treatment (10μM) abrogated 53BP1 focus formation 1 hour after IR in U2OS cell line irrespective of TRIP12/UBR5 depletion, suggesting TRIP12, UBR5 control RNF168 turnover through direct/indirect interaction with the proteolytic machinery! This contradiction in our results may be due to lower dose of MG132 used in our case, allowing persistence of some residual ubiquitin which can be still utilized by the abundant RNF168 molecules in absence of TRIP12 and UBR5 for establishment of the ubH2AK15 53BP1 docking site.
Overall, our results suggest that in the presence of elevated levels of the RNF168 ligase, recruitment of 53BP1 and its retention at DNA damage sites is less sensitive to quantity of free ubiquitin molecules than previously thought.

References

[1] Jackson SP, Bartek J. The DNA-damage response in human biology and disease. Nature. 2009; 461:1071-8.
[2] Lukas J, Lukas C, Bartek J. More than just a focus: The chromatin response to DNA damage and its role in genome integrity maintenance. Nat Cell Biol 2011; 13:1161-9.
[3] Delacote F. and Lopez B.S. Importance of the cell cycle phase for the choice of the appropriate DSB repair pathway, for genome stability maintenance: the trans-S double-strand break repair model. Cell Cycle 2007; 7:33-38.
[4] Moynahan M.E., Chiu J.W., Koller B.H., Jasin M. Brca1 controls homologous/directed DNA repair. Mol. Cell 1999; 4: 511-518.
[5] Dantuma NP, Groothuis TA, Salomons FA, Neefjes J. A dynamic ubiquitin equilibrium couples proteasomal activity to chromatin remodeling. J Cell Biol 2006; 173: 19-26.
[6] Fradet-Turcotte A, Canny MD, Escribano-Díaz C, Orthwein A, Leung CC, Huang H, Landry MC, Kitevski-LeBlanc J, Noordermeer SM, Sicheri F, Durocher D. 53BP1 is a reader of the DNA-damage-induced H2A Lys 15 ubiquitin mark. Nature 2013; 499:50-4.
[7] Huang D.T., Miller D.W., Mathew R., Cassel R., Holton J.M., Roussel M.F., Schulman B.A. A unique E1/E2 interaction recquired for optimal conjugation of the ubiquitin-like protein NEDD8. Nat. Struct. Mol. Biol. 2004; 11: 927-935.
[8] Duda D.M., Borg L.A., Scott D.C. Hunt H.W., Hammel M., Schulman B.A. Structural insight into NEDD8 activation of cullin-RING ligases: conformational control of conjugation. Cell 2008; 134: 995-1006.
[9] Gudjonsson T., Altmeyer M., Savic V., Toledo L., Dinant C. et al. TRIP12 and UBR5 suppress spreading of chromatin ubiquitylation at damaged chromosomes. Cell 2012; 150(4):697-709.

15.3 APPENDIX C

L Beresova, E Vesela, I Chamrád, J Voller, M Yamada, T Furst, R Lenobel, **K Chroma**, J Gursky, K Krizova, M Mistrik, and J Bartek, Role of DNA repair factor XPC in response to replication stress, revealed by DNA fragile site affinity chromatography and quantitative proteomics. J. Proteome Res. 2016 October 30., IF (2016): 4.173

Journal of proteome research

Article

pubs.acs.org/jpr

Role of DNA Repair Factor Xeroderma Pigmentosum Protein Group C in Response to Replication Stress As Revealed by DNA Fragile Site Affinity Chromatography and Quantitative Proteomics

Lucie Beresova,[†,‡] Eva Vesela,[†] Ivo Chamrad,[‡] Jiri Voller,[†] Masayuki Yamada,[†] Tomas Furst,[†] Rene Lenobel,[‡] Katarina Chroma,[†] Jan Gursky,[†] Katerina Krizova,[†] Martin Mistrik,*[,†] and Jiri Bartek*[,†,§,∥]

[†]Institute of Molecular and Translational Medicine, Faculty of Medicine and Dentistry, Palacky University, Olomouc, Czech Republic

[‡]Department of Protein Biochemistry and Proteomics, Centre of the Region Hana for Biotechnological and Agricultural Research, Faculty of Science, Palacky University, Olomouc, Czech Republic

[§]Danish Cancer Society Research Center, Copenhagen, Denmark

[∥]Science for Life Laboratory, Division of Translational Medicine and Chemical Biology, Department of Biochemistry and Biophysics, Karolinska Institute, Stockholm, Sweden

Supporting Information

ABSTRACT: Replication stress (RS) fuels genomic instability and cancer development and may contribute to aging, raising the need to identify factors involved in cellular responses to such stress. Here, we present a strategy for identification of factors affecting the maintenance of common fragile sites (CFSs), which are genomic loci that are particularly sensitive to RS and suffer from increased breakage and rearrangements in tumors. A DNA probe designed to match the high flexibility island sequence typical for the commonly expressed CFS (FRA16D) was used as specific DNA affinity bait. Proteins significantly enriched at the FRA16D fragment under normal and replication stress conditions were identified using stable isotope labeling of amino acids in cell culture-based quantitative mass spectrometry. The identified proteins interacting with the FRA16D fragment included some known CFS stabilizers, thereby validating this screening approach. Among the hits from our screen so far not implicated in CFS maintenance, we chose Xeroderma pigmentosum protein group C (XPC) for further characterization. XPC is a key factor in the DNA repair pathway known as global genomic nucleotide excision repair (GG-NER), a mechanism whose several components were enriched at the FRA16D fragment in our screen. Functional experiments revealed defective checkpoint signaling and escape of DNA replication intermediates into mitosis and the next generation of XPC-depleted cells exposed to RS. Overall, our results provide insights into an unexpected biological role of XPC in response to replication stress and document the power of proteomics-based screening strategies to elucidate mechanisms of pathophysiological significance.

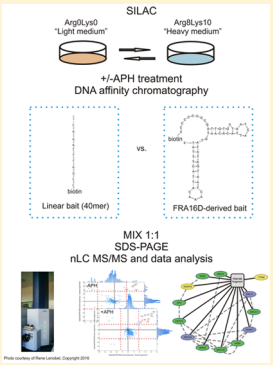

KEYWORDS: *DNA affinity chromatography, SILAC proteomics, common fragile sites, replication stress, FRA16D, mitosis, 53BP1 bodies, γH2AX, DNA damage response, Xeroderma pigmentosum complementation group C (XPC) protein*

INTRODUCTION

Common fragile sites (CFSs) are defined as a nonrandom distribution of breaks, gaps, and constrictions visible on metaphase chromosomes, especially under conditions of replication stress.[1] These sites are conserved among diverse mammalian species[2] and have been intensively studied mainly owing to their association with chromosomal aberrations (deletions, translocations, amplifications) that are found in many types of cancer[3] and may play a causative role in tumorigenesis.[4]

The molecular basis of CFS-associated chromosomal instability has been partially explained through structural analyses. Many CFSs contain AT-rich stretches that form highly flexible sequence islands. The common feature of all these atypical sequences is the formation of unusual secondary DNA structures that have been shown to compromise DNA replication in vitro.[5,6] Furthermore, an increased occurrence of replication fork collapse and DNA double strand break (DSB) formation in the flexible islands were reported for a yeast model with artificially introduced human CFS, FRA16D, upon replication stress.[7] An additional explanation for CFSs' instability may reflect frequent collisions between DNA replication and transcription machinery due to very large genes located in some of the CFSs.[8]

Aphidicolin (APH), an inhibitor of DNA polymerases α and ε is the most potent inducer of the majority of known CFSs and is used at a concentration that slows but does not arrest replication fork progression.[9,10] Such a RS scenario induces long stretches of single-stranded DNA as a consequence of the inhibited DNA polymerases lagging behind the advancing DNA helicase during DNA replication.[11] The cellular response to RS

Received: July 4, 2016
Published: October 30, 2016

DOI: 10.1021/acs.jproteome.6b00622
J. Proteome Res. 2016, 15, 4505−4517

and stabilization of CFSs involves multiple cellular factors as also documented by spontaneous expression of CFSs in cells from patients with genetic instability disorders such as Seckel syndrome.[12] Furthermore, genetic models based on experimental knock-down of checkpoint and/or DNA repair proteins like ATR or Chk1 kinases,[13,14] BRCA1,[15] FANCD2,[16] SMC1,[17] WRN,[18] and MSH2[19] show enhanced APH-induced CFS expression. Importantly, oncogenic stress evoked by mutated RAS,[20] Cyclin E, and E2F[21] overexpression leads to CFS-associated instability and deletions, and rearrangements in CFS areas are often detected in human premalignant lesions and xenografts experiencing high oncogenic activity.[22−24]

The roles of the aforementioned factors in the protection against fragility of CFSs were mostly discovered using methods of visual detection of chromosomal breaks and gaps on mitotic spreads. Several reports also utilized chromatin immunoprecipitation followed by quantitative PCR that allowed the detection of the studied protein at the CFS sequences.[25,26] Nevertheless, an unbiased proteome-wide screening for identification of new protein candidates that could contribute to CFS maintenance has not been reported.

As shown recently, quantitative mass spectrometry in combination with nucleic acid-based affinity chromatography is a powerful tool for proteome-wide screens of specific DNA and RNA binding proteins pointing to new protein candidates for deeper functional characterization.[27−29] In this regard, stable isotope labeling of amino acids in cell culture (SILAC) appears to be a method of choice that is straightforward, minimizes chances of bias caused by sample processing errors, and allows simple distinguishing of specific interactors from background binding proteins.[30,31] Here, we present a new strategy combining DNA-affinity chromatography with SILAC and mass spectrometry to isolate potential CFS protein interactors. Besides the advantages mentioned above, SILAC allowed us not only to identify CFS binding factors but also to distinguish between those bound under normal unperturbed cell growth and those enriched under conditions of APH-evoked replication stress. The results obtained with our combinatorial screening approach and functional characterization of XPC as a surprising new factor involved in CFS stability and overall cellular response to RS are presented below.

MATERIALS AND EXPERIMENTAL PROCEDURES

Chemicals

All chemicals used in this study were of analytical grade and purchased from Sigma-Aldrich unless stated otherwise.

Cell Culture

In this study, the following human cell types were used: cervical cancer cell line (HeLa S3; ATCC), normal diploid fibroblast strain (TIG3, ATCC), and osteosarcoma cell line (U-2 OS; ATCC).

For the SILAC screen, HeLa S3 cells were grown in RPMI 1640 medium with omitted lysine and arginine (Biowest) supplemented with 10% dialyzed fetal bovine serum and 1% penicillin/streptomycin solution. For quantitative SILAC-based MS analysis, the RPMI 1640 medium was supplemented separately with L-arginine and L-lysine (Arg^0, Lys^0) or L-[U-$^{13}C^6$, $^{15}N^4$]arginine, L-[U- $^{13}C^6$, $^{15}N^2$]lysine (Arg^{10}, Lys^8) (Cambridge Isotope Laboratories,Inc.). After five cellular doublings, the success rate of protein labeling was verified by in-solution digestion and a shotgun LC−MS/MS analysis.

The other cell types were cultured in Dulbecco's modified Eagle's medium (Invitrogen) supplemented with 10% fetal bovine serum and 1% penicillin/streptomycin. The doxycycline-inducible shRNA ATR knockdown model in the U-2 OS cell line was characterized previously.[32]

Affinity Ligands and Immobilization on Chromatography Media

As an affinity ligand mimicking CFS, an oligonucleotide with the sequence (5′-3′) CCC CCC CCC GAT TGT GAT AAT CAT TAC ACA ATG TAT ATA GTA ATC AAA TCA TTA CTT TAT was used. With the exception of the first nine cytosines that served as a linker, the sequence corresponds to a part of the common fragile site FRA16D.[7] The ability of the sequence to form the same secondary structures as the corresponding part of FRA16D was tested in the Mfold program.[33] Default parameters were modified to reflect our experimental conditions (150 mM Cl^-, 1 mM Mg^{2+}, 4 °C).

As a second ligand, a control oligonucleotide with linear structure, oligonucleotide (5′-3′) CAA ATT TTA GCC AGT CAT CCC ATA GTA TCG TCC GTT CAA G, was used. The oligonucleotide should not be able to form stable secondary structure and was designed in silico as follows.

One million random 40-mers were generated and T_m (melting temperature) of the most stable secondary structure was calculated in MFold (settings same as above). Five percent of sequences with the lowest T_m were selected, and all of the 20 bp subsequences were extracted. Another set of 40-mers was created by concatenation of random pairs from this pool. For avoiding the creation of oligonucleotides deprived of certain nucleotides or dominated by repetitions, sequences with the lowest variability (expressed as entropy) at the level of mono-, di-, tri-, and tetranucleotides were removed. After 20 rounds of this "selection" and "recombination", 100 40-mers with the lowest T_m together with their reverse sequences were selected for closer inspection. Sequences predicted to interact with single strand binding transcription factors by Transcription Element Search System web service[34] were removed. Final selection took into consideration the following parameters: T_m of the most stable structure, number of structures predicted by MFold, and sequence variability. The selected 40-mer is not able to form any structure with negative ΔG, and the corresponding T_m are lower than −47 °C.

Both oligonucleotide sequences were custom synthesized and modified with biotin at the 5′ end (Generi Biotech). Affinity beads were prepared by immobilization of the oligonucleotides to streptavidin-covered magnetic beads (Chemicell) according to the manufacturer's instructions. Briefly, SIMAG-streptavidin beads (1 mg) were washed three times with 1 mL of citrate buffer (150 mM NaCl, 15 mM trisodium citrate, pH 7.0) and resuspended in 0.5 mL of citrate buffer. Then, 200 pmol of the specific oligonucleotide was added, and immobilization was performed at room temperature under slow rotation of the beads in 15 min. Unbound oligonucleotides were removed by washing of affinity beads with three volumes of the citrate buffer. Before use, the prepared affinity beads were finally equilibrated to a starting condition for DNA affinity chromatography with 1 mL of a binding buffer (25 mM HEPES with 150 mM $NaCl_2$, 1 mM $MgCl_2$, pH 7.5) at 4 °C under slow rotation for 15 min.

DOI: 10.1021/acs.jproteome.6b00622
J. Proteome Res. 2016, 15, 4505−4517

Preparation of Cell Lysate and DNA Affinity Chromatography

Two differently labeled HeLa S3 cell populations, marked as light and heavy, were both cultivated with or without the presence of APH for induction of replication stress. In the first experiment, the light and heavy labeled cell populations were cultured under normal growth conditions and subsequently used in the SILAC comparative analysis of specific CFS binding proteins enriched by DNA affinity chromatography on the FRA16D fragment and control beads covered by the linear oligonucleotide. In the second experiment, both labeled cell populations were exposed to 0.4 μM APH for 24 h before harvesting and also employed for the isolation of specific CFS binding proteins in the same way as in the first experiment.

Briefly, HeLa S3 cells, light and heavy, were harvested, and the cellular pellets were resuspended in a buffer from a NEPPER nuclear and cytoplasmatic extraction kit (Thermo Scientific) for isolation of nuclear proteins. The concentrations of isolated nuclear proteins were determined by Bradford protein assay (Biorad) with BSA as a standard. Equal amounts of nuclear proteins (1 mg) isolated from light and heavy cell populations were mixed with 1 mL of the binding buffer and incubated with affinity beads containing either the FRA16D fragment or a control linear sequence. The association of the nuclear proteins with oligonucleotide beads was performed at 4 °C under continuous slow vertical rotation for 1 h. After the interaction of the proteins with oligonucleotide baits, the unbound proteins were removed by washing of the beads with 1 mL of the binding buffer (repeated five times). The retained proteins were eluted from the beads directly by the addition of 25 μL of SDS-PAGE sample buffer and boiling at 95 °C with continuous shaking for 10 min. The eluates were carefully removed from the beads and mixed 1:1. All affinity experiments were performed in two independent biological replicates. In one replicate, the FRA16D fragment was incubated with the heavy labeled nuclear proteins, and to the beads with control linear sequence, the light labeled nuclear proteins were added. In the second replicate, the labeled protein extracts added to the resins were swapped. The same SILAC comparative experiment with beads covered by the FRA16D fragment and control linear sequence was carried out with both HeLa S3 cell populations exposed to 0.4 μM APH for 24 h. This experiment was repeated in two independent biological replicates with swapping of the labeled nuclear proteins added to the affinity beads as well.

Protein Separation and Digestion

Proteins retained and eluted from both oligonucleotide affinity beads (FRA16D fragment sequence vs linear control sequence) were mixed in a 1:1 ratio, separated on 4−16% BIS-TRIS SDS-PAGE gradient gels (Biorad), and stained with colloidal Coomassie Blue. Each sample line was divided into 13 fractions, which were further cut into small pieces. Then, proteins were destained, reduced with DDT, and subsequently alkylated with iodacetamide and digested with rafinose-modified trypsin overnight.[35,36] The released peptides were extracted from the gel pieces with 5% formic acid in 30% acetonitrile (v/v) and purified using C18 StageTips.[37]

Nanoflow Liquid Chromatography Mass Spectrometry

The desalted peptides were analyzed by nanoflow liquid chromatography (nanoEASY-nLC System; Thermo Fisher Scientific) coupled to a UHR-Q-TOF maXis instrument equipped with online nanoESI source (Bruker Daltoniks). Peptides loaded on a precolumn (2 cm × 75 μm packed with ReproSil-Pur C18-AQ 5 μm resin) were eluted and separated on an analytical column with a multistep gradient at a flow rate of 200 nL/min for 185 min. The gradient was created by mixing of 0.4% (v/v) formic acid (solvent phase A) and 0.4% formic acid in 80% acetonitrile (v/v) (Table S-1). The analytical column was prepared in a 15 cm fused silica emitter with an inner diameter of 75 μm (New Objective) packed in-house with reverse phase ReproSil-Pur C18-AQ 3 μm resin (Dr. Maisch GmbH). The MS instrument was operated in data-dependent acquisition mode using the top five precursors with charge states $\geq$ 2. The selected precursors were fragmented with the use of collision-induced dissociation. The fragmented precursors were dynamically excluded for 18 s. Detailed settings of the MS analyzer are described in the Supporting Information. Each sample was analyzed in two technical replicates.

Data Processing

The collected raw data were processed using the DataAnalysis v 4.2 SP1 software (Bruker Daltonik). The XML files containing precursor and fragmentation data were created and used for consequent bioinformatics analysis. The XML files were uploaded to ProteinScape v 2.1 and searched by Mascot v2.2.07 (in-house server; Matrix Science) against a custom-prepared database containing human proteins downloaded from UniProt (20150107, 89706 seq; www.uniprot.org) supplemented with common contaminants (keratins, trypsin, bovine serum albumin) and reversed sequences of all human proteins for the determination of false discovery rate (FDR). The Mascot search was carried out with the following parameters: MS and MS/MS tolerances were set to ±25 ppm and ±0.05 Da, respectively; protease specificity was set to trypsin, and one missed cleavage was allowed; carbamidomethylation of cysteine was set as a fixed modification, and N-terminal protein acetylation, methionine oxidation, and heavy labeled $^{13}C(6)^{15}N(2)$lysine and $^{13}C(6)^{15}N(4)$arginine were set as a variable modification. Proteins identified by Mascot algorithm were subsequently processed in ProteinScape v2.1 with the following parameters: a minimum of two peptides with a score ≥15 and the FDR at 5% at the protein level were needed to accept protein identification. From the list of identified proteins, only those associated with at least three quantified peptide pairs were considered as quantifiable proteins and used for subsequent bioinformatics analysis.

The relative ratios of quantified proteins identified in both forward and reverse label-swap experiments were normalized by log2 transformation and plotted in a scatter plot. For significant differences in relative protein abundance, the normalized ratios of the proteins were statistically evaluated for their normal distribution, and protein abundance was considered as significantly different ($p < 0.01$) in the case of ratios differing from the mean by 2.58σ as determined from the normalized ratio distributions of the biological replicate analyses.[38] Such proteins, clustered at the right top corner of the scatter plot, represent candidates for FRA16D fragment-specific interactors.

Gene Ontology Annotation Analysis

To determine the significantly enriched gene ontology (GO) molecular function and biological process terms related to FRA16D fragment-associated proteins, ClueGO,[39] a Cytoscape[40] plug-in, was employed. A two-sided minimal-likelihood test on the hypergeometric distribution, an equivalent to the classical Fisher's exact test, was utilized for the enrichment

DOI: 10.1021/acs.jproteome.6b00622
J. Proteome Res. 2016, 15, 4505−4517

analysis with the human genome set as a background gene population. The *p*-values for all enriched GO terms were adjusted with the Benjamini−Hochberg correction method.

Antibodies

For immunoblotting, the following antibodies were used: XPC (Novus Biological, NB100-477, 1:1000), pChK1 (Ser345, Cell Signaling, 2348, 1:500), ChK1 (Santa Cruz, sc-8408, 1:500), GAPDH (GeneTex, GTX30666, 1:2000), and MCM7 (Santa Cruz, sc-65469, 1:100). HRP-conjugated secondary antibodies were as follows: antimouse (GE-Healthcare, NA931 V, 1:1000), antirabbit (GE-Healthcare, NA934 V, 1:1000), and antigoat (Santa Cruz, sc-2020, 1:1000).

For immunofluorescence microscopy, the following primary antibodies were used: ATR (Santa Cruz (N-19) sc-1887, 1:250), ATRIP (Cell Signaling, 2737, 1:250), γH2AX (pSer139, Millipore, 07-146, 1:500), 53BP1 (Santa Cruz, sc-22760, 1:500), Cyclin A (Leica, NCL-cyclinA, 1:200), and pH3 (pSer10, Millipore, 06-570, 1:1000). Secondary antimouse and antirabbit antibodies were Alexa Fluor 488 (A11001) and Alexa Fluor 568 (A11036) (Invitrogen, 1:1000).

Immunoblotting

For the analysis of checkpoint response, the same amounts of cells were resuspended in the SDS-PAGE sample buffer and incubated at 95 °C for 8 min with shaking (1400 rpm). The samples were resolved by SDS-PAGE (4−15% gradient) (Biorad) and subsequently transferred to a nitrocellulose membrane for immunoblotting detection by specific antibodies.

Gene Silencing

siGenome Human XPC (7508) siRNA SMART pool was purchased from Dharmacon (Cat. No. M-016040-01-0010), and transfection was conducted using siRNA MAX (Invitrogen) following the manufacturer's instructions. As a control siRNA, GGCUACGUCCAGGAGCGCACC from Eurofin MWG operon or siGenome RISC FREE control siRNA from Dharmacon (Cat. No. D-001220-01-05) were used. Both control siRNAs were tested to exclude cytotoxicity using the colony formation assay.

Biochemical Analysis of XPC Ubiquitination upon APH Treatment

U-2 OS were transfected with siXPC pool or control siRNA. Two days after the transfection, the cells were treated with 0.4 μM aphidicolin for 24 h and subjected to lysis or biochemical cell fractionation and then analyzed by immunoblotting as previously described.[41] The primary antibody used in this study was against XPC (Novus Biological, NB100-477).

Fluorescence Microscopy

Immunofluorescence Detection of DDR Factors. The transfected cells were seeded in 24 well plates and treated with 0.4 μM APH or 0.5% DMSO 24 h before fixation. The cells were either fixed directly with 10% formalin, followed by 5 min permeabilization with 0.5% TritonX (staining for 53BP1, cyclin A), or fixed after pre-extraction (ATR, ATRIP). Samples were stained with primary antibodies at 4 °C overnight and then with secondary antibodies at room temperature for 1 h and incubated with Hoechst 33342 at room temperature for 5 min before mounting. Images were automatically recorded using an inverted fluorescence microscope BX71 (Olympus) and ScanR Acquisition software (Olympus), analyzed with ScanR Analysis software (Olympus), and evaluated with Statistica software (StatSoft). On the basis of DNA cyclin A staining, the cell population was gated to G1 (cyclin A negative cells). Number of foci or signal intensity of respective markers was counted. Each experiment was performed with at least three biological replicates.

Immunofluorescence Analysis of Mitotic Cells. The transfected cells were seeded in a 24-well plate and treated with either 0.4 μM APH or 0.5% DMSO for 24 h. After treatment, the cells were fixed with 10% formalin, permeabilized by 0.5% Triton X, and stained for the specific markers. Images were taken using an inverted fluorescent microscope (Zeiss Observer Z.1, 63× oil objective). The plates were placed onto the sliding table of the microscope and automatically scanned. On the basis of phospho-H3 marker positivity, approximately 150 mitotic cells were chosen and subsequently scanned for phospho-H2AX (γH2AX) foci. γH2AX foci were analyzed in custom-made software implemented in MatLab. Each experiment was performed with at least three biological replicates.

Flow Cytometry Analysis of pH3-Positive Cells

The transfected cells were seeded on 6 cm diameter Petri dish and treated with 0.2 μM APH, 0.4 μM APH, or 0.5% DMSO 24 h before fixation with 100 ng/mL of nocodazole added 6 h before fixation. The cells were trypsinized, fixed with cold (4 °C) 10% formalin for 15 min at RT, and permeabilized with 0.5% Triton X for 5 min. Samples were stained with the primary antibody against pH3 for 1 h at RT and then with the secondary antibody for 1 h. Cells were centrifuged and resuspended in PBS + 2% FBS with 0.5 μg/mL of DAPI. Samples were analyzed with the BD FACSVerse flow cytometer, and pH3-positive cells were gated as indicated in Figure S-4.

RESULTS AND DISCUSSION

Experimental Strategy for the Identification of Potential CFS Interactors

The main goal of this work was to identify candidate CFS binding proteins and provide further insight into the biological function of selected hits. To perform the first unbiased proteome screen that would allow the detection of proteins bound to the structurally specific CFS sequence, we designed and performed DNA affinity chromatography[28] in combination with SILAC-based quantitative proteomics[42,43] (Figure 1).

The crucial step of our experimental approach was the DNA affinity chromatography that demanded the design and synthesis of baits suitable for isolation of specific CFS interacting proteins. We based our bait on the concept that CFSs arise as a consequence of specific DNA sequences, which under replication stress create stable secondary structures that are difficult to replicate. Thus, we used a fragment mimicking the high-flexibility island within the well-characterized CFS, FRA16D,[7] as the specific DNA bait. The ability of this sequence to form the hard-to-replicate secondary structure under our experimental conditions was verified in the Mfold program,[33] (for the final form, see Figure S-1). For distinguishing the candidate-specific CFS interactors from common DNA binding proteins, control bait with linear structure was designed and employed in parallel. Moreover, the nucleotide order was selected in a way to avoid resemblance with known promoters (for further details on control bait construction, see the Experimental Procedures). Both baits were modified at the 5′ end by adding biotin to facilitate their immobilization to streptavidin-covered magnetic beads. To identify FRA16D

DOI: 10.1021/acs.jproteome.6b00622
J. Proteome Res. 2016, 15, 4505−4517

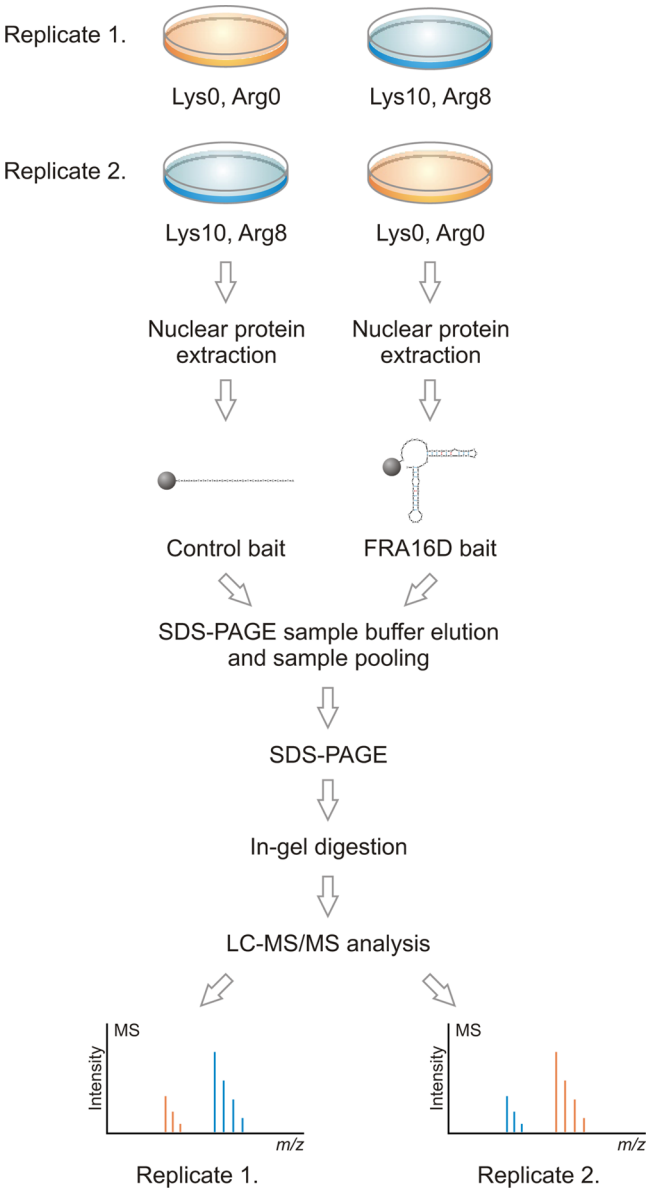

Figure 1. Experimental strategy for identification and quantification of specific FRA16D fragment interactors. Cells were grown in the SILAC "heavy" and "light" medium. The extracts of nuclear proteins were added to the resins covered by a specific FRA16D fragment as a bait and control linear sequence. After the affinity purification step, the eluates were mixed 1:1, separated by SDS-PAGE, and in-gel digested. Resulting peptide mixtures were analyzed by LC−MS/MS. The workflow was performed with cells cultured under normal conditions and also upon 0.4 μM APH for 24 h.

fragment binding proteins, we used the following experimental strategy.

First, we performed an experiment to obtain a list of nuclear proteins interacting with the FRA16D fragment-specific bait from lysates of HeLa S3 cells grown under normal conditions. In the next experiment, the HeLa S3 cells were exposed to replication stress induced by 0.4 μM APH, a concentration of the drug that reliably induces CFS expression.[9,10] Importantly, a comparison of FRA16D fragment interactors from cells under normal versus replication stress conditions revealed multiple interacting proteins (Figure 2), some of which have not yet been associated with CFS biology.

Analysis of CFS-Enriched Proteins

Using a stringent threshold for FDR at less than 5%, we identified in total 655 and 282 proteins binding to the FRA16D bait in APH-treated and control cells, respectively. Protein ratios for FRA16D fragment-specific versus control bait beads could be assessed for at least 559 and 228 proteins from the above two groups, of which 410 and 150 were detected in independent biological replicates. As documented by scatter plots of $\log_2$ transformed ratios (Figure 2), 13 distinct proteins appeared to specifically and robustly interact with the FRA16D fragment but not with the control bait.

Among these 13 selected hits, two and eight proteins were bound to FRA16D exclusively under normal and APH-induced stress conditions, respectively, and three proteins interacted with FRA16D under both conditions (Figure 3). A validation in the form of a proof of principle for our screen was provided by the following two results. First, examination of the GO annotations of the candidate CFS binders revealed a high enrichment of proteins involved in binding to various DNA structures and proteins implicated in mechanisms responsible for genome maintenance (Figure 4A and B). This is in agreement with the use of structured DNA as the specific bait. A second and possibly even more important validation was provided by the fact that our list of 13 hits included Werner helicase (WRN) and mismatch repair protein 2 (MSH2), both proteins previously characterized for their biological functions in the maintenance of CFS stability.[18,19]

According to the Kyoto encyclopedia of genes and genomes (KEGG) enrichment analysis, our 13 selected candidate FRA16D interactors play roles in several DNA repair pathways, including nonhomologous end-joining (NHEJ), mismatch repair (MMR), base excision repair (BER), and nucleotide excision repair (NER) (Figure 4C). The last mentioned, NER, is the pathway that operates anywhere within the genome to eliminate "bulky" DNA lesions.[45] DNA damage-binding protein 1 (DDB1), XPC, and Centrin-2 (CETN2) form the so-called initiation complex of global-genome NER (GG-NER), whereas XRCC1 and LIG3 are involved in sealing nicks or gaps after excision of the nucleotides.[46−49] Our observation that these proteins together accumulate at the FRA16D fragment under replication stress conditions together with their high interconnectivity (Figure 3) may suggest that GG-NER could be involved in resolution of DNA structures that occur within CFS regions under replication stress.

The GG-NER initiation is supported by XPC ubiquitylation, which is promoted by the UV-DDB-ubiquitin ligase complex.[47] This UV-DDB-mediated recognition of DNA damage by XPC is particularly observed in the case of UV-induced cyclobutane pyrimidine dimers and lesions that cause low distortion of DNA helix,[50] whereas direct recognition of (6−4) pyrimidine-pyrimidone photoproducts and some other lesions caused by chemical adducts could be UV-DDB independent. To verify whether the DNA structures created upon APH treatment in CFS loci are recognized through a process that involves XPC ubiquitylation, we performed cell fractionation and assessed the ubiquitylation status of chromatin-bound XPC after APH treatment through the electrophoretic mobility of XPC. In contrast to UV-induced ubiquitylation-mediated electrophoretic mobility shift, XPC did not show such altered mobility upon treatment of cells with APH (Figure S-2), indicating a mechanism distinct from the UV response and potentially direct recognition of these replication barriers by XPC.

DOI: 10.1021/acs.jproteome.6b00622
J. Proteome Res. 2016, 15, 4505−4517

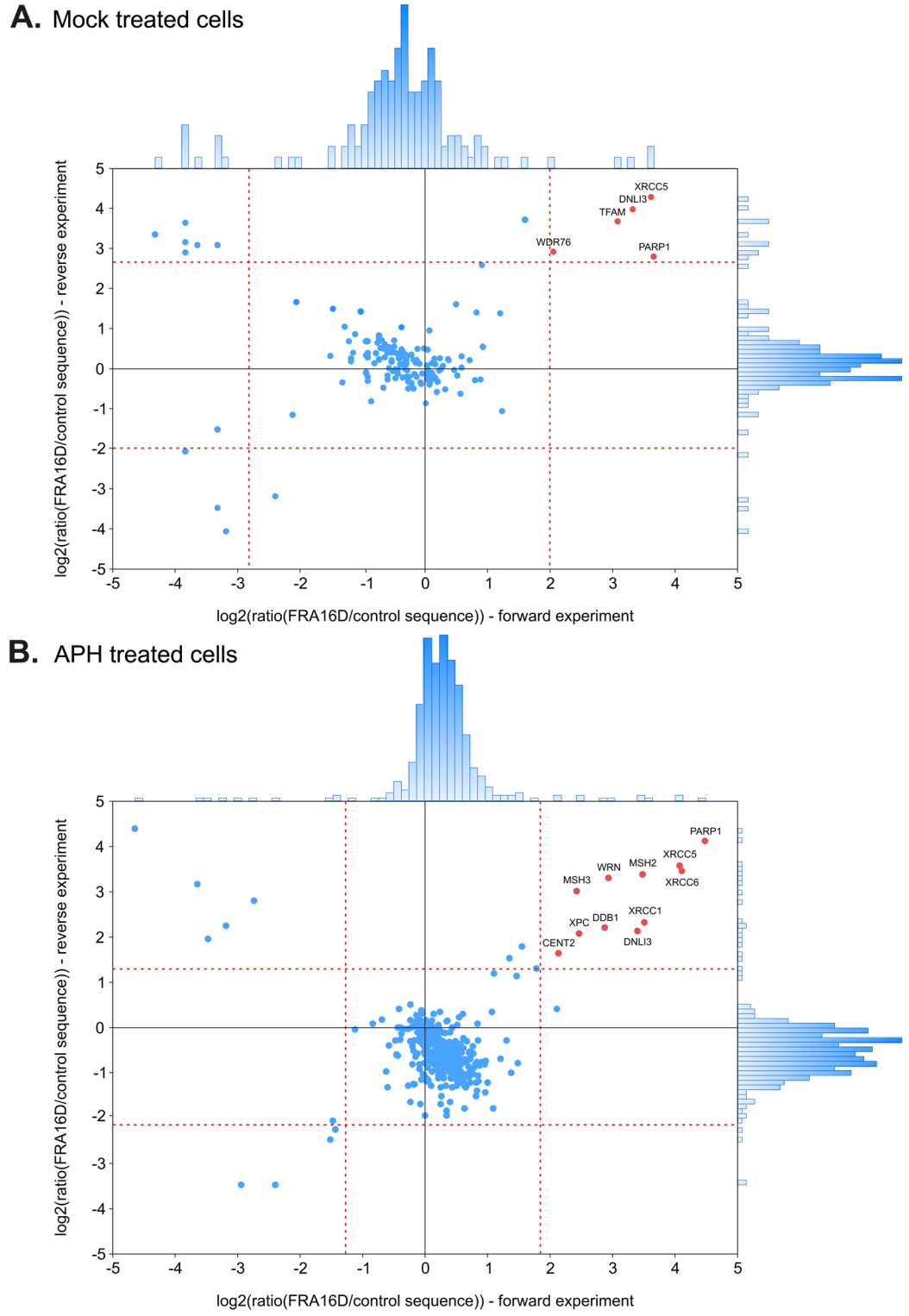

Figure 2. Determination of FRA16D fragment interaction partners. Graphs contain logarithmic ratios from both replicates "forward" H/L and "reverse" L/H plotted against each other. The specific FRA16D fragment interactors are clustered in the upper right corner (red points) because of the high ratio in both replicates of the experiment. Background proteins are centered to the origin with a 1:1 ratio in both replicates, and contaminants are observed in the upper left corner with a high ratio in the light form in both repetitions. (A) Cells cultured under normal conditions. (B) Cells exposed to 0.4 μM APH for 24 h.

Recent studies indicate that XPC is not only the main initiator of NER, but thanks to its substrate versatility, it seems to be a general sensor of aberrant structures such as DNA cross-links and various "DNA bubbles"[51,52] with the potential to be involved in other cellular mechanisms besides NER.[53] It was shown that XPC plays a role in the elimination of oxidative damage by regulating BER,[54,55] in chromatin remodeling and checkpoint response,[56,57] in regulation of transcription,[58] and in the maintenance of telomere stability.[59] On the basis of these emerging reports, we next developed an automated approach to

DOI: 10.1021/acs.jproteome.6b00622
J. Proteome Res. 2016, 15, 4505−4517

Figure 3. FRA16D fragment retained proteins and their mutual interactions. Interaction network for the proteins specifically enriched by the FRA16D fragment under normal and replication stress conditions. The depicted interactions were drawn in Cytoscape software[40] after importing the data from Figure 2 and downloading the protein−protein interactions from the String database.[44]

assess mitotic CFSs and tested the possibility that CFS regions (especially under replication stress) generate some secondary DNA structures that are "sensed" by XPC.

Method for Automated Evaluation of CFS Expression in Mitosis

The involvement of proteins in the maintenance of CFS stability is usually determined by scoring for chromosomal aberrations under unperturbed control and replication stress conditions with the protein of interest either absent (mutant, deleted, or knocked down) or overexpressed. For better resolution of individual CFS regions, Giemsa staining or the FISH method on mitotic spreads is usually used.[14,16,18] A major technical shortcoming associated with such standard approaches is high demand for the quality of mitotic spreads. Furthermore, such evaluations are very time-consuming, and a subset of smaller lesions may remain undetected. For these limitations to be overcome, a more precise method for the detection of phosphorylated histone H2AX (γH2AX) in mitosis was developed[60] and further optimized in our present project for our purposes (Figure S-5). γH2AX foci are commonly accepted as a marker of DNA double-stranded breaks,[61] and quantification of γH2AX immunofluorescence signal intensity, or rather the number of foci, can be used to estimate the extent of DNA damage or repair kinetics.[62]

Our quantitative method for CFS expression is principally based on the fact that, in APH-treated human lymphoblasts, the 20 most expressed CFSs account for 80% of all detectable mitotic DNA double strand breaks.[1] Because these mitotic breaks are marked by the γH2AX signal (Figure S-5A), the overall quantification of γH2AX foci in mitosis after APH treatment correlates with CFS expression. Our method was further optimized by combined immunofluorescence staining for γH2AX and serine 10-phosphorylated histone H3 (pH3), the latter a recognized marker of mitosis. Such a setup allows for high throughput analysis using automated microscopy-based detection of mitotic cells within the cell population followed by detailed γH2AX foci scoring selectively in the mitotic cells (Figure S-5B). The feasibility of our method for identification of factors involved in CFS stability was validated in a cellular model allowing inducible knockdown of ATR by shRNA. APH treatment resulted in an increase of γ-H2AX in mitotic cells that was strongly augmented after ATR depletion (Figure S-5C), consistent with published data regarding the ATR kinase and its involvement in CFS stability.[13]

XPC Participates in Replication Stress-Induced DNA Damage Response and in the Maintenance of CFS Stability

For testing if XPC plays a role in CFS stability, the human U-2 OS cells depleted of XPC by RNAi-mediated knockdown were treated with 0.4 μM APH for 24 h. The mitotic γH2AX foci were quantified by the automated routine described above. Surprisingly, in an analogous experiment as with ATR knockdown, XPC deficiency caused a significant decrease in the number of γH2AX foci after APH treatment (Figure 5A,B). This observation has two possible explanations. Either the depletion of XPC leads to such a prominent form of CFS-associated instability that the G2/M checkpoint blocks such cells from mitotic entry or the CFS-associated aberrant DNA structures are sensed by a cellular mechanism that may involve XPC and that is required for the signaling from such aberrant DNA structures and thereby for generation of the ensuing enhanced γH2AX signal. To address this intriguing observation further, we also compared the number of γH2AX foci in XPC-

DOI: 10.1021/acs.jproteome.6b00622
J. Proteome Res. 2016, 15, 4505−4517

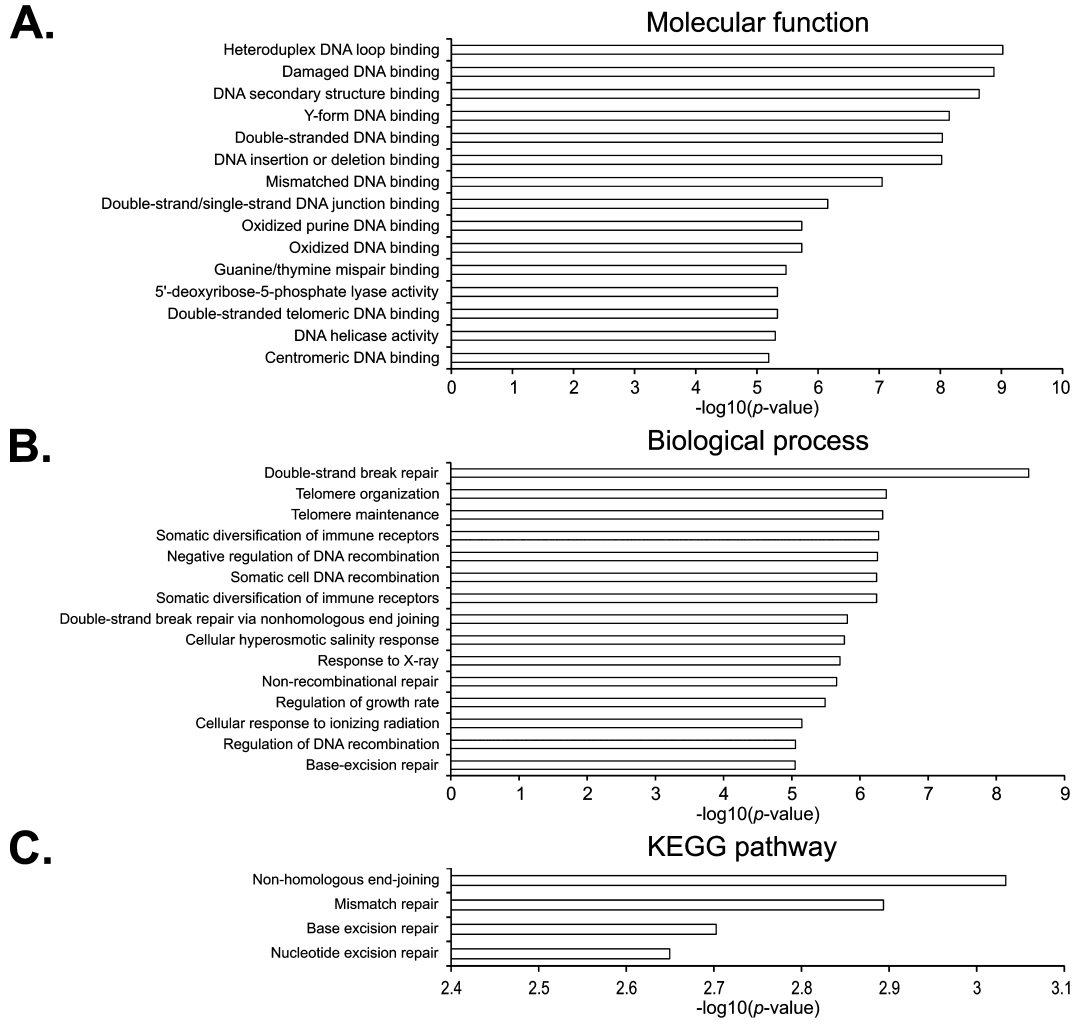

Figure 4. Gene ontology annotation enrichment analysis of identified FRA16D fragment interaction partners. Most significantly enriched terms of identified interaction proteins reveal structured DNA affinity, DNA damage signaling, and repair signatures as depicted in the graphs. (A) Molecular functions, (B) biological functions, and (C) significantly enriched KEGG pathways with significance expressed as −log10 of the respective *p* values.

depleted and ATR/XPC codepleted U-2 OS mitotic cells after APH treatment. XPC depletion resulted in decreased γH2AX foci in mitotic cells compared to that in control mock-depleted cells (Figure S-6). In addition, depletion of XPC in cells codepleted for ATR further decreased the number of γH2AX foci in mitotic cells compared to cells depleted of ATR alone (Figure S-6).

Given that ATR is the major checkpoint kinase whose signaling ensures arrest of cells with damaged DNA at the G2/M boundary,[63] we argued that the observed decrease or loss of mitotic γH2AX signaling might reflect a previously unrecognized positive role of XPC in promoting checkpoint signaling within CFSs. On the basis of our results with mitotic γH2AX, we suggest the possibility that XPC may bind to stalled replication forks to initiate incision of the DNA structures, which are difficult to replicate, such as the high-flexibility islands within CFSs. The XPC-driven incision process could then initiate and/or contribute to activation of the DDR signaling and create structures marked by γH2AX foci in mitosis. Thus, in the absence of XPC, at least a fraction of stalled replication forks are not turned into such "visible" lesions, leading to insufficient checkpoint response documented here by the impaired γH2AX signal. Provided that this proposed scenario is correct, XPC-deficient cells exposed to replication stress should accumulate unresolved replication fork intermediates, particularly in the vulnerable genomic loci in the vicinity of CFSs. Importantly, ineffective checkpoint signaling due to XPC depletion would make such cells largely unreceptive ("blind") to the accumulating aberrant and potentially hazardous structures at CFSs and allow entry into mitosis despite the danger of breaking the chromosomes.

To test if such unresolved abnormal replication intermediates are indeed present and transferred through mitosis to the next cell generation, we scored the so-called 53BP1 bodies in G1 cells, a commonly recognized feature of cells undergoing enhanced replication stress in the previous cell cycle.[64] Mechanistically, unresolved aberrant underreplicated loci that escape into mitosis may result in DNA double strand breaks during mitosis and then were recognized and stabilized in early postmitotic daughter cells by 53BP1 and related proteins, forming the microscopically recognizable G1 53BP1 bodies.[64]

Indeed, quantification of 53BP1 bodies in G1 cells in our experiments revealed a significant increase in the XPC-depleted cells upon 0.4 μM APH treatment, a result which is fully in line with the above hypothesis (Figure 5C,D).

On the basis of the obtained data, we conclude that XPC participates in detection and/or resolution of replication

DOI: 10.1021/acs.jproteome.6b00622
J. Proteome Res. 2016, 15, 4505−4517

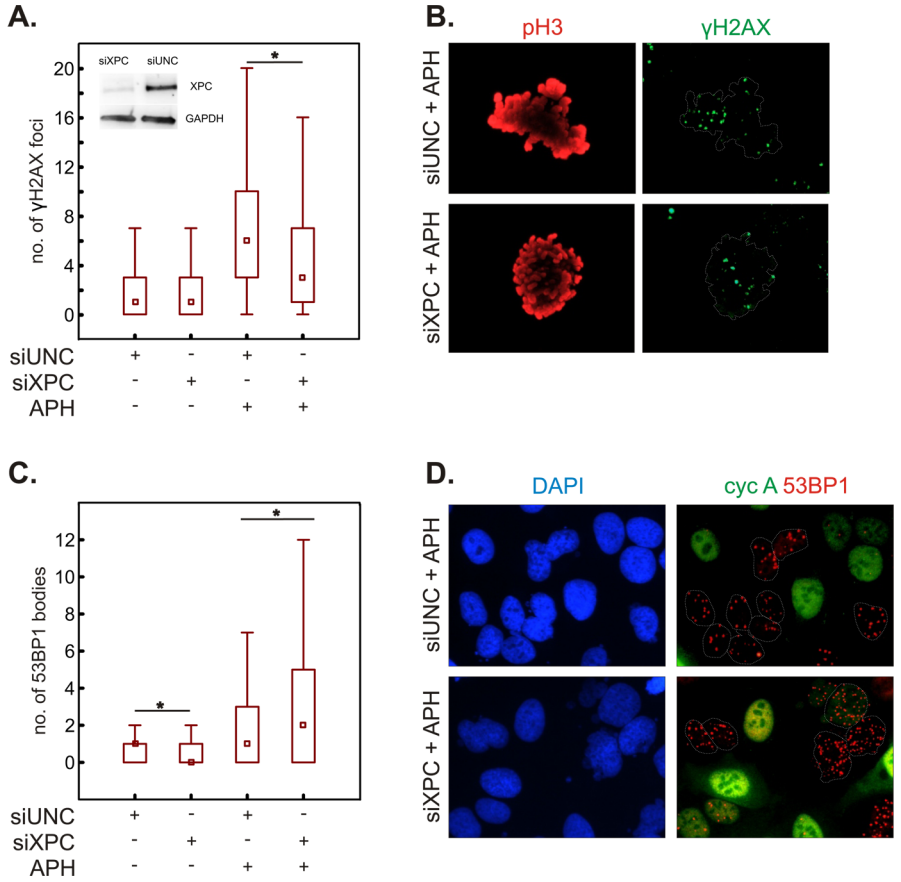

Figure 5. Analysis of DNA damage in XPC-depleted cells. Replication stress-induced DNA damage signaling is significantly altered in XPC-silenced cells. (A) Immunofluorescence detection shows a significant decrease of γH2AX foci signal in XPC-depleted mitotic cells. (B) Illustrative pictures depicting the evaluation based on pH3 immunostaining of mitotic cells and γH2AX foci. (C) Immunofluorescence detection shows a significant increase in G1 phase-associated 53BP1 bodies in XPC-depleted cells. (D) Illustrative pictures depicting the evaluation based on immunostaining of the S-G2 marker (Cyclin A) and 53BP1 bodies. Only cells negative for Cyclin A (encircled) were analyzed. The asterisks mean significance with a *p*-value < 0.05.

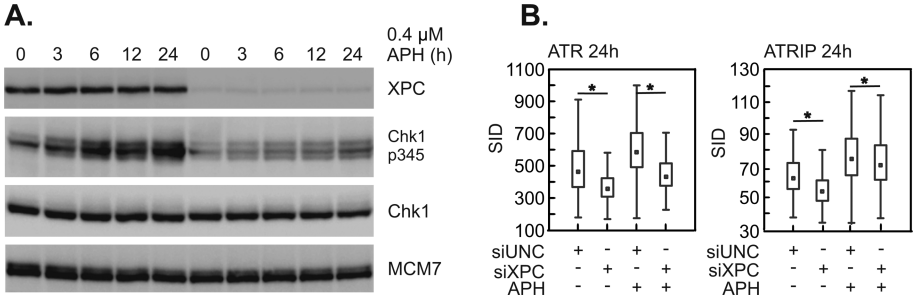

Figure 6. ATR-promoted checkpoint signaling is altered in XPC-depleted cells. (A) Western blot-based analysis of impaired phosphorylation of direct ATR target Chk1 in XPC-silenced cells. Cells were treated by APH and harvested at various time points. MCM7 served as a loading control. (B) Microscopy-based quantification of ATR and ATRIP recruitment to the chromatin shows a significant decrease in XPC-silenced cells under normal conditions and also after APH-induced replication stress.

barriers arising at CFS regions and promotes checkpoint activation.

XPC Influences Checkpoint Response after Replication Stress

To assess whether XPC depletion indeed influences checkpoint signaling after APH-induced replication stress, we tested phosphorylation of Chk1, the key ATR substrate and effector kinase promoting G2/M checkpoint arrest.[63] Consistent with our conceptual predictions, knockdown of XPC in two human cancer cell lines (U-2 OS, HeLa S3) and a diploid fibroblast strain (TIG-3) resulted in a prominent negative impact on Chk1 phosphorylation at early time points after treatment with 0.4 μM APH (Figure 6A and Figure S-3). In addition, the mitotic indices in such experiments, measured as the accumulation of nocodazole-arrested pH3 positive mitotic cells, were shifted toward unscheduled mitotic entry, pointing at impaired checkpoint function in the XPC-depleted cells (Figure S-4A,B). XPC-depleted U-2 OS cells treated with APH also showed elevated numbers of 53BP1 bodies in G1 phase after aberrant mitotic progression. Similarly, XPC-depleted

DOI: 10.1021/acs.jproteome.6b00622
J. Proteome Res. 2016, 15, 4505−4517

APH-treated TIG3 and Hela S3 cells did not show a prominent elevation of G1 53BP1 bodies, suggesting that this type of readout is not manifested in all cell lines, probably due to rapid elimination of the damaged cells (data not shown). As the ATR-Chk1 cascade represents a major checkpoint signaling "unit", we also performed quantitative immunofluorescence microscopy analysis of chromatin-bound ATR and its partner ATRIP. The chromatin-bound signal of both proteins was decreased in XPC-depleted cells (Figure 6B). How XPC promotes binding of the ATR/ATRIP complex to chromatin remains elusive, but it is known that the binding of ATR is a necessary prerequisite for subsequent ATR-dependent checkpoint activation,[63] thereby providing a plausible explanation for the impaired Chk1 phosphorylation detected in our experiments with XPC-depleted cells under replication stress.

Altogether, the data set obtained in our present study supports the idea of the XPC/ATR-Chk1 pathway interaction in response to replication stress and their functional link in promoting activation of checkpoint signaling. Notably, a broadly analogous function of XPC was described for the lesions induced by UV radiation where cells depleted for XPC displayed impaired ATR activation and phosphorylation of its downstream target Chk1.[57] On the other hand, signaling of UV-induced lesions reportedly relied on XPC during G1 phase but not during S phase.[65] Our data in response to APH on the other hand demonstrate an S-phase relevant ATR/Chk1-promoting role of XPC in checkpoint signaling, most likely reflecting the different nature of the APH-induced relative to UV-induced DNA lesions as well as the differential requirement for XPC ubiquitylation, which are important mechanistic differences demonstrated in our present study. In terms of the impact on DNA, APH generates long stretches of single-stranded DNA by uncoupling of DNA polymerases and helicases, thereby creating vulnerable secondary structures, especially at CFSs that become the substrate for XPC and possibly GG-NER. Upon UV irradiation, on the other hand, DNA cross-links are formed and rapidly processed either by translesion synthesis[66] or converted into DNA double-strand breaks.[67]

Overall, we propose that, in the absence of XPC, the replication problems that occur at CFSs are not properly recognized and/or processed during the S phase and become the source of subsequent genomic instability. Last but not least, our results also illustrate the power of innovative high-throughput screens based on quantitative proteomics and hypothesis-driven strategies to identify new components of fundamental mechanisms, such as cellular stress responses and maintenance of genomic integrity.

CONCLUSIONS

In this study, we performed the first unbiased proteome-wide screen to identify new putative proteins responsible for maintenance of CFS stability. Besides previously characterized WRN and MSH2 proteins, we also identified several additional candidates whose role in CFS maintenance warrants deeper characterization. Because of the fact that almost half of the identified proteins are implicated in NER, the XPC protein as the main initiator of the NER pathway was chosen for a follow-up functional study.

On the basis of our results, we propose a hypothesis for the role of XPC in preventing CFS expression by promoting checkpoint signaling under replication stress. We show that XPC deficient cells are incapable of proper checkpoint activation in response to RS, leading to increased genomic instability manifested as accumulation of specific DNA lesions marked by 53BP1 bodies in G1 cells. We further suggest that this phenotype may reflect a new role for XPC, or possibly the whole GG-NER repair pathway, in sensing aberrant replication structures and providing the incision step, a role that is particularly required at hard-to-replicate structures in CFS loci formed after RS. Thus, XPC deficiency leads to impaired CFS-associated signaling through the ATR/ATRIP-Chk1 axis, thereby allowing for inappropriate passage of cells with aberrant structures associated with stalled replication forks through mitosis. The fate of such damaged cells depends on the respective genetic background and fitness of cellular DDR. In the next cell generation of U-2 OS cells passing through the unscheduled mitosis, such aberrant DNA structures can be detected as DNA double strand breaks marked by focal accumulation of 53BP1 in the form of the 53BP1 bodies. In some other cell lines, represented here by HeLa S3 or TIG-3 cells, this aberrant scenario during the methaphase/anaphase transition and/or immediately after mitosis of APH-exposed cells is "solved" by elimination of such abnormal cells through apoptosis. This is consistent with the notion that CFSs are important sites of the genome that may serve as alarm sensors for elimination of cells with unstable genetic material arising upon replication stress. Through this mechanism, CFSs may contribute to the intrinsic cellular barrier against tumorigenesis.[68]

Apart from this important biological insight into the function of XPC protein and its relevance for chromosomal (in)stability and cancer, we also document that the strategy of using DNA structure-specific baits, which can be successfully combined with quantitative proteomics, can generate a wealth of results valuable for contemporary biomedicine.

ASSOCIATED CONTENT

Supporting Information

The Supporting Information is available free of charge on the ACS Publications website at DOI: 10.1021/acs.jproteome.6b00622.

Final structure of specific FRA16D fragment bait, verification of XPC ubiquitination upon APH, 53BP1 bodies in G1 cells, checkpoint response and MI of TIG-3, HeLa XPC KD cells, illustration of automated evaluation of γH2AX foci in mitosis, detection of γH2AX in XPC-silenced U-2 OS shATR mitotic cells, and description of MS analyzer settings and gradient for peptide separation during LC−MS/MS (PDF)

Quantification of FRA16D interactors with APH treatment with a comparison of normal vs reverse experiment (XLSX)

Quantification of FRA16D interactors with MOCK treatment with a comparison of normal vs reverse experiment (XLSX)

Detailed protein report of APH treatment normal experiment (PDF)

Detailed protein report of APH treatment reverse experiment. (PDF)

Detailed protein report of MOCK treatment normal experiment (PDF)

Detailed protein report of MOCK treatment reverse experiment (PDF)

DOI: 10.1021/acs.jproteome.6b00622
J. Proteome Res. 2016, 15, 4505−4517

Summary of complete protein identification and quantification MS data (XLSX)

AUTHOR INFORMATION

Corresponding Authors

*E-mail: martin.mistrik@upol.cz.
*E-mail: jb@cancer.dk.

Notes

The authors declare no competing financial interest.

ACKNOWLEDGMENTS

We would like to thank our colleagues Juraj Kramara for discussion of experiments and Iva Protivankova for assistance with western blot analyses. L.B., I.C., and R.L. were supported by grant LO1204 from the National Program of Sustainability I, MEYS. M.M. and J.B. were supported by the Kellner Family Foundation. L.B. and E.V. were supported by the internal grant IGA-LF-2016-030. J.B. was supported by the Danish Council for Independent Research (DFF-1331-00262B), the Novo Nordisk Foundation (grant 16584), and the Swedish Research Council. M.M., J.B. and M.Y. were supported by the Grant Agency of the Czech Republic 13-17555S and the Norwegian Financial Mechanism CZ09 (Project PHOSCAN 7F14061); E.V., M.M, J.B., T.F., J.G., K.C., and J.V. were supported by the grant LO1304 from the National Program of Sustainability I, MEYS. M.M. was supported by Czech-BioImaging project (LM2015062 funded by MEYS, CR). K.K. was supported by the Endowment Fund of Palacky University.

ABBREVIATIONS

APH, aphidicolin; BER, base excision repair; CFS, common fragile site; DDR, DNA damage response; DSB, double-stranded break; FDR, false discovery rate; GG-NER, global genome nucleotide excision repair; GO, gene ontology; KEGG, Kyoto encyclopedia of genes and genomes; pH3, mitotically phosphorylated histone H3; RS, replication stress; SILAC, stable isotope labeling of amino acids in cell culture; MMR, mismatch repair; NER, nucleotide excision repair; NHEJ, nonhomologous end joining; γH2AX, phosphohistone H2AX

REFERENCES

(1) Glover, T. W.; Berger, C.; Coyle, J.; Echo, B. DNA polymerase alpha inhibition by aphidicolin induces gaps and breaks at common fragile sites in human chromosomes. *Hum. Genet.* **1984**, *67*, 136−142.

(2) Ruiz-Herrera, A.; Ponsá, M.; Gargcía, F.; Egozcue, J.; García, M. Fragile sites in human and Macaca fascicularis chromosomes are breakpoints in chromosome evolution. *Chromosome Res.* **2002**, *10*, 33−44.

(3) Arlt, M. F.; Durkin, S. G.; Ragland, R. L.; Glover, T. W. Common fragile sites as targets for chromosome rearrangements. *DNA Repair* **2006**, *5*, 1126−1135.

(4) Durkin, S. G.; Ragland, R. L.; Arlt, M. F.; Mulle, J. G.; Warren, S. T.; Glover, T. W. Replication stress induces tumor-like microdeletions in FHIT/FRA3B. *Proc. Natl. Acad. Sci. U. S. A.* **2008**, *105*, 246−251.

(5) Schwartz, M.; Zlotorynski, E.; Kerem, B. The molecular basis of rare and common fragile sites. *Cancer Lett.* **2006**, *232*, 13−26.

(6) Zlotorynski, E.; Rahat, A.; Skaug, J.; Ben-Porat, N.; Ozeri, E.; Hershberg, R.; Levi, A.; Scherer, S. W.; Margalit, H.; Kerem, B. Molecular basis of expression of common and rare fragile sites. *Mol. Cell. Biol.* **2003**, *23*, 7143−7151.

(7) Zhang, H.; Freudenreich, C. H. An AT-Rich sequence in human common fragile site FRA16D causes fork stalling and chromosome breakage in *S. cerevisiae*. *Mol. Cell* **2007**, *27*, 367−379.

(8) Helmrich, A.; Ballarino, M.; Tora, L. Collisions between replication and transcription complexes cause common fragile site instability at the longest human genes. *Mol. Cell* **2011**, *44*, 966−977.

(9) Cheng, C. H.; Kuchta, R. D. DNA polymerase ε: Aphidicolin inhibition and the relationship between polymerase and exonuclease activity. *Biochemistry* **1993**, *32*, 8568−8574.

(10) Mrasek, K.; Schoder, C.; Teichmann, A. C.; Behr, K.; Franze, B.; Wilhelm, K.; Blaurock, N.; Claussen, U.; Liehr, T.; Weise, A. Global screening and extended nomenclature for 230 aphidicolin inducible fragile sites, including 61 yet unreported ones. *Int. J. Oncol.* **2010**, *36*, 929−940.

(11) Chang, D. J.; Lupardus, P. J.; Cimprich, K. A. Monoubiquitination of proliferating cell nuclear antigen induced by stalled replication requires uncoupling of DNA polymerase and mini-chromosome maintenance helicase activities. *J. Biol. Chem.* **2006**, *281*, 32081−32088.

(12) Casper, A. M.; Durkin, S. G.; Arlt, M. F.; Glover, T. W. Chromosomal instability at common fragile sites in Seckel Syndrome. *Am. J. Hum. Genet.* **2004**, *75*, 654−660.

(13) Casper, A. M.; Nghiem, P.; Arlt, M. F.; Glover, T. W. ATR regulates fragile site stability. *Cell* **2002**, *111*, 779−789.

(14) Durkin, S. G.; Arlt, M. F.; Howlett, N. G.; Glover, T. W. Depletion of Chk1, but not Chk2, induces chromosomal instability and breaks at common fragile sites. *Oncogene* **2006**, *25*, 4381−4388.

(15) Arlt, M. F.; Xu, B.; Durkin, S. G.; Casper, A. M.; Kastan, M. B.; Glover, T. W BRCA1 is required for common fragile site stability via its G2/M checkpoint function. *Mol. Cell. Biol.* **2004**, *24*, 6701−6709.

(16) Howlett, N. G.; Taniquchi, T.; Durkin, S. G.; D'Andrea, A. D.; Glover, T. W. The Fanconi anemia pathway is required for the DNA replication stress response and for the regulation of common fragile site stability. *Hum. Mol. Genet.* **2005**, *14*, 693−701.

(17) Musio, A.; Montagna, C.; Mariani, T.; Tilenni, M.; Focarelli, M. L.; Brait, L.; Indino, E.; Benedetti, P. A.; Chessa, L.; Albertini, A.; Ried, T.; Vezzoni, P. SMC1 involvement in fragile site expression. *Hum. Mol. Genet.* **2005**, *14*, 525−533.

(18) Pirzio, L. M.; Pichierri, P.; Bignami, M.; Franchitto, A. Werner syndrome helicase activity is essential in maintaining fragile site stability. *J. Cell Biol.* **2008**, *180*, 305−314.

(19) Turner, B. C.; Ottey, M.; Zimonjic, D. B.; Potoczek, M.; Hauck, W. W.; Pequignot, E.; Keck-Waggoner, C. L.; Sevignani, C.; Aldaz, C. M.; McCue, P. A.; Palazzo, J.; Huebner, K.; Popescu, N. C. The Fragile histidine triad/commn chromosome fragile site 3B locus and repair-deficient cancers. *Cancer Res.* **2002**, *61*, 4054−4060.

(20) Di Micco, R.; Fumagalli, M.; Cicalese, A.; Piccinin, S.; Gasparini, P.; Luise, C.; Schurra, C.; Garre, M.; Nuciforo, P. G.; Bensimon, A.; Maestro, R.; Pelicci, P. G.; d'Adda di Fagagna, F. Oncogene-induced senescence is a DNA damage response triggered by DNA hyper-replication. *Nature* **2006**, *444*, 638−642.

(21) Bester, A. C.; Roniger, M.; Oren, Y. S.; Im, M. M.; Sarni, D.; Chaoat, M.; Bensimon, A.; Zamir, G.; Shewach, D. S.; Kerem, B. Nucleotide deficiency promotes genomic instability in early stage of cancer development. *Cell* **2011**, *145*, 435−446.

(22) Bartkova, J.; Horejsi, Z.; Koed, K.; Kramer, A.; Tort, F.; Zieger, K.; Guldberg, P.; Sehested, M.; Nesland, J. M.; Lukas, C.; Ørntoft, T.; Lukas, J.; Bartek, J. DNA damage response as a candidate anti-cancer barrier in early human tumorigenesis. *Nature* **2005**, *434*, 864−870.

(23) Bartkova, J.; Rezaei, N.; Liontos, M.; Karakaidos, P.; Kletsas, D.; Issaeva, N.; Vassiliou, L. V.; Kolettas, E.; Niforou, K.; Zoumpourlis, V. C.; Takaoka, M.; Nakagawa, H.; Tort, F.; Fugger, K.; Johansson, F.; Sehested, M.; Andersen, C. L.; Dyrskjot, L.; Ørntoft, T.; Lukas, J.; Kittas, C.; Helleday, T.; Halazonetis, T. D.; Bartek, J.; Gorgoulis, V. G. Oncogene-induced senescence is part of the tumorigenesis barrier imposed by DNA damage checkpoints. *Nature* **2006**, *444*, 633−637.

(24) Gorgoulis, V. G.; Vassiliou, L. V.; Karakaidos, P.; Zacharatos, P.; Kotsinas, A.; Liloglou, T.; Venere, M.; Ditullio, R. A., Jr.; Kastrinakis, N. G.; Levy, B.; Kletsas, D.; Yoneta, A.; Herlyn, M.; Kittas, C.; Halazonetis, T. D. Activation of the DNA damage checkpoint and genomic instability in human precancerous lesions. *Nature* **2005**, *434*, 907−913.

DOI: 10.1021/acs.jproteome.6b00622
J. Proteome Res. 2016, 15, 4505−4517

(25) Lu, X.; Parvathaneni, S.; Hara, T.; Lal, A.; Sharma, S. Replication stress induces specific enrichment of RECQ1 at common fragile site FRA3B and FRA16D. *Mol. Cancer* **2013**, *12*, 1−12.
(26) Bergoglio, V.; Boyer, A. S.; Walsh, E.; Naim, V.; Legube, G.; Lee, M. Y.; Rey, L.; Rosselli, F.; Cazaux, C.; Eckert, K. A.; Hoffmann, J. S. DNA synthesis by Pol η promotes fragile site stability by preventing under-replicated DNA in mitosis. *J. Cell Biol.* **2013**, *201*, 395−408.
(27) Butter, F.; Scheibe, M.; Morl, M.; Mann, M. Unbiased RNA-protein interaction screen by quantitative proteomics. *Proc. Natl. Acad. Sci. U. S. A.* **2009**, *106*, 10626−10631.
(28) Mittler, G.; Butter, F.; Mann, M. A SILAC-based DNA protein interaction screen that identifies candidate binding proteins to functional DNA elements. *Genome Res.* **2009**, *19*, 284−293.
(29) Scheibe, M.; Arnoult, N.; Kappei, D.; Buchholz, F.; Decottignies, A.; Butter, F.; Mann, M. Quantitative interaction screen of telomeric repeat-containing RNA reveals novel TERRA regulators. *Genome Res.* **2015**, *23*, 2149−2157.
(30) Trinkle-Mulcahy, L.; Boulon, S.; Lam, Y. W.; Urcia, R.; Boisvert, F. M.; Vandermoere, F.; Morrice, N. A.; Swift, S.; Rothbauer, U.; Leonhardt, H.; Lamond, A. Identifying specific protein interaction partners using quantitative mass spectrometry and bead proteomes. *J. Cell Biol.* **2008**, *183*, 223−239.
(31) Hubner, N. C.; Bird, A. W.; Cox, J.; Splettstoesser, B.; Bandilla, P.; Poser, I.; Hyman, A.; Mann, M. Quantitative proteomics combined with BAC TransgeneOmics reveals in vivo protein interactions. *J. Cell Biol.* **2010**, *189*, 739−754.
(32) Danielsen, J. M. R.; Larsen, D. H.; Schou, K. B.; Freire, R.; Falck, J.; Bartek, J.; Lukas, J. HCLK2 is required for activity of the DNA damage response kinase ATR. *J. Biol. Chem.* **2009**, *284*, 4140−4147.
(33) Zuker, M. Mfold web server for nucleic acid folding and hybridization prediction. *Nucleic Acids Res.* **2003**, *31*, 3406−3415.
(34) Schug, J. Using TESS to predict transcription factor binding sites in DNA sequence. *Curr. Protoc Bioinformatics* **2008**, 1.
(35) Shevchenko, A.; Tomas, H.; Havlis, J.; Olsen, J. V.; Mann, M. In-gel digestion for mass spectrometric characterization of proteins and proteomes. *Nat. Protoc.* **2006**, *1*, 2856−2860.
(36) Sebela, M.; Stosova, T.; Havlis, J.; Wielsch, N.; Thomas, H.; Zdrahal, Z.; Shevchenko, A. Thermostable trypsin conjugates for high-throughput proteomics: synthesis and performance evaluation. *Proteomics* **2006**, *6*, 2959−2963.
(37) Rappsilber, J.; Mann, M.; Ishihama, Y. Protocol for micro-purification, enrichment, pre-fractionation and storage of peptides for proteomics using StageTips. *Nat. Protoc.* **2007**, *2*, 1896−1906.
(38) Oppermann, F. S.; Gnad, F.; Olsen, J. V.; Hornberger, R.; Greff, Z.; Keri, G.; Mann, M.; Daub, H. Large-scale proteomics analysis of the human kinome. *Mol. Cell. Proteomics* **2009**, *8*, 1751−1764.
(39) Bindea, G.; Mlecnik, B.; Hackl, H.; Charoentong, P.; Tosolini, M.; Kirilovsky, A.; Fridman, W. H.; Pages, F.; Trajanoski, Z.; Galon, J. ClueGO: a Cytoscape plug-in to decipher functionally grouped gene ontology and pathway annotation networks. *Bioinformatics* **2009**, *25*, 1091−1093.
(40) Shannon, P.; Markiel, A.; Ozier, O.; Baliga, N. S.; Wang, J. T.; Ramage, D.; Amin, N.; Schwikowski, B.; Ideker, T. Cytoscape: a software environment for integrated models of biomolecular interaction networks. *Genome Res.* **2003**, *13*, 2498−2504.
(41) Yamada, M.; Watanabe, K.; Mistrik, M.; Vesela, E.; Protivankova, I.; Mailand, N.; Lee, M.; Masai, H.; Lukas, J.; Bartek, J. ATR-Chk1-APC/C^{cdh1}-dependent stabilization of Cdc7-ASK (Dbf4) kinase is required for DNA lesion bypass under replication stress. *Genes Dev.* **2013**, *27*, 2459−2472.
(42) Ong, S. E.; Blagoev, B.; Kratchmarova, I.; Kristensen, D. B.; Steen, H.; Pandey, A.; Mann, M. Stable isotope labeling of amino acids in cell culture, SILAC, as a simple and accurate approach to expression proteomics. *Mol. Cell. Proteomics* **2002**, *1*, 376−386.
(43) Ong, S. E.; Mann, M. A practical recipe for stable isotope labeling by amino acids in cell culture (SILAC). *Nat. Protoc.* **2007**, *1*, 2650−2660.
(44) von Mering, C.; Huynen, M.; Jaeggi, D.; Schmidt, S.; Bork, S.; Snel, B. STRING: a database of predicted functional associations between proteins. *Nucleic acids Res.* **2003**, *31*, 258−261.
(45) Gillet, L. C. J.; Scharer, O. D. Molecular mechanisms of mammalian global genome nucleotide excision repair. *Chem. Rev.* **2006**, *106*, 253−276.
(46) Sugasawa, K.; Ng, J. M. Y; Masutani, Ch.; Iwai, S.; van der Spek, P. J.; Eker, A. P. M.; Hanaoka, F.; Bootsma, D.; Hoeijmakers, J. H. J Xeroderma pigmentosum group C protein complex is the initiator of Global Genome Nucleotide Excision repair. *Mol. Cell* **1998**, *2*, 223−232.
(47) Sugasawa, K.; Okuda, Y.; Saijo, M.; Nishi, R.; Matsuda, N.; Chu, G.; Mori, T.; Iwai, S.; Tanaka, K.; Hanaoka, F. UV-induced ubiquitylation of XPC protein mediated by UV-DDB-ubiquitin ligase complex. *Cell* **2005**, *121*, 387−400.
(48) Nishi, R.; Okuda, Y.; Watanabe, E.; Mori, T.; Iwai, S.; Masutani, C.; Sugasawa, K.; Hanaoka, F. Centrin-2 stimulates nucleotide excision repair by interacting with xeroderma pigmentousum group C protein. *Mol. Cell. Biol.* **2005**, *25*, 5664−5674.
(49) Moser, J.; Kool, H.; Giakzidis, I.; Caldecott, K.; Mullenders, L. H. F.; Fousteri, M. I. Sealing of chromosomal DNA nicks during nucleotide excision repair requires XRCC1 and DNA ligase III alpha in a cell-cycle-specific manner. *Mol. Cell* **2007**, *27*, 311−323.
(50) Fitch, M. E.; Nakajima, S.; Yasui, A.; Ford, J. M. In vivo recruitment of XPC to UV induced cyclobutane pyrimidine dimers by the DDB2 gene product. *J. Biol. Chem.* **2003**, *278*, 46906−46910.
(51) Sugasawa, K.; Shimizu, Y.; Iwai, S.; Hanaoka, F. A molecular mechanism for DNA damage recognition by the xeroderma pigmentosum group C protein complex. *DNA Repair* **2002**, *1*, 95−107.
(52) Krasikova, Y. S.; Rechkunova, N. Y.; Maltseva, E. A.; Anarbaev, R. O.; Pestryakov, P. E.; Sugasawa, K.; Min, J. H.; Lavrik, O. L. Human and yeast DNA damage recognition complexes bind with high affinity DNA structures mimicking in size transcription bubble. *J. Mol. Recognit.* **2013**, *26*, 653−661.
(53) Shell, S. M.; Hawkins, E. K.; Tsai, M. S.; Hlaing, A. S.; Rizzo, C. J.; Chazin, W. J. Xeroderma pigmentosum complementation group C protein (XPC) serves as a general sensor of damaged DNA. *DNA Repair* **2013**, *12*, 947−953.
(54) Melis, J. P. M.; Kuiper, R. V.; Zwart, E.; Robinson, J.; Pennings, J. L. A.; van Oostrom, C. T. M.; Luijten, M.; van Steeg, H. Slow accumulation of mutations in (XPC−/−)mice upon induction of oxidative stress. *DNA Repair* **2013**, *12*, 1081−1086.
(55) D'Errico, M.; Parlanti, E.; Teson, M.; de Jesus, B. M. B.; Degan, P.; Calcagnile, A.; Jaruga, P.; Bjoras, M.; Crescenzi, M.; Pedrini, A. M.; Egly, J. M.; Zambruno, G.; Stefanini, M.; Dizdaroglu, M.; Dogliotti, E. New functions of XPC in the protection of human skin cells from oxidative damage. *EMBO J.* **2006**, *25*, 4305−4315.
(56) Ray, A.; Mir, S. N.; Wani, G.; Zhao, Q.; Battu, A.; Zhu, Q.; Wang, Q. E.; Wani, A. A. Human SNF5/INI1, a component of the human SWI/SNF chromatin remodeling complex, promotes nucleotide excision repair by influencing ATM recruitment and downstream H2AX phosphorylation. *Mol. Cell. Biol.* **2009**, *29*, 6206−6219.
(57) Ray, A.; Milum, K.; Battu, A.; Wani, G.; Wani, A. A. NER initiation factors, DDB2 and XPC, regulate UV radiation response by recruiting ATR and ATM kinases to DNA damage sites. *DNA Repair* **2013**, *12*, 273−283.
(58) Le May, N.; Mota-Fernandes, D.; Velez-Cruz, R.; Iltis, I.; Biard, D.; Egly, J. M. NER factors are recruited to active promoters and facilitate chromatin modification for transcription in the absence of exogenous genotoxic attack. *Mol. Cell* **2010**, *38*, 54−66.
(59) Stout, G. J.; Blasco, M. A. Telomere length and telomerase activity impact the UV sensitivity syndrome xeroderma pigmentosum C. *Cancer Res.* **2013**, *73*, 1844−1854.
(60) Loffler, H.; Fechter, A.; Matuszewska, M.; Saffrich, R.; Mistrik, M.; Marhold, J.; Hornung, C.; Westermann, F.; Bartek, J.; Kramer, A. Cep63 recruits Cdk1 to the centrosome: Implications for regulation of mitotic entry, centrosome amplification and genome maintenance. *Cancer Res.* **2011**, *71*, 2129−2139.

DOI: 10.1021/acs.jproteome.6b00622
J. Proteome Res. 2016, 15, 4505−4517

(61) Rogakou, E. P.; Pilch, D. R.; Orr, A. H.; Ivanova, V. S.; Bonner, W. M. DNA double-stranded breaks induce histone H2AX phosphorylation on Serine 139. *J. Biol. Chem.* **1998**, *273*, 5858−5868.
(62) Ibuki, Y.; Shikata, M.; Toyooka, T. γH2AX is a sensitive marker of DNA damage induced by metabolically activated 4-(methylnitrosamino)-1-(3-pyridyl)-1-butanone. *Toxicol. In Vitro* **2015**, *29*, 1831−1838.
(63) Liu, Q. H.; Guntuku, S.; Cui, X. S.; Matsuoka, S.; Cortez, D.; Tamai, K.; Luo, G. B.; Carattini-Rivera, S.; DeMayo, F.; Bradley, A.; Donehower, L. A.; Elledge, S. J. Chk1 is an essential kinase that is regulated by ATR and required for the G(2)/M DNA damage checkpoint. *Genes Dev.* **2000**, *14*, 1448−1459.
(64) Lukas, C.; Savic, V.; Bekker-Jensen, S.; Doil, C.; Neumann, B.; Pedersen, R. S.; Grøfte, M.; Chan, K. L.; Hickson, I. D.; Bartek, J.; Lukas, J. 53BP1 nuclear bodies form around DNA lesions generated by mitotic transmission of chromosomes under replication stress. *Nat. Cell Biol.* **2011**, *13*, 243−253.
(65) Ray, A.; Blevins, Ch.; Wani, G.; Wani, A. A. ATR- and ATM-mediated DNA damage response is dependent on excision repair assembly during G but not in S phase of cell cycle. *PLoS One* **2016**, *11*, e0159344.
(66) Shachar, S.; Ziv, O.; Avkin, S.; Adar, S.; Wittschieben, J.; Reißner, T.; Chaney, S.; Friedberg, E. C.; Wang, Z.; Carell, T.; Geacintov, N.; Livneh, Z. Two-polymerase mechanisms dictate error-free and error-prone translesion DNA synthesis in mammals. *EMBO J.* **2009**, *28*, 383−393.
(67) Elvers, I.; Johansson, F.; Groth, P.; Erixon, K.; Helleday, T. UV stalled replication fork restart by re-priming in human fibroblasts. *Nucleic Acids Res.* **2011**, *39*, 7049−7057.
(68) Georgakilas, A. G.; Tsantoulis, P.; Kotsinas, A.; Michalopoulos, I.; Townsend, P.; Gorgoulis, V. G. Are common fragile sites merely structural domains or highly organized functional units susceptible to oncogenic stress? *Cell. Mol. Life Sci.* **2014**, *71*, 4519−4544.

DOI: 10.1021/acs.jproteome.6b00622
J. Proteome Res. 2016, 15, 4505−4517

15.4 APPENDIX D

E Vesela, **K Chroma**, Z Turi, M Mistrik. Common Chemical Inductors of Replication Stress: Focus on Cell-Based Studies. Biomolecules 2017 February 21., IF not defined yet

biomolecules

MDPI

Review

Common Chemical Inductors of Replication Stress: Focus on Cell-Based Studies

Eva Vesela [1,2], Katarina Chroma [1], Zsofia Turi [1] and Martin Mistrik [1,*]

[1] Institute of Molecular and Translational Medicine, Faculty of Medicine and Dentistry, Palacky University, Hnevotinska 5, Olomouc 779 00, Czech Republic; eva.vesela@upol.cz (E.V.); katarina.chroma@upol.cz (K.C.); zsofia.turi01@upol.cz (Z.T.)

[2] MRC Laboratory for Molecular Cell Biology, University College London, London WC1E 6BT, UK

* Correspondence: martin.mistrik@upol.cz; Tel.: +420-585-634-170

Academic Editor: Rob de Bruin

Received: 25 November 2016; Accepted: 10 February 2017; Published: 21 February 2017

Abstract: DNA replication is a highly demanding process regarding the energy and material supply and must be precisely regulated, involving multiple cellular feedbacks. The slowing down or stalling of DNA synthesis and/or replication forks is referred to as replication stress (RS). Owing to the complexity and requirements of replication, a plethora of factors may interfere and challenge the genome stability, cell survival or affect the whole organism. This review outlines chemical compounds that are known inducers of RS and commonly used in laboratory research. These compounds act on replication by direct interaction with DNA causing DNA crosslinks and bulky lesions (cisplatin), chemical interference with the metabolism of deoxyribonucleotide triphosphates (hydroxyurea), direct inhibition of the activity of replicative DNA polymerases (aphidicolin) and interference with enzymes dealing with topological DNA stress (camptothecin, etoposide). As a variety of mechanisms can induce RS, the responses of mammalian cells also vary. Here, we review the activity and mechanism of action of these compounds based on recent knowledge, accompanied by examples of induced phenotypes, cellular readouts and commonly used doses.

Keywords: replication stress; cisplatin; aphidicolin; hydroxyurea; camptothecin; etoposide; cancer

1. Introduction

The DNA molecule always has to keep the middle ground: it must be sufficiently rigid to maintain correct genetic information while at the same time available for ongoing processes. DNA is particularly vulnerable to insults during replication, a process where a copy of the genome is generated [1]. Replication must be tightly regulated because it is essential for genome integrity, and therefore the fate of a new cellular generation. Accurate coordination of several cellular pathways is needed to provide sufficient energy and material supply, precise timing and functional repair to overcome arising difficulties [1].

Transient slowing or disruption of replication fork (RF) progression is called replication stress (RS), which can be caused by a limitation of important factors and/or obstacles caused by intrinsic and extrinsic sources [2]. Intrinsic sources of RS involve the physiological properties of the DNA molecule, such as regions of heterochromatin structure, origin-poor regions or sites rich in some types of repetitive sequences [3–5]. Other intrinsic sources of RS are generated by deregulated pathways that cause over- and under-replication [6–8], re-replication (also known as re-duplication) [9,10], or by transcription and replication machinery collisions [9].

The most common extrinsic sources of RS are all wavelengths of ultraviolet radiation (UV) [11], ionising radiation (IR) [12] and special genotoxic chemical compounds [13] which are the main focus of this review. RS-inducing chemicals can cause a broad spectrum of DNA lesions. Alkylating

agents such as methyl-methane sulfonate (MMS) [14], temozolomide and dacarbazine [15] directly modify DNA by attaching an alkyl group that presents an obstacle to RF progression. Moreover, the bifunctional alkylating compounds (e.g., mustard gas) can cause the crosslinking of guanine nucleobases [16,17] that violate the DNA structure even further [18]. Typical crosslinking agents introduce covalent bonds between nucleotides located on the same strand (intrastrand crosslinks), like cisplatin, or opposite strands (interstrand crosslink), like mitomycin C, and psoralens [18]. Crosslinks make the strands unable to uncoil and/or separate and physically block RF progression [19]. Even a small amount of unrepaired crosslinks (approx. 100–500) is reported to be lethal to a mammalian cell [20]. Furthermore, single-strand DNA breaks (SSB) and double-strand DNA breaks (DSB) represent a specific problem for ongoing replication which is well manifested by increased sensitivity of replicating cells towards radiomimetic compounds (e.g., neocarzinostatin) [21]. Other compounds do not damage the DNA structure directly but rather interfere with replication-related enzymes. Aphidicolin, an inhibitor of replicative DNA polymerases leads to uncoupling of the replicon and generation of long stretches of single-stranded DNA (ssDNA) [22]. After hydroxyurea treatment, an inhibitor of ribonucleotide reductase (RNR), the metabolism of deoxyribonucleotide triphosphates (dNTPs) is disturbed, and subsequently, the RF progression is blocked [23]. Camptothecin and etoposide, inhibitors of topoisomerase I and topoisomerase II respectively, prevent DNA unwinding and halt relaxation of torsional stress [24,25]. The most common sources of RS are illustrated in Figure 1.

Several repair pathways are essential for rapid elimination of DNA distortions and lesions introduced by the action of RS inducing compounds [26]. Removal and replacement of single base damage (e.g., oxidised and alkylated bases), is performed by base excision repair (BER) [27]. More extensive damage affecting several adjacent bases is repaired by nucleotide excision repair pathway (NER). NER is essential for repair of UV-induced damage such as cyclobutane pyrimidine dimers, or pyrimidine-pyrimidone (6-4) photoproducts and also needed for crosslinks removal caused by for example cisplatin [28]. Single-strand break repair in higher eukaryotes rely on poly(ADP-Ribose) polymerase 1 (PARP1) and X-ray repair cross complementing 1 (XRCC1) depedent recognition of the lesion, followed by end processing and ligation [29]. Double-strand breaks (DSBs) are processed by either homologous recombination (HR), or non-homologous end-joining (NHEJ). HR is active predominantly in S and G2 phases using the sister chromatid as a template for repair with high fidelity [30]. NHEJ, considered as an error prone pathway, performs DSB repair in all cell cycle stages more rapidly by direct ligation of two unprocessed (or minimally processed) DNA ends [31].

All previously described specific structures and concomitant DNA lesions can challenge the progression of RF. If the RF encounters a lesion which the replicative polymerase is unable to process as a template, it becomes stalled [32]. Stalled RFs are vulnerable structures and may undergo spontaneous collapse which leads to DSBs and genomic instability (GI) [33,34]. To avoid the harmful consequences of stalled forks, several mechanisms—DNA damage tolerance pathways (DDT)—exist to bypass the lesions and enable fork restart. One well-described process of DDT is translesion synthesis (TLS). TLS promotes "polymerase switch" from the replicative polymerase to translesion polymerases, which are able to continue replication across the lesion. TLS polymerases possess low processivity and fidelity towards the template DNA strand. Therefore TLS is often referred to as the error-prone pathway of DDT [32,34–36]. Among the DNA lesions which block the progression of RFs, interstrand crosslinks (ICLs) belong to the most challenging to bypass [37]. Thus, a whole group of proteins called Fanconi anaemia (FA) proteins evolved to govern the bypass and the repair of ICLs. The FA network promotes the unhooking of the ICL by specific endonucleases, bypassing the lesion by TLS polymerases or the repair by HR [5–7]. Patients with a defect in the FA protein family suffer from premature ageing, show increased sensitivity to DNA crosslinking agents (e.g., cisplatin, mitomycin C) and predisposition to certain types of cancers due to increased GI [38–40]. Although the FA pathway is involved mainly in ICL repair, it contributes more generally to initial detection of RF arrest, processing and stabilisation of the forks and regulation of TLS [41,42].

DNA damage bypass can occur in an error-free manner through the activation of the other branch of DDT, called template switching (TS). The process utilises the newly synthesised strand of the sister duplex, using it as an undamaged template. TS can be promoted either by fork regression or by strand invasion mediated by HR [34,36,43,44]. RF restart can also be achieved by firing nearby dormant replication origins or by repriming events leaving behind lesion containing single-stranded DNA (ssDNA) gaps which are subsequentially processed by DTT pathways [45–50]. Altogether, these processes ensure the rapid resumption of DNA synthesis, preventing prolonged fork stalling and the potentially deleterious effects of replication fork collapse. However, upon persisting RS, or non-functional RS response, the RF may fail to restart and collapse, most probably due to destabilised, dysfunctional or displaced components of replication machinery [1,50–54]. Prolonged stalled replication forks are targeted by endonucleases followed by recombination-based restart pathways [55,56].

Among the features of RS belong accumulation of long stretches of ssDNA [46,57], resulting from the uncoupled activity of DNA polymerase and progression of DNA helicase [58,59]. The persisting ssDNA is rapidly coated by replication protein A (RPA) that in turn generates the signal triggering the checkpoint response through activation of Ataxia telangiectasia Rad3-related (ATR) checkpoint kinase [60–63]. Once activated, ATR and its downstream target checkpoint kinase 1 (CHK1) help the cell to faithfully complete DNA replication upon RS [52,53,64]. In addition, ATR as the central RS response kinase contributes to the stabilisation and restart of the stalled forks even after the stress has been removed [65]. The ATR-CHK1 pathway is responsible for cell cycle inhibition, suppression of new origin firing, DNA repair and to the overall improvement of cell survival [62,66]. The role of Ataxia telangiectasia mutated (ATM), another important checkpoint kinase, upon RS conditions is not as clear and straightforward as of ATR. ATM is preferentially activated by DSBs which are generated in later stages after RS induction, mostly after the RF collapse [67,68]. There is suggested interplay between ATM and ATR during replication stress which becomes apparent under concomitant depletion of both kinases [68]. Interplay between ATM, Werner helicase (WRN) and Bloom helicase (BLM) is needed for the resolution of replication intermediates and HR repair pathway that is important for RF restart [69,70].

Chronic replication stress conditions, particularly in the absence of proper DNA repair pathway and/or non-functional checkpoint responses might result in the transfer of RS-related DNA alterations to daughter cells, inducing mutations, GI and fuelling tumourigenesis [1].

From this point of view, the RS is a strong pro-carcinogenic factor driving selective pressure for acquisition of mutations overcoming cell cycle arrest or apoptosis [71,72]. This further leads to the progression of malignant transformation and faster selection of mutations allowing development of resistance to cancer treatment [73].

However, cells typically react on the prolonged exposure to RS by triggering mechanisms leading to permanent cell cycle arrest known as cellular senescence or apoptosis [74,75] acting as a natural barrier against tumour progression [76].

Several hereditary syndromes are linked to enhanced RS and GI. The spectrum of exhibited symptoms is broad and includes premature ageing, growth retardation, neurodegeneration, immunodeficiency, cancer predisposition and others. The disorders like Seckel syndrome (deficiency in ATR kinase) [77], Ataxia telangiectasia caused (loss of ATM kinase) [78], Xeroderma pigmentosum (XP); various defects in XP protein family group) [79] are caused by aberrations in DNA damage recognition and repair enzymes [80]. Bloom and Werner syndrome (deficiency of BLM and WRN helicase, respectively) [81,82], Fanconi anaemia (FA; mutations in FA pathway proteins) [83,84], or Rothmund-Thomson syndrome (defects in RECQ like helicase 1 protein) [85,86] are related to failure of replication fork progression and restart.

In general, RS is a potent inducer of variety of hereditary and non-hereditary diseases, including the oncogenic transformation. The knowledge and understanding of the processes during RS are crucial for choosing the most efficient therapy. The in vitro-based cell studies involving models

of chemical induction of RS are unique source of information about molecular interactions and undergoing mechanisms. For this review five compounds were chosen, all of them are commonly used for cell-based experiments to induce RS. Several aspects are discussed in detail: mechanism of action aimed at replication interference, proper dosing and common experimental setups. A brief overview of the medical use and important practical hints for laboratory use are also included.

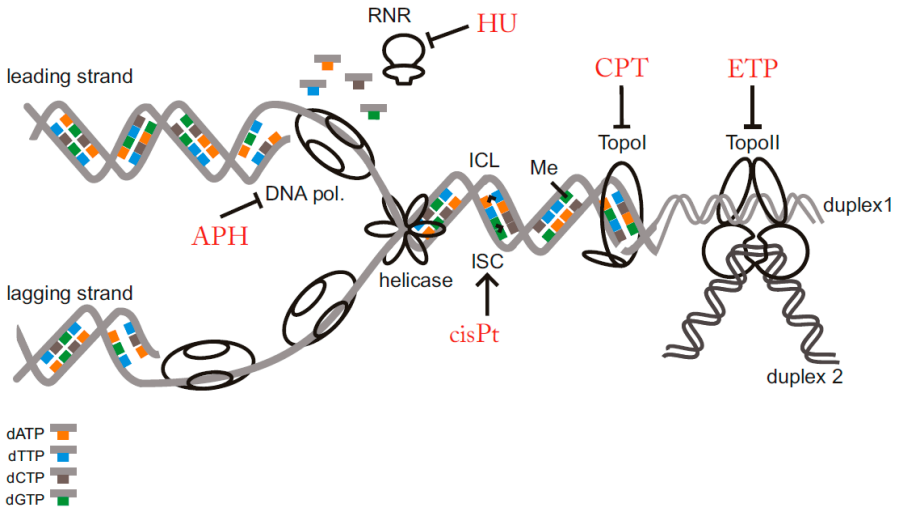

Figure 1. Schematic view of the most common lesions causing replication stress. In the scheme, several important replication stress (RS) inducing factors are illustrated: intra-strand crosslink (ISC), inter-strand crosslink (ICL), alkylated/modified base (Me) and inhibition of replication related enzymes. Compounds further described in the review are marked by red colour. RNR: ribonucleotide reductase; DNA pol.: DNA polymerase; TopoI: topoisomerase I; TopoII: topoisomerase II; APH: aphidicolin; HU: hydroxyurea; CPT: camptothecin; ETP: etoposide; cisPt: cisplatin; dATP: deoxyadenosine triphosphate; dTTP: deoxythymidine triphosphate; dCTP: deoxycytidine triphospahte; dGTP: deoxyguanine triphosphate.

2. Compounds

2.1. Cisplatin

Cisplatin (cisPt) is an inorganic platinum complex first synthesised by Italian chemist Michel Peyrone and originally known as 'Peyrone's chloride' (Figure 2). The cytostatic activity of cisPt was first reported by Barnett Rosenberg and co-workers in 1965 following accidental discovery of *Escherichia coli* growth inhibition induced by the production of cisPt from platinum electrodes [87]. It is generally considered as a cytotoxic drug for treating cancer cells by damaging DNA and inhibiting DNA synthesis. cisPt is a neutral planar coordination complex of divalent platinum [88] with two labile chloride groups and two relatively inert amine ligands. The *cis* configuration is necessary for the antitumour activity [89], 3D structure of monofunctional cisPt bound to DNA structure can be found here [90].

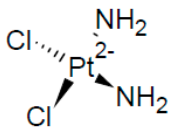

Figure 2. Cisplatin structure.

2.1.1. Mechanism of DNA Damage Induction

The cytotoxicity of cisPt is known to be due to the formation of DNA adducts, including intrastrand (96%) and interstrand (1%) DNA crosslinks, DNA monoadduct (2%) and DNA–protein

crosslinks (<1%) [91]. These structural DNA modifications block uncoiling and separation of DNA double-helix strands, events both necessary for DNA replication and transcription [92]. Inside a cell, cisPt forms an activated platinum complex, which triggers a nucleophilic substitution reaction via an attack on nucleophilic centres on purine bases of DNA, in particular, *N7* positions of guanosine (65%) and adenosine residues (25%) [93]. The two reactive sites of cisPt enable the formation of the most critical crosslink between two adjacent guanines (1,2-d(GpG)), resulting in the formation of DNA intrastrand crosslinks [94]. Also, platinum can align to guanine bases on the opposite DNA strand, thus creating DNA interstrand crosslinks, present in lower percentage [95]. These cisPt crosslinks create severe local DNA lesions that are sensed by cellular proteins, inducing repair, replication bypass or triggering apoptosis [96]. Several protein families can recognise cisPt–DNA adducts, including nucleotide excision repair (NER) proteins [97], homology-directed repair proteins (HDR) [98], mismatch repair (MMR) proteins [99] and non-histone chromosomal high mobility group proteins 1 and 2 (HMG1 and HMG2) [100]. The intrastrand cisPt structural alteration stalls RNA polymerase II. It is recognised and efficiently repaired by global genome NER (GG-NER) or its transcription-coupled sub-pathway (TC-NER) [101]. The second DNA repair system predominantly involved in coping with cisPt–DNA adducts is error-free HDR, which removes DNA DSBs remaining after cisPt adduct removal [98]. In contrast to the previously mentioned repair pathways that increase cell viability, MMR proteins have been shown to be essential for cisPt-mediated cytotoxicity [99]. cisPt is reported to enhance interactions between MMR proteins MLH1/PMS2 (MutL homolog 1/PMS1 homolog 2, MMR component) and p73, triggering apoptosis [102]. Therefore, mutations in MMR genes are known to be associated with cisPt resistance [103]. HMG1 and HMG2 recognise intrastrand DNA adducts between adjacent guanines, affecting cell cycle events and subsequently inducing apoptosis [100].

In addition to the previously mentioned repair proteins, specialised translesion DNA polymerase eta (η) can be loaded onto sites of cisPt–DNA adducts promoting TLS repair pathway [104]. cisPt also induces dose-dependent reactive oxygen species (ROS), which are responsible for the severe side effects of platinum-based therapy, including nephrotoxicity and hepatotoxicity [105]. When overwhelming the reduction capacity of the cell, cisPt-induced ROS might lead to lipid peroxidation, oxidative DNA damage, altered signal transduction pathway and calcium homoeostasis failure [105]. Extensive unrepaired cisPt-induced DNA damage can proceed to apoptotic cell death mediated by various signal transduction pathways, including calcium signalling [106], death receptor signalling [107] and activation of mitochondrial pathways [108]. At least two main pathways have been proposed to mediate cisPt-induced apoptosis in vitro. One involves the critical tumour suppressor protein p53 directly binding to cisPt-modified DNA [109] and promoting apoptosis via several mechanisms. p53 binds and counteracts the anti-apoptotic B-cell lymphoma-extra large (Bcl-xL) [110], contributes to inactivation of nutrient sensor AMP-kinase (AMPK) [111], activates caspase-6 and -7 [112] and the pro-apoptotic Bcl-2 family member PUMAα in renal tubular cells [113]. However, the role of p53 in response to cisPt seems to be controversial, as it has been described to contribute to cisPt cytotoxicity [114] and also to be involved in cisPt resistance in different cancer models [115]. The other cisPt-induced apoptotic pathway is mediated via a pro-apoptotic member of the p53 family, p73. cisPt has been shown to induce p73 in several cancer cell lines [116], which cooperates with the MMR system and c-Abl tyrosine kinase, known to be involved in DNA damage-induced apoptosis [117]. In response to cisPt, c-Abl phosphorylates p73, making it stable [118], and increases its pro-apoptotic function by binding transcription coactivator p300, which triggers transcription of pro-apoptotic genes [119]. Moreover, p73 forms a complex with c-Jun N-terminal kinase/stress-activated protein kinase (JNK), leading to cisPt-induced apoptosis [120]. Intrinsic signaling pathways involved in cisPt driven apoptosis include Akt [121], protein kinase C [122,123], and mitogen activated protein kinases—MAPK (e.g., extracellular signal-regulated kinases; ERK) [124–126], JNK [127–129] and p38 [130].

2.1.2. Other Effects

Besides DNA, the primary target of cisPt in cells, there is some evidence for the involvement of non-DNA targets in cisPt cytotoxicity [131]. cisPt interacts with phospholipids and phosphatidylserine

in membranes [132], disrupts the cytoskeleton and alters the polymerization of actin, probably due to conformational changes resulting from the formation of Pt–S bonds [133]. MicroRNAs (miR), which play a role in posttranscriptional gene silencing, have been shown to be involved in the modulation of cisPt resistance-related pathways in different cancer models. miR-378 was shown to reverse resistance to cisPt in lung adenocarcinoma cells [134], whereas miR-27a was shown to be upregulated in a multidrug resistant ovarian cancer cell line, contributing to cisPt resistance [135]. miR-21 increases the cisPt sensitivity of osteosarcoma-derived cells [136]. For references to particular studies using cisPt, refer to Table 1.

Table 1. Effects of various cisplatin treatments in vitro.

Concentration	Incubation Time	Observed Effect	Cell Line	Reference
300 μM	2 h	increase in polyADP ribosylation	O-342 rat ovarian tumour cells	[137]
100 μM	2 h before IR	sensitization to γ-radiation	hypoxic V-79 Chinese hamster cells	[138]
100 μM	2 h	increase in polyADP ribosylation	CV-l monkey cells	[139]
<20 μg/mL (<66 μM)	5 h	block of rRNA synthesis block of DNA replication	Hela	[140]
15 μM	1 h	induction of SCE (sister chromatid exchange) decreased cell survival	6 primary human tumour cell culture	[141]
10–30 μM	24 h, 48 h	induction of apoptosis	224 (melanoma cells) HCT116	[142]
10 μM	24 h	increase in antiapoptotic Bcl-2 mRNA synthesis (regulated by PKC and Akt2)	KLE HEC-1-A Ishikawa MCF-7	[143]
2–10 μM	72 h	induction of apoptosis	224 (melanoma cells) HCT116	[142]
5 μM	24 h	increase in p53 stability activation of ATR increased p53(ser15) phosphorylation	A2780	[144]
5 μM	24 h	activation of p21 activation of CHK2 increased p53(ser20) phosphorylation	HCT116	[144]
5 μM	24 h	induction of mitochondrial reactive oxygen species (ROS) response	A549 PC3 MEF	[143]
2 μM	24 h	G2/M arrest, subapoptic damage	MSC	[145]
>2 μM	24 h	decreased proliferation rate induction of apoptosis	TGCT H12.1 TGCT 2102EP	[145]
1–4 μg/mL	2 h	block of DNA synthesis block of transcription G2 arrest apoptosis	L1210/0 cells	[146]
2 μg/mL	48 h 144 h, 168 h	inhibition of mtDNA replication inhibition of mitochondrial genes transcription	Dorsal root ganglion (DRG) sensory neurons	[147]
1 μg/mL	2 h	transient G2 arrest	Hela	[148]
3.0 μM	4 h before	block of NHEJ	A2780	[138]
0.2–0.8 μM	IR 0.5 Gy 4 h	cisPt-IR synergistic interaction	MO59J MO59K	[138]
1–2.5 μM	24 h–48 h	block of DNA replication followed by cell apoptosis	Hela	[149]
0.3–1 μM	overnight	inhibition of RNA polymerase II-dependent transcription	Hela XPF	[144]
0.6 μM	2 h	90% reduction in clonogenic capacity detected after 7 days CHK1 phosphorylation causing CHK1 dependent S phase arrest	Hela	[148]
0.5 μM	24 h 48 h	loss of telomeres (TEL), or TEL repeats cell death	Hela	[139]

ATR: Ataxia telangiectasia Rad3-related; Bcl: B-cell lymphoma; CHK1: checkpoint kinase 1; CHK2: checkpoint kinase 2; IR: ionizing radiation; mtDNA: mitochondrial DNA; NHEJ: non-homologous end-joining; PKC: protein kinase C; polyADP: poly adenosine diphosphate; rRNA: ribosomal RNA.

2.1.3. Solubility

cisPt (molecular weight (MW) 300.05 g/mol) is water soluble at 2530 mg/L (at 25 °C), saline solution with a high chloride concentration (approx. 154 mmol/L) is recommended. In the absence of chloride, the cisPt chloride leaving group becomes aquated, replacing the chloride ligand with water and generating a mixture of species with increased reactivity and altered cytotoxicity [150,151]. Commonly used solutions for laboratory use are aqueous-based solutions in 0.9% NaCl (0.5 mg/mL), pH 3.5–5. Dissolved cisPt may degrade over a short time, the storage of aliquots is not recommended. However, the stability at −20 °C in the dark is reported to be 14 days. Solutions (in 2 mM phosphate buffered saline buffer with chloride concentration 140 mmol/L) stored at 4 °C should be stable for 7–14 days [152]. Undiluted cisPt is stable in the dark at 2–8 °C for several months [121,153]. Dimethyl sulfoxide (DMSO) can also be used for cisPt dilution, however it is not recommended. The nucleophilic sulphur can displace cisPt ligands, affecting the stability and reducing cisPt cytotoxicity [154]. DMSO introduced in combination studies with cisPt does not affect its activity [152].

2.1.4. Medical Use

Following the start of clinical trials in 1971, cisPt, marketed as Platinol (Bristol-Myers Squibb, New York, USA), was approved for use in ovarian and testicular cancer by the Food and Drug Administration (FDA) in 1979 [155]. cisPt is considered one of the most commonly used chemotherapy drugs for treating a wide range of malignancies, including head and neck, bladder, oesophagal, gastric and small cell lung cancer [156,157]. Moreover, cisPt has been shown to treat Hodgkin's [158] and non-Hodgkin's lymphomas [159], neuroblastoma [160], sarcomas [161], multiple myelomas [162], melanoma [163], and mesothelioma [164]. cisPt can reach concentrations of up to 10 μg/mL in human plasma [165]. cisPt is administrated either as a single agent or, in the main cases, in combination with other cytostatics (e.g., bleomycin, vinblastine, cyclophosphamide) or radiotherapy for the treatment of a variety of tumours, e.g., cervical carcinoma [153]. The most important reported side effect is nephrotoxicity, due to preferential accumulation and persistence of cisPt in the kidney [166], later ototoxicity and bone marrow depression. Pharmacokinetic and pharmacodynamic studies have shown that a maximal steady state cisPt plasma concentration of between 1.5 and 2 μg/mL has the most effective chemotherapeutical effect with minimal adverse nephrotoxicity [167]. Many cancers initially responding to cisPt treatment could become later resistant. Mechanisms involved in the development of cisPt resistance include changes in cellular uptake, drug efflux, drug inactivation by increased levels of cellular thiols, processing of cisPt-induced damage by increased NER and decreased MMR activity and inhibition of apoptosis [99,168]. To boost platinum drug cytotoxicity, overcome its resistance and achieve a synergistic effect, new platinum-based drugs, as well as their combinatorial therapy with other antineoplastic agents were developed for cancer treatment [169]. Besides of cisPt derivatives as carboplatin and oxaliplatin, are currently being used in the clinical practice, while nedaplatin, lobaplatin and nedaplatin acquired limited approval in clinical use [170,171]. Recent discoveries described the combination of cisPt with PARP inhibitor olaparib targeting DNA repair to acts synergistically in several non-small cell lung carcinoma cell lines [172]. This combinatorial therapy can be promising especially in patients with advanced breast and ovarian cancer-bearing BRCA1/2 (breast cancer 1/2) mutations [173].

2.1.5. Summary

cisPt is used in vitro in concentration range approx. 0.5–300 μM. The levels in human plasma can reach up to 10 μg/mL (33 μM) which should be beared in mind when interpreting in vitro data. Continuous treatment, or longer incubation time, or high cisPt concentration of 20 mg/mL lead to complete inhibition of DNA synthesis [174]. The concentration range of 15–30 μM results in a block of DNA replication and transcription and triggers DNA damage response (DDR) signalization

through ATM-CHK2, ATR-CHK1 DDR pathways resulting in p53-p21 driven cell cycle arrest or p53-mediated cell apoptosis [141–144]. However, in some cell lines also the synthesis of anti-apoptotic protein Bcl-2 was reported [143]. cisPt is in the majority of cell lines induces apoptosis above the concentration of approx. 2 μM [139,141,142,146]. cisPt block DNA replication [139,140,146] and inhibits RNA synthesis [140,175,176] and also influences the mitochondrial DNA synthesis and metabolism [147]. As a commonly used drug in clinics, many in vitro experiments have been conducted to address problems arising during treatment. Especially, the study of mechanisms underlying drug resistance [177], causes of toxic side effects [178], enhancement of synergistic effects [179] and ways how to improve drug delivery systems [180]. cisPt massively triggers the TLS repair pathways; defective FA proteins sensitise the cells towards this compound [181], defective MMR proteins establish cisPt resistance [103,182].

2.2. Aphidicolin

Aphidicolin (APH) is a tetracyclin diterpenoid antibiotic isolated from *Nigrospora sphaerica* (Figure 3) which interferes with DNA replication by inhibiting DNA polymerases α, ε and δ [183]. Specifically, only cells in S phase are affected, whereas cells in other phases of the cell cycle are left to continue until the G1/S checkpoint, where they accumulate [184].

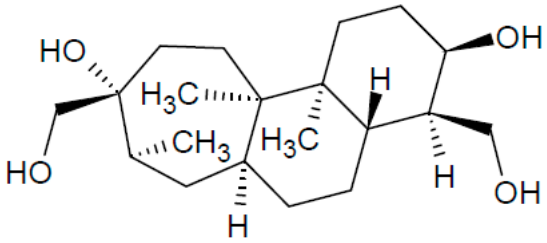

Figure 3. Aphidicolin structure.

2.2.1. Mechanism of DNA Damage Induction

APH binds to the active site of DNA polymerase α and rotates the template guanine, selectively blocking deoxycytidine triphosphate (dCTP) incorporation [185]. DNA polymerase α interacts with APH by its C18-binding OH group, APH forms a transient complex with polymerase and DNA [183]. The effect of APH on cell cultures is reversible if the cells are treated for no longer than 2 generations [186]. The exonuclease activity of APH-responding polymerases is only mildly affected, even at concentrations completely blocking the polymerase activity [183]. However, in the cell nucleus, the exonuclease activity is usually not retained because ternary complex APH–polymerase–DNA is formed and blocks the enzyme [183]; 3D structure of the complex can be found here [187].

Mechanistically, APH compromises the function of DNA polymerase, while helicase proceeds regularly (so called uncoupled/disconnected replicon), which leads to the generation of long stretches of single-stranded DNA [188]. The disconnected replicon is vulnerable structure prone for breakage preferentially at the so-called common fragile sites (CFSs) (also referred to as CFS expression) [189]. CFSs are specific genomic loci conserved in mammals generally prone to instability upon RS [190]. CFS expression is also common in precancerous and cancerous lesions [76]. Moreover, a causative role of CFS's in cancer development has been suggested [191]. APH reproducibly causes damage at the same sites, and thus low doses of APH are used to define APH-inducible CFSs, of which there are over 80 described in the human genome [22,192]. Other CFS inducers (hydroxyurea, camptothecin, hypoxia and folate deficiency) are not so specific, nor efficient as APH [193,194]. Importantly, APH efficiently induces CFS expression only when the rate of polymerase is slowed down but not completely blocked. The optimum concentration range usually spans 0.1–1 μM [195] (and refer to Table 2). Apart from disconnected replicon, there might be other explanations for the extraordinary potency of APH to induce CFS-associated genomic instability. First, APH has been shown to increase

the number of R-loops within certain CFSs, thus inducing replication/transcription collisions [196]. However, the mechanistic relationship between APH and increased R-loop formation is not clear. Second, re-licensing of replication origins is typical feature of oncogenic genetic backgrounds which are very prone to CFS expression. In such situations the CFS expression is explained as a result of DNA re-replication and subsequent collision of re-replicating forks within CFSs [10,197]. This phenomenon was studied in detail in yeasts at replication slow zones (analogs to CFSs in mammals) [198]. It is not clear whether the same re-licensing process is induced also by APH, however re-duplication would explain the reported APH-induced amplifications [191,199].

Prolonged treatment with low doses of APH induces cellular senescence response [74]. Interestingly, the most efficient doses were found to span the same range as doses used for CFS expression, which implies that CFSs might play a causative role in this process. Moreover, oncogene-induced senescence also displays increased CFSs-associated instability [10,197]. These phenotypical similarities between oncogenic stress and low doses of APH make this drug a good candidate for studying cellular processes in early stages of malignant transformation.

2.2.2. Other Effects

APH is a very specific DNA polymerase inhibitor, APH does not interact with mitochondrial DNA polymerases [186] nor proteins [200], DNA, RNA, metabolic intermediates, nor nucleic acid precursor synthesis [184,200,201]. Contradictory results have been obtained regarding the effect of APH on DNA repair synthesis (DRS). According to a radiography method, APH does not influence DRS [200], although when DRS was induced by tumor necrosis factor (TNF) or UV irradiation, APH was observed to inhibit the process [202,203]. For references to particular studies using APH, refer to Table 2.

Table 2. Effects of various aphidicolin treatments in vitro.

Concentration	Incubation Time	Observed Effect	Cell Line	Reference
0.2 mM	16 h, 10 h	formation of anaphase bridges and micronuclei	HeLa	[204]
30 μM	6 h	stalled replication forks	HCT116	[205]
30 μM	6 h	stalled replication forks	PD20 cells Bloom syndrome cells	[206]
5 μg/mL (14.3 μM)	4 h	DNA repair synthesis inhibition sensitization towards TNF treatment	L929 ovarian cancer cells A2780	[202]
5 μg/mL (14.3 μM)	2–8 h	S phase arrest kinetics and mechanism study	RKO 293T MEF	[207]
2.5 μg/mL (7.15 μM)	1 h	inhibition of DNA synthesis and DNA repair	Normal and XPA deficient human fibroblasts	[203]
10 μM	15 h	cell cycle synchronisation at the G1/S boundary	REF-52 HeLa	[208]
5–25 μM	24 h	inhibition of replicative polymerases	Werner syndrome cells Bloom syndrome cells	[209,210]
1 μM	1–24 h	CFS induction	HEK293T	[210]
1 μM	24 h	CFS induction	MEF HeLa	[211]
0.5 μM	2 h	transient attenuation of DNA synthesis,	DT40	[212]
0.1 μM	24 h	study of chromosome integrity and replication		
0.4 μM	24 h	CFS induction	U-2 OS	[213]
0.1 μM 0.2 μM	16 h	replication stress observed on telomeres	hESC (UCSF4)	[214]
0.2 μM	2 weeks	irreversible senescence induction	REF-52	[74]
0.2 μM	24 h	CFS induction	BJ-hTERT	[215]
0.05 μM 0.4 μM	24 h	CFS induction	Werner syndrome fibroblasts AG11395 cells	[216]

Table 2. *Cont.*

Concentration	Incubation Time	Observed Effect	Cell Line	Reference
0.3 μM	48 h	increased incidence of mitotic extra chromosomes replication stress	V79 hamster cell lines	[217]
0.3 μM	72 h	replication stress	Human fibroblasts HGMDFN090	[199]
2 μg/mL	not indicated	replication block	BJ BJ-tert HMEC	[197]
0.2 μM	7–24 h	cell synchronization	HeLa	[184]

CFS: common fragile site; TNF: tumour necrosis factor.

2.2.3. Solubility

APH (MW 338.48 g/mol) is soluble in DMSO (up to 10 mg/mL), ethanol (up to 1 mg/mL) and methanol (freely), not soluble in water. The stability of the powder is 3 years at 2–8 °C, ethanol solution for a week at 2–8 °C, DMSO solution for 6 weeks at −20 °C [218].

2.2.4. Medical Use

APH has limited use in clinical practice owing to its low solubility. Only APH-glycinate has so far been tested in clinical trial phase I. However, fast clearance from human plasma (no drug observed after 6–8 h of APH administration) and no anti-tumour activity was observed. Its use as a single agent or even in combination with other cytostatics is no longer being considered [219]. APH is metabolised by cytochrome P-450 dependent degradation [220]. APH and its derivatives are considered as potential therapeutics for parasitic diseases, e.g., Chagas disease [221].

2.2.5. Summary

APH is used for in vitro studies in concentration range approx. 0.01 μM to 0.2 mM. APH is mainly used for cell-based experiments involving CFS expression [222], cell cycle synchronization [223], replication fork stability and restart studies [224] and for cellular senescence induction [74]. The threshold between replication fork stalling and slowing down is around 1 μM. Upon higher concentrations (5 μM–0.2 mM) APH was reported to stall the DNA polymerase, leading to S phase arrest. Upon lower concentrations, when the DNA polymerases are just slowed down, CFS expression can be observed. Usually, longer incubation times (approx. one population doubling) are used, so more cells within the population are affected. APH treatment causes a significant amount of DNA damage, leading to rapid ATR kinase activation. In the case of longer APH treatment also ATM is activated probably as a consequence of DSB formed within the stalled replication forks [207]. Prolonged APH incubation in the range of days up to weeks at low concentrations (0.2–1 μM) induces cellular senescence [74].

2.3. Hydroxyurea

Hydroxyurea (HU) was first synthesised in the 19th century (Figure 4) and inhibits the incorporation of nucleotides by interfering with the enzyme ribonucleotide reductase (RNR) [225]. RNR converts nucleotide di- and tri-phosphates to deoxynucleotide di- and tri-phosphates, which is the rate-limiting step in nucleotide synthesis [226]. Without proper levels of dNTPs, DNA cannot be correctly replicated nor repaired [227].

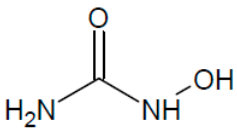

Figure 4. Hydroxyurea structure.

2.3.1. Mechanism of DNA Damage Induction

RNR is a large tetrameric enzyme comprising two R1 subunits and two small regulatory subunits R2 [228]. HU scavenges the tyrosyl radical of the R2 subunit which inactivates the RNR enzymatic activity [226]. Complete inhibition of RNR has been observed within 10 min after treatment with 0.1 mM HU and within 5 min after 3 mM of HU in murine 3T6 cells [229]. Consequently DNA synthesis is inhibited, selectively stopping the cells in S phase [230]. The inhibition is caused alterations in the dNTP pools. Each type of dNTP is affected in a different way. For example, after 280–560 μM HU treatment for 60 min, the dTTP pool was found to increase by 50%, whereas the dCTP pool is decreased by 50% [231]. HU slows down the initiation of replication and also the progression of replication forks. Moreover, after stopping the production of dNTPs, DNA repair and mitochondrial DNA synthesis are affected in all cells, regardless of the cell cycle stage [227]. HU treatment greatly affects the choice of replication origins and origin spacing in mammalian cells [232]. Although the mechanism of DNA damage induction may look similar to that for APH, HU induces a different spectrum of fragile sites, called early replicating fragile sites (ERFs) [233]. ERFs are also induced by c-Myc expression [11,12]. It was also reported that 10 μg/mL APH [234] (concentration that stalls the replication fork progression) leads to the generation of several kilobases long unwound DNA; however, HU treatment can generate only up to 100–200 nt long ssDNA [235].

2.3.2. Other Effects

HU induces copy number variants (CNVs) with similar frequency and size distribution as APH [236]. It was reported for yeast cells, that HU alters Fe–S centres, enzyme cofactors catalysing oxidation-reduction reactions, which interferes with various metabolic enzymes and affects the redox balance of cells. Similar mechanism is proposed also for mammalian cells [237].

HU has been negatively tested for mutagenicity, measured by single nucleotide variation (SNV) and insertion/deletion frequency [238]. On the other hand, low doses of HU have been reported to induce DNA damage [239]. Therefore, it is possible that the compound possesses some pro-mutagenic potential (see also below). For references to particular studies using HU, refer to Table 3.

Table 3. Effects of various hydroxyurea treatments in vitro.

Concentration	Incubation Time	Effect	Cell Line	Reference
200 mM	2 h	replication block	yeast cells	[240]
10–200 mM	3 h	replication block replication fork (RF) restart	yeast cells	[241]
5 mM	1 h	replication block	HEK293	[242]
2 mM	3 h	replication block		
50 μM–5 mM	40 min–2 h	replication stress	293T mouse ES cells	[243]
2 mM	1 h, 24 h	replication stress replication block	HCC1937 MCF7	[244]
2 mM	16 h	replication block	HEK293	[245]
2 mM	24 h	DNA damage induction during S phase	U-2 OS 293T	[246]
2 mM	15 h	replication block cell cycle synchronisation at the G1/S boundary	REF-52 HeLa	[208]
2 mM	5 h	dNTP depletion	REF52	[74]
2 mM	3 h	chromosomal aberrations FANCD2 pathway involvement	lymphoblastoid cell lines	[247]
1 mM	overnight	replication block	MCF7	[248]
0.5 mM	5 h–10 h	replication block	U-2OS	[249]
2 mM	2 h–24 h	replication block		
0.5 mM	90 min	nucleotides depletion stalled RF w/o DSBs formation	MEF	[250]

Table 3. *Cont.*

Concentration	Incubation Time	Effect	Cell Line	Reference
0.1–0.5 mM	2 h–72 h	γ-globin gene expression	K562	[251]
0.1–0.5 mM	2 h–8 h	replication stress	PC3	[252]
0.2–0.4 mM	4 days	cell differentiation ERK signalling pathway inhibition p38 signal transduction activation	K562	[253]
0.3 mM	10 days	microsatellite instability upon FANCJ depletion	GM08402 HeLa PD20F	[254]
0.15–0.2 mM	2 weeks	irreversible senescence induction	REF-52	[74]
0.2 mM	2 h–7 h	replication stress	MEF	[255]
0.15 mM	2 h	p53 activation	REF52	[74]
50–200 μM	20 h	HIF1 induction eNOS induction	HUVEC	[256]
25–200 μM	72 h	induction of apoptosis	AML cell lines (MV4-11, OCI-AML3, MOLM-13, and HL-60)	[257]
5 μM–0.5 mM	48 h	replication stress	V79 hamster cells	[217]
2 μM	12 h	replication stress	H1299	[258]

dNTP: deoxynucleotide triphosphate; DSBs: double-strand breaks; eNOS: endothelial nitric oxide synthase; ERK: extracellular signal-regulated kinases; FANCD2: Fanconi anaemia complementation group D2; FANCJ: Fanconi anaemia complementation group J; HIF: hypoxia induced factor 1.

2.3.3. Solubility

HU (MW 76.05 g/mol) is freely soluble in water at 100 mg/mL, soluble also in DMSO. The powder is stable at 4 °C for 12 months. Solutions are stable for 1 month at −20 °C (after defrosting, equilibration is recommended for 1 h at room temperature. It is recommended to prepare fresh solutions before use. HU decomposes in the presence of moisture; therefore, it is recommended that it is stored in air-tight containers in a dry atmosphere [259].

2.3.4. Medical Use

HU is a commonly used medicine first approved by the FDA for the treatment of neoplastic disorders in the 1960s [260]. Common plasma levels of HU range 100–200 μM [261]. It is used for the treatment of sickle cell disease, essential thrombocytosis [262], myeloproliferative disorders and psoriasis [260] and is commonly indicated as a cytoreductive treatment in polycythemia vera [263] and others. Synergistic effects have been reported when it is used in combination with antiretroviral pills [264] and also in indicated cases with radiotherapy [265]. HU may be used as an anti-retroviral agent, especially in HIV (human immunodeficiency virus) patients. HU may cause myelofibrosis development with increased time of use and AML/MDS syndrome (acute myeloid leukaemia/myelodysplastic syndrome) [266]. Adverse side-effects have been observed, mainly myelosuppression [267]. A 17-year follow-up study of 299 patients treated with HU as a long-term therapy showed no difference in the incidence of complications such as stroke, renal disease, hepatic disease, malignancy or sepsis [268], suggesting that HU is well-tolerated. However, CNVs are generated at therapeutic doses of HU, and data from reproductive studies and studies on subsequent generations have so far been rather limited [236,268].

2.3.5. Summary

HU is used in vitro approx. in the range 2 mM–5 mM. The most commonly used concentrations are around 2 mM. HU is used for cell cycle synchronization [269], replication fork stability studies [249,252], studies of recovery mechanisms after the release of RS [242] and checkpoint responses [241]. Lower concentrations are used for RS induction [254], induction of senescence [74], apoptosis [257],

and repair pathways induction [217]. HU reaches plasma concentrations around 0.1 mM; this should be bear in mind when interpreting the data for clinical relevance [261]. The MRN (Mre11-Rad50-Nbs1) complex members Mre11 (Meiotic recombination 11) and Nbs1 (Nijmegean breakage syndrome 1) are required for efficient recovery of replication after treatment with replication stalling agents such as hydroxyurea [12]. HU causes rapid generation of ssDNA as indicated by RPA loading 40 min after treatment [270]. Subsequently, ATR-CHK1 signalling is activated, and HR repair pathway is induced.

Cells deficient in XRCC2 or other homologous recombination components exhibit hypersensitivity to HU [271]. It was reported that for hamster V79 cells, low concentrations of HU (5–10 μM) mimics the replication dynamics of untreated HR deficient cells [217]. Cellular senescence after long term replication stress caused by HU is dependent on p53-p21 signalling pathway and independent of p16 [74]. HU influences mutiple cellular pathways, e.g., JNK pathway, mitochondrial and peroxisome biogenesis, expression of several heat shock response proteins, autophagy pathways stimulation (beclin-1 expression), hemoglobin type F induction (in sickle cell disease, β-thalasemmia patients), etc. [272]. There are several cell lines that response to HU treatment in a specific manner, e.g., K562 cell line undergoes differentiation [253], T-cells activation is decreased [264], the morphology of vascular endothelial cells is affected [273].

2.4. Camptothecin

Camptothecin (CPT) is a pentacyclic quinoline alkaloid first isolated from the Chinese tree *Camptotheca acuminata* (Nyssaceae) by Wall et al. [274] (Figure 5). CPT has a unique intracellular target, topoisomerase I (TopoI), a nuclear enzyme that reduces the torsional stress of supercoiled DNA [24]. This activity enables specific regions of DNA to become sufficiently exposed and relaxed to facilitate essential cellular processes, such as DNA replication, recombination and transcription [275].

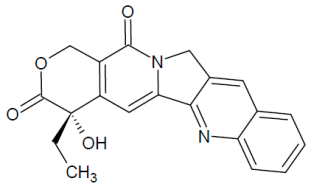

Figure 5. Camptothecin structure.

2.4.1. Mechanism of DNA damage induction

TopoI binds covalently to double-stranded DNA through a reversible transesterification reaction, generating a SSB [276], 3D structure can be found here [277]. This so-called TopoI–DNA cleavage complex (Top1cc) facilitates the relaxation of torsional strain in supercoiled DNA, either by allowing passage of the intact single strand through the nick or by free rotation of the DNA around the uncleaved strand [278]. CPT covalently and reversibly stabilises the normally transient DNA Top1cc by inhibiting religation of the scissile strand, thereby prolonging the half-life of Top1cc and increasing the number of DNA SSBs [279,280]. Moreover, trapping of the enzyme on the DNA leads to rapid depletion of the TopoI pool [281]. The effect of CPT is readily reversible after removal of the drug. However, prolonged stabilisation of Top1cc can cause multiple problems. Firstly, failure to relieve supercoiling generated by such processes as transcription and replication can lead to RS by creating torsional strain within the DNA [279,281,282]. Furthermore, the collision of the RF with the ternary drug-enzyme-DNA complex generates DSBs with serious cellular consequences, including cell death [283,284].

Because ongoing DNA synthesis is important for CPT-induced cytotoxicity, CPT is considered an S phase-specific drug. The repair of CPT-induced DSBs involves multiple DNA damage repair proteins. Recent studies have highlighted that functional cooperation between BRCA2, FANCD2, RAD18 and RAD51 proteins are essential for repair of replication-associated DSBs through HR. Loss of any of these proteins causes disruption of HR repair, chromosomal aberrations and sensitization of cells to

CPT [285]. A close link between CPT and HR has also been demonstrated in experiments measuring sister chromatid exchange events (SCEs), which are common consequence of elevated HR repair process and found to be induced by low doses of CPT [270]. CPT is applied in early S phase cells for triggering G2 arrest accompanied by blockage of the p34cdc2/cyclin B complex, a consequence of either DNA breakage, the arrest of the replication fork or both [286]. In addition, CPT driven TopoI–DNA cleavable complex and associated strand breaks were shown to increase transcription of the c-Jun early response gene, which occurs in association with internucleosomal DNA fragmentation, a characteristic mark of apoptosis [287]. Noncytotoxic concentrations of CPT can induce the differentiation of human leukaemia cells [288], and an antiangiogenic effect is suggested [289,290]. Interestingly, when used in combined treatment with APH, CPT reduces the APH-induced RPA (an indicator of ssDNA) signal and has a rescuing effect on CFS expression [291]. For references to particular studies using CPT, refer to Table 4.

Table 4. Effects of various camptothecin treatments in vitro.

Concentration	Incubation Time	Observed Effect	Cell Line	Reference
20 μM	30 min	DNA fragmentation in G1 and S phase cells	Hela	[292]
10 μM	24 h	increase in cell sensitivity to TRAIL-mediated apoptosis	Hep3B	[293]
10 μM	4 h	formation of replication mediated DNA DSBs	HT29	[294]
5 μM	60 min	inhibition of RNA synthesis	CSA	[295]
1 μM	60 min	inhibition of DNA synthesis	CSB	[296]
1 μM	60 min	replication block DSB formation cell death	U2OS	[297]
1 μM	60 min	formation of stabilised TopoI-cc complex DSB formation phosphorylation of CHK1 (S317) CHK2 (T68), RPA (S4/S8)	HCT116	[294]
1 μM	60 min	inhibition of DNA replication suggested DNA DSB formation	L1210 mouse lymphoblastic leukaemic cells	[293]
200 nM–1 μM	50 min	DSB formation	CSB	[298]
100 nM–10 nM	60 min	DSB formation	HCT116	[299]
25 nM	60 min	checkpoint activation (ATM-CHK2, ATR-CHK1) replication fork stalling replication fork reversal formation of specific DNA structures	U-2O-S	[300]
10 nM–100 nM	60 min	inhibition of EIAV (equine infectious anemia virus) replication	CF2Th	[295]
10 nM–20 nM	60 min	inhibition of HIV-1 replication block of viral protein expression	H9	[281]
6 nM	6 h	accumulation of cells in early S phase	Normal lymphocytes	[296]
	24 h	apoptosis, DNA fragmentation	MOLT-4	
6.25 nM	48 h	specific suppression of oral cancer cells growth	KB oral cancer cells	[281]
2.5 nM	48 h	increase in SCE upon depletion of Fbh1 helicase	BJ	[281]

ATM: Ataxia telangiectasia mutated; HIV: Human immunodeficiency virus; RPA: replication protein A; SCE: sister chromatid exchange; TopoI-cc: Topoisomerase I cleavage complex; TRAIL: TNF alpha related apoptosis inducing ligand, TNF: tumour necrosis factor.

2.4.2. Solubility

CPT (MW 348.35 g/mol) is soluble in DMSO (up to 10 mg/mL), methanol (40 mg/mL), 0.1 N sodium hydroxide (50 mg/mL) or acetic acid, insoluble in water. At higher concentrations, heating is required to dissolve the product completely (approx. 10 min at 95 °C), but some precipitation occurs upon cooling to room temperature [301].

2.4.3. Medical Use

CPT cannot be used in clinical practice because of its poor solubility in aqueous solutions, instability and toxicity, but modifications at selected sites have improved the pharmacologic and activity profile [283]. Currently, three water-soluble CPT-derivates, i.e., irinotecan (CPT-11), topotecan (TPT) and belotecan (CKD-602), are available for cancer therapy. However, despite their selectivity for TopoI and unique mechanism of action, they all have critical limitations. In particular, they become inactivated against TopoI within minutes at physiological pH due to spontaneous lactone E-ring opening [302] and diffuse rapidly from the TopoI–DNA cleavage complex due to their noncovalent binding. To overcome these problems, five-membered E-ring CPT-keto non-lactone analogues S38809 and S39625 have been synthesised and selected for advanced preclinical development based on their promising activity in tumour models. Their chemical stability and ability to produce high levels of persistent Top1cc makes them useful candidates for future treatment [303].

2.4.4. Summary

Camptothecin is used in concentration range 2.5 nM up to 20 μM. CPT is a potent DSBs inducer in a wide concentration range, approx. 10 nM–10 μM. Upon higher concentration (20 μM–10 μM), CPT was reported to be cytotoxic, increasing cell apoptosis via DNA fragmentation predominantly in S phase cells with ongoing DNA synthesis [292,293]. The most frequently used concentration of 1 μM CPT was shown to block DNA synthesis and induce DSBs resulting from the collision of RF due to prolonged stabilisation of TopoI DNA cleavage complex. The main implication of lower CPT concentrations is the induction of replication fork slowing and reversal, as a rapid response to TopoI inhibition is the increase in topological stress of DNA locally [300]. CPT activates predominantly ATR-CHK1 and ATM-CHK2 signalling, and leading to G2 checkpoint arrest [300]. Even at low doses of CPT HR repair pathway is triggered.

2.5. Etoposide

Etoposide (ETP) is a derivative of podophyllotoxin first synthetised in 1966 and approved for treatment as an antineoplastic agent in 1983 [304]. ETP structure comprises of polycyclic A–D rings, an E-ring and aglycone core (Figure 6). ETP compromises the proper function of the enzyme topoisomerase II (TopoII), 3D structure can be found here [305]. TopoII performs cleavage of both strands of a DNA duplex and enables passage of a second intact duplex through the transient break, ATP is used to power the strand transition [306]. As a result, relaxation, unknotting and decatenation of DNA are achieved enabling processes like replication and transcription [25].

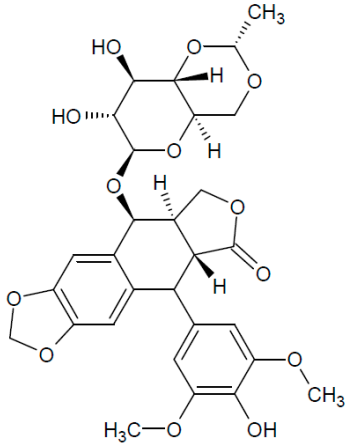

Figure 6. Etoposide structure.

2.5.1. Mechanism of DNA Damage Induction

Two modes of action were suggested for ETP to interfere with TopoII [25]. As a poison, it stabilises TopoII:DNA complexes, whereas as an inhibitor ETP interacts with the catalytic site of TopoII, decreasing the number of active cleavage complexes [307]. ETP acts as a poison by stabilizing the cleavage complex of TopoII via decoupling the key catalytic residues, thus preventing the religation of cleaved DNA ends [308]. As a result, the number of TopoII-associated DNA breaks are increased [309]. ETP's A, B and D-rings mediate the drug-enzyme interaction, whereas the aglycon core binds to DNA [262,308]. E–ring substituents are important for ETP activity but do not contribute to ETP-enzyme binding [310]. ETP is metabolised by cytochrome P3A4 (CYP3A4) to two metabolites, ETP-quinone and ETP-catechol. Both active against the TopoII enzyme. ETP-quinone is approx. 100× more efficient at inhibiting TopoII than ETP. ETP-quinone can block binding of the enzyme to DNA by stabilisation of the N-terminal clamp [307]. In cases where the enzyme still binds to DNA, the metabolite can stabilise the enzyme:DNA complex by inhibiting the religation step thus leading to higher levels of DSBs [307]. The ETP-catechol metabolite works similarly to the parent compound but can also be oxidised to the quinone [311]. ETP induces DSBs directly in all phases of the cell cycle, as observed by γH2AX foci formation (a marker of DSBs) [312,313]. ETP does not require S-phase to induce damage, but ongoing replication enhances its cytotoxic effect [314]. ETP causes disassembly of replication factories (sites of ongoing replication), as measured by the distribution of proliferating cell nucelar antigen protein (PCNA) [315]. Moreover, the cytotoxic effect of ETP is partially reduced by inhibitors of DNA synthesis, such as APH and HU [316]. There are two isoforms of the TopoII enzyme in mammals, called TopoIIα and TopoIIβ, sharing 68% homology [317]. TopoIIα activity is upregulated during cell cycle progression, peaks in mitosis and is essential for proliferating cells [318]. TopoIIβ is needed during transcription and DNA repair, and its levels are more stable during the cell cycle [319]. ETP is not selective between these two paralogs, and the inhibition of TopoIIβ is believed to be the reason for ETP therapy-related secondary malignancies [320]. TopoIIα seems to be a better target for therapy. Therefore, new compounds and analogues of ETP have been synthesised to be selective only for TopoIIα [321].

2.5.2. Other Effects

A strong mutagenic effect has been measured for ETP in mammalian cells by several assays, e.g., HPRT assay (hypoxanthine phosphoribosyl transferase), SCE and detection of mutations at the locus of the adenosine kinase gene [322]. In prokaryotic organisms (*E. coli*, *Salmonella typhimurium*), no significant genotoxic effect was observed [322]. For references to particular studies using ETP, refer to Table 5.

Table 5. Effects of various etoposide treatments in vitro.

Concentration	Incubation Time	Effect	Cell Line	References
up to 450 μM	40 min	SSB and DSB formation, induction of H2AX phosphorylation with slow kinetics	SV-40 transformed human fibroblasts G361	[323]
1–100 μM	30 min	formation of TopoII-blocked DSBs, activation of ATM-mediated repair	MEF HEK293T BJ1 AT	[324]
2–100 μM	6 h–48 h	senescence, apoptosis induction of p53 response	HepG2 U2OS	[325]
2–100 μM	1–3 h	disassembly of replication factories	AT1 BR AT3 BR HeLa	[315]
50–100 μM	3–6 h/16 h	apoptosis (activation of intrinsic (mitochondrial) pathway)	Hela HCT116	[326]
50 μM	15 h	apoptosis	BJAB Hut78	[327]

Table 5. *Cont.*

Concentration	Incubation Time	Effect	Cell Line	References
50 μM	48 h	growth arrest (accumulation of cells at G2/M boundary) induction of p53 response	MCF-7 ZR75-1 T-47D	[328]
25 μM	1 h	SSB and DSB formation γH2AX, pATM, pDNA-PKcs, MDC1 foci formation persisting DSBs cell death	HeLa HCT116	[329]
20 μM	16 h	increase in γH2AX levels reduction of proliferation rate (accumulation of cells in S and G2/M boundary)	U2OS	[330]
20 μM	1 h	repairable DSBs	HEK293T COS-7 BJ-hTERT H1299	[331,332]
	16 h	irrepairable DSBs, ATM-dependent HIC1 SUMOylation, induction of p53-dependent apoptotic response		
20 μM	1–5 h	apoptosis	A549 HeLa, T24	[333]
10 μM	1 h	DNA damage induction	A549	[334]
1–10 μM	48 h	apoptosis	HCC1937 BT-549	[335]
8 μM	1 h	induction of p53 response,	SH-SY-5Y SH-EP1	[336]
0.75–3 μM	72 h	senescence, apoptosis	A549	[337]
0.75 μM	24 h	cell cycle arrest in G2/M phase, DNA damage induction, induction of p53 response	MSC TGCT H12.1 TGCT 2102EP	[145]

DSBs: Double strand breaks; HIC1: Hypermethylated In Cancer 1; MDC1: Mediator of DNA Checkpoint 1; pATM: phosphorylated Ataxia elangiectasia Mutated; pDNA-PKcs: phosphorylated DNA Protein Kinase catalytic subunit; SSB: single-strand DNA break; TopoII: Topoisomerase II.

2.5.3. Solubility

ETP (MW 588.56 g/mol) is soluble in organic solvents (ethanol, methanol, DMSO), poorly soluble in water. It is recommended that stock solutions in organic solvents be diluted so 0.1% organic solvent is present in the final solution. The stability in aqueous solution is best at pH 4–5, but it can be improved by adding polysorbate 80 (Tween80), polyethylene glycol 300, citric acid and alcohol. ETP is unstable under oxidative conditions [338]. Under acidic conditions (pH < 4), the glycosidic linkage and lactone ring are hydrolysed, whereas, under basic conditions (pH > 6), *cis*-lactone epimers are formed [304]. Aqueous solutions are stable for several hours, depending on the concentration of the solution but irrespective of the temperature. ETP is sensitive to UV irradiation, both in solution and as a powder [338].

2.5.4. Medical Use

According to pharmacokinetic studies, plasma levels of ETP peak at concentrations of 20–70 μM [339]. ETP is approved for the treatment of refractory testicular tumors and small cell lung cancer. Various chemical modifications with potential higher efficacy have also been tested for clinical use, e.g., 4′-phosphorylation or 4′-propyl carboxy derivatives [340]. In the field of so-called personalised medicine, combined subsequent treatment of ETP and cisPt has been shown to be beneficial for patients suffering from ERCC1-incompetent lung adenocarcinoma [341]. ETP is reported to cause therapy-related leukaemias [320] and specific chromosomal translocations. Chromosomal rearrangements at the 11q23 chromosome band were found in patients and seemed to be related to the CYP3A4 metabolic conversion of ETP [342]. In mouse embryonic stem cells, an increase

in fusion chimeric products was observed at a 1.5 kb "hot spot" between exons 9 and 11 (analogous region to MLL (mixed lineage leukaemia) breakpoint cluster in human leukaemia) [343]. MLL gene encodes lysine (K)-specific histone methyltransferase 2A therefore influencing histone methylation and gene expression [344]. Leukaemogenic MLL translocations lead to expression of MLL fusion proteins. Patients with such translocations exhibit poor prognosis [345]. MLL fusion proteins are efficient in transforming the hematopoetic cells into leukaemia stem cells [346]. Many studies have attempted to solve the adverse side effects of ETP treatment and understand the underlying molecular mechanisms, e.g., multi-drug resistance [347], or unwanted toxicity [348]. The search for compounds that may improve ETP treatment usually starts with cell-based experiments, e.g., protective compounds shielding healthy cells [349], compounds selectively enhancing ETP toxicity [350] or targeted delivery [351].

2.5.5. Summary

ETP is commonly used for the induction of apoptosis [352]. Indeed, several studies reported that higher doses of the compound (25–100 μM) activate apoptosis, mostly in a manner dependent on p53 [325–327,329]. Prolonged treatment at lower concentrations of ETP can also lead to induction of the p53 pathway, cell cycle arrest, senescence and apoptosis [145,325,330,335,337]. ETP induces the formation of irreversible DNA–TopoII cleavage complexes (TopoIIcc) and DNA damage regardless of concentration or incubation time [323,324,329–332,334,353]. The initial displacement of TopoIIcc requires the coordinated action of several processes, such as cleavage by the 5′-tyrosyl DNA phosphodiesterase (TTRAP) and proteasome-dependent degradation of TopoII [354,355]. Furthermore, the MRN complex, CtIP (RBBP8 protein) and BRCA1 play a critical role in the removal of such DNA-protein adducts [356]. The remaining DNA lesions are often referred as DSBs, which are accompanied by the activation of ATM-mediated signalling or repair pathways, usually quantified by the formation of γH2AX [323,324,329–332]. However, several studies argue against the ability of ETP to primarily induce DSBs, showing that majority of the DNA lesions formed upon ETP treatment are SSBs [323,329]. Despite the discrepancy, pathways engaged in DSB repair are activated after the exposure to the drug, and among them, NHEJ is seemingly predominant [329,356–358]. ETP used in relatively high concentration (20–25 μM) might lead to persistent or irreparable DSB formation [329,331,332].

3. Conclusions

Replication stress is a significant contributor to genomic instability, a major factor for the conservation of mutations [1], relevant promoter of tumourigenesis [8] and also one of the main features of cancer cells [76]. Owing to its complexity, replication can be disturbed by multiple mechanisms. In this review, we focused on several compounds known to be RS inducers and often used in cell-based assays. Some of the compounds have been shown to be effective in cancer treatment. Importantly, the chemicals have been primarily chosen to cover various mechanisms of action, resulting in different treatment-induced phenotypes resembling those of RS in carcinogenesis. Induction of RS in vitro, e.g., by chemicals inducing DNA damage, is a crucial research tool. Precise knowledge about the mechanism of DNA damage induction and cellular pathways involved in the RS response is particularly important for the development of appropriate cellular assays for investigating carcinogenesis and cancer treatment. The above-mentioned publications in separate compound-related tables were chosen to help with the practical aspects of such assay design. Dose and time-dependent effects related to the genetic backgrounds (i.e., dependent on the cell line used) and proper readout are important issues for experiment design. Moreover, other practical information has been included so that readers can use this review as a brief guide for choosing an appropriate model and dose scheme for cell-based studies.

Acknowledgments: The work was supported by Grant Agency of the Czech Republic 13-17555S, Internal Grant of Palacky University IGA-LF-2016-030, the Norwegian Financial Mechanism CZ09 (Project PHOSCAN 7F14061).

Author Contributions: E.V. wrote the chapter 2.3, contributed to chapters 2.2 and 2.5, prepared the figures. K.C. wrote the chapters 2.1 and 2.4, Z.T. contributed to chapter 2.5, M.M. contributed to chapter 2.2. All authors participated on the introduction part and revised the manuscript.

Conflicts of Interest: The authors declare no conflict of interest.

References

1. Zeman, M.K.; Cimprich, K.A. Causes and consequences of replication stress. *Nat. Cell Biol.* **2014**, *16*, 2–9. [CrossRef] [PubMed]
2. Burhans, W.C.; Weinberger, M. DNA replication stress, genome instability and aging. *Nucleic Acids Res.* **2007**, *35*, 7545–7556. [CrossRef] [PubMed]
3. Huh, M.S.; Ivanochko, D.; Hashem, L.E.; Curtin, M.; Delorme, M.; Goodall, E.; Yan, K.; Picketts, D.J. Stalled replication forks within heterochromatin require ATRX for protection. *Cell Death Dis.* **2016**, *7*, e2220. [CrossRef] [PubMed]
4. Gelot, C.; Magdalou, I.; Lopez, B.S. Replication stress in Mammalian cells and its consequences for mitosis. *Genes* **2015**, *6*, 267–298. [CrossRef] [PubMed]
5. Krasilnikova, M.M.; Mirkin, S.M. Replication stalling at Friedreich's ataxia $(GAA)_n$ repeats in vivo. *Mol. Cell. Biol.* **2004**, *24*, 2286–2295. [CrossRef] [PubMed]
6. Neelsen, K.J.; Zanini, I.M.Y.; Mijic, S.; Herrador, R.; Zellweger, R.; Ray Chaudhuri, A.; Creavin, K.D.; Blow, J.J.; Lopes, M. Deregulated origin licensing leads to chromosomal breaks by rereplication of a gapped DNA template. *Genes Dev.* **2013**, *27*, 2537–2542. [CrossRef] [PubMed]
7. Porter, A.C. Preventing DNA over-replication: A Cdk perspective. *Cell Div.* **2008**, *3*, 3. [CrossRef] [PubMed]
8. Burrell, R.A.; McClelland, S.E.; Endesfelder, D.; Groth, P.; Weller, M.-C.; Shaikh, N.; Domingo, E.; Kanu, N.; Dewhurst, S.M.; Gronroos, E.; et al. Replication stress links structural and numerical cancer chromosomal instability. *Nature* **2013**, *494*, 492–496. [CrossRef] [PubMed]
9. Liu, B.; Alberts, B.M. Head-on collision between a DNA replication apparatus and RNA polymerase transcription complex. *Science* **1995**, *267*, 1131–1137. [CrossRef] [PubMed]
10. Bartkova, J.; Rezaei, N.; Liontos, M.; Karakaidos, P.; Kletsas, D.; Issaeva, N.; Vassiliou, L.-V.F.; Kolettas, E.; Niforou, K.; Zoumpourlis, V.C.; et al. Oncogene-induced senescence is part of the tumorigenesis barrier imposed by DNA damage checkpoints. *Nature* **2006**, *444*, 633–637. [CrossRef] [PubMed]
11. Vallerga, M.B.; Mansilla, S.F.; Federico, M.B.; Bertolin, A.P.; Gottifredi, V. Rad51 recombinase prevents Mre11 nuclease-dependent degradation and excessive PrimPol-mediated elongation of nascent DNA after UV irradiation. *Proc. Natl. Acad. Sci. USA* **2015**, *112*, E6624–E6633. [CrossRef] [PubMed]
12. Mazouzi, A.; Velimezi, G.; Loizou, J.I. DNA replication stress: Causes, resolution and disease. *Exp. Cell Res.* **2014**, *329*, 85–93. [CrossRef] [PubMed]
13. Jekimovs, C.; Bolderson, E.; Suraweera, A.; Adams, M.; O'Byrne, K.J.; Richard, D.J. Chemotherapeutic compounds targeting the DNA double-strand break repair pathways: The good, the bad, and the promising. *Front. Oncol.* **2014**, *4*, 86. [CrossRef] [PubMed]
14. Beranek, D.T. Distribution of methyl and ethyl adducts following alkylation with monofunctional alkylating agents. *Mutat. Res.* **1990**, *231*, 11–30. [CrossRef]
15. Kondo, N.; Takahashi, A.; Mori, E.; Noda, T.; Su, X.; Ohnishi, K.; McKinnon, P.J.; Sakaki, T.; Nakase, H.; Ono, K.; et al. DNA ligase IV is a potential molecular target in ACNU sensitivity. *Cancer Sci.* **2010**, *101*, 1881–1885. [CrossRef] [PubMed]
16. Brookes, P.; Lawley, P.D. The reaction of mono- and di-functional alkylating agents with nucleic acids. *Biochem. J.* **1961**, *80*, 496–503. [CrossRef] [PubMed]
17. Lawley, P.D.; Brookes, P. The action of alkylating agents on deoxyribonucleic acid in relation to biological effects of the alkylating agents. *Exp. Cell Res.* **1963**, *24* (Suppl. S9), 512–520. [CrossRef]
18. Noll, D.M.; Mason, T.M.; Miller, P.S. Formation and repair of interstrand cross-links in DNA. *Chem. Rev.* **2006**, *106*, 277–301. [CrossRef] [PubMed]
19. Schärer, O.D. DNA Interstrand Crosslinks: Natural and Drug-Induced DNA Adducts that Induce Unique Cellular Responses. *ChemBioChem* **2005**, *6*, 27–32. [CrossRef] [PubMed]
20. Lawley, P.D.; Phillips, D.H. DNA adducts from chemotherapeutic agents. *Mutat. Res.* **1996**, *355*, 13–40. [CrossRef]

21. Bhuyan, B.K.; Scheidt, L.G.; Fraser, T.J. Cell cycle phase specificity of antitumor agents. *Cancer Res.* **1972**, *32*, 398–407. [PubMed]
22. Glover, T.W.; Arlt, M.F.; Casper, A.M.; Durkin, S.G. Mechanisms of common fragile site instability. *Hum. Mol. Genet.* **2005**, *14*, R197–R205. [CrossRef] [PubMed]
23. Koç, A.; Wheeler, L.J.; Mathews, C.K.; Merrill, G.F. Hydroxyurea arrests DNA replication by a mechanism that preserves basal dNTP pools. *J. Biol. Chem.* **2004**, *279*, 223–230. [CrossRef] [PubMed]
24. Hsiang, Y.H.; Lihou, M.G.; Liu, L.F. Arrest of replication forks by drug-stabilized topoisomerase I-DNA cleavable complexes as a mechanism of cell killing by camptothecin. *Cancer Res.* **1989**, *49*, 5077–5082. [PubMed]
25. Deweese, J.E.; Osheroff, N. The DNA cleavage reaction of topoisomerase II: Wolf in sheep's clothing. *Nucleic Acids Res.* **2009**, *37*, 738–748. [CrossRef] [PubMed]
26. Helleday, T.; Petermann, E.; Lundin, C.; Hodgson, B.; Sharma, R.A. DNA repair pathways as targets for cancer therapy. *Nat. Rev. Cancer* **2008**, *8*, 193–204. [CrossRef] [PubMed]
27. Krokan, H.E.; Bjørås, M. Base Excision Repair. *Cold Spring Harb. Perspect. Biol.* **2013**, *5*, a012583. [CrossRef] [PubMed]
28. Gillet, L.C.J.; Schärer, O.D. Molecular mechanisms of mammalian global genome nucleotide excision repair. *Chem. Rev.* **2006**, *106*, 253–276. [CrossRef] [PubMed]
29. Caldecott, K.W. Protein ADP-ribosylation and the cellular response to DNA strand breaks. *DNA Repair* **2014**, *19*, 108–113. [CrossRef] [PubMed]
30. Heyer, W.-D.; Ehmsen, K.T.; Liu, J. Regulation of homologous recombination in eukaryotes. *Annu. Rev. Genet.* **2010**, *44*, 113–139. [CrossRef] [PubMed]
31. Davis, A.J.; Chen, D.J. DNA double strand break repair via non-homologous end-joining. *Transl. Cancer Res.* **2013**, *2*, 130–143. [PubMed]
32. Bi, X. Mechanism of DNA damage tolerance. *World J. Biol. Chem.* **2015**, *6*, 48–56. [CrossRef] [PubMed]
33. Aguilera, A.; Gómez-González, B. Genome instability: A mechanistic view of its causes and consequences. *Nat. Rev. Genet.* **2008**, *9*, 204–217. [CrossRef] [PubMed]
34. Chang, D.J.; Cimprich, K.A. DNA damage tolerance: When it's OK to make mistakes. *Nat. Chem. Biol.* **2009**, *5*, 82–90. [CrossRef] [PubMed]
35. Ghosal, G.; Chen, J. DNA damage tolerance: A double-edged sword guarding the genome. *Transl. Cancer Res.* **2013**, *2*, 107–129. [PubMed]
36. Saugar, I.; Ortiz-Bazán, M.Á.; Tercero, J.A. Tolerating DNA damage during eukaryotic chromosome replication. *Exp. Cell Res.* **2014**, *329*, 170–177. [CrossRef] [PubMed]
37. Deans, A.J.; West, S.C. DNA interstrand crosslink repair and cancer. *Nat. Rev. Cancer* **2011**, *11*, 467–480. [CrossRef] [PubMed]
38. Longerich, S.; Li, J.; Xiong, Y.; Sung, P.; Kupfer, G.M. Stress and DNA repair biology of the Fanconi anemia pathway. *Blood* **2014**, *124*, 2812–2819. [CrossRef] [PubMed]
39. Gaillard, H.; García-Muse, T.; Aguilera, A. Replication stress and cancer. *Nat. Rev. Cancer* **2015**, *15*, 276–289. [CrossRef] [PubMed]
40. Mamrak, N.E.; Shimamura, A.; Howlett, N.G. Recent discoveries in the molecular pathogenesis of the inherited bone marrow failure syndrome Fanconi anemia. *Blood Rev.* **2016**. [CrossRef] [PubMed]
41. Kennedy, R.D.; D'Andrea, A.D. The Fanconi Anemia/BRCA pathway: New faces in the crowd. *Genes Dev.* **2005**, *19*, 2925–2940. [CrossRef] [PubMed]
42. Thompson, L.H.; Hinz, J.M. Cellular and molecular consequences of defective Fanconi anemia proteins in replication-coupled DNA repair: Mechanistic insights. *Mutat. Res.* **2009**, *668*, 54–72. [CrossRef] [PubMed]
43. Branzei, D. Ubiquitin family modifications and template switching. *FEBS Lett.* **2011**, *585*, 2810–2817. [CrossRef] [PubMed]
44. Xu, X.; Blackwell, S.; Lin, A.; Li, F.; Qin, Z.; Xiao, W. Error-free DNA-damage tolerance in *Saccharomyces cerevisiae*. *Mutat. Res. Rev. Mutat. Res.* **2015**, *764*, 43–50. [CrossRef] [PubMed]
45. Ge, X.Q.; Jackson, D.A.; Blow, J.J. Dormant origins licensed by excess Mcm2–7 are required for human cells to survive replicative stress. *Genes Dev.* **2007**, *21*, 3331–3341. [CrossRef] [PubMed]
46. Lopes, M.; Foiani, M.; Sogo, J.M. Multiple mechanisms control chromosome integrity after replication fork uncoupling and restart at irreparable UV lesions. *Mol. Cell* **2006**, *21*, 15–27. [CrossRef] [PubMed]

47. Woodward, A.M.; Göhler, T.; Luciani, M.G.; Oehlmann, M.; Ge, X.; Gartner, A.; Jackson, D.A.; Blow, J.J. Excess Mcm2–7 license dormant origins of replication that can be used under conditions of replicative stress. *J. Cell Biol.* **2006**, *173*, 673–683. [CrossRef] [PubMed]
48. Elvers, I.; Johansson, F.; Groth, P.; Erixon, K.; Helleday, T. UV stalled replication forks restart by re-priming in human fibroblasts. *Nucleic Acids Res.* **2011**, *39*, 7049–7057. [CrossRef] [PubMed]
49. McIntosh, D.; Blow, J.J. Dormant origins, the licensing checkpoint, and the response to replicative stresses. *Cold Spring Harb. Perspect. Biol.* **2012**, *4*, a012955. [CrossRef] [PubMed]
50. De Piccoli, G.; Katou, Y.; Itoh, T.; Nakato, R.; Shirahige, K.; Labib, K. Replisome stability at defective DNA replication forks is independent of S phase checkpoint kinases. *Mol. Cell* **2012**, *45*, 696–704. [CrossRef] [PubMed]
51. Tercero, J.A.; Diffley, J.F.X. Regulation of DNA replication fork progression through damaged DNA by the Mec1/Rad53 checkpoint. *Nature* **2001**, *412*, 553–557. [CrossRef] [PubMed]
52. Lopes, M.; Cotta-Ramusino, C.; Pellicioli, A.; Liberi, G.; Plevani, P.; Muzi-Falconi, M.; Newlon, C.S.; Foiani, M. The DNA replication checkpoint response stabilizes stalled replication forks. *Nature* **2001**, *412*, 557–561. [CrossRef] [PubMed]
53. Cobb, J.A.; Bjergbaek, L.; Shimada, K.; Frei, C.; Gasser, S.M. DNA polymerase stabilization at stalled replication forks requires Mec1 and the RecQ helicase Sgs1. *EMBO J.* **2003**, *22*, 4325–4336. [CrossRef] [PubMed]
54. Ragland, R.L.; Patel, S.; Rivard, R.S.; Smith, K.; Peters, A.A.; Bielinsky, A.-K.; Brown, E.J. RNF4 and PLK1 are required for replication fork collapse in ATR-deficient cells. *Genes Dev.* **2013**, *27*, 2259–2273. [CrossRef] [PubMed]
55. Hanada, K.; Budzowska, M.; Davies, S.L.; van Drunen, E.; Onizawa, H.; Beverloo, H.B.; Maas, A.; Essers, J.; Hickson, I.D.; Kanaar, R. The structure-specific endonuclease Mus81 contributes to replication restart by generating double-strand DNA breaks. *Nat. Struct. Mol. Biol.* **2007**, *14*, 1096–1104. [CrossRef] [PubMed]
56. Forment, J.V.; Blasius, M.; Guerini, I.; Jackson, S.P. Structure-specific DNA endonuclease Mus81/Eme1 generates DNA damage caused by Chk1 inactivation. *PLoS ONE* **2011**, *6*, e23517. [CrossRef] [PubMed]
57. Zellweger, R.; Dalcher, D.; Mutreja, K.; Berti, M.; Schmid, J.A.; Herrador, R.; Vindigni, A.; Lopes, M. Rad51-mediated replication fork reversal is a global response to genotoxic treatments in human cells. *J. Cell Biol.* **2015**, *208*, 563–579. [CrossRef] [PubMed]
58. Pacek, M.; Walter, J.C. A requirement for MCM7 and Cdc45 in chromosome unwinding during eukaryotic DNA replication. *EMBO J.* **2004**, *23*, 3667–3676. [CrossRef] [PubMed]
59. Byun, T.S.; Pacek, M.; Yee, M.; Walter, J.C.; Cimprich, K.A. Functional uncoupling of MCM helicase and DNA polymerase activities activates the ATR-dependent checkpoint. *Genes Dev.* **2005**, *19*, 1040–1052. [CrossRef] [PubMed]
60. Zou, L.; Elledge, S.J. Sensing DNA damage through ATRIP recognition of RPA-ssDNA complexes. *Science* **2003**, *300*, 1542–1548. [CrossRef] [PubMed]
61. MacDougall, C.A.; Byun, T.S.; Van, C.; Yee, M.; Cimprich, K.A. The structural determinants of checkpoint activation. *Genes Dev.* **2007**, *21*, 898–903. [CrossRef] [PubMed]
62. Nam, E.A.; Cortez, D. ATR signalling: More than meeting at the fork. *Biochem. J.* **2011**, *436*, 527–536. [CrossRef] [PubMed]
63. Maréchal, A.; Zou, L. DNA damage sensing by the ATM and ATR kinases. *Cold Spring Harb. Perspect. Biol.* **2013**, *5*, a012716. [CrossRef] [PubMed]
64. Lucca, C.; Vanoli, F.; Cotta-Ramusino, C.; Pellicioli, A.; Liberi, G.; Haber, J.; Foiani, M. Checkpoint-mediated control of replisome-fork association and signalling in response to replication pausing. *Oncogene* **2004**, *23*, 1206–1213. [CrossRef] [PubMed]
65. Petermann, E.; Orta, M.L.; Issaeva, N.; Schultz, N.; Helleday, T. Hydroxyurea-stalled replication forks become progressively inactivated and require two different RAD51-mediated pathways for restart and repair. *Mol. Cell* **2010**, *37*, 492–502. [CrossRef] [PubMed]
66. Labib, K.; De Piccoli, G. Surviving chromosome replication: The many roles of the S-phase checkpoint pathway. *Philos. Trans. R. Soc. Lond. B Biol. Sci.* **2011**, *366*, 3554–3561. [CrossRef] [PubMed]
67. Ozeri-Galai, E.; Schwartz, M.; Rahat, A.; Kerem, B. Interplay between ATM and ATR in the regulation of common fragile site stability. *Oncogene* **2008**, *27*, 2109–2117. [CrossRef] [PubMed]

68. Ciccia, A.; Elledge, S.J. The DNA damage response: Making it safe to play with knives. *Mol. Cell* **2010**, *40*, 179–204. [CrossRef] [PubMed]
69. Ammazzalorso, F.; Pirzio, L.M.; Bignami, M.; Franchitto, A.; Pichierri, P. ATR and ATM differently regulate WRN to prevent DSBs at stalled replication forks and promote replication fork recovery. *EMBO J.* **2010**, *29*, 3156–3169. [CrossRef] [PubMed]
70. Bachrati, C.Z.; Hickson, I.D. RecQ helicases: Suppressors of tumorigenesis and premature aging. *Biochem. J.* **2003**, *374*, 577–606. [CrossRef] [PubMed]
71. Hills, S.A.; Diffley, J.F.X. DNA replication and oncogene-induced replicative stress. *Curr. Biol.* **2014**, *24*, R435–R444. [CrossRef] [PubMed]
72. Macheret, M.; Halazonetis, T.D. DNA replication stress as a hallmark of cancer. *Annu. Rev. Pathol.* **2015**, *10*, 425–448. [CrossRef] [PubMed]
73. Murga, M.; Campaner, S.; Lopez-Contreras, A.J.; Toledo, L.I.; Soria, R.; Montaña, M.F.; D'Artista, L.; Schleker, T.; Guerra, C.; Garcia, E.; et al. Exploiting oncogene-induced replicative stress for the selective killing of Myc-driven tumors. *Nat. Struct. Mol. Biol.* **2011**, *18*, 1331–1335. [CrossRef] [PubMed]
74. Marusyk, A.; Wheeler, L.J.; Mathews, C.K.; DeGregori, J. p53 mediates senescence-like arrest induced by chronic replicational stress. *Mol. Cell. Biol.* **2007**, *27*, 5336–5351. [CrossRef] [PubMed]
75. Bai, G.; Smolka, M.B.; Schimenti, J.C. Chronic DNA Replication Stress Reduces Replicative Lifespan of Cells by TRP53-Dependent, microRNA-Assisted MCM2–7 Downregulation. *PLoS Genet.* **2016**, *12*, e1005787. [CrossRef] [PubMed]
76. Bartkova, J.; Horejsí, Z.; Koed, K.; Krämer, A.; Tort, F.; Zieger, K.; Guldberg, P.; Sehested, M.; Nesland, J.M.; Lukas, C.; et al. DNA damage response as a candidate anti-cancer barrier in early human tumorigenesis. *Nature* **2005**, *434*, 864–870. [CrossRef] [PubMed]
77. O'Driscoll, M.; Ruiz-Perez, V.L.; Woods, C.G.; Jeggo, P.A.; Goodship, J.A. A splicing mutation affecting expression of ataxia-telangiectasia and Rad3-related protein (ATR) results in Seckel syndrome. *Nat. Genet.* **2003**, *33*, 497–501. [CrossRef] [PubMed]
78. McKinnon, P.J. ATM and ataxia telangiectasia. *EMBO Rep.* **2004**, *5*, 772–776. [CrossRef] [PubMed]
79. DiGiovanna, J.J.; Kraemer, K.H. Shining a light on xeroderma pigmentosum. *J. Investig. Dermatol.* **2012**, *132*, 785–796. [CrossRef] [PubMed]
80. Callén, E.; Surrallés, J. Telomere dysfunction in genome instability syndromes. *Mutat. Res.* **2004**, *567*, 85–104. [CrossRef] [PubMed]
81. Lauper, J.M.; Krause, A.; Vaughan, T.L.; Monnat, R.J. Spectrum and risk of neoplasia in Werner syndrome: A systematic review. *PLoS ONE* **2013**, *8*, e59709. [CrossRef] [PubMed]
82. Bernstein, K.A.; Gangloff, S.; Rothstein, R. The RecQ DNA helicases in DNA repair. *Annu. Rev. Genet.* **2010**, *44*, 393–417. [CrossRef] [PubMed]
83. Kim, H.; D'Andrea, A.D. Regulation of DNA cross-link repair by the Fanconi anemia/BRCA pathway. *Genes Dev.* **2012**, *26*, 1393–1408. [CrossRef] [PubMed]
84. Joenje, H.; Patel, K.J. The emerging genetic and molecular basis of Fanconi anaemia. *Nat. Rev. Genet.* **2001**, *2*, 446–457. [CrossRef] [PubMed]
85. Larizza, L.; Roversi, G.; Volpi, L. Rothmund-Thomson syndrome. *Orphanet J. Rare Dis.* **2010**, *5*, 2. [CrossRef] [PubMed]
86. Lu, H.; Shamanna, R.A.; Keijzers, G.; Anand, R.; Rasmussen, L.J.; Cejka, P.; Croteau, D.L.; Bohr, V.A. RECQL4 Promotes DNA End Resection in Repair of DNA Double-Strand Breaks. *Cell Rep.* **2016**, *16*, 161–173. [CrossRef] [PubMed]
87. Rosenberg, B.; Vancamp, L.; Krigas, T. Inhibition of cell division in *Escherichia coli* by electrolysis products from a platinum electrode. *Nature* **1965**, *205*, 698–699. [CrossRef] [PubMed]
88. Todd, R.C.; Lippard, S.J. Inhibition of transcription by platinum antitumor compounds. *Metallomics* **2009**, *1*, 280–291. [CrossRef] [PubMed]
89. Zamble, D.B.; Lippard, S.J. Cisplatin and DNA repair in cancer chemotherapy. *Trends Biochem. Sci.* **1995**, *20*, 435–439. [CrossRef]
90. Available online: http://www.rcsb.org/pdb/explore/explore.do?structureId=3CO3 (accessed on 23 January 2017).

91. Fichtinger-Schepman, A.M.; van der Veer, J.L.; den Hartog, J.H.; Lohman, P.H.; Reedijk, J. Adducts of the antitumor drug *cis*-diamminedichloroplatinum(II) with DNA: Formation, identification, and quantitation. *Biochemistry* **1985**, *24*, 707–713. [CrossRef] [PubMed]
92. Harder, H.C.; Rosenberg, B. Inhibitory effects of anti-tumor platinum compounds on DNA, RNA and protein syntheses in mammalian cells in virtro. *Int. J. Cancer* **1970**, *6*, 207–216. [CrossRef] [PubMed]
93. Eastman, A. Reevaluation of interaction of *cis*-dichloro(ethylenediamine)platinum(II) with DNA. *Biochemistry* **1986**, *25*, 3912–3915. [CrossRef] [PubMed]
94. Sherman, S.E.; Gibson, D.; Wang, A.H.; Lippard, S.J. X-ray structure of the major adduct of the anticancer drug cisplatin with DNA: *cis*-[Pt(NH3)2(d(pGpG))]. *Science* **1985**, *230*, 412–417. [CrossRef] [PubMed]
95. Eastman, A. Separation and characterization of products resulting from the reaction of *cis*-diamminedichloroplatinum (II) with deoxyribonucleosides. *Biochemistry* **1982**, *21*, 6732–6736. [CrossRef] [PubMed]
96. Desoize, B. Cancer and metals and metal compounds: Part I—Carcinogenesis. *Crit. Rev. Oncol. Hematol.* **2002**, *42*, 1–3. [CrossRef]
97. Köberle, B.; Masters, J.R.; Hartley, J.A.; Wood, R.D. Defective repair of cisplatin-induced DNA damage caused by reduced XPA protein in testicular germ cell tumours. *Curr. Biol.* **1999**, *9*, 273–276. [CrossRef]
98. Borst, P.; Rottenberg, S.; Jonkers, J. How do real tumors become resistant to cisplatin? *Cell Cycle* **2008**, *7*, 1353–1359. [CrossRef] [PubMed]
99. Sedletska, Y.; Fourrier, L.; Malinge, J.-M. Modulation of MutS ATP-dependent functional activities by DNA containing a cisplatin compound lesion (base damage and mismatch). *J. Mol. Biol.* **2007**, *369*, 27–40. [CrossRef] [PubMed]
100. Brown, R.; Clugston, C.; Burns, P.; Edlin, A.; Vasey, P.; Vojtěsek, B.; Kaye, S.B. Increased accumulation of p53 protein in cisplatin-resistant ovarian cell lines. *Int. J. Cancer* **1993**, *55*, 678–684. [CrossRef] [PubMed]
101. Damsma, G.E.; Alt, A.; Brueckner, F.; Carell, T.; Cramer, P. Mechanism of transcriptional stalling at cisplatin-damaged DNA. *Nat. Struct. Mol. Biol.* **2007**, *14*, 1127–1133. [CrossRef] [PubMed]
102. Shimodaira, H.; Yoshioka-Yamashita, A.; Kolodner, R.D.; Wang, J.Y.J. Interaction of mismatch repair protein PMS2 and the p53-related transcription factor p73 in apoptosis response to cisplatin. *Proc. Natl. Acad. Sci. USA* **2003**, *100*, 2420–2425. [CrossRef] [PubMed]
103. Aebi, S.; Kurdi-Haidar, B.; Gordon, R.; Cenni, B.; Zheng, H.; Fink, D.; Christen, R.D.; Boland, C.R.; Koi, M.; Fishel, R.; et al. Loss of DNA mismatch repair in acquired resistance to cisplatin. *Cancer Res.* **1996**, *56*, 3087–3090. [PubMed]
104. Alt, A.; Lammens, K.; Chiocchini, C.; Lammens, A.; Pieck, J.C.; Kuch, D.; Hopfner, K.-P.; Carell, T. Bypass of DNA lesions generated during anticancer treatment with cisplatin by DNA polymerase eta. *Science* **2007**, *318*, 967–970. [CrossRef] [PubMed]
105. Brozovic, A.; Ambriović-Ristov, A.; Osmak, M. The relationship between cisplatin-induced reactive oxygen species, glutathione, and BCL-2 and resistance to cisplatin. *Crit. Rev. Toxicol.* **2010**, *40*, 347–359. [CrossRef] [PubMed]
106. Splettstoesser, F.; Florea, A.-M.; Büsselberg, D. IP_3 receptor antagonist, 2-APB, attenuates cisplatin induced Ca^{2+}-influx in HeLa-S3 cells and prevents activation of calpain and induction of apoptosis. *Br. J. Pharmacol.* **2007**, *151*, 1176–1186. [CrossRef] [PubMed]
107. Shamimi-Noori, S.; Yeow, W.-S.; Ziauddin, M.F.; Xin, H.; Tran, T.L.N.; Xie, J.; Loehfelm, A.; Patel, P.; Yang, J.; Schrump, D.S.; et al. Cisplatin enhances the antitumor effect of tumor necrosis factor-related apoptosis-inducing ligand gene therapy via recruitment of the mitochondria-dependent death signaling pathway. *Cancer Gene Ther.* **2008**, *15*, 356–370. [CrossRef] [PubMed]
108. Qian, W.; Nishikawa, M.; Haque, A.M.; Hirose, M.; Mashimo, M.; Sato, E.; Inoue, M. Mitochondrial density determines the cellular sensitivity to cisplatin-induced cell death. *Am. J. Physiol. Cell Physiol.* **2005**, *289*, C1466–C1475. [CrossRef] [PubMed]
109. Wetzel, C.C.; Berberich, S.J. p53 binds to cisplatin-damaged DNA. *Biochim. Biophys. Acta* **2001**, *1517*, 392–397. [CrossRef]
110. Kutuk, O.; Arisan, E.D.; Tezil, T.; Shoshan, M.C.; Basaga, H. Cisplatin overcomes Bcl-2-mediated resistance to apoptosis via preferential engagement of Bak: Critical role of Noxa-mediated lipid peroxidation. *Carcinogenesis* **2009**, *30*, 1517–1527. [CrossRef] [PubMed]

111. Kim, H.-S.; Hwang, J.-T.; Yun, H.; Chi, S.-G.; Lee, S.-J.; Kang, I.; Yoon, K.-S.; Choe, W.-J.; Kim, S.-S.; Ha, J. Inhibition of AMP-activated protein kinase sensitizes cancer cells to cisplatin-induced apoptosis via hyper-induction of p53. *J. Biol. Chem.* **2008**, *283*, 3731–3742. [CrossRef] [PubMed]
112. Yang, C.; Kaushal, V.; Haun, R.S.; Seth, R.; Shah, S.V.; Kaushal, G.P. Transcriptional activation of caspase-6 and -7 genes by cisplatin-induced p53 and its functional significance in cisplatin nephrotoxicity. *Cell Death Differ.* **2008**, *15*, 530–544. [CrossRef] [PubMed]
113. Jiang, M.; Wei, Q.; Wang, J.; Du, Q.; Yu, J.; Zhang, L.; Dong, Z. Regulation of PUMA-alpha by p53 in cisplatin-induced renal cell apoptosis. *Oncogene* **2006**, *25*, 4056–4066. [CrossRef] [PubMed]
114. Righetti, S.C.; Della Torre, G.; Pilotti, S.; Ménard, S.; Ottone, F.; Colnaghi, M.I.; Pierotti, M.A.; Lavarino, C.; Cornarotti, M.; Oriana, S.; et al. A comparative study of p53 gene mutations, protein accumulation, and response to cisplatin-based chemotherapy in advanced ovarian carcinoma. *Cancer Res.* **1996**, *56*, 689–693. [PubMed]
115. Johnson, C.L.; Lu, D.; Huang, J.; Basu, A. Regulation of p53 stabilization by DNA damage and protein kinase C. *Mol. Cancer Ther.* **2002**, *1*, 861–867. [PubMed]
116. Gong, J.G.; Costanzo, A.; Yang, H.Q.; Melino, G.; Kaelin, W.G.; Levrero, M.; Wang, J.Y. The tyrosine kinase c-Abl regulates p73 in apoptotic response to cisplatin-induced DNA damage. *Nature* **1999**, *399*, 806–809. [PubMed]
117. Preyer, M.; Shu, C.-W.; Wang, J.Y.J. Delayed activation of Bax by DNA damage in embryonic stem cells with knock-in mutations of the Abl nuclear localization signals. *Cell Death Differ.* **2007**, *14*, 1139–1148. [CrossRef] [PubMed]
118. Tsai, K.K.C.; Yuan, Z.-M. c-Abl stabilizes p73 by a phosphorylation-augmented interaction. *Cancer Res.* **2003**, *63*, 3418–3424. [PubMed]
119. Levy, D.; Adamovich, Y.; Reuven, N.; Shaul, Y. Yap1 phosphorylation by c-Abl is a critical step in selective activation of proapoptotic genes in response to DNA damage. *Mol. Cell* **2008**, *29*, 350–361. [CrossRef] [PubMed]
120. Jones, E.V.; Dickman, M.J.; Whitmarsh, A.J. Regulation of p73-mediated apoptosis by c-Jun N-terminal kinase. *Biochem. J.* **2007**, *405*, 617–623. [CrossRef] [PubMed]
121. Hayakawa, J.; Ohmichi, M.; Kurachi, H.; Kanda, Y.; Hisamoto, K.; Nishio, Y.; Adachi, K.; Tasaka, K.; Kanzaki, T.; Murata, Y. Inhibition of BAD phosphorylation either at serine 112 via extracellular signal-regulated protein kinase cascade or at serine 136 via Akt cascade sensitizes human ovarian cancer cells to cisplatin. *Cancer Res.* **2000**, *60*, 5988–5994. [PubMed]
122. Isonishi, S.; Andrews, P.A.; Howell, S.B. Increased sensitivity to *cis*-diamminedichloroplatinum(II) in human ovarian carcinoma cells in response to treatment with 12-*O*-tetradecanoylphorbol 13-acetate. *J. Biol. Chem.* **1990**, *265*, 3623–3627. [PubMed]
123. Basu, A.; Teicher, B.A.; Lazo, J.S. Involvement of protein kinase C in phorbol ester-induced sensitization of HeLa cells to *cis*-diamminedichloroplatinum(II). *J. Biol. Chem.* **1990**, *265*, 8451–8457. [PubMed]
124. Wang, X.; Dhalla, N.S. Modification of beta-adrenoceptor signal transduction pathway by genetic manipulation and heart failure. *Mol. Cell. Biochem.* **2000**, *214*, 131–155. [CrossRef] [PubMed]
125. Basu, A.; Tu, H. Activation of ERK during DNA damage-induced apoptosis involves protein kinase Cdelta. *Biochem. Biophys. Res. Commun.* **2005**, *334*, 1068–1073. [CrossRef] [PubMed]
126. Nowak, G. Protein kinase C-alpha and ERK1/2 mediate mitochondrial dysfunction, decreases in active Na^+ transport, and cisplatin-induced apoptosis in renal cells. *J. Biol. Chem.* **2002**, *277*, 43377–43388. [CrossRef] [PubMed]
127. Sánchez-Pérez, I.; Benitah, S.A.; Martínez-Gomariz, M.; Lacal, J.C.; Perona, R. Cell stress and MEKK1-mediated c-Jun activation modulate NFκB activity and cell viability. *Mol. Biol. Cell* **2002**, *13*, 2933–2945. [CrossRef] [PubMed]
128. Jones, J.A.; Stroud, R.E.; Kaplan, B.S.; Leone, A.M.; Bavaria, J.E.; Gorman, J.H.; Gorman, R.C.; Ikonomidis, J.S. Differential protein kinase C isoform abundance in ascending aortic aneurysms from patients with bicuspid versus tricuspid aortic valves. *Circulation* **2007**, *116*, I144–I149. [CrossRef] [PubMed]
129. Zanke, B.W.; Boudreau, K.; Rubie, E.; Winnett, E.; Tibbles, L.A.; Zon, L.; Kyriakis, J.; Liu, F.F.; Woodgett, J.R. The stress-activated protein kinase pathway mediates cell death following injury induced by *cis*-platinum, UV irradiation or heat. *Curr. Biol.* **1996**, *6*, 606–613. [CrossRef]

130. Hernández Losa, J.; Parada Cobo, C.; Guinea Viniegra, J.; Sánchez-Arevalo Lobo, V.J.; Ramón y Cajal, S.; Sánchez-Prieto, R. Role of the p38 MAPK pathway in cisplatin-based therapy. *Oncogene* **2003**, *22*, 3998–4006. [CrossRef] [PubMed]
131. Wang, S.J.; Bourguignon, L.Y.W. Hyaluronan-CD44 promotes phospholipase C-mediated Ca^{2+} signaling and cisplatin resistance in head and neck cancer. *Arch. Otolaryngol. Head Neck Surg.* **2006**, *132*, 19–24. [CrossRef] [PubMed]
132. Speelmans, G.; Staffhorst, R.W.; Versluis, K.; Reedijk, J.; de Kruijff, B. Cisplatin complexes with phosphatidylserine in membranes. *Biochemistry* **1997**, *36*, 10545–10550. [CrossRef] [PubMed]
133. Huihui, Z.; Baohuai, W.; Youming, Z.; Kui, W. Calorimetric studies on actin polymerization and a comparison of the effects of cisplatin and transplatin. *Thermochim. Acta* **1995**, *265*, 31–38. [CrossRef]
134. Chen, X.; Jiang, Y.; Huang, Z.; Li, D.; Chen, X.; Cao, M.; Meng, Q.; Pang, H.; Sun, L.; Zhao, Y.; et al. miRNA-378 reverses chemoresistance to cisplatin in lung adenocarcinoma cells by targeting secreted clusterin. *Sci. Rep.* **2016**, *6*, 19455. [CrossRef] [PubMed]
135. Zhu, H.; Wu, H.; Liu, X.; Evans, B.R.; Medina, D.J.; Liu, C.-G.; Yang, J.-M. Role of MicroRNA miR-27a and miR-451 in the regulation of MDR1/P-glycoprotein expression in human cancer cells. *Biochem. Pharmacol.* **2008**, *76*, 582–588. [CrossRef] [PubMed]
136. Vanas, V.; Haigl, B.; Stockhammer, V.; Sutterlüty-Fall, H. MicroRNA-21 Increases Proliferation and Cisplatin Sensitivity of Osteosarcoma-Derived Cells. *PLoS ONE* **2016**, *11*, e0161023. [CrossRef] [PubMed]
137. Douple, E.B.; Richmond, R.C. Platinum complexes as radiosensitizers of hypoxic mammalian cells. *Br. J. Cancer Suppl.* **1978**, *3*, 98–102. [PubMed]
138. Boeckman, H.J.; Trego, K.S.; Turchi, J.J. Cisplatin sensitizes cancer cells to ionizing radiation via inhibition of nonhomologous end joining. *Mol. Cancer Res.* **2005**, *3*, 277–285. [CrossRef] [PubMed]
139. Ishibashi, T.; Lippard, S.J. Telomere loss in cells treated with cisplatin. *Proc. Natl. Acad. Sci. USA* **1998**, *95*, 4219–4223. [CrossRef] [PubMed]
140. Jordan, P.; Carmo-Fonseca, M. Cisplatin inhibits synthesis of ribosomal RNA in vivo. *Nucleic Acids Res.* **1998**, *26*, 2831–2836. [CrossRef] [PubMed]
141. Tofilon, P.J.; Vines, C.M.; Baker, F.L.; Deen, D.F.; Brock, W.A. *cis*-Diamminedichloroplatinum(II)-induced sister chromatid exchange: An indicator of sensitivity and heterogeneity in primary human tumor cell cultures. *Cancer Res.* **1986**, *46*, 6156–6159. [PubMed]
142. Berndtsson, M.; Hägg, M.; Panaretakis, T.; Havelka, A.M.; Shoshan, M.C.; Linder, S. Acute apoptosis by cisplatin requires induction of reactive oxygen species but is not associated with damage to nuclear DNA. *Int. J. Cancer* **2007**, *120*, 175–180. [CrossRef] [PubMed]
143. Rouette, A.; Parent, S.; Girouard, J.; Leblanc, V.; Asselin, E. Cisplatin increases B-cell-lymphoma-2 expression via activation of protein kinase C and Akt2 in endometrial cancer cells. *Int. J. Cancer* **2012**, *130*, 1755–1767. [CrossRef] [PubMed]
144. Damia, G.; Filiberti, L.; Vikhanskaya, F.; Carrassa, L.; Taya, Y.; D'incalci, M.; Broggini, M. Cisplatinum and taxol induce different patterns of p53 phosphorylation. *Neoplasia* **2001**, *3*, 10–16. [CrossRef] [PubMed]
145. Lützkendorf, J.; Wieduwild, E.; Nerger, K.; Lambrecht, N.; Schmoll, H.-J.; Müller-Tidow, C.; Müller, L.P. Resistance for Genotoxic Damage in Mesenchymal Stromal Cells Is Increased by Hypoxia but Not Generally Dependent on p53-Regulated Cell Cycle Arrest. *PLoS ONE* **2017**, *12*, e0169921. [CrossRef] [PubMed]
146. Sorenson, C.M.; Barry, M.A.; Eastman, A. Analysis of events associated with cell cycle arrest at G2 phase and cell death induced by cisplatin. *J. Natl. Cancer Inst.* **1990**, *82*, 749–755. [CrossRef] [PubMed]
147. Podratz, J.L.; Knight, A.M.; Ta, L.E.; Staff, N.P.; Gass, J.M.; Genelin, K.; Schlattau, A.; Lathroum, L.; Windebank, A.J. Cisplatin induced mitochondrial DNA damage in dorsal root ganglion neurons. *Neurobiol. Dis.* **2011**, *41*, 661–668. [CrossRef] [PubMed]
148. Wagner, J.M.; Karnitz, L.M. Cisplatin-induced DNA damage activates replication checkpoint signaling components that differentially affect tumor cell survival. *Mol. Pharmacol.* **2009**, *76*, 208–214. [CrossRef] [PubMed]
149. Bürkle, A.; Chen, G.; Küpper, J.H.; Grube, K.; Zeller, W.J. Increased poly(ADP-ribosyl)ation in intact cells by cisplatin treatment. *Carcinogenesis* **1993**, *14*, 559–561. [CrossRef] [PubMed]
150. Jennerwein, M.; Andrews, P.A. Drug accumulation and DNA platination in cells exposed to aquated cisplatin species. *Cancer Lett.* **1994**, *81*, 215–220. [CrossRef]

151. Shirazi, F.H.; Molepo, J.M.; Stewart, D.J.; Ng, C.E.; Raaphorst, G.P.; Goel, R. Cytotoxicity, accumulation, and efflux of cisplatin and its metabolites in human ovarian carcinoma cells. *Toxicol. Appl. Pharmacol.* **1996**, *140*, 211–218. [CrossRef] [PubMed]
152. Hall, M.D.; Telma, K.A.; Chang, K.-E.; Lee, T.D.; Madigan, J.P.; Lloyd, J.R.; Goldlust, I.S.; Hoeschele, J.D.; Gottesman, M.M. Say no to DMSO: Dimethylsulfoxide inactivates cisplatin, carboplatin, and other platinum complexes. *Cancer Res.* **2014**, *74*, 3913–3922. [CrossRef] [PubMed]
153. Available online: http://www.webcitation.org/6mEemW8DM (accessed on 23 November 2016).
154. Massart, C.; Le Tellier, C.; Gibassier, J.; Leclech, G.; Nicol, M. Modulation by dimethyl sulphoxide of the toxicity induced by *cis*-diamminedichloroplatinum in cultured thyrocytes. *Toxicol. Vitro* **1993**, *7*, 87–94. [CrossRef]
155. Wiltshaw, E.; Subramarian, S.; Alexopoulos, C.; Barker, G.H. Cancer of the ovary: A summary of experience with *cis*-dichlorodiammineplatinum(II) at the Royal Marsden Hospital. *Cancer Treat. Rep.* **1979**, *63*, 1545–1548. [PubMed]
156. Galanski, M. Recent developments in the field of anticancer platinum complexes. *Recent Pat. Anticancer Drug Discov.* **2006**, *1*, 285–295. [CrossRef] [PubMed]
157. Lebwohl, D.; Canetta, R. Clinical development of platinum complexes in cancer therapy: An historical perspective and an update. *Eur. J. Cancer* **1998**, *34*, 1522–1534. [CrossRef]
158. Baetz, T.; Belch, A.; Couban, S.; Imrie, K.; Yau, J.; Myers, R.; Ding, K.; Paul, N.; Shepherd, L.; Iglesias, J.; et al. Gemcitabine, dexamethasone and cisplatin is an active and non-toxic chemotherapy regimen in relapsed or refractory Hodgkin's disease: A phase II study by the National Cancer Institute of Canada Clinical Trials Group. *Ann. Oncol.* **2003**, *14*, 1762–1767. [CrossRef] [PubMed]
159. Crump, M.; Baetz, T.; Couban, S.; Belch, A.; Marcellus, D.; Howson-Jan, K.; Imrie, K.; Myers, R.; Adams, G.; Ding, K.; et al. Gemcitabine, dexamethasone, and cisplatin in patients with recurrent or refractory aggressive histology B-cell non-Hodgkin lymphoma: A Phase II study by the National Cancer Institute of Canada Clinical Trials Group (NCIC-CTG). *Cancer* **2004**, *101*, 1835–1842. [CrossRef] [PubMed]
160. Pearson, A.D.J.; Pinkerton, C.R.; Lewis, I.J.; Imeson, J.; Ellershaw, C.; Machin, D.; European Neuroblastoma Study Group; Children's Cancer and Leukaemia Group (CCLG formerly United Kingdom Children's Cancer Study Group). High-dose rapid and standard induction chemotherapy for patients aged over 1 year with stage 4 neuroblastoma: A randomised trial. *Lancet Oncol.* **2008**, *9*, 247–256. [PubMed]
161. Reichardt, P. The treatment of uterine sarcomas. *Ann. Oncol.* **2012**, *23* (Suppl. S10), x151–x157. [CrossRef] [PubMed]
162. Dadacaridou, M.; Papanicolaou, X.; Maltesas, D.; Megalakaki, C.; Patos, P.; Panteli, K.; Repousis, P.; Mitsouli-Mentzikof, C. Dexamethasone, cyclophosphamide, etoposide and cisplatin (DCEP) for relapsed or refractory multiple myeloma patients. *J. BUON* **2007**, *12*, 41–44. [PubMed]
163. Glover, D.; Glick, J.H.; Weiler, C.; Fox, K.; Guerry, D. WR-2721 and high-dose cisplatin: An active combination in the treatment of metastatic melanoma. *J. Clin. Oncol.* **1987**, *5*, 574–578. [PubMed]
164. Berghmans, T.; Paesmans, M.; Lalami, Y.; Louviaux, I.; Luce, S.; Mascaux, C.; Meert, A.P.; Sculier, J.P. Activity of chemotherapy and immunotherapy on malignant mesothelioma: A systematic review of the literature with meta-analysis. *Lung Cancer* **2002**, *38*, 111–121. [CrossRef]
165. Hanada, K.; Nishijima, K.; Ogata, H.; Atagi, S.; Kawahara, M. Population pharmacokinetic analysis of cisplatin and its metabolites in cancer patients: Possible misinterpretation of covariates for pharmacokinetic parameters calculated from the concentrations of unchanged cisplatin, ultrafiltered platinum and total platinum. *Jpn. J. Clin. Oncol.* **2001**, *31*, 179–184. [PubMed]
166. Daugaard, G.; Abildgaard, U. Cisplatin nephrotoxicity. A review. *Cancer Chemother. Pharmacol.* **1989**, *25*, 1–9. [CrossRef] [PubMed]
167. Nagai, N.; Kinoshita, M.; Ogata, H.; Tsujino, D.; Wada, Y.; Someya, K.; Ohno, T.; Masuhara, K.; Tanaka, Y.; Kato, K.; et al. Relationship between pharmacokinetics of unchanged cisplatin and nephrotoxicity after intravenous infusions of cisplatin to cancer patients. *Cancer Chemother. Pharmacol.* **1996**, *39*, 131–137. [CrossRef] [PubMed]
168. Kartalou, M.; Essigmann, J.M. Mechanisms of resistance to cisplatin. *Mutat. Res.* **2001**, *478*, 23–43. [CrossRef]
169. Olszewski, U.; Hamilton, G. A better platinum-based anticancer drug yet to come? *Anticancer Agents Med. Chem.* **2010**, *10*, 293–301. [CrossRef] [PubMed]

170. Dieras, V.; Girre, V.; Guilhaume, M.-N.; Laurence, V.; Mignot, L. Oxaliplatin and ovarian cancer. *Bull. Cancer* **2006**, *93* (Suppl. S1), S35–S39. [PubMed]
171. Ganjavi, H.; Gee, M.; Narendran, A.; Parkinson, N.; Krishnamoorthy, M.; Freedman, M.H.; Malkin, D. Adenovirus-mediated p53 gene therapy in osteosarcoma cell lines: Sensitization to cisplatin and doxorubicin. *Cancer Gene Ther.* **2006**, *13*, 415–419. [CrossRef] [PubMed]
172. Michels, J.; Vitale, I.; Senovilla, L.; Enot, D.P.; Garcia, P.; Lissa, D.; Olaussen, K.A.; Brenner, C.; Soria, J.-C.; Castedo, M.; et al. Synergistic interaction between cisplatin and PARP inhibitors in non-small cell lung cancer. *Cell Cycle* **2013**, *12*, 877–883. [CrossRef] [PubMed]
173. Balmaña, J.; Tung, N.M.; Isakoff, S.J.; Graña, B.; Ryan, P.D.; Saura, C.; Lowe, E.S.; Frewer, P.; Winer, E.; Baselga, J.; et al. Phase I trial of olaparib in combination with cisplatin for the treatment of patients with advanced breast, ovarian and other solid tumors. *Ann. Oncol.* **2014**, *25*, 1656–1663. [CrossRef] [PubMed]
174. Sorenson, C.M.; Eastman, A. Influence of *cis*-diamminedichloroplatinum(II) on DNA synthesis and cell cycle progression in excision repair proficient and deficient Chinese hamster ovary cells. *Cancer Res.* **1988**, *48*, 6703–6707. [PubMed]
175. Vichi, P.; Coin, F.; Renaud, J.P.; Vermeulen, W.; Hoeijmakers, J.H.; Moras, D.; Egly, J.M. Cisplatin- and UV-damaged DNA lure the basal transcription factor TFIID/TBP. *EMBO J.* **1997**, *16*, 7444–7456. [CrossRef] [PubMed]
176. Cullinane, C.; Mazur, S.J.; Essigmann, J.M.; Phillips, D.R.; Bohr, V.A. Inhibition of RNA polymerase II transcription in human cell extracts by cisplatin DNA damage. *Biochemistry* **1999**, *38*, 6204–6212. [CrossRef] [PubMed]
177. Kumar, S.; Kumar, A.; Shah, P.P.; Rai, S.N.; Panguluri, S.K.; Kakar, S.S. MicroRNA signature of *cis*-platin resistant vs. *cis*-platin sensitive ovarian cancer cell lines. *J. Ovarian Res.* **2011**, *4*, 17. [PubMed]
178. Ciarimboli, G.; Ludwig, T.; Lang, D.; Pavenstädt, H.; Koepsell, H.; Piechota, H.-J.; Haier, J.; Jaehde, U.; Zisowsky, J.; Schlatter, E. Cisplatin nephrotoxicity is critically mediated via the human organic cation transporter 2. *Am. J. Pathol.* **2005**, *167*, 1477–1484. [CrossRef]
179. Gressette, M.; Vérillaud, B.; Jimenez-Pailhès, A.-S.; Lelièvre, H.; Lo, K.-W.; Ferrand, F.-R.; Gattolliat, C.-H.; Jacquet-Bescond, A.; Kraus-Berthier, L.; Depil, S.; et al. Treatment of Nasopharyngeal Carcinoma Cells with the Histone-Deacetylase Inhibitor Abexinostat: Cooperative Effects with Cis-platin and Radiotherapy on Patient-Derived Xenografts. *PLoS ONE* **2014**, *9*, e91325. [CrossRef] [PubMed]
180. Rout, S.R.; Behera, B.; Maiti, T.K.; Mohapatra, S. Multifunctional magnetic calcium phosphate nanoparticles for targeted platin delivery. *Dalton Trans.* **2012**, *41*, 10777–10783. [CrossRef] [PubMed]
181. Kitao, H.; Takata, M. Fanconi anemia: A disorder defective in the DNA damage response. *Int. J. Hematol.* **2011**, *93*, 417–424. [CrossRef] [PubMed]
182. Sawant, A.; Kothandapani, A.; Zhitkovich, A.; Sobol, R.W.; Patrick, S.M. Role of mismatch repair proteins in the processing of cisplatin interstrand cross-links. *DNA Repair* **2015**, *35*, 126–136. [CrossRef] [PubMed]
183. Cheng, C.H.; Kuchta, R.D. DNA polymerase epsilon: Aphidicolin inhibition and the relationship between polymerase and exonuclease activity. *Biochemistry* **1993**, *32*, 8568–8574. [CrossRef] [PubMed]
184. Pedrali-Noy, G.; Spadari, S.; Miller-Faurès, A.; Miller, A.O.; Kruppa, J.; Koch, G. Synchronization of HeLa cell cultures by inhibition of DNA polymerase alpha with aphidicolin. *Nucleic Acids Res.* **1980**, *8*, 377–387. [CrossRef] [PubMed]
185. Baranovskiy, A.G.; Babayeva, N.D.; Suwa, Y.; Gu, J.; Pavlov, Y.I.; Tahirov, T.H. Structural basis for inhibition of DNA replication by aphidicolin. *Nucleic Acids Res.* **2014**, *42*, 14013–14021. [CrossRef] [PubMed]
186. Spadari, S.; Pedrali-Noy, G.; Falaschi, M.C.; Ciarrocchi, G. Control of DNA replication and cell proliferation in eukaryotes by aphidicolin. *Toxicol. Pathol.* **1984**, *12*, 143–148. [CrossRef] [PubMed]
187. Available online: http://www.rcsb.org/pdb/explore/explore.do?structureId=4Q5V) (accessed on 23 January 2017).
188. Chang, D.J.; Lupardus, P.J.; Cimprich, K.A. Monoubiquitination of proliferating cell nuclear antigen induced by stalled replication requires uncoupling of DNA polymerase and mini-chromosome maintenance helicase activities. *J. Biol. Chem.* **2006**, *281*, 32081–32088. [CrossRef] [PubMed]
189. Sutherland, G.R. Chromosomal fragile sites. *Genet. Anal. Tech. Appl.* **1991**, *8*, 161–166. [CrossRef]
190. Shiraishi, T.; Druck, T.; Mimori, K.; Flomenberg, J.; Berk, L.; Alder, H.; Miller, W.; Huebner, K.; Croce, C.M. Sequence conservation at human and mouse orthologous common fragile regions, FRA3B/FHIT and Fra14A2/Fhit. *Proc. Natl. Acad. Sci. USA* **2001**, *98*, 5722–5727. [CrossRef] [PubMed]

191. Hellman, A.; Zlotorynski, E.; Scherer, S.W.; Cheung, J.; Vincent, J.B.; Smith, D.I.; Trakhtenbrot, L.; Kerem, B. A role for common fragile site induction in amplification of human oncogenes. *Cancer Cell* **2002**, *1*, 89–97. [CrossRef]
192. Durkin, S.G.; Ragland, R.L.; Arlt, M.F.; Mulle, J.G.; Warren, S.T.; Glover, T.W. Replication stress induces tumor-like microdeletions in FHIT/FRA3B. *Proc. Natl. Acad. Sci. USA* **2008**, *105*, 246–251. [CrossRef] [PubMed]
193. Bristow, R.G.; Hill, R.P. Hypoxia and metabolism. Hypoxia, DNA repair and genetic instability. *Nat. Rev. Cancer* **2008**, *8*, 180–192. [CrossRef] [PubMed]
194. MacGregor, J.T.; Schlegel, R.; Wehr, C.M.; Alperin, P.; Ames, B.N. Cytogenetic damage induced by folate deficiency in mice is enhanced by caffeine. *Proc. Natl. Acad. Sci. USA* **1990**, *87*, 9962–9965. [CrossRef] [PubMed]
195. Koundrioukoff, S.; Carignon, S.; Técher, H.; Letessier, A.; Brison, O.; Debatisse, M. Stepwise activation of the ATR signaling pathway upon increasing replication stress impacts fragile site integrity. *PLoS Genet.* **2013**, *9*, e1003643. [CrossRef] [PubMed]
196. Helmrich, A.; Ballarino, M.; Tora, L. Collisions between replication and transcription complexes cause common fragile site instability at the longest human genes. *Mol. Cell* **2011**, *44*, 966–977. [CrossRef] [PubMed]
197. Di Micco, R.; Fumagalli, M.; Cicalese, A.; Piccinin, S.; Gasparini, P.; Luise, C.; Schurra, C.; Garre', M.; Nuciforo, P.G.; Bensimon, A.; et al. Oncogene-induced senescence is a DNA damage response triggered by DNA hyper-replication. *Nature* **2006**, *444*, 638–642. [CrossRef]
198. Cha, R.S.; Kleckner, N. ATR homolog Mec1 promotes fork progression, thus averting breaks in replication slow zones. *Science* **2002**, *297*, 602–606. [CrossRef] [PubMed]
199. Arlt, M.F.; Mulle, J.G.; Schaibley, V.M.; Ragland, R.L.; Durkin, S.G.; Warren, S.T.; Glover, T.W. Replication stress induces genome-wide copy number changes in human cells that resemble polymorphic and pathogenic variants. *Am. J. Hum. Genet.* **2009**, *84*, 339–350. [CrossRef] [PubMed]
200. Hardt, N.; Pedrali-Noy, G.; Focher, F.; Spadari, S. Aphidicolin does not inhibit DNA repair synthesis in ultraviolet-irradiated HeLa cells. A radioautographic study. *Biochem. J.* **1981**, *199*, 453–455. [CrossRef] [PubMed]
201. Pedrali-Noy, G.; Belvedere, M.; Crepaldi, T.; Focher, F.; Spadari, S. Inhibition of DNA replication and growth of several human and murine neoplastic cells by aphidicolin without detectable effect upon synthesis of immunoglobulins and HLA antigens. *Cancer Res.* **1982**, *42*, 3810–3813. [PubMed]
202. Gera, J.F.; Fady, C.; Gardner, A.; Jacoby, F.J.; Briskin, K.B.; Lichtenstein, A. Inhibition of DNA repair with aphidicolin enhances sensitivity of targets to tumor necrosis factor. *J. Immunol.* **1993**, *151*, 3746–3757. [PubMed]
203. Waters, R. Aphidicolin: An inhibitor of DNA repair in human fibroblasts. *Carcinogenesis* **1981**, *2*, 795–797. [CrossRef] [PubMed]
204. Wang, F.; Stewart, J.; Price, C.M. Human CST abundance determines recovery from diverse forms of DNA damage and replication stress. *Cell Cycle* **2014**, *13*, 3488–3498. [CrossRef] [PubMed]
205. Yeo, J.E.; Lee, E.H.; Hendrickson, E.A.; Sobeck, A. CtIP mediates replication fork recovery in a FANCD2-regulated manner. *Hum. Mol. Genet.* **2014**, *23*, 3695–3705. [CrossRef] [PubMed]
206. Chaudhury, I.; Stroik, D.R.; Sobeck, A. FANCD2-controlled chromatin access of the Fanconi-associated nuclease FAN1 is crucial for the recovery of stalled replication forks. *Mol. Cell. Biol.* **2014**, *34*, 3939–3954. [CrossRef] [PubMed]
207. Hammond, E.M.; Green, S.L.; Giaccia, A.J. Comparison of hypoxia-induced replication arrest with hydroxyurea and aphidicolin-induced arrest. *Mutat. Res.* **2003**, *532*, 205–213. [CrossRef] [PubMed]
208. Borel, F.; Lacroix, F.B.; Margolis, R.L. Prolonged arrest of mammalian cells at the G1/S boundary results in permanent S phase stasis. *J. Cell Sci.* **2002**, *115*, 2829–2838. [PubMed]
209. Basile, G.; Leuzzi, G.; Pichierri, P.; Franchitto, A. Checkpoint-dependent and independent roles of the Werner syndrome protein in preserving genome integrity in response to mild replication stress. *Nucleic Acids Res.* **2014**, *42*, 12628–12639. [CrossRef] [PubMed]
210. Nguyen, G.H.; Dexheimer, T.S.; Rosenthal, A.S.; Chu, W.K.; Singh, D.K.; Mosedale, G.; Bachrati, C.Z.; Schultz, L.; Sakurai, M.; Savitsky, P.; et al. A small molecule inhibitor of the BLM helicase modulates chromosome stability in human cells. *Chem. Biol.* **2013**, *20*, 55–62. [CrossRef] [PubMed]

211. Schmidt, L.; Wiedner, M.; Velimezi, G.; Prochazkova, J.; Owusu, M.; Bauer, S.; Loizou, J.I. ATMIN is required for the ATM-mediated signaling and recruitment of 53BP1 to DNA damage sites upon replication stress. *DNA Repair* **2014**, *24*, 122–130. [CrossRef] [PubMed]
212. Fujita, M.; Sasanuma, H.; Yamamoto, K.N.; Harada, H.; Kurosawa, A.; Adachi, N.; Omura, M.; Hiraoka, M.; Takeda, S.; Hirota, K. Interference in DNA replication can cause mitotic chromosomal breakage unassociated with double-strand breaks. *PLoS ONE* **2013**, *8*, e60043. [CrossRef] [PubMed]
213. Beresova, L.; Vesela, E.; Chamrad, I.; Voller, J.; Yamada, M.; Furst, T.; Lenobel, R.; Chroma, K.; Gursky, J.; Krizova, K.; et al. Role of DNA Repair Factor Xeroderma Pigmentosum Protein Group C in Response to Replication Stress As Revealed by DNA Fragile Site Affinity Chromatography and Quantitative Proteomics. *J. Proteome Res.* **2016**, *15*, 4505–4517. [CrossRef] [PubMed]
214. Janson, C.; Nyhan, K.; Murnane, J.P. Replication Stress and Telomere Dysfunction Are Present in Cultured Human Embryonic Stem Cells. *Cytogenet. Genome Res.* **2015**, *146*, 251–260. [CrossRef] [PubMed]
215. Miron, K.; Golan-Lev, T.; Dvir, R.; Ben-David, E.; Kerem, B. Oncogenes create a unique landscape of fragile sites. *Nat. Commun.* **2015**, *6*, 7094. [CrossRef] [PubMed]
216. Murfuni, I.; De Santis, A.; Federico, M.; Bignami, M.; Pichierri, P.; Franchitto, A. Perturbed replication induced genome wide or at common fragile sites is differently managed in the absence of WRN. *Carcinogenesis* **2012**, *33*, 1655–1663. [CrossRef] [PubMed]
217. Wilhelm, T.; Magdalou, I.; Barascu, A.; Técher, H.; Debatisse, M.; Lopez, B.S. Spontaneous slow replication fork progression elicits mitosis alterations in homologous recombination-deficient mammalian cells. *Proc. Natl. Acad. Sci. USA* **2014**, *111*, 763–768. [CrossRef] [PubMed]
218. Available online: https://www.google.cz/url?sa=t&rct=j&q=&esrc=s&source=web&cd=3&cad=rja&uact=8&ved=0ahUKEwibvoX5jL_QAhULVSwKHQfLCXwQFggsMAI&url=https%3A%2F%2Fwww.sigmaaldrich.com%2Fcontent%2Fdam%2Fsigma-aldrich%2Fdocs%2FSigma%2FDatasheet%2F6%2Fa0781dat.pdf&usg=AFQjCNEPSqAi (accessed on 23 November 2016).
219. Sessa, C.; Zucchetti, M.; Davoli, E.; Califano, R.; Cavalli, F.; Frustaci, S.; Gumbrell, L.; Sulkes, A.; Winograd, B.; D'Incalci, M. Phase I and clinical pharmacological evaluation of aphidicolin glycinate. *J. Natl. Cancer Inst.* **1991**, *83*, 1160–1164. [CrossRef] [PubMed]
220. Edelson, R.E.; Gorycki, P.D.; MacDonald, T.L. The mechanism of aphidicolin bioinactivation by rat liver in vitro systems. *Xenobiotica* **1990**, *20*, 273–287. [CrossRef] [PubMed]
221. Santos, G.B.; Krogh, R.; Magalhaes, L.G.; Andricopulo, A.D.; Pupo, M.T.; Emery, F.S. Semisynthesis of new aphidicolin derivatives with high activity against *Trypanosoma cruzi*. *Bioorg. Med. Chem. Lett.* **2016**, *26*, 1205–1208. [CrossRef] [PubMed]
222. Glover, T.W.; Berger, C.; Coyle, J.; Echo, B. DNA polymerase alpha inhibition by aphidicolin induces gaps and breaks at common fragile sites in human chromosomes. *Hum. Genet.* **1984**, *67*, 136–142. [CrossRef] [PubMed]
223. Kurose, A.; Tanaka, T.; Huang, X.; Traganos, F.; Darzynkiewicz, Z. Synchronization in the cell cycle by inhibitors of DNA replication induces histone H2AX phosphorylation: An indication of DNA damage. *Cell Prolif.* **2006**, *39*, 231–240. [CrossRef] [PubMed]
224. Trenz, K.; Smith, E.; Smith, S.; Costanzo, V. ATM and ATR promote Mre11 dependent restart of collapsed replication forks and prevent accumulation of DNA breaks. *EMBO J.* **2006**, *25*, 1764–1774. [CrossRef] [PubMed]
225. Krakoff, I.H.; Brown, N.C.; Reichard, P. Inhibition of ribonucleoside diphosphate reductase by hydroxyurea. *Cancer Res.* **1968**, *28*, 1559–1565. [PubMed]
226. Reichard, P. Interactions between deoxyribonucleotide and DNA synthesis. *Annu. Rev. Biochem.* **1988**, *57*, 349–374. [CrossRef] [PubMed]
227. Håkansson, P.; Hofer, A.; Thelander, L. Regulation of mammalian ribonucleotide reduction and dNTP pools after DNA damage and in resting cells. *J. Biol. Chem.* **2006**, *281*, 7834–7841. [CrossRef] [PubMed]
228. Eriksson, M.; Uhlin, U.; Ramaswamy, S.; Ekberg, M.; Regnström, K.; Sjöberg, B.M.; Eklund, H. Binding of allosteric effectors to ribonucleotide reductase protein R1: Reduction of active-site cysteines promotes substrate binding. *Structure* **1997**, *5*, 1077–1092. [CrossRef]
229. Bianchi, V.; Pontis, E.; Reichard, P. Changes of deoxyribonucleoside triphosphate pools induced by hydroxyurea and their relation to DNA synthesis. *J. Biol. Chem.* **1986**, *261*, 16037–16042. [PubMed]

230. Skog, S.; Tribukait, B.; Wallström, B.; Eriksson, S. Hydroxyurea-induced cell death as related to cell cycle in mouse and human T-lymphoma cells. *Cancer Res.* **1987**, *47*, 6490–6493. [PubMed]
231. Akerblom, L. Azidocytidine is incorporated into RNA of 3T6 mouse fibroblasts. *FEBS Lett.* **1985**, *193*, 203–207. [CrossRef]
232. Anglana, M.; Apiou, F.; Bensimon, A.; Debatisse, M. Dynamics of DNA replication in mammalian somatic cells: Nucleotide pool modulates origin choice and interorigin spacing. *Cell* **2003**, *114*, 385–394. [CrossRef]
233. Barlow, J.H.; Faryabi, R.B.; Callén, E.; Wong, N.; Malhowski, A.; Chen, H.T.; Gutierrez-Cruz, G.; Sun, H.-W.; McKinnon, P.; Wright, G.; et al. Identification of early replicating fragile sites that contribute to genome instability. *Cell* **2013**, *152*, 620–632. [CrossRef] [PubMed]
234. Lönn, U.; Lönn, S. Extensive regions of single-stranded DNA in aphidicolin-treated melanoma cells. *Biochemistry* **1988**, *27*, 566–570. [CrossRef] [PubMed]
235. Recolin, B.; Van der Laan, S.; Maiorano, D. Role of replication protein A as sensor in activation of the S-phase checkpoint in Xenopus egg extracts. *Nucleic Acids Res.* **2012**, *40*, 3431–3442. [CrossRef] [PubMed]
236. Arlt, M.F.; Ozdemir, A.C.; Birkeland, S.R.; Wilson, T.E.; Glover, T.W. Hydroxyurea induces de novo copy number variants in human cells. *Proc. Natl. Acad. Sci. USA* **2011**, *108*, 17360–17365. [CrossRef] [PubMed]
237. Huang, M.-E.; Facca, C.; Fatmi, Z.; Baïlle, D.; Bénakli, S.; Vernis, L. DNA replication inhibitor hydroxyurea alters Fe–S centers by producing reactive oxygen species in vivo. *Sci. Rep.* **2016**, *6*, 29361. [CrossRef] [PubMed]
238. Szikriszt, B.; Póti, Á.; Pipek, O.; Krzystanek, M.; Kanu, N.; Molnár, J.; Ribli, D.; Szeltner, Z.; Tusnády, G.E.; Csabai, I.; et al. A comprehensive survey of the mutagenic impact of common cancer cytotoxics. *Genome Biol.* **2016**, *17*, 99. [CrossRef] [PubMed]
239. Mistrik, M.; Oplustilova, L.; Lukas, J.; Bartek, J. Low-dose DNA damage and replication stress responses quantified by optimized automated single-cell image analysis. *Cell Cycle* **2009**, *8*, 2592–2599. [CrossRef] [PubMed]
240. Ohouo, P.Y.; Bastos de Oliveira, F.M.; Liu, Y.; Ma, C.J.; Smolka, M.B. DNA-repair scaffolds dampen checkpoint signalling by counteracting the adaptor Rad9. *Nature* **2013**, *493*, 120–124. [CrossRef] [PubMed]
241. Morafraile, E.C.; Diffley, J.F.X.; Tercero, J.A.; Segurado, M. Checkpoint-dependent RNR induction promotes fork restart after replicative stress. *Sci. Rep.* **2015**, *5*, 7886. [CrossRef] [PubMed]
242. Kim, H.-S.; Kim, S.-K.; Hromas, R.; Lee, S.-H. The SET Domain Is Essential for Metnase Functions in Replication Restart and the 5′ End of SS-Overhang Cleavage. *PLoS ONE* **2015**, *10*, e0139418. [CrossRef] [PubMed]
243. Masuda, T.; Xu, X.; Dimitriadis, E.K.; Lahusen, T.; Deng, C.-X. "DNA Binding Region" of BRCA1 Affects Genetic Stability through modulating the Intra-S-Phase Checkpoint. *Int. J. Biol. Sci.* **2016**, *12*, 133–143. [CrossRef] [PubMed]
244. Yarden, R.I.; Metsuyanim, S.; Pickholtz, I.; Shabbeer, S.; Tellio, H.; Papa, M.Z. BRCA1-dependent Chk1 phosphorylation triggers partial chromatin disassociation of phosphorylated Chk1 and facilitates S-phase cell cycle arrest. *Int. J. Biochem. Cell Biol.* **2012**, *44*, 1761–1769. [CrossRef] [PubMed]
245. Awate, S.; De Benedetti, A. TLK1B mediated phosphorylation of Rad9 regulates its nuclear/cytoplasmic localization and cell cycle checkpoint. *BMC Mol. Biol.* **2016**, *17*, 3. [CrossRef] [PubMed]
246. Ahlskog, J.K.; Larsen, B.D.; Achanta, K.; Sørensen, C.S. ATM/ATR-mediated phosphorylation of PALB2 promotes RAD51 function. *EMBO Rep.* **2016**, *17*, 671–681. [CrossRef] [PubMed]
247. Molina, B.; Marchetti, F.; Gómez, L.; Ramos, S.; Torres, L.; Ortiz, R.; Altamirano-Lozano, M.; Carnevale, A.; Frias, S. Hydroxyurea induces chromosomal damage in G2 and enhances the clastogenic effect of mitomycin C in Fanconi anemia cells. *Environ. Mol. Mutagen.* **2015**, *56*, 457–467. [CrossRef] [PubMed]
248. Croke, M.; Neumann, M.A.; Grotsky, D.A.; Kreienkamp, R.; Yaddanapudi, S.C.; Gonzalo, S. Differences in 53BP1 and BRCA1 regulation between cycling and non-cycling cells. *Cell Cycle* **2013**, *12*, 3629–3639. [CrossRef] [PubMed]
249. Yamada, M.; Watanabe, K.; Mistrik, M.; Vesela, E.; Protivankova, I.; Mailand, N.; Lee, M.; Masai, H.; Lukas, J.; Bartek, J. ATR-Chk1-APC/CCdh1-dependent stabilization of Cdc7-ASK (Dbf4) kinase is required for DNA lesion bypass under replication stress. *Genes Dev.* **2013**, *27*, 2459–2472. [CrossRef] [PubMed]
250. Hu, L.; Kim, T.M.; Son, M.Y.; Kim, S.-A.; Holland, C.L.; Tateishi, S.; Kim, D.H.; Yew, P.R.; Montagna, C.; Dumitrache, L.C.; et al. Two replication fork maintenance pathways fuse inverted repeats to rearrange chromosomes. *Nature* **2013**, *501*, 569–572. [CrossRef] [PubMed]

251. Lou, T.-F.; Singh, M.; Mackie, A.; Li, W.; Pace, B.S. Hydroxyurea generates nitric oxide in human erythroid cells: Mechanisms for gamma-globin gene activation. *Exp. Biol. Med.* **2009**, *234*, 1374–1382. [CrossRef] [PubMed]
252. Vassileva, I.; Yanakieva, I.; Peycheva, M.; Gospodinov, A.; Anachkova, B. The mammalian INO80 chromatin remodeling complex is required for replication stress recovery. *Nucleic Acids Res.* **2014**, *42*, 9074–9086. [CrossRef] [PubMed]
253. Park, J.I.; Choi, H.S.; Jeong, J.S.; Han, J.Y.; Kim, I.H. Involvement of p38 kinase in hydroxyurea-induced differentiation of K562 cells. *Cell Growth Differ.* **2001**, *12*, 481–486. [PubMed]
254. Barthelemy, J.; Hanenberg, H.; Leffak, M. FANCJ is essential to maintain microsatellite structure genome-wide during replication stress. *Nucleic Acids Res.* **2016**, *44*, 6803–6816. [CrossRef] [PubMed]
255. Kunnev, D.; Rusiniak, M.E.; Kudla, A.; Freeland, A.; Cady, G.K.; Pruitt, S.C. DNA damage response and tumorigenesis in Mcm2-deficient mice. *Oncogene* **2010**, *29*, 3630–3638. [CrossRef] [PubMed]
256. Da Guarda, C.C.; Santiago, R.P.; Pitanga, T.N.; Santana, S.S.; Zanette, D.L.; Borges, V.M.; Goncalves, M.S. Heme changes HIF-α, eNOS and nitrite production in HUVECs after simvastatin, HU, and ascorbic acid therapies. *Microvasc. Res.* **2016**, *106*, 128–136. [CrossRef] [PubMed]
257. Leitch, C.; Osdal, T.; Andresen, V.; Molland, M.; Kristiansen, S.; Nguyen, X.N.; Bruserud, Ø.; Gjertsen, B.T.; McCormack, E. Hydroxyurea synergizes with valproic acid in wild-type p53 acute myeloid leukaemia. *Oncotarget* **2016**, *7*, 8105–8118. [PubMed]
258. Liu, K.; Graves, J.D.; Scott, J.D.; Li, R.; Lin, W.-C. Akt switches TopBP1 function from checkpoint activation to transcriptional regulation through phosphoserine binding-mediated oligomerization. *Mol. Cell. Biol.* **2013**, *33*, 4685–4700. [CrossRef] [PubMed]
259. Available online: https://www.google.cz/url?sa=t&rct=j&q=&esrc=s&source=web&cd=3&cad=rja&uact=8&ved=0ahUKEwiVt4Lulb_QAhUBGSwKHbcOB_kQFggsMAI&url=https%3A%2F%2Fwww.sigmaaldrich.com%2Fcontent%2Fdam%2Fsigma-aldrich%2Fdocs%2FSigma%2FProduct_Information_Sheet%2F2%2Fh8627pis.pdf& (accessed on 23 January 2017).
260. Segal, J.B.; Strouse, J.J.; Beach, M.C.; Haywood, C.; Witkop, C.; Park, H.; Wilson, R.F.; Bass, E.B.; Lanzkron, S. *Hydroxyurea for the Treatment of Sickle Cell Disease*; Evidence Reports/Technology Assessments; Agency for Healthcare Research and Quality (US): Rockville, MD, USA, 2008; pp. 1–95.
261. Kühr, T.; Burgstaller, S.; Apfelbeck, U.; Linkesch, W.; Seewann, H.; Fridrik, M.; Michlmayr, G.; Krieger, O.; Lutz, D.; Lin, W.; et al. A randomized study comparing interferon (IFNα) plus low-dose cytarabine and interferon plus hydroxyurea (HU) in early chronic-phase chronic myeloid leukemia (CML). *Leuk. Res.* **2003**, *27*, 405–411. [CrossRef]
262. Aruch, D.; Mascarenhas, J. Contemporary approach to essential thrombocythemia and polycythemia vera. *Curr. Opin. Hematol.* **2016**, *23*, 150–160. [CrossRef] [PubMed]
263. Barbui, T.; Finazzi, M.C.; Finazzi, G. Front-line therapy in polycythemia vera and essential thrombocythemia. *Blood Rev.* **2012**, *26*, 205–211. [CrossRef] [PubMed]
264. Benito, J.M.; López, M.; Lozano, S.; Ballesteros, C.; González-Lahoz, J.; Soriano, V. Hydroxyurea exerts an anti-proliferative effect on T cells but has no direct impact on cellular activation. *Clin. Exp. Immunol.* **2007**, *149*, 171–177. [CrossRef] [PubMed]
265. Gurberg, J.; Bouganim, N.; Shenouda, G.; Zeitouni, A. A case of recurrent anaplastic meningioma of the skull base with radiologic response to hydroxyurea. *J. Neurol. Surg. Rep.* **2014**, *75*, e52–e55. [CrossRef] [PubMed]
266. Kiladjian, J.-J.; Chevret, S.; Dosquet, C.; Chomienne, C.; Rain, J.-D. Treatment of polycythemia vera with hydroxyurea and pipobroman: Final results of a randomized trial initiated in 1980. *J. Clin. Oncol.* **2011**, *29*, 3907–3913. [CrossRef] [PubMed]
267. Charache, S.; Barton, F.B.; Moore, R.D.; Terrin, M.L.; Steinberg, M.H.; Dover, G.J.; Ballas, S.K.; McMahon, R.P.; Castro, O.; Orringer, E.P. Hydroxyurea and sickle cell anemia. Clinical utility of a myelosuppressive "switching" agent. The Multicenter Study of Hydroxyurea in Sickle Cell Anemia. *Medicine* **1996**, *75*, 300–326. [CrossRef] [PubMed]
268. Steinberg, M.H.; McCarthy, W.F.; Castro, O.; Ballas, S.K.; Armstrong, F.D.; Smith, W.; Ataga, K.; Swerdlow, P.; Kutlar, A.; DeCastro, L.; et al. The risks and benefits of long-term use of hydroxyurea in sickle cell anemia: A 17.5 year follow-up. *Am. J. Hematol.* **2010**, *85*, 403–408. [CrossRef] [PubMed]

269. Darzynkiewicz, Z.; Halicka, H.D.; Zhao, H.; Podhorecka, M. Cell synchronization by inhibitors of DNA replication induces replication stress and DNA damage response: Analysis by flow cytometry. *Methods Mol. Biol.* **2011**, *761*, 85–96. [PubMed]
270. Fugger, K.; Mistrik, M.; Danielsen, J.R.; Dinant, C.; Falck, J.; Bartek, J.; Lukas, J.; Mailand, N. Human Fbh1 helicase contributes to genome maintenance via pro- and anti-recombinase activities. *J. Cell Biol.* **2009**, *186*, 655–663. [CrossRef] [PubMed]
271. Liu, N.; Lim, C.-S. Differential roles of XRCC2 in homologous recombinational repair of stalled replication forks. *J. Cell. Biochem.* **2005**, *95*, 942–954. [CrossRef] [PubMed]
272. Brose, R.D.; Shin, G.; McGuinness, M.C.; Schneidereith, T.; Purvis, S.; Dong, G.X.; Keefer, J.; Spencer, F.; Smith, K.D. Activation of the stress proteome as a mechanism for small molecule therapeutics. *Hum. Mol. Genet.* **2012**, *21*, 4237–4252. [CrossRef] [PubMed]
273. Adragna, N.C.; Fonseca, P.; Lauf, P.K. Hydroxyurea affects cell morphology, cation transport, and red blood cell adhesion in cultured vascular endothelial cells. *Blood* **1994**, *83*, 553–560. [PubMed]
274. Wall, M.E.; Wani, M.C.; Cook, C.E.; Palmer, K.H.; McPhail, A.T.; Sim, G.A. Plant Antitumor Agents. I. The Isolation and Structure of Camptothecin, a Novel Alkaloidal Leukemia and Tumor Inhibitor from *Camptotheca acuminata*[1,2]. *J. Am. Chem. Soc.* **1966**, *88*, 3888–3890. [CrossRef]
275. Gupta, M.; Fujimori, A.; Pommier, Y. Eukaryotic DNA topoisomerases I. *Biochim. Biophys. Acta* **1995**, *1262*, 1–14. [CrossRef]
276. Champoux, J.J. Mechanism of the reaction catalyzed by the DNA untwisting enzyme: Attachment of the enzyme to 3′-terminus of the nicked DNA. *J. Mol. Biol.* **1978**, *118*, 441–446. [CrossRef]
277. Available online: http://www.rcsb.org/pdb/explore/explore.do?structureId=1T8I (accessed on 23 January 2017).
278. Stivers, J.T.; Harris, T.K.; Mildvan, A.S. Vaccinia DNA topoisomerase I: Evidence supporting a free rotation mechanism for DNA supercoil relaxation. *Biochemistry* **1997**, *36*, 5212–5222. [CrossRef] [PubMed]
279. Koster, D.A.; Palle, K.; Bot, E.S.M.; Bjornsti, M.-A.; Dekker, N.H. Antitumour drugs impede DNA uncoiling by topoisomerase I. *Nature* **2007**, *448*, 213–217. [CrossRef] [PubMed]
280. Staker, B.L.; Hjerrild, K.; Feese, M.D.; Behnke, C.A.; Burgin, A.B.; Stewart, L. The mechanism of topoisomerase I poisoning by a camptothecin analog. *Proc. Natl. Acad. Sci. USA* **2002**, *99*, 15387–15392. [CrossRef] [PubMed]
281. Regairaz, M.; Zhang, Y.-W.; Fu, H.; Agama, K.K.; Tata, N.; Agrawal, S.; Aladjem, M.I.; Pommier, Y. Mus81-mediated DNA cleavage resolves replication forks stalled by topoisomerase I–DNA complexes. *J. Cell Biol.* **2011**, *195*, 739–749. [CrossRef] [PubMed]
282. Palle, K.; Vaziri, C. Rad18 E3 ubiquitin ligase activity mediates Fanconi anemia pathway activation and cell survival following DNA Topoisomerase 1 inhibition. *Cell Cycle* **2011**, *10*, 1625–1638. [CrossRef] [PubMed]
283. Pommier, Y. Topoisomerase I inhibitors: Camptothecins and beyond. *Nat. Rev. Cancer* **2006**, *6*, 789–802. [CrossRef] [PubMed]
284. Tuduri, S.; Crabbé, L.; Conti, C.; Tourrière, H.; Holtgreve-Grez, H.; Jauch, A.; Pantesco, V.; De Vos, J.; Thomas, A.; Theillet, C.; et al. Topoisomerase I suppresses genomic instability by preventing interference between replication and transcription. *Nat. Cell Biol.* **2009**, *11*, 1315–1324. [CrossRef] [PubMed]
285. Tripathi, K.; Mani, C.; Clark, D.W.; Palle, K. Rad18 is required for functional interactions between FANCD2, BRCA2, and Rad51 to repair DNA topoisomerase 1-poisons induced lesions and promote fork recovery. *Oncotarget* **2016**, *7*, 12537–12553. [PubMed]
286. Tsao, Y.P.; D'Arpa, P.; Liu, L.F. The involvement of active DNA synthesis in camptothecin-induced G2 arrest: Altered regulation of p34cdc2/cyclin B. *Cancer Res.* **1992**, *52*, 1823–1829. [PubMed]
287. Kharbanda, S.; Rubin, E.; Gunji, H.; Hinz, H.; Giovanella, B.; Pantazis, P.; Kufe, D. Camptothecin and its derivatives induce expression of the *c-jun* protooncogene in human myeloid leukemia cells. *Cancer Res.* **1991**, *51*, 6636–6642. [PubMed]
288. Aller, P.; Rius, C.; Mata, F.; Zorrilla, A.; Cabañas, C.; Bellón, T.; Bernabeu, C. Camptothecin induces differentiation and stimulates the expression of differentiation-related genes in U-937 human promonocytic leukemia cells. *Cancer Res.* **1992**, *52*, 1245–1251. [PubMed]
289. Clements, M.K.; Jones, C.B.; Cumming, M.; Daoud, S.S. Antiangiogenic potential of camptothecin and topotecan. *Cancer Chemother. Pharmacol.* **1999**, *44*, 411–416. [CrossRef] [PubMed]

290. O'Leary, J.J.; Shapiro, R.L.; Ren, C.J.; Chuang, N.; Cohen, H.W.; Potmesil, M. Antiangiogenic effects of camptothecin analogues 9-amino-20(*S*)-camptothecin, topotecan, and CPT-11 studied in the mouse cornea model. *Clin. Cancer Res.* **1999**, *5*, 181–187. [PubMed]
291. Arlt, M.F.; Glover, T.W. Inhibition of topoisomerase I prevents chromosome breakage at common fragile sites. *DNA Repair* **2010**, *9*, 678–689. [CrossRef] [PubMed]
292. Horwitz, S.B.; Horwitz, M.S. Effects of camptothecin on the breakage and repair of DNA during the cell cycle. *Cancer Res.* **1973**, *33*, 2834–2836. [PubMed]
293. Jayasooriya, R.G.P.T.; Choi, Y.H.; Hyun, J.W.; Kim, G.-Y. Camptothecin sensitizes human hepatoma Hep3B cells to TRAIL-mediated apoptosis via ROS-dependent death receptor 5 upregulation with the involvement of MAPKs. *Environ. Toxicol. Pharmacol.* **2014**, *38*, 959–967. [CrossRef] [PubMed]
294. Strumberg, D.; Pilon, A.A.; Smith, M.; Hickey, R.; Malkas, L.; Pommier, Y. Conversion of topoisomerase I cleavage complexes on the leading strand of ribosomal DNA into 5′-phosphorylated DNA double-strand breaks by replication runoff. *Mol. Cell. Biol.* **2000**, *20*, 3977–3987. [CrossRef] [PubMed]
295. Priel, E.; Showalter, S.D.; Roberts, M.; Oroszlan, S.; Blair, D.G. The topoisomerase I inhibitor, camptothecin, inhibits equine infectious anemia virus replication in chronically infected CF2Th cells. *J. Virol.* **1991**, *65*, 4137–4141. [PubMed]
296. Bruno, S.; Giaretti, W.; Darzynkiewicz, Z. Effect of camptothecin on mitogenic stimulation of human lymphocytes: Involvement of DNA topoisomerase I in cell transition from G0 to G1 phase of the cell cycle and in DNA replication. *J. Cell. Physiol.* **1992**, *151*, 478–486. [CrossRef] [PubMed]
297. Squires, S.; Ryan, A.J.; Strutt, H.L.; Johnson, R.T. Hypersensitivity of Cockayne's syndrome cells to camptothecin is associated with the generation of abnormally high levels of double strand breaks in nascent DNA. *Cancer Res.* **1993**, *53*, 2012–2019. [PubMed]
298. Ding, X.; Matsuo, K.; Xu, L.; Yang, J.; Zheng, L. Optimized combinations of bortezomib, camptothecin, and doxorubicin show increased efficacy and reduced toxicity in treating oral cancer. *Anticancer Drugs* **2015**, *26*, 547–554. [CrossRef] [PubMed]
299. Zhang, J.; Walter, J.C. Mechanism and regulation of incisions during DNA interstrand cross-link repair. *DNA Repair* **2014**, *19*, 135–142. [CrossRef] [PubMed]
300. Ray Chaudhuri, A.; Hashimoto, Y.; Herrador, R.; Neelsen, K.J.; Fachinetti, D.; Bermejo, R.; Cocito, A.; Costanzo, V.; Lopes, M. Topoisomerase I poisoning results in PARP-mediated replication fork reversal. *Nat. Struct. Mol. Biol.* **2012**, *19*, 417–423. [CrossRef] [PubMed]
301. Available online: http://www.sigmaaldrich.com/content/dam/sigma-aldrich/docs/Sigma/Product_Information_Sheet/c9911pis.pdf (accessed on 23 November 2016).
302. Jaxel, C.; Kohn, K.W.; Wani, M.C.; Wall, M.E.; Pommier, Y. Structure-activity study of the actions of camptothecin derivatives on mammalian topoisomerase I: Evidence for a specific receptor site and a relation to antitumor activity. *Cancer Res.* **1989**, *49*, 1465–1469. [PubMed]
303. Takagi, K.; Dexheimer, T.S.; Redon, C.; Sordet, O.; Agama, K.; Lavielle, G.; Pierré, A.; Bates, S.E.; Pommier, Y. Novel E-ring camptothecin keto analogues (S38809 and S39625) are stable, potent, and selective topoisomerase I inhibitors without being substrates of drug efflux transporters. *Mol. Cancer Ther.* **2007**, *6*, 3229–3238. [CrossRef] [PubMed]
304. Hande, K.R. Etoposide: Four decades of development of a topoisomerase II inhibitor. *Eur. J. Cancer* **1998**, *34*, 1514–1521. [CrossRef]
305. Available online: http://www.rcsb.org/pdb/explore/explore.do?structureId=3QX3 (accessed on 23 January 2017).
306. Liu, L.F.; Rowe, T.C.; Yang, L.; Tewey, K.M.; Chen, G.L. Cleavage of DNA by mammalian DNA topoisomerase II. *J. Biol. Chem.* **1983**, *258*, 15365–15370. [PubMed]
307. Gibson, E.G.; King, M.M.; Mercer, S.L.; Deweese, J.E. Two-Mechanism Model for the Interaction of Etoposide Quinone with Topoisomerase IIα. *Chem. Res. Toxicol.* **2016**, *29*, 1541–1548. [CrossRef] [PubMed]
308. Wu, C.-C.; Li, T.-K.; Farh, L.; Lin, L.-Y.; Lin, T.-S.; Yu, Y.-J.; Yen, T.-J.; Chiang, C.-W.; Chan, N.-L. Structural basis of type II topoisomerase inhibition by the anticancer drug etoposide. *Science* **2011**, *333*, 459–462. [CrossRef] [PubMed]

309. Bender, R.P.; Jablonksy, M.J.; Shadid, M.; Romaine, I.; Dunlap, N.; Anklin, C.; Graves, D.E.; Osheroff, N. Substituents on etoposide that interact with human topoisomerase IIalpha in the binary enzyme-drug complex: Contributions to etoposide binding and activity. *Biochemistry* **2008**, *47*, 4501–4509. [CrossRef] [PubMed]
310. Wilstermann, A.M.; Bender, R.P.; Godfrey, M.; Choi, S.; Anklin, C.; Berkowitz, D.B.; Osheroff, N.; Graves, D.E. Topoisomerase II—Drug interaction domains: Identification of substituents on etoposide that interact with the enzyme. *Biochemistry* **2007**, *46*, 8217–8225. [CrossRef] [PubMed]
311. Jacob, D.A.; Mercer, S.L.; Osheroff, N.; Deweese, J.E. Etoposide quinone is a redox-dependent topoisomerase II poison. *Biochemistry* **2011**, *50*, 5660–5667. [CrossRef] [PubMed]
312. Rogakou, E.P.; Pilch, D.R.; Orr, A.H.; Ivanova, V.S.; Bonner, W.M. DNA double-stranded breaks induce histone H2AX phosphorylation on serine 139. *J. Biol. Chem.* **1998**, *273*, 5858–5868. [CrossRef] [PubMed]
313. Terasawa, M.; Shinohara, A.; Shinohara, M. Canonical non-homologous end joining in mitosis induces genome instability and is suppressed by M-phase-specific phosphorylation of XRCC4. *PLoS Genet.* **2014**, *10*, e1004563. [CrossRef] [PubMed]
314. Zhao, H.; Rybak, P.; Dobrucki, J.; Traganos, F.; Darzynkiewicz, Z. Relationship of DNA damage signaling to DNA replication following treatment with DNA topoisomerase inhibitors camptothecin/topotecan, mitoxantrone, or etoposide. *Cytometry A* **2012**, *81*, 45–51. [CrossRef] [PubMed]
315. Montecucco, A.; Rossi, R.; Ferrari, G.; Scovassi, A.I.; Prosperi, E.; Biamonti, G. Etoposide Induces the Dispersal of DNA Ligase I from Replication Factories. *Mol. Biol. Cell* **2001**, *12*, 2109–2118. [CrossRef] [PubMed]
316. Holm, C.; Covey, J.M.; Kerrigan, D.; Pommier, Y. Differential requirement of DNA replication for the cytotoxicity of DNA topoisomerase I and II inhibitors in Chinese hamster DC3F cells. *Cancer Res.* **1989**, *49*, 6365–6368. [PubMed]
317. Austin, C.A.; Sng, J.H.; Patel, S.; Fisher, L.M. Novel HeLa topoisomerase II is the II beta isoform: Complete coding sequence and homology with other type II topoisomerases. *Biochim. Biophys. Acta* **1993**, *1172*, 283–291. [CrossRef]
318. Niimi, A.; Suka, N.; Harata, M.; Kikuchi, A.; Mizuno, S. Co-localization of chicken DNA topoisomerase IIalpha, but not beta, with sites of DNA replication and possible involvement of a C-terminal region of alpha through its binding to PCNA. *Chromosoma* **2001**, *110*, 102–114. [CrossRef] [PubMed]
319. Ju, B.-G.; Lunyak, V.V.; Perissi, V.; Garcia-Bassets, I.; Rose, D.W.; Glass, C.K.; Rosenfeld, M.G. A topoisomerase IIβ-mediated dsDNA break required for regulated transcription. *Science* **2006**, *312*, 1798–1802. [CrossRef] [PubMed]
320. Azarova, A.M.; Lyu, Y.L.; Lin, C.-P.; Tsai, Y.-C.; Lau, J.Y.-N.; Wang, J.C.; Liu, L.F. Roles of DNA topoisomerase II isozymes in chemotherapy and secondary malignancies. *Proc. Natl. Acad. Sci. USA* **2007**, *104*, 11014–11019. [CrossRef] [PubMed]
321. Nitiss, J.L. DNA topoisomerase II and its growing repertoire of biological functions. *Nat. Rev. Cancer* **2009**, *9*, 327–337. [CrossRef] [PubMed]
322. Gupta, R.S.; Bromke, A.; Bryant, D.W.; Gupta, R.; Singh, B.; McCalla, D.R. Etoposide (VP16) and teniposide (VM26): Novel anticancer drugs, strongly mutagenic in mammalian but not prokaryotic test systems. *Mutagenesis* **1987**, *2*, 179–186. [CrossRef] [PubMed]
323. Muslimović, A.; Nyström, S.; Gao, Y.; Hammarsten, O. Numerical Analysis of Etoposide Induced DNA Breaks. *PLoS ONE* **2009**, *4*, e5859. [CrossRef]
324. Álvarez-Quilón, A.; Serrano-Benítez, A.; Lieberman, J.A.; Quintero, C.; Sánchez-Gutiérrez, D.; Escudero, L.M.; Cortés-Ledesma, F. ATM specifically mediates repair of double-strand breaks with blocked DNA ends. *Nat. Commun.* **2014**, *5*, 3347. [CrossRef] [PubMed]
325. Nagano, T.; Nakano, M.; Nakashima, A.; Onishi, K.; Yamao, S.; Enari, M.; Kikkawa, U.; Kamada, S. Identification of cellular senescence-specific genes by comparative transcriptomics. *Sci. Rep.* **2016**, *6*, 31758. [CrossRef] [PubMed]
326. Brasacchio, D.; Alsop, A.E.; Noori, T.; Lufti, M.; Iyer, S.; Simpson, K.J.; Bird, P.I.; Kluck, R.M.; Johnstone, R.W.; Trapani, J.A. Epigenetic control of mitochondrial cell death through PACS1-mediated regulation of BAX/BAK oligomerization. *Cell Death Differ.* **2017**. [CrossRef] [PubMed]

327. Martin, R.; Desponds, C.; Eren, R.O.; Quadroni, M.; Thome, M.; Fasel, N. Caspase-mediated cleavage of raptor participates in the inactivation of mTORC1 during cell death. *Cell Death Discov.* **2016**, *2*, 16024. [CrossRef] [PubMed]
328. Brekman, A.; Singh, K.E.; Polotskaia, A.; Kundu, N.; Bargonetti, J. A p53-independent role of Mdm2 in estrogen-mediated activation of breast cancer cell proliferation. *Breast Cancer Res.* **2011**, *13*, R3. [CrossRef] [PubMed]
329. Soubeyrand, S.; Pope, L.; Haché, R.J.G. Topoisomerase IIα-dependent induction of a persistent DNA damage response in response to transient etoposide exposure. *Mol. Oncol.* **2010**, *4*, 38–51. [CrossRef] [PubMed]
330. Velma, V.; Carrero, Z.I.; Allen, C.B.; Hebert, M.D. Coilin levels modulate cell cycle progression and γH2AX levels in etoposide treated U2OS cells. *FEBS Lett.* **2012**, *586*, 3404–3409. [CrossRef] [PubMed]
331. Dehennaut, V.; Loison, I.; Dubuissez, M.; Nassour, J.; Abbadie, C.; Leprince, D. DNA double-strand breaks lead to activation of hypermethylated in cancer 1 (HIC1) by SUMOylation to regulate DNA repair. *J. Biol. Chem.* **2013**, *288*, 10254–10264. [CrossRef] [PubMed]
332. Paget, S.; Dubuissez, M.; Dehennaut, V.; Nassour, J.; Harmon, B.T.; Spruyt, N.; Loison, I.; Abbadie, C.; Rood, B.R.; Leprince, D. HIC1 (hypermethylated in cancer 1) SUMOylation is dispensable for DNA repair but is essential for the apoptotic DNA damage response (DDR) to irreparable DNA double-strand breaks (DSBs). *Oncotarget* **2017**, *8*, 2916–2935. [CrossRef] [PubMed]
333. Sypniewski, D.; Bednarek, I.; Gałka, S.; Loch, T.; Błaszczyk, D.; Sołtysik, D. Cytotoxicity of etoposide in cancer cell lines in vitro after BCL-2 and C-RAF gene silencing with antisense oligonucleotides. *Acta Pol. Pharm.* **2013**, *70*, 87–97.
334. Rybak, P.; Hoang, A.; Bujnowicz, L.; Bernas, T.; Berniak, K.; ZarÄ Bski, M.A.; Darzynkiewicz, Z.; Dobrucki, J. Low level phosphorylation of histone H2AX on serine 139 (γH2AX) is not associated with DNA double-strand breaks. *Oncotarget* **2016**, *7*, 49574–49587. [CrossRef] [PubMed]
335. Chen, L.; Cui, H.; Fang, J.; Deng, H.; Kuang, P.; Guo, H.; Wang, X.; Zhao, L. Glutamine deprivation plus BPTES alters etoposide- and cisplatin-induced apoptosis in triple negative breast cancer cells. *Oncotarget* **2016**, *7*, 54691–54701. [CrossRef] [PubMed]
336. Rodriguez-Lopez, A.M.; Xenaki, D.; Eden, T.O.; Hickman, J.A.; Chresta, C.M. MDM2 mediated nuclear exclusion of p53 attenuates etoposide-induced apoptosis in neuroblastoma cells. *Mol. Pharmacol.* **2001**, *59*, 135–143.
337. Litwiniec, A.; Gackowska, L.; Helmin-Basa, A.; Żuryń, A.; Grzanka, A. Low-dose etoposide-treatment induces endoreplication and cell death accompanied by cytoskeletal alterations in A549 cells: Does the response involve senescence? The possible role of vimentin. *Cancer Cell Int.* **2013**, *13*, 9. [CrossRef] [PubMed]
338. Akhtar, N.; Talegaonkar, S.; Khar, R.K.; Jaggi, M. A validated stability-indicating LC method for estimation of etoposide in bulk and optimized self-nano emulsifying formulation: Kinetics and stability effects. *Saudi Pharm. J.* **2013**, *21*, 103–111. [CrossRef] [PubMed]
339. Available online: http://www.sigmaaldrich.com/content/dam/sigma-aldrich/docs/Sigma/Product_Information_Sheet/e1383pis.pdf (accessed on 23 Novermber 2016).
340. Wrasidlo, W.; Schröder, U.; Bernt, K.; Hübener, N.; Shabat, D.; Gaedicke, G.; Lode, H. Synthesis, hydrolytic activation and cytotoxicity of etoposide prodrugs. *Bioorg Med Chem Lett.* **2002**, *12*, 557–560. [CrossRef]
341. Jokić, M.; Vlašić, I.; Rinneburger, M.; Klümper, N.; Spiro, J.; Vogel, W.; Offermann, A.; Kümpers, C.; Fritz, C.; Schmitt, A.; et al. Ercc1 Deficiency Promotes Tumorigenesis and Increases Cisplatin Sensitivity in a Tp53 Context-Specific Manner. *Mol. Cancer Res.* **2016**, *14*, 1110–1123. [CrossRef] [PubMed]
342. Felix, C.A.; Walker, A.H.; Lange, B.J.; Williams, T.M.; Winick, N.J.; Cheung, N.K.; Lovett, B.D.; Nowell, P.C.; Blair, I.A.; Rebbeck, T.R. Association of CYP3A4 genotype with treatment-related leukemia. *Proc. Natl. Acad. Sci. USA* **1998**, *95*, 13176–13181. [CrossRef] [PubMed]
343. Blanco, J.G.; Edick, M.J.; Relling, M.V. Etoposide induces chimeric Mll gene fusions. *FASEB J.* **2004**, *18*, 173–175. [CrossRef] [PubMed]
344. Thirman, M.J.; Gill, H.J.; Burnett, R.C.; Mbangkollo, D.; McCabe, N.R.; Kobayashi, H.; Ziemin-van der Poel, S.; Kaneko, Y.; Morgan, R.; Sandberg, A.A. Rearrangement of the MLL gene in acute lymphoblastic and acute myeloid leukemias with 11q23 chromosomal translocations. *N. Engl. J. Med.* **1993**, *329*, 909–914. [CrossRef] [PubMed]

345. Cerveira, N.; Lisboa, S.; Correia, C.; Bizarro, S.; Santos, J.; Torres, L.; Vieira, J.; Barros-Silva, J.D.; Pereira, D.; Moreira, C.; et al. Genetic and clinical characterization of 45 acute leukemia patients with MLL gene rearrangements from a single institution. *Mol. Oncol.* **2012**, *6*, 553–564. [CrossRef] [PubMed]
346. Krivtsov, A.V.; Armstrong, S.A. MLL translocations, histone modifications and leukaemia stem-cell development. *Nat. Rev. Cancer* **2007**, *7*, 823–833. [CrossRef] [PubMed]
347. Zhang, L.; Chen, F.; Zhang, Z.; Chen, Y.; Lin, Y.; Wang, J. Design, synthesis and evaluation of the multidrug resistance-reversing activity of pyridine acid esters of podophyllotoxin in human leukemia cells. *Bioorg. Med. Chem. Lett.* **2016**, *26*, 4466–4471. [CrossRef] [PubMed]
348. Lee, K.-I.; Su, C.-C.; Yang, C.-Y.; Hung, D.-Z.; Lin, C.-T.; Lu, T.-H.; Liu, S.-H.; Huang, C.-F. Etoposide induces pancreatic β-cells cytotoxicity via the JNK/ERK/GSK-3 signaling-mediated mitochondria-dependent apoptosis pathway. *Toxicol. Vitro* **2016**, *36*, 142–152. [CrossRef] [PubMed]
349. Pellegrini, G.G.; Morales, C.C.; Wallace, T.C.; Plotkin, L.I.; Bellido, T. Avenanthramides Prevent Osteoblast and Osteocyte Apoptosis and Induce Osteoclast Apoptosis in Vitro in an Nrf2-Independent Manner. *Nutrients* **2016**, *8*, 423. [CrossRef] [PubMed]
350. Papież, M.A.; Krzyściak, W.; Szade, K.; Bukowska-Straková, K.; Kozakowska, M.; Hajduk, K.; Bystrowska, B.; Dulak, J.; Jozkowicz, A. Curcumin enhances the cytogenotoxic effect of etoposide in leukemia cells through induction of reactive oxygen species. *Drug Des. Dev. Ther.* **2016**, *10*, 557–570. [CrossRef] [PubMed]
351. Zhang, S.; Lu, C.; Zhang, X.; Li, J.; Jiang, H. Targeted delivery of etoposide to cancer cells by folate-modified nanostructured lipid drug delivery system. *Drug Deliv.* **2016**, *23*, 1838–1845. [CrossRef] [PubMed]
352. Lindsay, G.S.; Wallace, H.M. Changes in polyamine catabolism in HL-60 human promyelogenous leukaemic cells in response to etoposide-induced apoptosis. *Biochem. J.* **1999**, *337 Pt 1*, 83–87. [CrossRef] [PubMed]
353. Kumar, A.; Ehrenshaft, M.; Tokar, E.J.; Mason, R.P.; Sinha, B.K. Nitric oxide inhibits topoisomerase II activity and induces resistance to topoisomerase II-poisons in human tumor cells. *Biochim. Biophys. Acta* **2016**, *1860*, 1519–1527. [CrossRef] [PubMed]
354. Zhang, A.; Lyu, Y.L.; Lin, C.-P.; Zhou, N.; Azarova, A.M.; Wood, L.M.; Liu, L.F. A protease pathway for the repair of topoisomerase II–DNA covalent complexes. *J. Biol. Chem.* **2006**, *281*, 35997–36003. [CrossRef] [PubMed]
355. Ledesma, F.C.; El Khamisy, S.F.; Zuma, M.C.; Osborn, K.; Caldecott, K.W. A human 5′-tyrosyl DNA phosphodiesterase that repairs topoisomerase-mediated DNA damage. *Nature* **2009**, *461*, 674–678. [CrossRef] [PubMed]
356. Aparicio, T.; Baer, R.; Gottesman, M.; Gautier, J. MRN, CtIP, and BRCA1 mediate repair of topoisomerase II–DNA adducts. *J. Cell Biol.* **2016**, *212*, 399–408. [CrossRef] [PubMed]
357. Quennet, V.; Beucher, A.; Barton, O.; Takeda, S.; Löbrich, M. CtIP and MRN promote non-homologous end-joining of etoposide-induced DNA double-strand breaks in G1. *Nucleic Acids Res.* **2011**, *39*, 2144–2152. [CrossRef] [PubMed]
358. Adachi, N.; Suzuki, H.; Iiizumi, S.; Koyama, H. Hypersensitivity of nonhomologous DNA end-joining mutants to VP-16 and ICRF-193: Implications for the repair of topoisomerase II-mediated DNA damage. *J. Biol. Chem.* **2003**, *278*, 35897–35902. [CrossRef] [PubMed]